Multi-wavelength study of variability in Blazars

A THESIS

submitted for the Award of Ph.D. degree at

MOHANLAL SUKHADIA UNIVERSITY

in the

Faculty of Science

BY

Sunil Chandra

Under the Supervision of

Prof. K. S. Baliyan

Physical Research Laboratory, Ahmedabad

Department of Physics

MOHANLAL SUKHADIA UNIVERSITY

UDAIPUR

Year of submission: 2013

To

My parents and grand parents

DECLARATION

I, **Sunil Chandra**, S/o Mr. Ramesh Chandra, resident of Room No. 103, Thaltej students hostel, Thaltej, Ahmedabad-380054, hereby declare that the research work incorporated in the present PhD thesis entitled, **"Multi-wavelength Study of Variability in Blazars"** is my own work and is original. This work (in part or in full) has not been submitted to any University for the award of a Degree or a Diploma. I have properly acknowledged the material collected from secondary sources wherever required. I solely own the responsibility for the originality of the entire content.

Date:

Sunil Chandra

(Author)

CERTIFICATE

I take pleasure in certifying that the thesis entitled, **"Multi-wavelength Study of Variability in Blazars"** by Mr. Sunil Chandra embodies the work done by him under my guidance. He has completed the following requirements as per Ph.D regulations of the University.

(a) Course work as per the university rules.

(b) Residential requirements of the university.

(c) Regularly submitted six monthly progress reports.

(d) Presented his work in the departmental committee.

(e) Published minimum of one research papers in a referred research journal.

I recommend the submission of thesis.

Date:

Kiran Singh Baliyan
(Thesis Supervisor)
Professor, Astronomy & Astrophysics, Division
Physical Research Laboratory,
(unit of Dept. of Space, Government of India)
Ahmedabad - 380 009.

Countersigned by

Head of the Department

Acknowledgements

This dissertation is an outcome of my patient work that has been conducted over a span of five years. In this interminable period of time, I have interacted with several scholars, scientists, colleagues, friends who have imparted in various ways during this tenure. At the very outset of winding up my doctoral thesis, it gives me immense pleasure to acknowledge my heartiest gratitude to all.

First and foremost, I express my sincere gratitude to my thesis advisor-cum-mentor, Prof. K.S. Baliyan, who has introduced me to the joy of Astronomy, an offbeat impression of the universe. The work presented in this dissertation was brushed up under the aegis of his guidance. His passionate support and magnanimous co-operation was the one which led my immature thoughts to a scientific sense. His deep insights in the subject and vast experience helped me immensely in learning the subject and necessary tools. His friendly behaviour always made our discussions more pleasant and decisive. Being personally connected to his family members also, especially Aunty Ji, I thank her for providing a family ambience even several thousand kilometres away from home.

I am thankful to Prof. J.N. Goswami, Director, PRL, for providing needful facilities required during this work. I would also like to express my sincere thanks to Prof. Utpal Sarkar, Dean, PRL; Prof. A. Singhvi and Prof. A. S. Joshipura, former Deans, PRL and PRL academic committee for their continuous support and help.

I take this opportunity to offer my profound indebtedness to Dr. Shashikiran Ganesh who always helped like a true friend and counsellor throughout this period. His deep insight in the instrumentation and astronomy always attracted and fascinated me to learn. I acknowledge his prompt support whenever and wherever I asked. In particular, I am very much delighted to thank his family members, especially Gayatri, his daughter. Her sweet talks and childishness always made me feel to be a part of her family.

I also offer gratitude to my collaborator, Prof. Wim Hermsen, from Space Research Organizations Netherlands (SRON). As a mentor and Guardian, he *taught many aspects of research and life. In the same time, I also thank Prof. Luigi Foschini from Osservatorio de Berea, Italy for attending even my naive questions and nurturing my understanding. Ever motivating facts were his tremendous insights into the subject and dedication towards science. I also acknowledge Prof. Gulab Dewangan from IUCAA, Pune and Dr. Sachindra Naik from PRL for their valuable discussions about X-ray astronomy.*

On this occasion, I can not forget to mention the supports provided by Prof. N. M. Ashok from PRL. His valuable comments and suggestions, as a critical reviewer, always helped in shaping my research. In addition, his friendly behaviour, as well known, is now inscribed in my mind. I also acknowledge the discussion sessions with Prof. Umesh Joshi and Prof. Ashok Singal on various topics which were always a kick-out for me from the puddles of confusion.

I also thank Dr. Santosh Vadawale, PRL for his unforgettable support during the infanthood of my research career. As a project guide, he helped me whenever I faced even nascent problems related to computers and programming. I also thank his family members for their caring behaviour. I always miss the company of his daughters Devyani and Arohi. Further, being with Devyani and Gayatri (Shashi's daughter), I could again travel-back in the precious time of my childhood.

I acknowledge the support provided by PRL faculty members such as Prof. B.G. Anandrao, Prof. T. Chandrashekhar, Prof. Hari Om Vats, Prof. Rajmal Jain, Prof. P. Janardhan, Prof. D.P.K. Banerjee and Dr. A. Chakraborty. I also take this opportunity to thank all scientists and staff members of Thaltej Campus, PRL, where my most of the research time was spent. Especially I thanks Mr. Amish B. Shah, Mr. V. Venkat, Mr. Dipak Panda, Mr. Mahajan, Mr. Vadher, Mr. Nambiar, Mr. Muralidhran, Mr. Bhagirath for their whole-hearted support.

I acknowledge my teachers especially Prof. R. Ramesh, Dr. Raghvan Rangrajan, Dr. Bhas Bapat, Dr. Namit Mahajan, Dr. A. Chakraborty, Prof. Vinod Prakash, Prof. Ranjana Prakash and Prof. H. Prakash for building the base of scientific culture. I feel privileged of being their student.

Undoubtedly, a significant period of my PhD tenure was spent at Mount Abu for observations. I cherished every moment spent there. I take this opportunity to express my heartfelt thanks to all the staff members at the Observatory for providing a supportive ambience. In particular, I am grateful to Mr. Jinesh K. Jain and Mr. G. S. Rajpurohit who taught me how to handle the instruments with utmost care and to carry out the observations. My thanks are due to Mr. Rajesh Shah and Mr. Mathur for their continuous and unconditional technical supports whenever needed. I also thank engineering trainees in PRL especially Nishant, Pavan, Bhavin, Tanmay, Twinkle and Nishta for their help in observations.

It is a pleasure to express my gratitude to Mr. & Mrs. J. K. Jain and Mr. & Mrs. Rajpurohit as well as their family for their affection and hospitality. I always recall the days at Abu with happiness for having the nice company of Chinki, the younger daughter of Jinesh Ji.

In the conducive atmosphere of the student community, life at hostel is always a memorable experience for all. I take this opportunity to thank all Research Scholars, Post Doctoral Fellows, Project Associates and trainees from both Navrangpura and Thaltej hostels, who were important to me in many ways. Listing all the names is impossible which demands apology. However, collective and individual acknowledgements are passed on to my colleagues cum friends: Das Bhaiya, Blesson Da, Lokesh Ji, Tapas Da, Ashish, Vishal Bhai, Susanta, Arun, Tanmoy, Priyanka, Anjali Varun, Vaibhav and Gaurava. I have learnt many things in the form of valuable discussions in either A & A students discussion sessions or individually. I especially convey my heartiest thanks to Priyanka, Susanta, Tapas, Tanmoy and Sonam for critically reading this thesis. I am always grateful to my batchmates cum collegues Siddhartha, Abhishek, Koushik, Amrendra, Arun, Susanta, Vema, Vivek, Parul, Chinmay and Yogita for their affections and supports at several stages of my research. When talking about the friends I can never deny the contributions of Arun, my friend and classmate from college days for his encouragement and unconditional mental support throughout my research period. This section would re-

main incomplete if I do not mention about Vimal, Thakur, Jha Ji, Pankaj Ji, Vinni bhai, Arko, Diganta, Zulfikar, Prajakta, Yashpal, Naveen, Nandi, Girish (Senior + Junior), Tomar, Rajlaxmi, Rishi, Gulab, Mono, Arun Pandey, Lalit, Dipti, Deepak, Mondal, Tinkal, and many more. I always enjoyed their company during parties, hostel festivals and Volleyball/Badminton matches.

I would like to convey my sincere thanks to Nishtha Madam, Mrs. Uma Desai, Mrs. Pragya Pandey, Mr. Indrabadan and other library staff for providing prompt help in my library works. Further, I would like to express my thanks to whole PRL staff for their support. I express my special regards to Mr B. M. Joshi, Mr. Senthil Babu, Pradeep Ji, Kayur Bhai, Mr. Dilip Gandhi and Parul Madam for their ever-willingly help. I also thank the staffs from computer centre (Mr. Jigar, Mr. Alok, Mr. Tejas, and Mr. Hitendra), PRL for providing the necessary computational facilities. My thanks are also due to PRL medical and canteen staffs for their services.

Behind any scientific work, support from the host organization and funding agencies is inevitable. In this regard, I acknowledge Physical Research Laboratory (PRL) for providing me an opportunity to be a part of it and conduct this research work. PRL provided its full support in terms of science, culture and livelihood. I also acknowledge the Black-hole Universe Consortium and International Astronomical Union (IAU) as well as Prof. Stefan Wagner (LSW, Heidelberg, Germany) and Prof. Luigi Foschini (Osservatorio de Milano, Italy) to extend financial support towards my scientific tours and to present my work.

I acknowledge different data archival resources and observatories to provide permission to use their data. In this list, I also acknowledge NED, HEASARC, Swift, Fermi, Planck, WISE, SIMBAD, MOJAVE, Steward Observatory, University of Arizona, SMARTS/Fermi group at Yale University, Blazar group at Boston University, and CRTS. It would have never been possible to lead to the scientific outcomes presented in this thesis without the direct or indirect support offered. I am also very grateful to the NASA/ADS service and google search engine for providing me needful and prompt informations about the subject.

The last but not the least, I wish to express my sincere regards and offer deepest gratitude to my parents who are the sole motivation of each and every achievement made by me during the course of research. In spite of me being their elder son, they always tried to keep me free of all the social responsibilities including family issues. I was always supported morally, financially and emotionally by other family members: Tau Ji, Dr. Anirudhh Sharma (uncle), Aunty Ji, Bua Ji, Amma Ji, Bhaiyya Ji, Sudhir, Vikal, Pawan, Prabhat, Praveen, Monu and all others. No doubt, this thesis would has never seen the daylight without their unfailing inspiration, kind support and remarkable patience. I am always owed to the continuous moral boosting by my friends Pawan, Kshitiz and Manish during this period. This acknowledgement is incomplete if I do not mention the moral support by Purnima Yadav. She supported me even in the situations when I was completely broken morally and emotionally. Without her continuous love and mental support, this dream would have never come true. In this flow, I wish to mention my little angels Shraddha, Namrata, Priya, Riya, Anshu and Sanju. Their memories have always kept me dynamic, joyous and socially connected. I also pay tribute to my grand parents for their effort to flourish the educational environments in the family.

Sunil Chandra
23 October, 2013

ABSTRACT

Active Galactic Nuclei (AGNs) are centers of galaxy, very compact in size but emitting huge energy, sometimes more than hundred times the total energy emitted by a normal galaxy. The mechanism of energy generation is understood to be accretion of mater onto a supermassive (10^6 to $10^9 M_\odot$ mass) black hole through accretion disk. Most of them have outflows (jets) of magnetized plasma moving at relativistic speed perpendicular to the disk. In a sub-class of source, emission is dominated by the non-thermal emission from the jet, directed at a small angle to the line of sight, ranging from radio to $\gamma-$rays. Such sources are known as blazars. However, the exact structure of the jet, its origin, acceleration, collimation and the physical mechanisms behind such huge energy output are not clearly understood. The central energy source is too compact to be resolvable by any present day, and even any new facility in near future. However, the variability in flux and polarization, the defining property of blazars, provides one of the important tools to probe the inner regions of AGNs.

In the present work we have used variability in multi-frequency flux and optical polarization for several blazars. Optical photometric and polarimetry obervations for more than 7 years carried out from Mt Abu Observatory as well as data at UV, X-ray from Swift and high energy $\gamma-$ray from Fermi space observatory are used to explore short and long-term variations and their behaviour at various wavelengths. Shortest time scale variation at a particular wavelength provides information about the size of the emission region. Study of polarization is used to understand the extent of magnetic fields in the emission region.

The intra- and inter-night variations in blazar S5 716+714 are used to determine fastest rate of variation and size of the emission region which is very compact ($\approx 10^{15}$cm). Long term study of the source is used to determine duty cycle of variation which is very high (84%). Bluer when brighter nature of flux variations indicates to be shock-in-jet model describing the generation of emission. The work also describes the statistical study on the nature of polarization in blazars and its application in classifying the same. We propose source CGRaBS J0211+1051 to be an LBL based on this and confirm the status by carrying out multiwavelngth study for spectral energy distribution (SED). A detailed study of source PKS 1510-089 using multiwavelength data is made and reasons behind the generation of several outbursts and flares is discussed.

The thesis also reports several statistical methods developed/used in the study as well as development of a pipeline to analyse large amount of optical data obtained from Mt Abu Observatory over tens of years. It makes it possible to reduce and analyse such large amount of data in short span of time.

Keywords: BL Lacertae objects : individual (S5 0716+714, CGRaBS J0211+1051); Flat spectrum quasars : individual (PKS 1510-089); galaxies: active; multi-wavelength: (photometry, polarimetry)

LIST OF PUBLICATIONS

0.1 Refreed Journals

1. **"Rapid optical variability in blazar S5 0716+71 During 2010 March"**

   S. Chandra, K. S. Baliyan, S. Ganesh and U.C. Joshi.

   Astrophysical Journal, **731**, 118 (2011)

2. **"Optical polarimetry of the blazars CGRABsJ0211+1051 from Mt. Abu Infrared Observatory"**

   S. Chandra, K. S. Baliyan, S. Ganesh and U.C. Joshi

   Astrophysical Journal, **749**, 92 (2012)

3. **"Precursor flares in OJ 287"**

   Pihajoki, P. and 21 others,

   Astrophysical Journal, **746**, 5 (2013)

4. **"Understanding the nature of blazars CGRABsJ0211+1051"**

   S. Chandra, K. S. Baliyan, L. Foschini and S. Ganesh

   Astrophysical Journal, 2013, **Submitted**.

5. **"Variability study of bright blazars using Mt. Abu Infrared Observatory"**

   S. Chandra, K. S. Baliyan, S. Ganesh

   MNRAS, 2013, **In prepration**.

0.2 Astronomical Telegrams

1. **"Photopolarimetry of Blazar 3c454.3 from MIRO"**
   Baliyan, K.S, Ganesh,S., Chandra, Sunil and Joshi, U.C.
   Astronomical Telegram # 2345 (Pub. Date 12/2009).

2. **"Detection of high and variable optical polarization in Blazar S5 0716+71 from MIRO"**
   Baliyan, K.S, Ganesh,S., Chandra, Sunil and Joshi, U.C.
   Astronomical Telegram # 2347 (12/2009).

3. **"High optical polarization detected in blazar CGRaBS J0211+1051 from MIRO"**
   Chandra, Sunil; Ganesh, S.; Baliyan, K. S.; Joshi, U. C.
   Astronomical Telegram # 3136 (01/2011).

4. **"NIR observations of S5 0716+71 from MIRO"**
   Chandra, Sunil.;Baliyan, K. S.; Mathew, B.
   Astronomical Telegram # 3704 (10/2011).

5. **"CCD Monitoring of Blazar OJ287 from MIRO"**
   Chandra, Sunil; Ganesh, Shashikiran; Baliyan, K. S.
   Astronomical Telegram # 3704 (04/2012).

6. **"GRB090426: Observation for optical counterpart from MIRO"**
   Chandra, Sunil; Ganesh, Shashikiran; Baliyan, K. S.
   GCN CIRCULAR # 9258 (26/042009 16:36:42 GMT).

Contents

List of Figures

List of Tables

Chapter 1

Introduction

1.1 Active Galactic Nuclei

Active Galactic Nuclei (AGN), are the centres of galaxies which show unusual activities at their nucleus. These central regions of active galaxies emit huge amount of radiation ($\sim 1 \times 10^{48-51} erg/s$) which is approximately 10^2 to 10^3 times the total energy output of a normal galaxy. The sizes of the AGN are very compact (V $\leq pc^3$). The huge energy output from these compact objects makes them observable even located at very large distances and hence underlines their utility as cosmological candles. In the present time which is known as era of Swift, Fermi, VERITAS, SDSS and other facilities equipped with modern technological instruments, the AGN are observed lying at the other end of observable universe at almost all the frequencies. They emit broad continuum emission across the spectrum which follows a power law, indicating to its non-thermal nature. The continuum emission from a normal galaxy, on the other hand, is thermal black body radiation from all constituent stars. The huge non-thermal broad band continuum emission from a tiny volume [$\ll pc^3$] of AGN cannot be explained using the usual thermonuclear processes at work in stellar systems. The continuum emission from most of the AGN are highly polarized. In addition to non-thermal continuum, optical spectroscopy of AGN reveal that majority of these sources exhibit emission dominant spectra unlike the absorption dominant stellar spectra. The emission lines observed

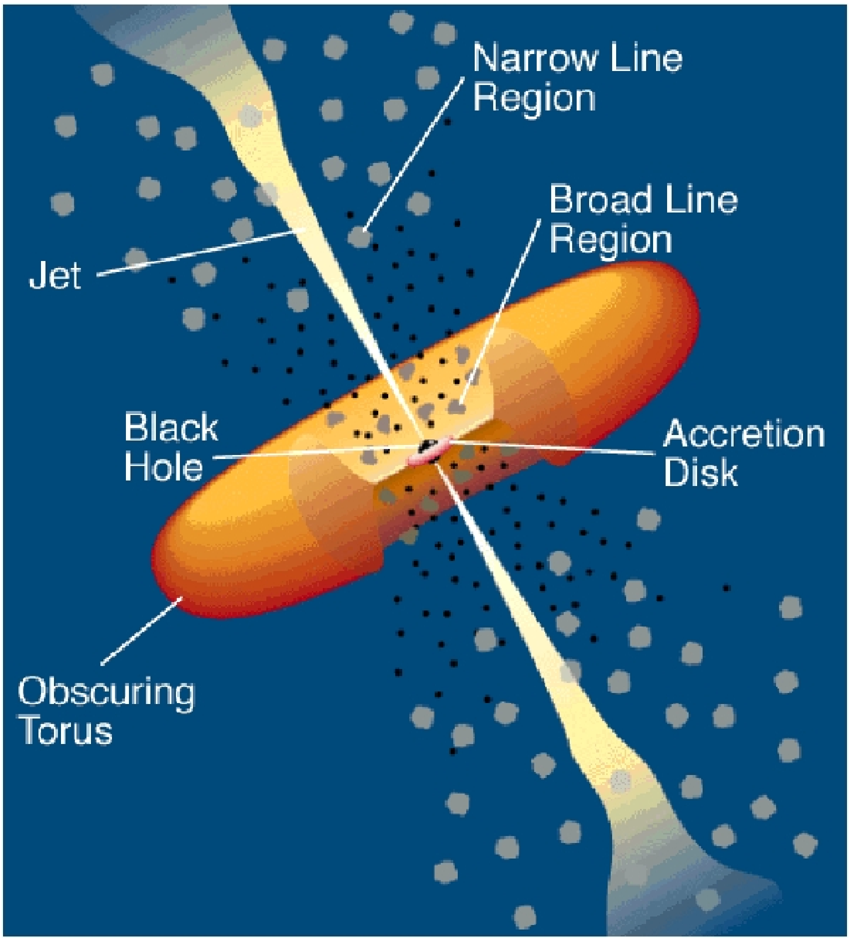

Figure 1.1 The model to explain the emission in active galactic nuclei (AGN) by Blandford and Rees (1992).

are mostly strong and broadend. The large width of these emission lines, if interpreted because of normal line broadening hypothesis, is indicative of highly dynamic surrounding of these centers, indicating to very high velocities. The question arises, what fuels such a high energy output from these sources. Many hypotheses were putforth and Fig.- 1.1 shows the schematic of a well accepted model of Active Galactic Nuclei proposed by Blandford and Rees (1992) in order to explain the observed properties of AGN.

According to this model a supermassive black-hole [M $\sim$ 10^{6-9} $M_{\odot}$] is sitting at the centers of active galaxies and mass is being accreted onto it. The gravitational potential energy of accreted material is partly converted to radiation. The accretion process is explained in many text books, such as

Frank et al. (2002) and Longair (1994). A twin jet of relativistic plasma is emanated from very close to the central part of these systems which provides the means for pumping the part of material and radiation into the space. A fast moving highly ionized hot cloud of molecular gases swirls around the central engine. This extremely fast moving, highly ionized, molecular gas cloud is the host of emission of broad lines in optical spectra and hence is known as Broad Line Region (BLR). Lowly ionized slowly moving component swirling around this system, lying at larger distances, is known as Narrow Line Region(NLRs). The whole system is surrounded by a cold envelope of dust and gas, known as torus (Urry and Padovani, 1995; Blandford and Königl, 1979b). The following section summarizes the energy extraction mechanism at work in AGN in brief.

1.2 Energy extraction in AGN through accretion

The following equation give a general expression of the energy extraction through the accretion phenomenon.

$$\frac{GM(m_p + m_e)}{r^2} \geq \frac{L\sigma_T}{4\pi r^2 c} \tag{1.1}$$

where the left part represents the effective gravitational pull on individual electron-proton pair because of central massive object (Mass $\sim$ M). The direction of this force is always towards the central object. The expression on the right hand side of above equation represents the radiation pressure working on each pair in outward direction i.e. opposing the inward motion. Therefore in order for accretion to take place, the gravitational pull should always be greater than the radiation pressure. The radiation pressure on individual pairs is directly proportional to the luminosity of the central object. Therefore there will be a limiting luminosity for central object with mass (M) at which the accretion will vanish. This limiting luminosity is known as Eddington luminosity (L_{edd}) and is given by.

$$L_{edd} = \frac{4\pi G M m_p c}{\sigma_T} \equiv 1.3 \times 10^{38} (M/M_\odot) ergs^{-1} \tag{1.2}$$

Above equation clearly states that the Eddington luminosity (L_{edd}) is only a function of mass of the central object. For the accretion powered objects the Eddington luminosity puts a limit on the steady accretion rate, $\dot{M}$ (gm s^{-1}). If part of the kinetic energy of in-falling material is given up as radiation close to the event horizon ($R_g \sim \frac{2GM}{c^2}$), the theoretical observable limit of central black hole, then the resulting accretion luminosity (L_{acc}) is given by

$$L_{acc} = \eta \frac{2GM\dot{M}}{R_G} = \eta \dot{M} c^2 \tag{1.3}$$

where η is the efficiency of accretion which quantifies the conversion of gravitational potential energy into radiation. In the case of accretion onto massive black holes, a reasonable value of $\eta \sim 0.1$ can be adopted while the thermonuclear process occurring in stellar systems has an efficiency (η) ~ 0.007) only.

1.3 Classification of Active Galactic Nuclei (AGN)

Based on their observational properties, Active Galactic Nuclei (AGN) are classified in several categories. In the following broad classification schemes are discussed in brief.

1.3.1 Based on radio properties

Depending on the radio observations of AGN they are broadly classified in two sub categories 1.) Radio Loud, and 2.) Radio Quiet. The radio loud AGN emit significantly at radio frequencies in comparison to optical. These are the sources discovered in radio surveys. Their morphology is often described broadly in terms of two components, 'extended' (spatially resolved) and 'compact' (unresolved at $\sim$ 1" resolution), which have different spectral characteristics, although the synchrotron processes seems to be at work in both the components. The position of compact component often coincides with the optical source or center of galaxy. The major difference between two components is that the extended component is optically thin for it's own radio synchrotron emission, whereas this is not true for the compact sources.

The extended radio structures are further classified into two luminosity classes (Fanaroff and Riley, 1974). The class I (FR-I) structures are relatively weaker radio sources brighter at centers with decreasing surface brightness towards edges. In contrast the class -II (FR-II) are overall radio bright sources. These sources are limb brightened and often show regions of enhanced emission either at the edge of the structure or embedded within the structure. According to Bridle and Perley (1984) the transition luminosity between both the classes is $L_\nu(1.4GHz) = 10^{32}$ erg $cm^{-1}s^{-1}Hz^{-1}$. The characteristics of compact sources are entirely different from the extended sources. The observing facility with the best spatial resolution at VLBI provides only an upper limit to the size of the compact sources, typically no better than $\sim$ 0.01 pc. The radio spectra of compact sources are flat ($\alpha \leq 0.5$) whereas the extended structures have steep radio spectra. In addition to the compact and extended components the radio sources often show features known as jets, which are extended linear structures (Bridle and Perley, 1984).

The radio quiet AGN are mainly discovered by the survey at optical frequencies. The UV-excess technique was the first to be used to discover such AGN (Ryle and Sandage, 1964). The long-wavelength SEDs of optically selected or radio quiet AGN are markedly different from those of radio-selected ones in that the radio emission (relative to UV-Opt-IR) is typically around 100 times lower.

1.3.2 Based on general physical properties

The Active Galactic Nuclei (AGN) are generally classified on the basis of the similarities and fundamental differences between the observed properties at various frequencies. Following are the popular classification based on this theme.

Seyfert Galaxies

The seyfert galaxies or seyferts are the low power AGN, generally radio-quiet and most often spiral in nature. The seyferts were first defined on morphological basis by Seyfert (1943) having high surface brightness nuclei and are identified by the presence of strong, high ionization emission lines. While studying the spectra of Seyferts Khachikian and Weedman (1974) realized two classes of Seyferts distinguished by the presence or absence of broad permitted emission lines. The first subclass of Seyferts are known as type-I and are characterized by the presence of narrow emission lines with equivalent width upto several hundred Km/second indicating presence of low-density (electron density, $n_e \approx 10^3 - 10^6 cm^{-3}$) ionized gas, and broad emission lines (with equivalent width upto several tens of thousands Km/second), characteristics of high density (electron density, $n_e \approx 10^9 cm^{-3}$ or higher) ionized gas. The broad line features are only seen in permitted lines. Seyfert type-II differs from type-I in that the only narrow lines are present in their spectra.

Quasars

Quasars or quasi-stellar objects are one of the brightest source in the universe. Around 5-10% of the quasars are radio-loud in nature. These are distinguished from Seyferts in that they are spatially resolved [smaller than $7''$]. Most of them have ellipticals as host galaxy. Many of them are surrounded by a low surface brightness halo (sometimes called as 'quasar fuzz') which appears to be the starlight from the host galaxies. Some quasars show the jet like morphology even in optical band [e.g., 3C273]. The quasar optical spectra is different from the Seyferts spectra by 1.) The stellar absorption features are extremely weak if present and 2.) the narrow lines are weaker in comparison to the broad lines than is the case in Seyfert galaxies. Since these are very bright, quasars are observed at very large distances. The most distant quasar is observed at a redshift which is equivalent to the time when the universe was only few hundred million years old.

Radio Galaxies

The radio galaxies emit huge emission at radio frequencies. They are known to show spatially extended structures containing core and two lobes. They exhibit structures ranging upto Mega-parsec distances. Many of them have shown the relativistic motion of plasma in the jet. They are classified into two classes FR-I and FR-II which are already discussed in section 1.3.1. Mostly these are ellipticals in nature. The optical counterpart of these galaxies are point like central bright spot. The optical spectra of radio galaxies show two subclasses: broad line radio galaxy (BLRG) and narrow line radio galaxy (NLRG) analogous to the Seyferts-I and Seyferts-II.

LINERs

A low luminosity class of low-ionization nuclear emission-line region galaxies (LINERs) was first identified by Heckman et al. (1980). Spectroscopically they resemble the Seyfert type-II galaxies except that these have low-ionization lines, e.g., [O I] $\lambda6300$ and [N II] $\lambda6548, 6583$ which are relatively stronger. Peterson (1997) describe these sources in great detail.

Blazars: BL Lacs & FSRQs

The blazars form the set of sources having featureless continuum emission, which is dominantly non-thermal. These sources are seen at a very small angle to the relativistic jet axis. They constitute flat spectrum quasars (FSRQs) and BL Lac objects. Out of all AGN, blazars show most violent variability at all wavelengths, ranging from radio to γ-rays. They show amplitude of variation in brightness which is often large (e.g., $\Delta m \geq$0.5 mag in visible band) even at short (intranight) time scale. In addition to such rapid variations in total flux, the emission is highly polarized ($\Delta p \geq 3\%$). The detailed discussions about the general properties of blazars is given in section 5.

Narrow Line Seyfert-1 Galaxies : NLS1

The Narrow Line Seyfert-1 Galaxies were first systematically described by Osterbrock and Pogge (1985). Their subsequent discovery in large numbers in soft X-ray surveys and the recognition that they possess optical spectra very different from other AGN made them very interesting to study. The nuclear spectra of these galaxies are generally like those of Seyfert 1s (strong Fe II, [O III] relatively weak compared to the Balmer), but with the width much narrower. The optical spectroscopic studies present following criteria for AGN to be categorized as NLS1 galaxy (Pogge et al., 2011).

- Narrow permitted lines only slightly broader than the forbidden lines.
- [O III] / H_β <3, but exceptions are allowed if strong [Fe VII] and [Fe X] are present, unlike what is seen in Seyfert 2s.
- FWHM (H_β) <2000 km s^{-1}.

The first two criteria were introduced in (Osterbrock and Pogge, 1985) whereas the third one is introduced later by Goodrich (1989). Relativistic jet is detected at least in one, NLS1 PMN 0948+0022, case using γ-ray energy Fermi observations (Abdo et al., 2009; Foschini et al., 2009, 2011a). There are significant fraction of total number of NLS1s [7%] which are radio loud (Komossa et al., 2006). The detection of radio structures in these objects makes them even more interesting. Based on present understanding of these objects, NLS1s are thought to form the bridge between galactic micro-quasars and AGN.

1.4 Polarization property of AGN

The detection of high polarization in the radio-galaxies and AGN confirmed the synchrotron nature of emission from these sources, radiated by relativistic electrons moving in magnetic field. This emission is non-thermal in nature. It has, therefore, played a pivotal role in the study of AGN and radio galaxies, in addition to other astronomical sources where it is contributed mostly by the scattering. Polarization measurements provide information which is not available from photometry and spectroscopy, such as magnetic field configuration. In AGN polarization helps diagnose several properties like the physical mechanisms behind energy generation and morphology of the object. The jet emission in AGN is mainly synchrotron emission and expected to be highly polarized, at least in jet dominated AGN, such as blazars as described above. The synchrotron emission is intrinsically highly polarized (≥ 60 %) depending upon the ordering of the magnetic field. The emission from other components in AGN namely disk, torus, BLR and host galaxy are thermal in nature and hence dilutes the intrinsic polarization from nuclear source. Even in blazars, extent of polarization will change depending upon the strength and alignment of magnetic field and orientation of the relativistic jet with respect to line of sight. The polarization properties are derived from stokes parameters, defined as,

$$m_l = \frac{\sqrt{Q^2 + U^2}}{I} \tag{1.4}$$

$$m_c = \frac{V}{I} \tag{1.5}$$

$$m_t = \frac{\sqrt{Q^2 + U^2 + V^2}}{I} \tag{1.6}$$

$$\chi = \frac{1}{2} tan^{-1} \frac{U}{Q} \tag{1.7}$$

where I, Q, U and V are known as stokes parameters. m_l, m_c, m_t and χ are termed as fractional linear polarization, fractional circular polarization, fractional polarization and position angle of the plane of polarization respectively.

Most of the synchrotron sources are linearly polarized to some degree ranging from 3-60 % depending on the ordering of magnetic field. The typical circular polarization in AGN is usually small (≤ 0.1 %). Therefore, the measurement of fractional linear polarization and position angle are often used to describe the polarization properties of the jet dominated AGN. Now onwards through this dissertation we will use degree of polarization (DP) for percentage of linear polarization unless otherwise specified. A detailed review on the polarization properties of AGN is given by Angel and Stockman (1980). They discuss various issues related to the polarization in AGN and even sub-classify BL Lacs based on polarization. This issue has been addressed by several other researchers (Andruchow et al., 2005; Fan et al., 1997). In general, the BL Lac objects show decrease in fractional linear polarization or degree of polarization (DP) from LBLs to HBLs. The FSRQs show simillar DP as LBLs. (Jannuzi et al., 1993; Fan et al., 1997; Andruchow et al., 2005; Ikejiri et al., 2009) reported the high DP as the characteristics of FSRQs and LBLs. Recently Heidt and Nilsson (2011) have discovered only a marginal difference in polarization behaviour of LBLs and HBLs as inferred from their sample of blazar candidates taken from sloan digital sky survey (SDSS).

1.5 Enigmatic Blazars

The term "Blazars" was coined by Edward A. Spiegel during a banquet speech at 1978 Pittsburg meeting on BL Lacs to represent Flat Spectrum Quasars (FSRQs) and BL Lac objects (Bl LAc + QuaSARS). They have been observed to show following properties:

- Broad band nonthermal continuum emission ranging from radio to high energy γ-rays
- Continuum featureless or with very weak emission lines
- Violent, high amplitude variability in flux over time scales ranging from few years down to few hours
- High and variable polarization at optical and radio frequencies
- Observed at low angle to the relativistic jet giving rise to Doppler boosting
- Superluminal velocity

Blazars show bimodality in broad band spectral energy distributions (SEDs). The first component of SED peaks at lower energies i.e. somewhere in sub-mm to soft X-rays energy domain whereas the second component peaks in MeV - GeV/TeV energies. There are many blazars observed at extreme γ-ray energies (TeV) using ground based cherenkov telescopes (e.g., MAGIC (Flix and MAGIC Collaboration, 2004), HESS(Kohnle, 1999), VARITAS (Weekes et al., 1997), TACTIC (Koul et al., 1993)). The detection of very high energy (VHE) emission from these objects throws a challenge for physical processes responsible for energizing particles to produce such energetic emission.

1.5.1 Spectral Energy Distribution of Blazars

As already pointed out, the SED of blazars show two humps one peaking at lower energies [sub-mm to UV] and other peaking at high energies [MeV-GeV]. The bimodality of blazar SED implies two different physical processes responsible for the emission. The low energy component of SED is mainly emitted by synchrotron processes in the relativistic jet where relativistic electrons spiral in magnetic field. The high polarization at Optical and Radio frequencies observed in blazars confirm it's synchrotron origin. However, the physical process responsible for high energy component of blazar SED is still not well understood. Depending on the nature of the jet material (leptons or hadrons), two different emission models have been proposed during last decade, namely (1) Hadronic model, and (2) Leptonic model.

Hadronic models

The hadronic model was first proposed by Mannheim and Biermann (1989) to explain the high energy emission (γ-ray) in blazars. According to this model, both relativistic electron and proton population exist in the emitting magnetized "blob" which itself moves with relativistic speed along the jet axis. The relativistic electrons, co-moving with the protons, contribute the low energy component of SED through synchrotron processes in the jet, while the high energy emission is generated because of photo-meson production, proton and muon synchrotron radiation, and subsequent synchrotron-pair cascading in the highly magnetized environment. For such reactions to take place, the protons are accelerated to high energeis, $E_p \geq 10^{19}$ eV. Either the external (i.e. from an accretion disk and/or torus) or internal photon fields (i.e. produced by synchrotron radiation from the co-accelerated electrons) serve as the target for photo-pion production. The hadronic origin of high energy emission in blazars can be verified by the detection of high energy neutrinos generated in decay chains of mesons during photoproduction interactions (Learned and Mannheim, 2000). Mücke and Protheroe (2001); Mücke et al. (2003); Beall and Bednarek (1999); Böttcher (2007) have given a good discussion of hadronic model and its application to explain the observed blazars SED. Generally a single isotropic region is thought to be responsible for blazar emission where most of the dissipation occurs. The electrons(e^-) and protons(p^+) are co-accelerated at the same site.

Due to the pitch-angle scattering, resulting particle distribution is expected to be quasi-isotropic. The relativistic protons are injected instantaneously into the highly magnetized emission region. The loss of energy takes place due to proton-photon interactions (meson production and Bethe-Heitler pair production), proton synchrotron radiation and adiabatic expansion. The pion photoproduction and Bethe-Heitler pair-production are shown in Figure 1.4. The top diagram sketches the charged pian production while the lower one shows the neutral pion production. The neutral pions are unstable and produce the γ-ray photons when they decay. The e^- and e^+ produced in pion photoproduction processes may be annihilated and produce γ-rays as end product. In the third diagram the Bethe-Heitler pair production process is shown. Here energetic protons give rise to the (e^-, e^+) pairs after interacting with the low energy seed photons. These pairs may produce γ-Rays after annihilation. The (e^-, e^+) may also give rise to synchrotron photons which again suffer the pair production and feed the cascade development.

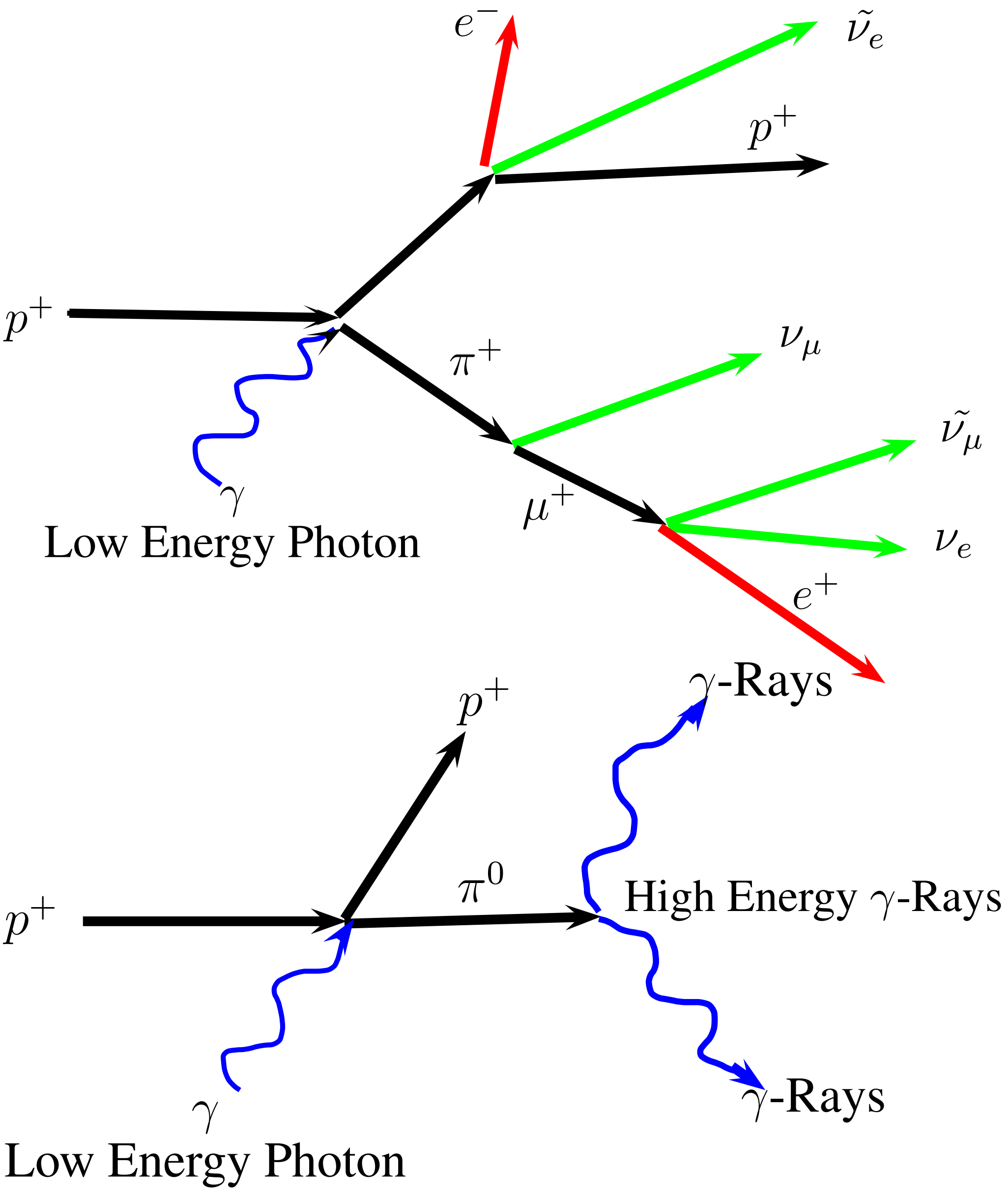

Figure 1.2 Pion Photoproduction.

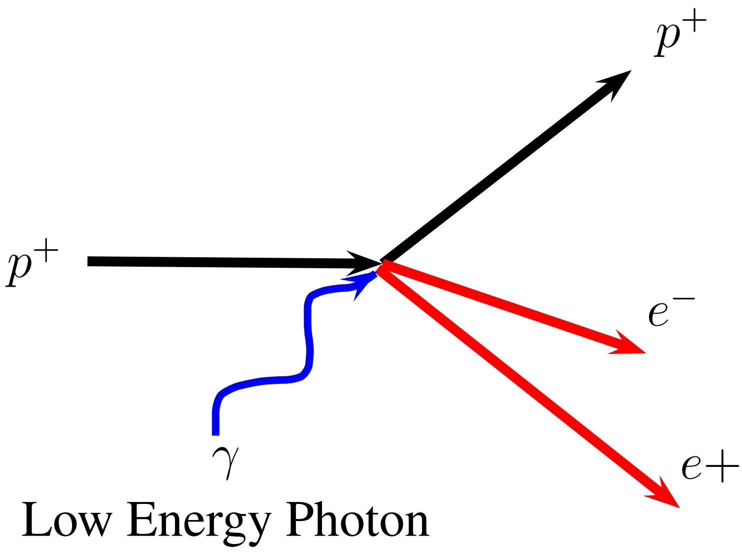

Figure 1.3 Bethe-Heither pair-production.

Leptonic models

In the leptonic models of blazar emission, the jet is composed of relativistic electrons & positrons. The protons are relatively cool and move slowly, therefore they do not play very important role in dissipation. The low energy component is emitted because of synchrotron processes in the magnetized jet. While, the high frequency component of SED is generated because of Inverse Compton scattering of low energy seed photons. The source of low energy seed photons decides the nature of scattering and the dominance of 2nd component. If the synchrotron photons are up-scattered by the same population of relativistic e^-/e^+, the process is known as Self Synchrotron Comptonization (SSC) (Marscher and Gear, 1985b; Ghisellini et al., 1985; Maraschi et al., 1992; Bloom and Marscher, 1996). However If the scattered seed photons are external to the emission region, the process is termed as External Comptonization (EC) (Dermer et al., 1992; Sikora et al., 2009; Agudo et al., 2011). The major possible sources of external seed photons are accretion disk (Dermer et al., 1992; Dermer and Schlickeiser, 1993), reprocessed UV, Optical radiation from circumnuclear material (Sikora et al., 1994; Blandford and Levinson, 1995; Ghisellini and Madau, 1996; Dermer et al., 1997, e.g., BLR) and infrared emission from dusty torus (Błażejowski et al., 2000) or synchrotron emission from other region of jet itself (Georganopoulos and Kazanas, 2003a,b; Ghisellini and Tavecchio, 2008). The dominant contribution of seed photons of various origins define the characteristics of SED. In many cases the single SSC is enough to explain the observed SEDs while in few cases only EC is sufficient. However, in few cases a combination of SSC & EC is required to explain the SEDs. The ratio of synchrotron energy density to the external contributions decides the dominant process i.e. SSC or EC. Therefore, the study of SED can reveal the governing processes behind blazars emission or in general jet emission in AGN. The modelling of SEDs require a simultaneous, multi-wavelength study of blazar emission over longest possible duration. The present time appears to be a golden era for such studies as we have coverage of almost all the wavebands from Radio to high energy γ-rays with sufficient resolutions involving observations from ground and space borne facilities.

1.5.2 Blazar sequence

BL Lac objects are well known sub-class of blazars, named after their progenitor BL Lacertae, which was originally classified as a blue star and found to have a radio counterpart VRO 42.22.01 (Schmitt, 1968). The observational property that makes BL Lacs different from other AGN are their featureless nonthermal continuum and strong variability. The lack of emission lines in the BL Lac spectra is debated by the community since the discovery of these objects. The most convincing and well accepted explanation was proposed by Blandford and Rees (1978). According to this, blazars are a class of AGN which are seen almost along the relativistic jet of plasma emanated from very close to the central engine, perpendicular to the accretion disk. Therefore the emission is highly boosted and hence any line emission, if present, will be swept out. The BL Lac objects are supposed to possess a limiting boosting. The boosting in a relativistic jet is quantified by Doppler boosting factor (δ) and given by

$$\delta = \frac{1}{\Gamma[1 - \beta cos(\theta)]} \tag{1.8}$$

where β is velocity in units of c, speed of light, and θ is the angle between jet direction and line of sight. The Γ is the bulk Lorentz factor, given by $\Gamma = \frac{1}{\sqrt{1-\beta^2}}$. However, some BL Lac objects are observed to show weak lines in their spectra at high resolution when in low brightness state (Maesano et al., 1997).

Based on the wavebands at which the BL Lac objects are discovered these are sub-classified in two categories namely, RBL and XBL, the radio selected and x-ray selected BL Lacs, respectively. Based on SED peaks, BL Lacs are also sub-categorized in low energy peaked BL Lac objects (LBLs), Intermediate energy peaked BL Lac objects (IBLs) and high energy peaked BL Lac objects (HBLs). If the low frequency component of SED peaks at low frequency (ν) $\leq 1 \times 10^1 4Hz$ the BL Lac is termed as LBL and when it peaks beyond $1 \times 10^1 6Hz$ the BL Lac objects are known as HBLs. However, if the peak lies somewhere in between these two limits of frequency, BL Lac is known as IBLs. The terms LBL, HBL and RBL, XBL are used interchangeably in literature. Flat Spectrum Quasars (FSRQs), on the other hand, share majority of the properties with the BL Lac Objects, except that FSRQ have flat radio spectra i.e. $\alpha > 0.5$, with $F_\nu \propto \nu^{-\alpha}$ and detectable emission lines in their spectra. The presence of weak lines indicate the significant contribution of emission from accretion disk and line emitting regions (BLR and NLR). The degree of polarization (DP) of FSRQs may range from few degree to few tens of degrees, just like LBLs. Based on optical polarization FSRQs themselves are sub-classified as high polarization quasars (HPQ) and low polarization quasars (LPQ)(Abdo et al., 2010a). The peak frequency of low energy component of SED lies at lower energies as compared to those for LBLs. Therefore, peak frequency of synchrotron component increases from FSRQ towards LBL, IBL and HBL.

In addition to the difference in frequencies at which synchrotron component peaks in various sub-classes of blazars, these sources show other distinct properties as well which suggest existence of a sequence in blazars in which several properties differ significantly from one sub-class to other. According to this, the total luminosity, jet power, dominance of high energy IC component decreases in the sequence FSRQ $> LBL > IBL > HBL$. In general, FSRQs & LBLs show high Compton Dominance (CD) which is defined as the ratio of peak Compton (L_C) luminosity to the peak synchrotron (L_{Sy}) luminosity, while both the luminosities are comparable in HBLs. Also, degree of polarization shows a tendency to decrease from FSRQ to HBL. (Fossati et al., 1998) has presented a nice discussion about this trend which was verified by Ghisellini et al. (1998) using canonical SED modelling. High energy IC component is mostly contributed by scattering of external photons in FSRQs, while its strength decreases towards HBLs which is explained mostly based on the synchrotron self Compton models. Such difference in properties in FSRQ, LBL and HBLs prompted people to propose a sequence of blazars. However, it has been felt that this is also becoming only of historical importance with more and more sources being detected with properties which fall in between those of FSRQ, LBL, IBL and HBL.

1.6 Variability in blazars

As already pointed out in last section that the blazars are one of the most violently variable objects among the AGN. These show such variability over the complete spectrum ad at several time scales, ranging from years, to months, to days and hours. The flux variations corresponding to a timescale of few hours or less are known as microvariations or Intraday/Intranight variability whereas the same corresponding to the larger timescales are referred as Internight/Interday variability. These also show large flares and outbursts lasting several days to years. It is an important property which helps discriminate models of emission and puts upper limit to the size of emission regions. The variability was first introduced to investigate the physical processes in these objects by Matthews and Sandage (1963), just after the discovery of quasars. They had derived the size of emission region based to shortest time scale of variation and light travel time argument [causality argument]. The causality argument gives the upper limit of the size of emission region using following equations.

$$R \leq \frac{\delta}{1+z} c\Delta_t \tag{1.9}$$

where the δ and z refer to the Doppler boosting factor and redshift of the object whereas δ_t is the variability timescale. This variability timescale is defined as the minimum time required for the significant change in flux. The quantitative definition of this observed parameter depends on the frequency of observations. Matthews and Sandage (1963) had also found that the brightness of the BL Lac object 3C48 changes by 0.04 mag in V band in 15 minutes, but their result was not taken seriously because of large instrumental errors. Soon after this many other observations reported significant flux variability over diverse timescales. For examples, in optical waveband, the detection of intraday variation in 3c279 (Oke, 1967), identification of radio source VRO 42.22.01 as variable star and later as prototype of a AGN class BL Lac (Hoffmeister et al., 1992; Schmitt, 1968), the day scale optical variability in AP Lib which was later identified as BL Lac objects based on fast variability (Miller, 1975) and many other blazars for variability with timescales of minutes, hours to several days (Racine, 1970; Bertaud et al., 1973; Grauer, 1984) were reported. IR flux variations were also reported almost during same time by Epstein et al. (1972); Rieke et al. (1977). The early radio observations of couple blazars at cm & mm frequencies also provide the evidence of significant variability (Sholomitskii, 1965; Dent, 1965; Kinman and Conklin, 1971; Hackney et al., 1972; Andrews et al., 1974). These authors had witnessed the probable correlations of variations in optical and radio wavebands on timescales of days and months, respectively, in OJ 287 and BL Lac. MacLeod et al. (1971) confirmed rapid radio flares in BL Lac but could not confirm any correlation with optical variability. The last few decades of 20th century proved era for blazars variability studies because of the advancement of technology and application of sophisticated detectors in Astronomical observatories. The frequent radio flux variability on various timescales were studied in detail by Heeschen and Rickett (1987); Witzel et al. (1986); Quirrenbach et al. (1991). Flux variations in X-rays were also reported by Snyder et al. (1980). The very short timescale variations indicate the highly beamed origin sources. The investigations of correlations or anti-correlations between the flux variations at different frequencies are widely performed by the community world wide to gain important informations.

With the advent of Extreme Gamma-Ray Energy Telescope (EGRET) onborad Compton Gamma-Ray Observatory (CGRO) a handful of blazars were detected at γ-Ray energies [$E \sim 100$ MeV - 1 GeV] which were well known variable blazars at radio and optical frequencies [e.g., 0716+714, 0804+499]. Many of the EGRET blazars were reported for flux variability at γ-rays (Michelson et al., 1994; Kniffen et al., 1993). The early EGRET observations for 3C279 showed a doubling of flux within 2 days with a subsequent fall within next 24 hours (Kniffen et al., 1993). The similar behaviour was observed for a number of other blazars namely PKS 0528+134 (Hunter et al., 1993), 3C454.3 (Hartman et al., 1993) and 1633+382, all of which show a significant rise and fall in flux within 48 hours. Few blazars have also shown variability at TeV energies [Mrk421; (Kerrick et al., 1995)]. After the successful launch of Fermi Gamma-ray Observatory, a successor to CGRO with improved sensitivity, the understanding of variability in blazars is completely revolutionized. The population of detectable blazars increased by orders of magnitude (see the first and second Fermi catalog). A lot of bright blazars are reported to be variable at γ-Rays on diverse timescales as discussed by Abdo et al. (2010c) in great detail. While Foschini et al. (2010) established the flux doubling within a timescale as short as few hours. There are many other instances when the variations at γ-rays are found to be correlated with variations at other frequencies.

The AGN are frequently reported to show variable X-ray flux. The characteristics of X-ray variations are entirely different in radio-loud and radio-quiet AGN. The X-ray variability in blazars are usually described by low-amplitude fluctuations around a steady mean with occasional flares superposed (Giommi et al., 1990). The long exposure EXOSAT studies shows that blazars spend only 10% time in spectacular flares, rest of the time they remain in quiet phase. A weak spectral variability is also reported (Giommi et al., 1990; Sambruna et al., 1993; Tashiro et al., 1994; Sembay et al., 1993; Thomas and Fink, 1994). Recent studies of blazars done by using RXTE, Chandra, Suzaku & Swft changed the view of X-Ray emission in blazars. The short variations as detected by many authors established very close locations for emission region with respect to the central engine (Foschini et al., 2010). In some cases quasi-periodic variations in X-ray are alos reported (Pian, 2002; Kataoka et al., 2001; Rani et al., 2009; Gierliński et al., 2008; Fan et al., 2002).

UV variability of blazars are somewhat less studied in comparison to other wavelengths. The early UV studies by Maraschi et al. (1986) report fast variations in PKS 2155-304 and OJ 287 (Δt) $\sim$ 1 and 2 days] respectively. A low amplitude variability (15 %) on timescales of 0.04 days was found in far UV at 100 A by Marshall et al. (1993). Blazars are extensively studied for variability at optical frequencies since their discovery. Various variability patterns are witnessed during last few decades. The campaigns organized by Webb et al. (1988) have been very successful for correlated variability study. Among other older studies are 1 days oscillations in PKS 2155-304 (Smith et al., 1992; Courvoisier et al., 1995), well defined rapid and symmetric flares with exponential slopes in 0954+658 (Wagner et al., 1993), spectral changes in BL Lac objects during brighter states (Miller, 1981), fast variabilities during flares of hour timescales (most spectacular 0.05 mag change in 10 minutes) (Miller et al., 1989; Carini et al., 1990). There are few older reports about the possibilities of periodicities at optical wavebands. On longer timescales the BL Lac object OJ 287 shows a periodicity of 12.07 years in historical light-curves longer than 100 years. This periodicity is explained using binary black hole paradigm (Sillanpaa, 1991; Valtonen et al., 1999; Shi et al., 2007; Valtonen et al., 2008, 2010b,a,c). The studies of a sample of blazars (Stickel et al., 1991) by Heidt and Wagner (1996) revealed high (80%) detection of IDV blazars. In other words around 80 % of the blazars in that sample are found to be variable on short time scales [$\Delta t \leq days$]. Later during 2003-2007 many observing campaigns were organized to study several sources for the variability simultaneously in more than one energy band (Villata et al., 2009a,b, 2008a, 2007, 2006, 2004a,a; Nesci et al., 2003, 2005a,b; Böttcher et al., 2003). The emission models responsible were constrained using the color dependence observed. The ealy reports of radio variability were for BL Lac (e.g., Harvey et al., 1972), 3C273 (e.g., Efanov et al., 1977), Cen A (e.g., Kellermann, 1974) and OJ287 (e.g., Andrews et al., 1974; Epstein et al., 1972; Kikuchi et al., 1973; Dreher et al., 1986; de Bruyn, 1988). The fast variability at radio wavelengths were established as a frequent phenomenon for S5-radio sample (Kuehr et al., 1981) by Witzel et al. (1986); Heeschen and Rickett (1987). Later on many of the blazars were established to show flux and polarization variations at radio frequencies over diverse timescales (Wagner and Witzel, 1995a; Gabuzda et al., 1989).

Earlier independent studies of polarization in blazars uncover many important properties of blazars (Bjornsson, 1985; Antonucci, 1986; Kulshrestha et al., 1987; Impey et al., 1989; Berriman et al., 1990; Wills et al., 1992; Takalo et al., 1994; Sagar et al., 2004; Dominici et al., 2004, and many more). Bjornsson (1985) studied the frequency dependence of polarized emission from blazars. (Ballard et al., 1990; Brindle et al., 1986; Valtaoja et al., 1991) carried out simultaneous observations of blazars at optical and Infrared wavelengths and established the correlations between polarization at both frequencies. Gabuzda et al. (2006) discovered the co-spatiality of radio and optical polarization which indicates the low energy radio and optical emission from same part of the jet. Impey et al. (1989) established the existence of a mini-blazar in 3C 273 using his photo-polarimetric studies. High degree of polarization in blazars empower the jet scenario of blazar emission as expected to be generated mainly because of synchrotron processes in the jet. Many studied were carried out to establish the correlations between polarization at optical and radio wavelengths with the total flux other frequencies(Takalo et al., 1992, 1994; Brindle, 1996; Wagner, 1996; Villata et al., 1997a). The total optical flux and polarized components are found to show mixed behaviour, sometime showing correlated variation.

It is clear from above discussions that the variability is an intrinsic characteristics of the blazars. The evidence of diverse time scale flux variation are witnessed over multiple frequencies. The high and variable radio and optical polarization is also witnessed in many of the blazars. It makes variability a very powerful tool to study blazar properties, which is the goal of the present study.

1.6.1 Explanation of variability in blazars

As discussed above in details, blazars show flux variability with diverse timescales ranging from tens of years down to few minutes over the complete electromagnetic spectrum. The flux variability at different timescales refer to the different physical processes responsible for such variations. Depending upon time scale of variation, several models are proposed to explain the flux variations in blazars. Some of the well accepted models are discussed below. Broadly the models are proposed based on two types of mechanisms, intrinsic (inherent to the source) and extrinsic (caused by outside effects), which are responsible for variations in flux and polarization.

Extrinsic mechanisms

Variability in the flux of the source may be caused by the effects external to the source of interest (of geometrical or atmospheric origin). The models falling in this category assume the flux variability to be merely a propagation effect. According to general theory of relativity proposed by Einstein a massive object distorts the space-time surrounding it. The space-time curve defines the trajectory of other surrounding objects. Even the light rays (massless photons) are affected by this highly distorted space time. Consequently, in the presence of very massive objects [quasars, galaxies, clusters, massive stars etc.] in the foreground, the light rays travelling from distant sources suffers change in trajectory, resulting change in apparent luminosity. This effect is known as microlensing effect because the foreground massive object works as a lens (Nilsson et al., 1996). The variability caused due to microlensing effect is achromatic in nature, does not depend on wavelength. The timescales of variations are also expected to range from tens of days to few months. The achromatic behaviour i.e. no color dependence and periodicity in observed variations distinguish this from other possibilities. The radio emission is highly affected by the intervening plasma in interstellar medium (ISM). The plasma motions in ISM form structures or irregularities that effectively scatter the incoming radio emission, the process known as interstellar scintillation(ISS). The rapid changes in the shape and sizes of these structures may introduce fluctuations in the intensity, received by the observer at ground. The possible timescales introduced because of this effect ranges from few tens of minutes to few hours. The observed very fast fluctuations ($\Delta t \sim$ few minutes) in the radio flux was very difficult task to explain assuming it to be because of intrinsic to the system. As the radio flux is thought to be generated in relatively cooled plasma at larger distances from centres. The *interstellar scintillation effect* becomes the best diagnosis to deal with such variations. However, ISS does not affect at higher frequencies and if correlated variations are observed in radio and optical, it rules out ISS as cause for radio variations.

As we know in the case of relativistic outflows in blazars jets, a slight change in the viewing angle may result a large change in overall flux. The change in viewing angle may be caused by many reasons. The *global bending of jet* (Marscher and Gear, 1985a; Romero, 1995) at some point downstream the jet may reflect a significant change in doppler boosting factor (δ) and hence effectively in observed flux. This bending of jet may be because of change in ambient medium, any obstacle in the path of the jet etc. The nature of this explanation is also achromatic and the timescale associated with such variations are large [Δ few months to several years]. The global bending of jet approach is favoured by a sudden jump in electron vector position angles or position angle(PA). In additions, emission shock moving in spiral motion or with ha helical trajectory introduces geometric effect which causes change in viewing angle and Doppler factor as a consequence. This results in periodic variation in the observed flux.

Intrinsic mechanisms

The observed flux variations may be triggered by the physical mechanisms happening within the system itself. It may be due to some instabilities either in the **accretion disk** or disturbances in the jet. Any hot spot in the accretion disk will be manifested in periodic variation in the flux as it passes through the line of sight(Mangalam and Wiita, 1993; Rani et al., 2010). However, only effect which may contribute to the intra-day time scale variation in flux is viscous disk instability depending upon the accretion disk thickness. However the disk mainly contributes in IR, Optical-UV regime of energy spectrum. Nonetheless, disk driven instability may trigger perturbations in the jet which might give rise to variations.

If the jet traverses a **helical trajectory** then the Doppler factor will change periodically and therefore a periodic, frequency independent variation in overall flux will result. The timescales associated with such variations are normally larger [$\Delta t \sim$ few days or more]. At larger timescale, quasi-periodic, frequency independent flux variations may be associated with precession of jet along it's axis. Other larger timescale variations observed in OJ287 [$\Delta \sim 11.6$ years] are caused by binary black hole system. These are periodic variations when one black hole passes through the accretion disk of other one. However a detailed study about the precursors of such outbursts, is done by Pihajoki et al. (2013).

The most accepted explanation for flux variability observed at a variety of timescales over the energy spectrum is given by **shock in jet model**. The standard relativistic jet model used as the paradigm for interpreting observations of compact jets was first presented by (Blandford and Rees, 1978) and improved upon by (Blandford and Königl, 1979b), with certain aspects added later by (Reynolds, 1982; Marscher, 1980; Konigl, 1981). Based on this relativistic jet model of active galactic nuclei Marscher and Gear (1985b) introduced the shock in jet model to explain flares in the blazar 3c273 observed in 1983 (Robson et al., 1983). In last few decades, with the availability of observational data, this model is further improved from time to time (Hughes et al., 1989; Hughes, 1991; Valtaoja and Valtonen, 1992; Sikora et al., 1994; Spada et al., 2001; Türler et al., 2006). The very basic assumption of the shock in jet model is that the initial parameters of the jet are not steady and the bulk speed of the outflow at the jet base is variable. When a slower shell of plasma outflow is followed by a faster moving shell, they necessarily collide with each other, forming a transverse shock propagating with relativistic speed. The shock formed in this way compresses the plasma which causes an increase in the density as well as an adiabatic increase in the internal energy and hence enhances the component of magnetic field that lies parallel to the shock front. It also accelerates the electrons to higher energies which then cool down emitting radiations. The amplitude of variation and time scale of variation depends on the power spectrum of the turbulence and shock thickness. Sharp flares can be understood if turbulence passes through a standing shock, the flow gets compressed and magnetic field and density get enhanced, giving rise to higher flux and polarization. It also accelerates the electrons to higher energies which emit making the features bright.

Marscher (2001) proposed that the different wavelength emissions are generated at different distances from central blackhole based on the hypothesis that higher the energy of synchrotron photon the higher energy electrons/positrons will be required for emission. This model naturally leads to bluer when brighter phenomenon. Here luminosity increases with injection of fresh population of electrons with an electron distribution harder than the previous, partially cooled ones(Mastichiadis and Kirk, 2002). A short term fluctuation in the spectral index may also result in BWB effect.

None of the models is able to consistently explain various type of variabilities observed in the light curves of the blazars. While it is possible to associate a mechanism to a specific variability feature in source at one time, it might fail to explain the same for different sourceor same source at different epoch. More data, continuous and simultaneous in all possible frequencies, for a large number of sources are required to limit the number of free parameters to constrain the models.

1.7 Multi-wavelength variability in blazars: a tool to study AGN

The problem of huge energy output from AGN and their structure largely remain unsolved since spatial resolutions available using most sophisticated observing facilities of today, and of near future, are unable to resolve the central engine. Hence the intrinsic property of flux variation is one of the best possible means to study them. Since blazar emisson is produced in the relativistic jets emanated from very close to the energy engine[$100 - 1000R_g$: $R_g = \frac{2GM}{R^2}$], variability in blazar flux provides deepest probe of the central engine. One of the most direct application of the detection of shortest variability time scale is to put upper limit to the size of the emission region.

As the multi-wavelength variability is well established observed property of blazars [section 1.5 reviews the historical observations of variability]. A single band observations contain only a part of information about the physical processes at work. Therefore investigations over the all possible frequencies are essential for a complete diagnostics of physics behind any event through estimation of the delays in variation. The pattern of variability at different wavelength regions can have important implications for the modelling of the emission processes. If the variability in two bands are correlated, then one can conclude that the radiation in the two bands are most likely produced by the same mechanism and in the same geometric region. However, if the variation in one band systematically lags behind the other one, then propagation from one region to another is involved. Multi-band variability studies therefore complement the information that can be obtained from single epoch broad band spectra. For an example the simultaneous multi-wavelength flux variations along with the optical polarization are used to constrain the physical mechanism responsible for 2009 flaring activity in blazar 3c279 (Abdo et al., 2010d).

These multi-wavelength campaigns are, however, difficult to organize as they involve the simultaneous observations of sources, spread over long period of time, using a number of terrestrial and space borne facilities with diverse instruments. Present era is best period for such studies as Fermi, Swift, Planck, VERITAS, HESS, VLBI and many other sophisticated ground based facilities are regularly providing good quality data.

The observed optical/UV flux may be generated in the disk and corona but in case of blazars, highly boosted jet emission rules out any significant role of disk component to the variability. However few blazars are observed showing disk emission when in fainter state (Ghisellini and Tavecchio, 2009; Ghisellini et al., 2011). The high optical polarization from blazars confirms the jet origin of any variability feature. X-ray emission are mainly generated in the jet by Synchrotron and Inverse-Compton processes in the jet. The reflection of disk emission by hot corona may also contribute in the quiscent phase. A significant progress has been made in the understanding of the variability at larger timescales [$\Delta t \sim$ few days or greater]. Multi-wavelength campaigns organized during last one decade for selected bright blazars have established many aspects of variability(Raiteri et al., 2009; Villata et al., 2008b; Abdo et al., 2010d; Agudo et al., 2011; Marscher et al., 2010; Orienti et al., 2011, 2013; Vercellone et al., 2010). In spite of some limitations, the shock in jet model has been extensively used to explain the variations with a range of time scales [few weeks down to few hours](Celotti and Ghisellini, 2008; Chatterjee et al., 2008). The pattern of variability observed in blazars are random and may not repeat during events at other epochs even for the same source. Therefore a large number of sources are needed to be studied over large possible time duration, covering the multiple flaring episodes, to map emission model in blazars. As part of this dissertation we have aimed to study the blazar PKS1510-089 using the multi-wavelength data covering more than two year of monitoring consisting of multiple flaring episodes. The observed data is discussed in view of shock in jet model as indicated by the observed frequency dependent variations.

Well sampled, high temporal resolution optical observations can present a unique picture of processes which are unseen at other frequencies. During last decade, many authors have claimed repeated detection of extremely violent variability events in many blazars with amplitudes $\Delta m \sim 1$ mag in few tens of minutes (Bai et al., 1998; Xie et al., 2001, 2002, 2004). For example these authors reported a 2 mag variation in 40 minutes for the HPQ PKS 1510-089; they have also showed several sudden($\Delta t \leq 15$ min) dips of ∼0.9 mag in the lightcurve of EGRET blazar OJ248 (0827+243). If confirmed, these extremely violent phenomenon require a complete reassessment of the mechanisms responsible for the energy generation in blazars. As an illustration, the size of emission region corresponding to the variability timescales of few tens of minutes imply the sizes smaller than the gravitational radii of central black holes of certain objects. The claims made by Xie et al. (2001, 2002) are discarded by Romero et al. (2002) as they did not find such violent variability for 20 EGRET blazars observed with ∼ 20 minutes time resolutions. They suggested that the high variability observed by Xie et al's may be due to wrong choice of comparison stars used for photometry as inappropriate choice may reflect spurious variations in differential lightcurves. In an independent study Miller et al. (2001) have witnessed a very systematic variations in optical observations BL Lac [∼0.2 mag/hr]. So there is still concern on such rapid variations and hence the underline physics is still not understood. Therefore, a detailed study is needed for better understanding of the nature of microvariations or intranight variability. On the other hand, few authors have recently reported very rapid quasi-periodic variations in several blazars. For example Rani et al. (2010) observed periodic variations in BL Lac object S5 0716+714 with a change of ∼ 0.09 mag within 15 minutes time period. Such short timescale periodicity is generally uncommon in blazars and very difficult to explain. A long stretch of intranight observations comprising various brightness states are required in order to confirm and understand the mechanism behind such variations. The study of nature of microvariation in blazar is one of the major motivations for this study. We have, therefore, used variability in flux and polarization in several sources to understand the nature of variations and estimate various physical quantities related to the structure and emission mechanisms operating in the blazars.

Work carried out in this thesis

In an attempt to understand the energetics of AGN in general and blazars in particular, we carry out a study on several blazars. First two chapters introduce the subject and the facilities and techniques employed. Rest of the report deals with our efforts to establish the realm of existence and explore the nature of the intranight (INV) and longer term variability in blazars. The intranight optical variability provides important clues to the mechanisms of blazar emission as intra-night variations are not easy to observe at other wavelengths. The optical emission, being emitted from jet at pc-scale, indicates the rapid fluctuations to be the intrinsic properties of blazars. We use blazar S5 0716+714 to investigate nature of the rapid variations. MIRO has monitored this source for more than 160 nights in optical R, V, B and I bands during last seven years. MIRO has detected the most rapid fluctuations ever detected for this source during its 2010, March optical flare [0.9 mag in 15 min]. Apart from rapid variations, several interesting variability patterns were detected during the course of this flaring event. The observed variability event which is used to constrain the possible physical mechanisms responsible for this event and estimate physical size of the emission region are the main focus of chapter 3. It provides details of the technique and its application to address optical intra-night and inter-night variability in order to get an insight into possible physical activities at work in blazar jets.

The 58 ideal photometric nights with a continuous monitoring of same objects for 2 hours or more are used for investigating the nature of INVs over different brightness states and frequency of such variations. More than 82% of the monitoring nights are detected to show significant INVs. The extent of variability quantified by the amplitude of variability are seen to depend on overall brightness level of blazar continuum. Interesting aspect of larger amplitude of variation during the relatively faint brightness level is noticed. This is well explained using shock in jet scenario of blazars in Chapter 4. The rest of this chapter discusses long time scale variations observed in S5 0716+714. A mild color dependence is noticed indicating to bluer when brighter phenomenon. The poor time sampling for long term data prohibits us to discuss any periodic behaviour but several episodes of large flaring activity is evident from the light-curve. We also notice a slow trend of decrease in brightnes with time.

The first detailed polarization study for a BL Lac object CGRABs J0211+1051 was made using PRLPOL at MIRO during it's major gamma-ray flare in January 2011. Observations from Mt Abu Observatory during January 30 to February 3 revealed intranight variation in the degree of polarization during at least three nights while PA remained stable during individual nights. Significant inter-night variations in DP and PA were noticed alongwith a mild bluer when brighhter trend indicating to fresh injection of plasma in the emission region as cause of change in DP and PA. Many authors have shown LBL to show higher polarization as compared to HBLs but many others claim no significant difference in polarization property. To resolve this issue, we carried out a systematic study of polarization behaviour with a larger sample of blazars. Our results strongly favour the results obtained by (Andruchow et al., 2005; Fan et al., 1997) that LBLs/FSRQs show much higher DP than HBL blazars. Therefor, degree of polarization can be used to classify blazars. Based on the high DP observed for CGRaBS J0211+1051, we propose this source to be a low energy peaked BL Lac objects (LBL).

Chapter 6 deals with a multi-wavelength study of the source CGRaBS J0211+1051 by constructing its spectral energy distribution and light curves. The low energy synchrotron peak of its SED falls at near IR region, confirming the proposition based on high polarization that the source is an LBL. However, the Compton dominance factor of this BL Lac object makes this source very interesting. The multi-wavelength lightcurve is used to discuss the possible physical processes at work. The shock in jet model again seems to be appropriate model to explain this source. Data used for this source is obtained from Fermi, Swift, MOJAVE and our own observations.

The multi-wavelength variability study of FSRQs PKS 1510-089 is carried out for diagnosing the physics responsible for various episodes of gamma-ray activity in this source during the course of mid 2011 to early 2012. All multi-wavelength data available from various resources are used to construct the multi-wavelength lightcurves and discuss the individual flaring events. Various shapes of flares in gamma-rays are seen in individual outbursts, suggesting different mechanisms of their origins. A systematic study of these outbursts are discussed in the last 7th chapter of this dissertation. The part of this work was presented at GA-IAU-2012 in Beijing and black hole meeting at Kathmandu, Nepal in 2013.

Last part of the thesis summarizes the conclusions of this work with future directions in this field.

Chapter 2

Observations and analysis methodology

2.1 Introduction

Astronomical sources emit radiation and sometimes high energy particles which are analysed to gain information about them. The photons, therefore, act as a true messengers which carry information on whatever is happening far away in deep universe. The study of astronomical sources, therefore, is the study on the photon as all the information is encoded there. Naturally, more number of photons we get, better knowledge we have about the source of interest. Some of the astronomical sources are far away and photons take very long to arrive at earth, even the light from our nearest star, the sun, takes about 8 minutes We are also aware that intensity of light decays as square of the distance travelled and hence very few of them arrive on earth when distances are really large. In order to collect more photons, we require large photon collection facilities, that we call telescopes. Further, we need detectors to convert these photons into electrical signals which analysed to get any meaningful scientific information. Most of the sources radiate their dominant emission at a particular wavelength depending upon their temperature, for example, just like a black body. However, some source radiate significant emission through complete electromagnetic spectrum. The objects of interest for the present study, blazars, are one of them. Their continuum emission cover almost complete energy spectrum and therefore require facilities to collect photons at all the energies. Therefore, the study of blazars requires collection and analysis of data at radio, IR, optical, UV, X-ray and $\gamma - ray$ frequencies. It is only relatively recent that we are able to get information at later two domains of energy which has completely revolutionized our understanding of astronomical sources, blazars in particular.

The photon collecting telescopes, observation techniques, instrumental calibration, and data reduction & analysis procedures to get end product are extremely dependent on the instruments used and the energy band of emission under study. In the present study we have dealt with multi-wavelength data for the variability studies. The optical/IR data have been obtained largely using Mt Abu InfraRed Observatory and other ground-based facilities, X-Ray/UV and γ Ray data are obtained from space based facilities SWIFT and Fermi. The data, from these, are analysed for generating the light-curve and spectral energy distribution (SED) for various studies. In the following sections, the overview of telescopes, instruments, observational strategies, and reduction procedures are given in brief detail.

2.2 Overview of observatories & instruments used

2.2.1 Mt. Abu InfraRed Observatory (MIRO)

Mount Abu Infrared Observatory (MIRO) operated by the Physical Research Laboratory, Ahmedabad, is located at Gurushikhar, Mt Abu, in Rajasthan, which is about 240 km from Ahmedabad. The Gurushikhar is the highest peak in the Aravali range. The altitude of the MIRO is 1680 meter from sea level with latitude and longitude of 24° 39' 10"N and 72° 46' 47" E, respectively. The Observatory houses astronomical telescopes and Aeronomy Laboratory for atmospheric studies. The weather conditions at the observatory site are of moderate type. The typical humidity at the observatory site is below 20-30 % throughout the year, except monsoon season. The wind speed during normal nights ranges between 5 - 50 km/h. The site is 20 km away from nearest

Figure 2.1 Mt. Abu Infrared Observatory, Rajasthan, India located at highest peak of Arravali Hills.

town and is shielded by a hillside and is almost free of stray light. One can easily get more than 200 photometric nights over an year. This observatory became fully functional for regular scientific observations in 1995 with a 1.2m telescope. Since last 18 years of regular operations the observatory has made a significant contribution to the astronomical community by collecting large amount of data on several sources. Figure 2.1 shows an image of MIRO taken from an adjacent peak.

MIRO operates two moderate sized optical telescopes at this site. Both are equatorial mount systems. The larger telescope (Figure 2.2) at MIRO has a parabolic mirror as primary with diameter of 1.2 meter while the secondary mirror is of 0.6 meter and hyperbolic in shape. The parabolic-hyperbolic combination (Ritchey-Chretien; RC configuration) of mirrors for primary and secondary provides a beam nearly free of all kind of optical aberrations like coma etc. RC configuration is adopted by most of the professional astronomical telescopes. The following are the instruments being regularly used as backend instrument at f/13 Cassegrain focus of this telescope:

- PRL made Optical Polarimeter (PRLPOL)
- Liquid Nitrogen cooled Optical CCD Camera
- Near Infrared Camera and Spectrograph (NICMOS)
- PRL-NICs
- Two Channel IR photometer
- Fabery-Perot Spectrograph

There is provision for Coude focus also and following instruments make use of this,

- Optical Fiber Fed Spectrograph
- PRL Advanced Radial Velocity All-Sky Search (PARAS)

Since blazars emit significant non-thermal emission which is highly polarized, we use polarimeter to detect and analyze such emission. Therefore, for the present study we have made use of PRLPOL built in-house and optical CCD camera as backend instruments mounted on the 1.2 meter telescope at MIRO. In the following two sections we have described the instruments in detail.

2.2.2 PRL Optical Polarimeter (PRLPOL)

PRLPOL (Fig- 2.3) is an in-house built photo-polarimeter (Deshpande et al., 1985; Joshi et al., 1987) which is one of the major instruments used as a backend instrument at MIRO since 1995. This instrument works on the principle of rapid modulation by a rotating half-wave plate (Frecker and Serkowski, 1976). Before the MIRO being fully functional this instrument was being used at many other observatories in India namely UPSO (Uttar Pradesh State Observatory,

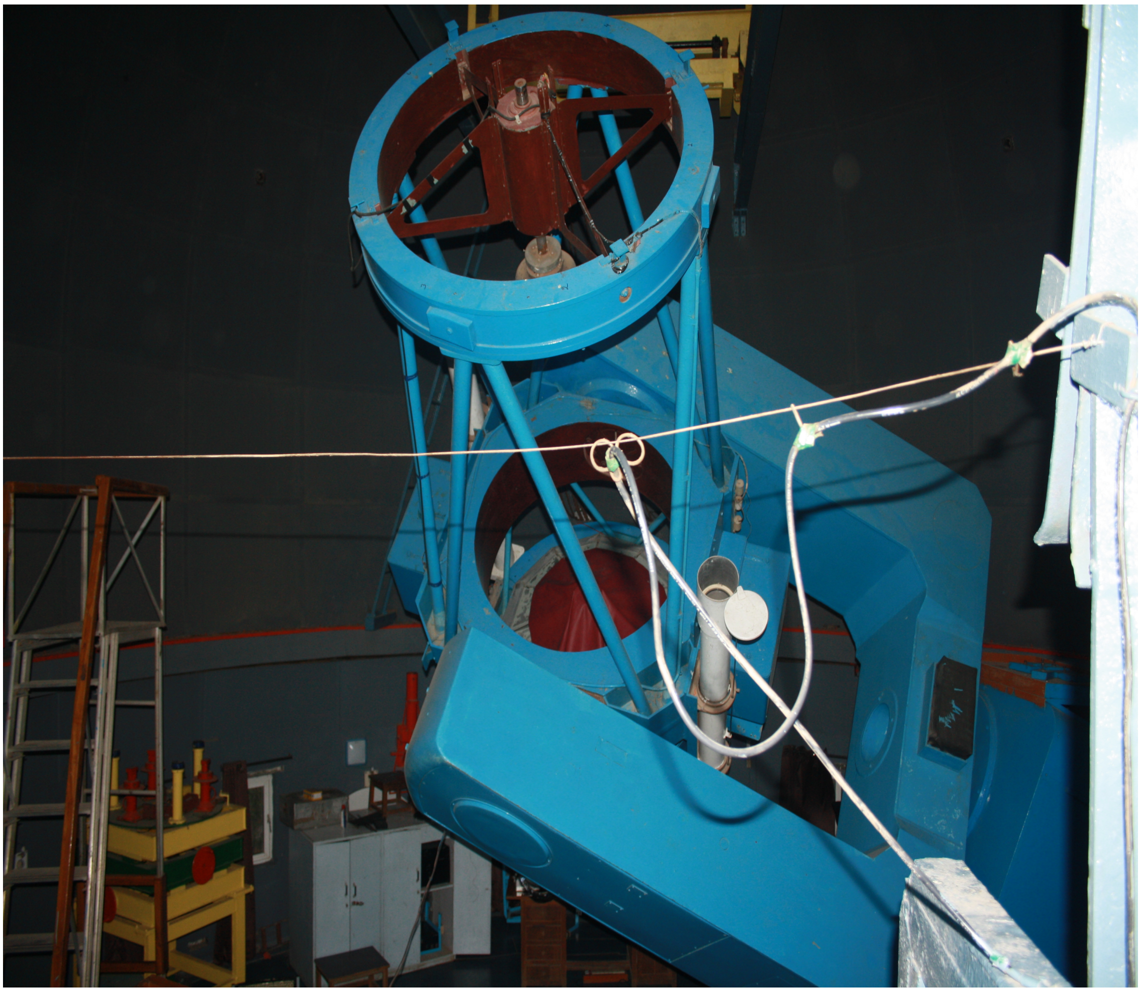

Figure 2.2 1.2 meter Telescope at Mt. Abu Infrared Observatory (MIRO).

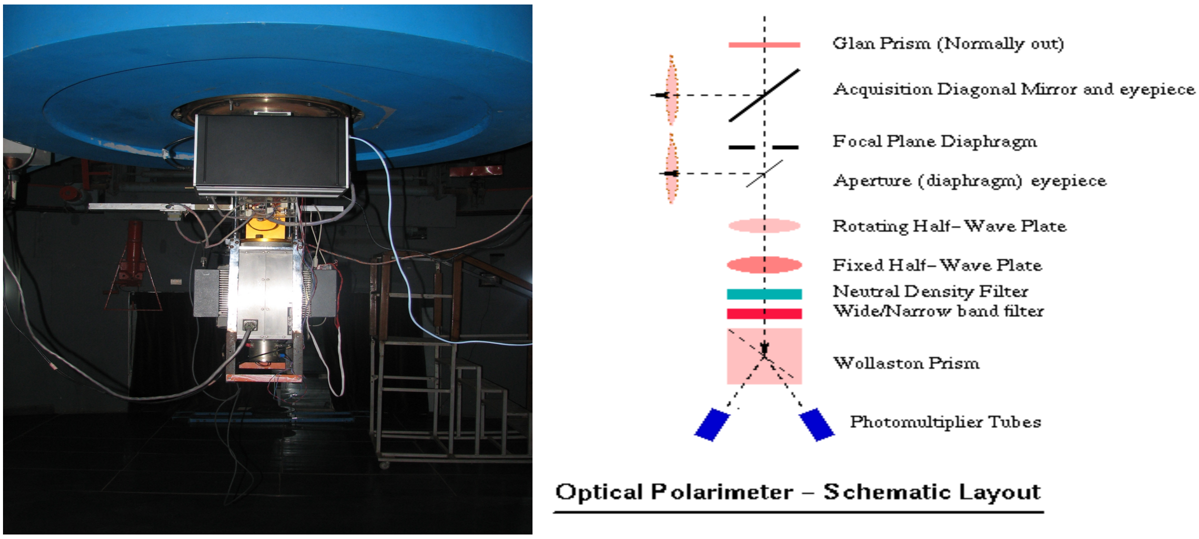

Figure 2.3 The left figures is PRL made Optical Polarimeter (PRLPOL) installed at the backend of telescope at MIRO. The right one is the full sketch of components of instrument.

Nainital - now known as ARIES,Uttarakhand) and Vainu Bappu Observatory, Kavalur, Tamil Nadu. The older version of the instrument set-up was very complex. The main instrument was being put at Cassegrain focus of telescope and all the power supplies and supporting electronics, computer, printer etc were needed to be put on the telescope floor. A lot of manual interventions, apart from technical support, were needed while observing. The matching of the field and guiding was being done manually through eyepeice. Apart from the technical difficulties the poor time sampling and lack of larger time exposures were basic limitations of original setup. However, this system was widely used in observing comets, variable stars and Active Galactic Nuclei (AGN).

The system was fully refurbished using improved version of electronics and high speed computers (Ganesh et al., 2009). The current version of PRLPOL is highly efficient and semi-automated system. The dozens of boxes with electronics and power supplies are now reduced to a single moderate size box on board the instrument. The errors introduced because of human intervention during observations are reduced by replacing the eyepieces with guiding CCD cameras which were used to locate the star positions in the aperture in the display at monitor. This system is using GNU/Linux (FSF,2008) with an RTAI (Real Time Application Interface) enabled kernel running on pc/104 based embedded CPU board for making its operation completely automated. Onyx PC/104 counter/timer and digital I/O bards are employed to record the counts coming from photo-multipliers in the photon counting mode. One in-house developed PC/104 board is used to rotate the half-wave plate to generate the fast modulation of incoming light beam. This motor was previously driven by an ISA bus board with external driver which provided the timing pulses and the current driver circuitry. The Atmel microcontrollers are used to drive stepper motors, incorporating the functionalities of the mechanical operations like optical filters, apertures etc. One independent mini PC is employed to control the USB interfaced CCD camera to provide a view of observing aperture and field being observed by the instrument. This arrangement effectively remove the human intervention for guiding the source within aperture. The SXV-H9 CCD camera from Starlight-Xpress, 1392 $\times$ 1040 pixel 16-bit thermoelectrically cooled CCD with compact driver electronics, is used to serve the purpose of viewing and keeping the source at the center of aperture. This replaces the aperture eyepiece in old version of instrument. There is also a provision for using a second CCD camera with relatively larger field of view for auto-guiding the telescope. The SXVF-M25C CCD Camera from Starlight-Xpress, a single shot colour camera, with a relatively large field of view is used as an autoguider to nullify the tracking error of telescope. It has 3024 $\times$ 2016 pixels in a Bayer matrix. This camera is mounted in the place of acquisition eyepiece (see Figure 2.3). The GNU/Linux and in house developed control system facilitate the operation of instrument remotely from anywhere over the PRL local area network (LAN). This system is presently being operated remotely from telescope control room, adjacent to the telescope dome; however, in principle, it can be used remotely from PRL campus Ahmedabad.

The working of this instrument is based on the prescriptions discussed in Frecker and Serkowski (1976). The main detectors used in this instrument are two identical photomultiplier tubes (PMTs) in photon counting mode to derive the parameters defining polarization of astronomical objects. The refurbishment of this instrument does not change the basic structure. It was just to improve the functionality and achieve better time sampling over longer period of monitoring of astronomical objects. The left panel of Figure 2.3 shows the picture of recent version of instrument installed at the Cassegrain focus of the 1.2m telescope. The right panel shows the basic layout of the optical path of the instrument. The first optical component (top) is a Glan prism which is used for calibrating the instrument for 100 % polarization. The next optical component in the layout is a diagonal mirror which reflects the light into acquisition eyepiece mounted perpendicular to the main incoming beam which is being used for guiding the field of interest. This eyepiece in the new version of system is replaced with auto-guider CCD camera and the whole guiding procedure is made automated. In the focal plane an array of different sized diaphragm serving as different apertures are mounted in such a way that at a time only one aperture will be in light path. The aperture movement is completely motor driven and controlled by the software itself. Just below the focal plane a diagonal flip mirror is mounted in coordination of another CCD camera serving for verifying the source position in aperture. The movement of flip mirror is controlled by motor in coordination of other controlling drivers such a way that after every acquisition light is reflected to the CCD camera and source can be seen in the field over the computer screen otherwise enter into the next optical component i.e. a set of two half-wave plates. The top half-wave plate is rotated around the optical axis which is common with the direction of incoming beam. The rotation of first half-wave plate is incorporated to minimize the effect of rapid fluctuations in the atmospheric conditions on intrinsic polarization of the source. The bottom half wave-plate is kept fixed exactly parallel to the first one. This arrangement is used to extract the informations about the position angle (PA) which will be defined later in section below. The next optical component which intervene the path of incoming light beam is neutral density filter. This is normally kept out while observing the faint sources. This is used when observing the bright stars for polarization. A set of narrow as well as broad filters are used in a linear array controlled by a stepper motor attached. This movement of filters can be automatically controlled by the observer through GUI. At a time only one filter will be in light path. The last optical component just above the detector is a Wollaston prism. This prism is mounted such a way the two bifurcated beams (Ordinary and Extra-ordinary) directly enters in the two separate but identical PMTs (EMI 9863B). A high achromatism converging lens system is glued on the lower side of prism. This lens system re-image the primary mirror onto both the PMTs so that the inaccuracies introduced due to inequality over the detector surface is removed.

The incoming light is passed through the rotating highly achromatic half-wave plate, modulated by a stepper motor at 5 or 10 rotations per second with 96 steps per rotation resulting in sampling time of 1 or 2 msec per step. The modulated beam after passing through the filter is then split into ordinary and extra-ordinary polarised components by a Wallaston prism and the respective counts are registered by two independent identical PMTs. The resulting counts follows a sine wave pattern in 24 steps following the modulations introduced. Since these counts exhibits the contributions from sky therefore an equally large nearby source free area is observed for the same exposure and subtracted from the source counts. Switching the exposures between the sky-source-sky is the typical observational strategy used for monitoring the polarization for astronomical objects. The sky corrected counts (I_j) are then fitted by the following function

$$I_j = \frac{1}{2}\Big\{I_0 \pm Qcos4\theta_j \pm Usin4\theta_j\Big\} \tag{2.1}$$

where I_0, Q and U are known as stokes parameters. θs are the postions of the half-wave plate (angle θ_j). From these parameters the linear fractional polarization or degree of polarization(DP), p, and position angle (PA), Θ, are given by:

$$p = \sqrt{Q^2 + U^2} \quad \Theta = \frac{1}{2} tan^{-1} \left\{ \frac{U}{Q} \right\} \tag{2.2}$$

The control program and embedded electronics onboard the instrument automatically complete all the required calculations and provide the degree of linear polarization and position angle as output in data files. The mean error in P is estimated from the deviation of the actual counts from the fitted curve. Polarization standard stars are regularly observed every night to determine the zero point for the P.A. and the instrumental polarization, which was found to be negligibly small ($\leq 0.02\%$). Three consecutive measurements are averaged to enhance the signal to noise ratio.

The standard Johnson and Cousins optical filters are used for monitoring the blazar sample of interst (Bessell and Brett, 1988; Bessell, 1995, 1990). The transmission characteristics of the filter are checked every year before the start of observing season. The field of view of the instrument is decided by the size of aperture used.

2.2.3 Optical CCD Camera

The Optical CCD Camera is being used as a backend instrument on 1.2m telescope at MIRO (Fig- 2.4). The main part of this instrument is an optical CCD camera (1296 $\times$ 1152 pixels) with a pixel size of 22 μm. The CCD chip is mounted within a chamber cooled by liquid nitrogen. A circular filter wheel is attached on the top of the camera to enable the use of different filters for imaging purpose. The movement of filters are driven by a stepper motor which is again controlled by MOXA Ethernet controller unit onboard the instrument. The camera unit is operated by a Windows XP based computer in telescope control room through a data cable. A vector camera shutter aperture is mounted on the top of filter wheel. This shutter is used to control the exposure onto the CCD chip. The chip is only exposed to the sky only when this shutter is open. Therefore the time resolution of this instrument is limited by the moment of shutter. The shutter closing and opening arrangement is

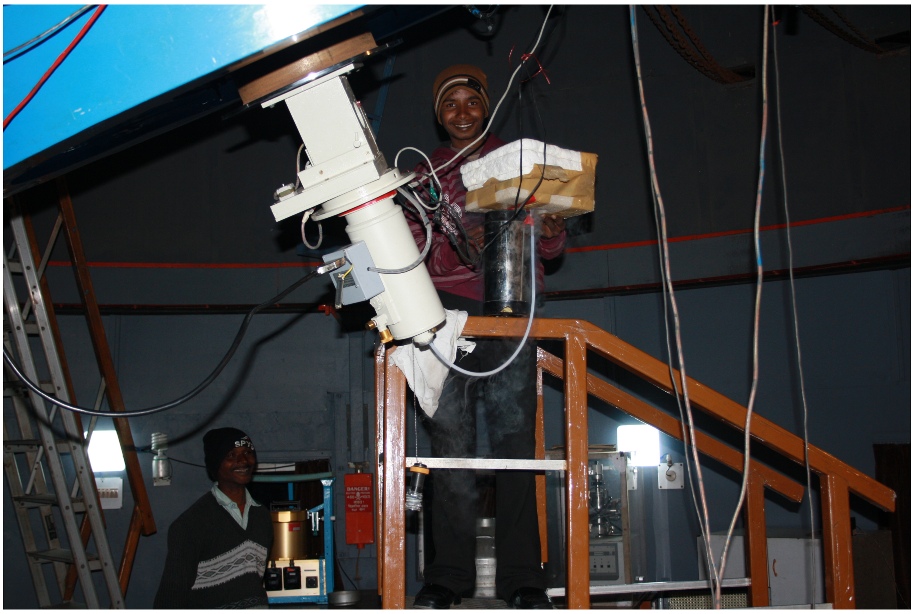

Figure 2.4 The Optical CCD Camera at MIRO attached at the backend of telescope. This camera is attached with a filter wheel containing five Johnson/Cousins filters (UBVRI).

fast enough to provide proper image for the exposures of more than 500 msec. The total field of view covered by this instrument as backend instrument at 1.2 m telescope at MIRO is 6.5 $\times$ 5.5 arcmin. This field of view is large enough to be used for differential photometry of astronomical objects. The details of differential photometry technique is discussed in subsequent sections.

2.2.4 Automated Telescope for Variability Studies: ATVS

"Automated telescope for variability studies "or ATVS is a newly installed observing facility at MIRO observatory (Fig- 2.5). This is a CDK20 system provided by PlaneWave Instruments Pvt. Ltd. The PlaneWave Instruments CDK20 is a 20 inch (0.51 meter) f/6.8 corrected Dall-Kirkham Astrograph Telescope. This is again an equatorial mount system. The primary mirror is a prolate ellisoidal mirror while the secondary mirror is of spherical geometry. A lens group, free of astigmatism, is mounted in the baffle i.e. in the light path. This lens system correct the sky image for field curvature effect, off-axis coma, and astigmatism. This telescope system is known to have minimal optical

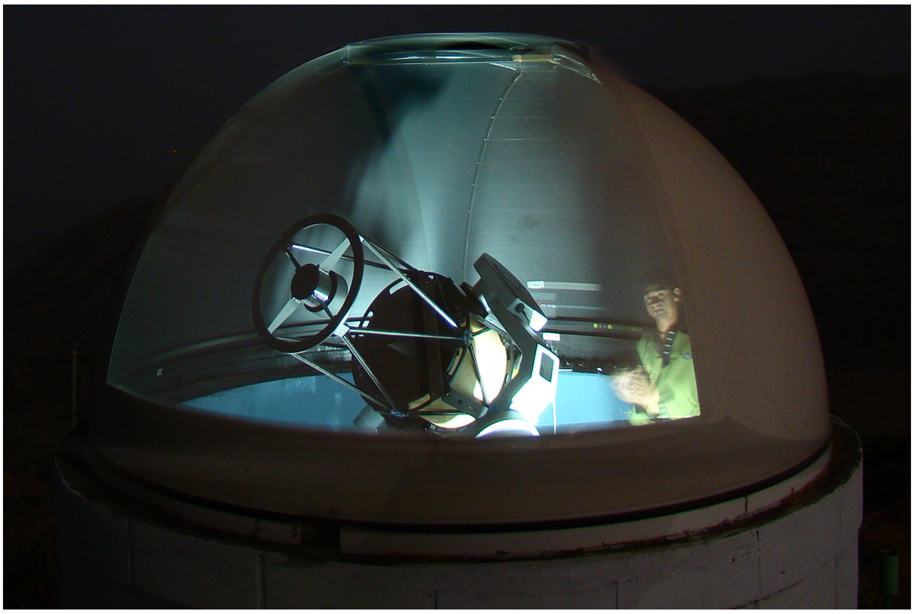

Figure 2.5 A long exposure image of ATVS with rotating dome. This gives an inner view of telescope in the dome.

aberrations. Therefore the optical tube is perfect for astronomical observations. The secondary mirror in this tube is kept fixed unlike the 1.2m telescope. The focusing is performed by moving the backend instrument/eyepiece up and down. A focuser arrangement is provided which is driven by a stepper motor and controlled by the controller installed as a part of tube. A set of three fans and a temperature sensor are installed in the back side of mirror to automatically maintain and measure the temperature of primary mirror, respectively.

ATVS is completely automated robotic telescope and hence can be operated remotely from anywhere in PRL network. Apart form the backend instrument, ATVS system comprises Boltwood cloud sensor, all sky camera, shutter drive and control system, and dome drive and control system as auxiliary devices coordinating in robotic operation. The Remote Telescope System 2nd version (RTS2), an open integrated source package for remote observatory control under the Linux operating system, is used to interface and operate different devices including the detector. The driver for operating the different components of ATVS system are developed in house. The cloud sensor is connected

Figure 2.6 The imaging instrument attached at the f/6.8 casslegrain focus of ATVS. This instrument is using EMCCD as detector.

to the controlling computer through serial cable and send the sky information regularly. The sensor measurements with the proper setting of parameters define the favourable sky conditions and make decisions autonomously about the starting of observations. The shutter drive wait for the ok signal from the cloud sensor then open the shutter. Now the telescope is ready to take commands for observations. The source coordinates and respective exposures are provided automatically by *scheduler* program. This program defines the observational strategy for ATVS. The dome and telescope drives are synchronized with sufficient accuracies. Dome drive synchronizes with telescope position every 3 seconds.

Figure 2.6 shows the picture of imaging instrument attached as the backend of the ATVS. This imager contains two filter wheels one containing the broad band filters and other having polaroids at 0°, 45° and 90° with few vacant slots. The filter wheel containing polaroids are only used when using this instrument as imaging polarimeter otherwise the vacant slot is kept in light path. The standard Johnsons and Cousins filters (UVBRI) are being used for using this as imager. Electron Multiplying Charge Coupled Device (EMCCD), 1k × 1k, provided by ANDOR Technologies Ltd is used as detector. The filter movement and EMCCD operation both are handled using in-house written scripts and using RTS2 platform. This system does not need a separate shutter for the camera because the EMCCD architecture has a storage area of the same size as the imaging area into which the image is quickly shifted electronically at the end of the exposure. A very detailed study of performance and noise estimation of the EMCCD for Astronomical objects can be found in Smith et al. (2004); Dussault and Hoess (2004); Smith et al. (2008); Giltinan et al. (2011). The total field of view of sky covered by ATVS is 13 $\times$ 13 arcmin.

The twilight and dawn sky flats are regularly taken for calibrating the non-uniformity of detector chip. The EMCCD chip is cooled below $-80°$C using the embedded thermoelectric cooling. The recycling running water cooling is optional which can further reduce the chip temperature upto $-100°$C. However $-80°$C is enough to reduce the dark current upto negligibly small level.

2.3 General techniques for data handling

2.3.1 Image Analysis

The optical images obtained using both the imaging instruments require pre-processing followed by the proper image analysis before generating any science results. The preprocessing of astronomical images require the reduction of detector, atmospheric and other artificial contributions to the intrinsic source flux. The nonuniformity in the pixel response may add the artificiality in the measured flux. Therefore the detector calibration for the same is required. The signal may be significantly affected by the thermally generated electrons. This is known as dark current. The cooling of photosenstive area (photon collecting area of detector) in general reduce the thermal electrons (dark current) significantly. The CCD and EMCCD detectors used for imaging at MIRO are cooled using liquid nitrogen ($-120°$) and thermoelectric cooling ($-80°$), respectively. These conditions are favorable enough to neglify the dark current in both the detectors.

All the preprocessing and image analysis used in this study are performed using a recent version of (V2.16) the 'Image Reduction and Analysis Facility (IRAF)', a general purpose software system for analysis of astronomical data. IRAF is written and supported by the National Optical Astronomy Observatories (NOAO) in Tucson, Arizona. NOAO is operated by the Association of Universities for Research in Astronomy (AURA), Inc. under cooperative agreement with the National Science Foundation.

It is clear from the above discussion that the images acquired by both the detectors are almost free of dark current. The twilight and/or dawn sky *flat* fields are taken every observing day. The *bias* frames are taken before and after observing the target. The *flat* field images are the frames grabbed with uniform illumination of detector while the *bias* frames are the images taken without exposing the detector i.e zero second exposure images. The *bias* frames presents the base level counts/pixel i.e before the starting the exposure. This is always constant throughout the detector area. In the CCD camera used at MIRO a thin vertical strip on left side of light sensitive chip (width 10 pixels) is kept unexposed to the sky. This region is known as overscan region and can be used in place of *bias* correction. The bias/overscan and flat field correction is performed to all the astronomical images. The nature of bias/overscan is additive so needed to be subtracted from all the frames. While the *flat* fields presents the nature of non-uniformity of detector chip. Therefore all the astronomical images should be divided by $flat$ fields after the *bias* subtraction. For this purpose all the *bias* frames captured overnight are median combined using the IRAF task *zerocombine* to generate the *master bias* frame. Similarly all the *flats* are combined filter wise using the IRAF task *flatcombine* to get the *master flat*. The resulting master bias and master flat files are used to correct the individual target images. This is performed using task *ccdproc*. *ccdproc* first perform bias correction on individual images + flat and then divide them by corrected flat image. The images taken from EMCCD at ATVS are bias clamped so only flat corrections are needed. The resulting images are then used for photometry in order to get the flux from the point sources in the field. The field of view of both the detectors are large enough (FOV_{CCD} 6.5 × 5.5 arcmin & FOV_{EMCCD}: 12.5 × 12.5) to accommodate at least three comparison stars (reference sources) around the source of interest. Therefore *differential photometry* is ideal technique for deriving the flux from these images. Differential photometry measures the difference between the target source and number of nearby reference sources (usually stars) to provide a potentially high precision differential measurement. Inherent in this technique is the assumption that the objects nearby to the target of interest are equally affected by variations in the atmosphere. This approach has long been recognized as the most effective technique for achieving the highest precision photometry (Young et al., 1991; Howell, 2006). For performing the photometry of corrected images *phot* task, provided in IRAF as a part of *aaphot*, is used. This task requires many basic parameters about the detector like gain, binning, exposure time etc and intrinsically to individual image like fwhm of point sources, standard deviation of back ground etc. Therefore individual images are examined for fwhm of point sources and standard deviation of background using IRAF task *imexamine* before using for photometry. The *phot* task performs the aperture photometry of the target along with the reference stars. A proper size of aperture and sky annulus are also required as input parameters for fitting the sky. Therefore aperture photometry is best for moderately rich fields without overlap of point spread functions (PSFs). For our purpose we have used a number of different sized apertures usually multiples of the full-width at half maximum (fwhm). The *phot* task generate a text file output containing the magnitudes and respective photometric uncertainties for the target and reference stars as well. The proper size of aperture is chosen by plotting the magnitudes of different point sources in the field vs the size of apertures. From our analysis the proper size of aperture is always roughly equal to 2.35-3.0 × FWHM. The difference of target and reference stars is called the *differential magnitude* for the source. This is always limited by the standard deviation of differential magnitudes of reference stars. A series of frames taken at different epochs can be used to present the high precision light-curve of the target as reference stars are not expected to vary with time except the statistical fluctuations. The target flux can be calibrated with the known flux of reference stars.

The whole procedure described above is scripted as a photometry pipeline developed during the present study. This is completely automated script giving the lightcurves and data-files as output. The point source identifications are carried out using the freely available package *Astrometry.net* and *WCSTools*. This script has made it possible to analyse large amount of data collected during more than last ten years or so.

2.4 Analysing archival data

We have also made use of archival data from Swift and Fermi for part of this study. These data in raw form are freely available on HEASARC website.

2.4.1 Swift data

Swift is effectively a multi-wavelength space based observatory by NASA, launched in November 2004. Many of the institutions form Europian and USA has actively collaborated in the concept and design of the observatory. The basic motive of this observatory was to detect and follow mysterious Gamma-Ray Bursts (GRBs), a cosmic explosions on tremendous scale. Swift has a compliment of three co-aligned instruments for studying gamma-ray bursts and afterglows or other heavenly objects: the Burst Alert Telescope (BAT; CdZnTe, Detecting Area: 5200 cm^2, FOV 2.0 sr, ΔE $\sim$ 15-150 KeV)(Barthelmy, 2004), the X-ray Telescope (XRT; XMM EPIC CCD, Effective area 135 cm^2, FOV 23.6' $\times$ 23.6', ΔE $\sim$ 0.3-10 KeV)(Burrows et al., 2005), and the Ultravoilet/Optical Telescope, a modified Ritchey-Chretien Telescope (f/12.7), (UVOT; Intensified CCD: 2048 $\times$ 2048 pixels, FOV 17' $\times$ 17', $\lambda \sim$ 170-600 nm)(Roming et al., 2005). The largest instrument onboard the Swift is BAT, which can view approximately 1/6 of the entire sky at one time. As soon as it detects some GRB within few seconds of detection of bursts, the spacecraft swiftly and autonomously repoint itself to aim the XRT and UVOT at the burst to enable the high precision X-ray and optical positions and spectra to be determined. Apart form the GRB detection and follow-up, Swift observes many micro-quasars, pulsars, AGN etc as part of regular observational strategy. The observed data become public within 24 hours of the observations. A sample of bright blazars are being regularily monitored by Swift. The XRT observes in pointing mode while UVOT takes few snapshots every pointing. The data from XRT and UVOT are downloaded from HEASARC data portal, maintained by NASA. The standard procedures prescribed by respective instrument team are used for analysis. We have used recent version of HEASOFT package (v6.12) along with the updated calibration database (dated 25 March 2012) for serving the purpose. The following sections discuss the data analysis methodology to generate the science product using different instrument data.

XRT

The XRT is a sensitive, flexible, autonomous X-ray CCD imaging spectrometer designed to measure the position, spectrum, and brightness of gamma-ray bursts (GRBs) and afterglows over a wide dynamic range covering more than 7 orders of magnitude in flux. The Beppo-SAX satellite showed that accurate positions of gamma ray bursts can be effectively determined using a high-resolution X-ray telescope, since all of the GRBs observed within 6-8 hours after the burst by the Beppo-SAX X-ray telescopes have fading X-ray counterparts or afterglows, whereas only about 60% have optical afterglows. However, by the time that Beppo-SAX is able to observe a typical X-ray afterglow, its intensity has already dropped by 4-5 orders of magnitude. The Swift XRT will begin observations before the GRB ends in many cases, and will fill in the large time gap during which the Lorentz factor of the relativistic blast wave changes from 100 to < 10. It will refine the BAT positions (1-4' uncertainty) to 2.5 arcseconds within 10 seconds of target acquisition for typical bursts, allowing ground-based optical telescopes to begin immediate spectroscopic observations of the afterglow. GRB positions and X-ray spectra are transmitted in near real time through TDRSS to the GCN network on the ground for broadcast to the world-wide gamma ray burst community.

The standard procedures, prescribed by the instrument team, are used to generate the science product using the raw event files downloaded from HEASARC. The *xrtpipeline* script, a part of HEASOFT package, is used to generate the level-2 cleaned event file. This script makes use of default parameters as inputs. The pipeline generates the spectrum and lightcurves as products. However, we performed proper grade and region filtering to generate the lightcurve and spectrum using level-2 cleaned event files. The grades 0-12 and 0-2 are selected for *pc* and *wt* modes of XRT, respectively. The source specrtum and lightcurve are then generated using appropriate region filtering. The 15° circular area centred at source position was used as source region. While the background light curve and spectrum are generated after using the four source free circular regions (each with radius of 50 pixels) near the source as background region. The required ancillary response matrix is generated by using task *xrtmkarf* followed by *xrtcentroid*. The response matrix file provided with the CALDB distribution is used for further analysis. The resulting spectrum were then fitted using *XSPEC* utility.

The data used for spectral fitting range between 0.2 10.0 KeV. The *simple power* law along with the warm absorption (*wabs*) gives the best fit for almost all the observations of interest. The model parameter $N_{\rm H}$, the galactic column density, is kept fixed at a value of 5.5×10^{22} cm^{-2} (Kalberla et al., 2005). The fitted model flux is then used for constructing lightcurve. However in many places we have used the count rate for generating the lightcurves.

For constructing SEDs, we estimated the photon flux in several small energy bins using interactive plotting utility (IPLOT), a part of PGPLOT, while fitting with XSPEC. The Galactic extinction correction is done by using unabsorbed flux in the following manner. First of all, modelled photon flux is calculated for all small energy bands using IPL with an appropriate value of parameter nH for that direction (as already discussed above). Then the same is repeated using $N_{\rm H} = 0$ which assumes no absorbing material in that particular line of sight. The ratio between absorbed and unabsorbed model photon fluxes gives the absorption factor. This factor is then used to correct the observed photon flux calculated by IPL in order to get intrinsic photon flux. The galactic extinction corrected photon flux respective to different energy bins are then converted into energy flux using proper conversion factor and used to construct SEDs.

UVOT

UVOT is an UV/Optical telescope coaligned with the XRT making Swift a complete multiwavelength facility. Co-aligned with the XRT, UVOT provides simultaneous ultraviolet and optical coverage (170-650 nm) in a 17' × 17' field. Despite its limited aperture, UVOT is a powerful complement to other instruments because of its UV capabilities and the absence of atmospheric extinction, diffraction, and background. Since UVOT has photon counting detectors, which are able to retain individual photon positions and timing information, it operates in a mode more similar to typical x-ray telescopes than to typical optical telescopes. The UVOT is a 30 cm modified Ritchey-Chretien UV/optical telescope coaligned with the X-ray Telescope and mounted on the telescope platform common to all instruments. An 11-position filter wheel allows low-resolution grism spectra of bright GRBs, magnification, and broadband UV/visible photometry. Photons register on a microchannel plate intensified CCD (MIC).

UVOT snapshots with the six filters, V (5468 $\AA$), B (4392 $\AA$), U (3465 $\AA$), UVW1 (2600 $\AA$), UVM2(2246 $\AA$) and UVW2 (1928 $\AA$) for all the obsIds (Tables.1), were integrated with the *uvotimsum* task and analysed by using *uvotsource* task, with a source region of 5 arcsec, while the background was extracted from an annular region centered on the blazar with external radius of 40" and internal radii of 7" Foschini et al. (2010). The observed magnitudes from all obsId are then corrected for extinction according to the model described in Cardelli et al. (1989). The magnitudes thus obtained are converted to energy flux (erg^2 cm^{-2} s^{-1} Å^{-1}) using following equation:

$$F_\lambda = FCF \times 10^{(ZPT-m)/2.5} \tag{2.3}$$

where ZPT is zero point flux, FCF is the flux conversion factor [erg^2 cm^{-2} count^{-1} Å^{-1}] and m is the observed magnitude in a particular filter. These values are taken from instruments calibration database (CALDB, Young et al. (1991); Howell (2006)). The light-curves are then constructed by using flux values in filters V, B, U, UVW1, UVM2, and UVW2. The UVOT flux averaged over the period of interest, are used to construct the Spectral Energy Distribution (SED) of the source.

2.4.2 Fermi-LAT data

The Fermi Gamma-ray Space Telescope, formerly GLAST, has opened up high-energy world to exploration and helping us answer many questions. With Fermi, astronomers have a superior tool to study how black holes, notorious for pulling matter in, can accelerate jets of gas outward at fantastic speeds. Physicists are able to study subatomic particles at energies far greater than those seen in ground-based particle accelerators. And cosmologists are gaining valuable information about the birth and early evolution of the Universe. In principle Fermi can be thought as an extension of Compton Gamma-Ray Observatory (CGRO) with better sensitivity over broad energy coverage. Fermi observatory have two instruments onboard 1.) Large Area Telescope (LAT: ΔE 0.03 - 300 GeV) and 2.) Gamma-Ray Burst Monitor (GBM). The Fermi spacecraft orbits the earth in about 96 minutes. It is oriented to point the LAT upward at all time, so the earth does not block the view. On alternate orbits Fermi rocks to the left and right, allowing the LAT to cover more of the sky. Thus the whole sky can be surveyed in two orbits. This mode of operation allows for constant monitoring of any gamma-ray emitter over days, weeks, months and years. When a strong gamma-ray burst occurs, Fermi will point itself at the location of the burst for a few hours to collect extra data.

The Large Area Telescope (LAT) is the principal scientific instrument on the Fermi Gamma Ray Space Telescope spacecraft. Originally called the Gamma-Ray Large Area Space Telescope (GLAST), the mission was renamed for the physicist Enrico Fermi. The Fermi spacecraft was launched into a near-earth orbit on 11 June 2008. The design life of the mission is 5 years and the goal for mission operations is 10 years. The Fermi LAT instrument collaboration is an international effort, funded by agencies in several countries. The LAT is an imaging high-energy gamma-ray telescope covering the energy range from about 20 MeV to more than 300 GeV. Such gamma rays are emitted only in the most extreme conditions, by particles moving very nearly at the speed of light. The LAT's field of view covers about 20% of the sky at any time, and it scans continuously, covering the whole sky every three hours. This instrument is having a series of 9 stacks of slicon-strip detectors (SSDs) being used as tracker, enabling the direction determination of incoming photons (Atwood et al., 2007). Below to these SSDs a Calorimeter is used (Grove et al., 2007). The primary purpose of calorimeter is two fold i) to measure the energy deposition due to electromagnetic particle shower that results from $e^{-}e^{+}$ pairs produced by incident photons, and ii) image the shower development profile, thereby providing an important background discriminator and estimator of the shower energy leakage fluctuations. Each calorimeter module has 96 CSI(Tl) crystals, with each of size 2.7 cm $\times$ 2.0 cm $\times$ 32.6 cm. More technical details about the instrument design and working can be found in (Atwood et al., 2009). The data is freely available to the scientific community within few hours. These data can be downloaded from Fermi-Science support center, NASA, USA.

The *gamma*-rays observations [0.03 - 200 GeV] made by Large Area Telescope (LAT) onboard Fermi telescope gamma-Ray observatory are analysed for few blazars. The PASS7 event data are used for constructing science product. We have used most recent version of ScienceTools (v9r27) software packages provided by Fermi-team is used following the standard prescriptions. The procedures, in detail, for data handling and simple caveats for generating scientific products are given by Fermi Science Support Center (FSSC)[1].

The PASS7 photon data set with a region of interest of 15° for CGRaBS J0211+1051 was obtained from Fermi data archive. The latest version of

[1]http://fermi.gsfc.nasa.gov/ssc/data/analysis/scitools/

ScienceTool (v9r27) and calibration files are used. The photon data with zenith angle $\geq 100°$ are discarded in order to avoid the contributions from earth albedo. The unbinned likelihood analysis method is used to reconstruct the source energy spectrum. For this, first of all coordinate, time, energy and region selection are performed on the raw event file to avoid unwanted contributions. The output file of previous step is again corrected for detector live time. A source model is constructed using the contributory python script *make2FGLxml* incorporating the latest *Fermi*-LAT catalog *gll_psc_v07.fit*, diffuse background components *gal_2yearp7v6_v0.fits* and extra-galactic background *iso_p7v6source.txt*. The Galactic diffuse emission model is generated using the GALPROP package and available online as a contributory file, while the extra-galactic one is described by a simple power law (Abdo et al., 2009).

The light-curve and SED are generated using likelihood analysis. Aperture photometry was also performed to cross check the the trends observed in lightcurves. We have adopted the similar methodology as used by Foschini et al. (2010); Foschini (2011); Foschini et al. (2011c,b) and discussed here briefly. First, the complete data are used for likelihood analysis using energy band of 0.1 to 100 GeV in order to determine the best fit source model. We found that *powerlaw2* model is the best fit source model as indicated by high test statistics (**530.9**). The powerlaw index value for the present fit is 2.03 ± 0.06. The same source model with this power law index is used for constructing light curve. The one day and three day time bins are used when generating light-curve. The flux with TS ≥ 9, equivalent to $\sigma \sim 3$, are used for constructing lightcurve.

For extracting SED the event file is binned in several energy bins (*100MeV - 500MeV, 500MeV - 1GeV, 1GeV - 5GeV and 5GeV - 50GeV, 50GeV - 100 GeV and 100GeV - 200GeV*) and likelihood analysis is performed for each energy bin to get energy flux for respective energy bands. The source model used are source dependent and are discussed in detail wherever used. For each energy bin the source under investigation and all nearby sources in the region of interest (ROI) are described by one parameter representing the integral flux in that energy bin. The diffuse background components are modelled with one single parameter, describing the normalization. The upper-limit estimation is done for the energy bins with TS ≤ 9 [$\sim 3\sigma$].

The following tools provided as a part of software distributions are used for the analysis done here. The *gtselect* and *gtmktime* are used for event selection and live time correction respectively. The *gtltcube*, *gtdiffrsp* and *gtexpmap* are used for generating livetime cube, Galactic diffuse response, and exposure map respectively. Last tool which is used for final likelihood analysis is *gtlike*. It provides the test statistics for source model fit along with the other model parameters.

2.4.3 Other archival data

In order to study the spectral energy distribution and lightcurves we have also made use of data from other resources namely MOJAVE, NED, VLBI etc. We have also used the optical polarization measurements observed by Steward Observatory, University of Arizona, USA. Most of these data are archival and in almost usable form. More detailed about the data resources and analysis procedures, if required, are discussed separately wherever used.

Chapter 3

Intranight optical variability in BL Lac object *S5 0716+714*

3.1 Introduction

The variability at almost all energy regimes is a defining property of the active galactic nuclei and therefore, can be used to study structure and physical mechanisms responsible for their emission. The variations occur at time scales ranging from sub-hour to several years. Short term variations put constraints on the size of the emission regions. In this chapter, we discuss rapid variations in blazar S5 0716+714 during a flaring epoch and estimate various physical entities.

S5 0716+714 is a well studied BL Lac object which was first detected by a Radio Survey in 1979 by Kuehr et al. (1981). It was included in the S5 catalog of the Strong Source Survey performed at 4.9 GHz (Kuehr et al., 1981, 1987; Witzel, 1987; Witzel et al., 1988). The source also belongs to the bright ($S_{5GHz} < 1Jy$) flat spectrum sub-sample of S5 catalog which has been studied extensively at radio frequencies. The radio maps obtained from several such studies clearly show a compact core-jet structure and extended emission looks like a double source perhaps of a Fanaroff-Riley class II (FR II, cf Chapter 1) object embedded in an oval cocoon (Antonucci, 1986; Gabuzda et al., 1998). The kinematic study of this source established the existence of superluminal motion (Gabuzda et al., 1998). According to a recent study by Jorstad and Marscher (2001), S5 0716+714 shows the value of proper motion as 11-15 $h^{-1}c$. The Very Long Baseline Array (VLBA) studies show evidence of quasi periodic ejection of emitting blobs occurring every $\sim$ 0.7 years. Multi-frequency Very Long Baseline Imaging (VLBI) study of S5 0716+71 by a group at Bonn (Bach et al., 2002, 1992-2002), presents a very consistent scenario of faster motion to the Jorstad and Marscher (2001). The combination of around 26 VLBI observations at 5-22 GHz results in apparent velocities of 5-10 $h^{-1}c$, with different component moving at slightly different speed. The polarization studies of this source at 6 cm revealed the rapid variability in polarization which is probably produced at about 25 mas from the nucleus (Gabuzda et al., 2000b,a).

BL Lac objects either show very weak or absolutely no emission line feature in their optical spectra. The optical spectroscopic observations of S5 0716+714 failed to reveal any spectral feature (Stickel, 1993; Rector and Stocke, 2001) making estimation of its redshift difficult. There are several other methods one can use to determine redshift of BL Lac objects but with relatively poor precession. Wagner (1996) inferred an upper limit of $z \geq 0.3$ from the absence of host galaxy and small angular size of the extended halo in radio maps. Later Nilsson et al. (2008) estimated the redshift of this blazar to be $z \geq 0.3 \pm 0.08$ based on assumption that the host galaxy of S5 0716+714 is of average luminosity. They performed deep I-band photometry during it's optically faint state and could get a weak signature of host. The host galaxy was found to have an I-band magnitude of 17.5 $\pm$ 0.5 and an effective radius of 2.7 $\pm$ 0.8 arcsec.

One of the very well known characteristics of the blazars is variable continuum emission throughout the energy spectrum. The flux variations for S5 0716+714 are observed with various timescales at almost all the frequencies (Wagner, 1996; Raiteri et al., 2003; Baliyan et al., 2005; Foschini et al., 2006; Carini et al., 2011; Chandra et al., 2011a, and references there-in). Very short time scale variability is also seen in optical polarization studies (Impey et al., 2000). The possible quasi-periodicities observed in Impey et al. (2000) is 12.5, 2.5 and 1.4 days. The flux variations with timescales of days or greater known as Interday while the variations corresponding to the timescales of less than few hours are known as Intranight/Intraday or microvariations. The flux variation in blazars are direct manifestations of the physical processes occurring in the jet. The optical emission in blazars is mostly dominated by synchrotron processes in the jet (particularly when the source is flaring) while other components coming from the regions exterior to the jet namely disk, corona, BLR and NLR may also contribute, depending upon the brightness state of source. The component dominating the overall emission governs the characteristics of the energy output. The different timescales of flux variations observed at different energies indicate the mechanisms responsible for blazar emission. The extensive study of flux variations for this source with a range of timescales over different frequencies have been performed by many workers (e.g., Quirrenbach et al., 2000; Villata et al., 2000; Nesci et al., 2002; Xie et al., 2004; Nesci et al., 2005a; Pollock et al., 2007; Gupta et al., 2008; Poon et al., 2009; Rani et al., 2010; Fan et al., 2011; Chandra et al., 2011a; Dai et al., 2013; Larionov et al., 2013). The flux variations down to a timescale of few days can be interpreted well with our present understanding of the emission processes and blazar jets. The most reliable models used are shock in jet model, micro-lensing effect, helical jet model and bending of jet (e.g., Gopal-Krishna and Subramanian, 1991; Mangalam and Wiita, 1993; Marscher and Gear, 1985b; Qian et al., 1991; Marscher, 1996a,b; Gopal-Krishna and Wiita, 1992). Rani et al. (2010); Chandra et al. (2011a); Nesci et al. (2005b) reported rapid optical variations with timescales of 15-20 minutes which can not be explained using traditional models. Since the associated size of the region estimated using light travel time argument [Equ. 1.5] will be smaller than the lowest stable orbit of the black hole, it can not be used to infer the size of the emission region. The Physical processes responsible for micro-variations are not understood and therefore an extensive monitoring of blazars for longer durations is required.

The position of blazar S5 0716+714 in the sky [RA 07 21 35.5 DEC

71 35 36.35] makes the object very suitable for the study of microvariations. Being close to celestial north, this source can continuously be monitored for more than 5 hours every night during an observing season at observatories in northern hemisphere. At our observatory (MIRO: Longitude 23.1, Latitude 72.5) this source can be continuously monitored for more than 6 hours every night. We have conducted variability study of Blazar S5 0716+714 during the course of approximately seven years from Mt. Abu Infrared Observatory. In this chapter we have investigated in detail the intranight optical variations observed during March 2010 optical flaring state. This event was reported by an Astronomical Telegram. The following sections will discuss how intranight variability study can be used to reveal several properties of the blazars.

3.2 Observations & data analysis

The photometric observations were carried out by using the liquid nitrogen cooled CCD-Camera mounted at the f/13 Cassegrain focus of the 1.2 m Telescope at Mt. Abu Infrared Observatory, Gurushikhar, Rajasthan, operated by the Physical Research Laboratory, Ahmedabad, India. The PIXELLANT CCD Camera has 1296 $\times$ 1152 square pixels each with 22 micron size and a total read out time of about 13 seconds. With a scale of 0.29 arcsec per pixel, the total field of view is about 6.5X 5.5 arcmin^2. The CCD read-out noise is 4 electrons and the dark current is negligible when cooled. The CCD-photometric system is equipped with Johnson-Cousin UBVRI filter set. The source was observed in two observing slots; during 2010 March 08-10 and 2010 March 19-20. All the observation nights were photometric with a seeing better than 1".5. Several bias frames were taken every night at the beginning and the end of the observations. To construct master flats, we have taken large number of evening twilight sky flats in all the bands each night. Observation strategy was to take 4-frames each in B,V, R and I band and then to monitor the source in R-band for several hours. The field of view was large enough to accommodate several standard stars in the target frame to facilitate calibration. The exposure times were 30 secs in I, R and V bands and 60 secs in B band.

Date	T_{start}(UT)	Duration (h)	No of images
2010 March 08	14:53:51	3.2	248
2010 March 09	14:39:36	3.4	265
2010 March 10	14:44:44	4.0	294
2010 March 19	14:24:16	0.06	5
	17:24:27	0.30	24
2010 March 20	14:11:53	3.3	201

Table 3.1: Observation log for monitoring in R-band

Table 1 presents the details of the observations, giving date, time (UT) of starting observation, duration of monitoring (hours) and total number of observation points on the source. The data reduction is performed using standard routines in IRAF[1] (Image Reduction and Analysis Facility) software. On the bias subtracted, flat fielded images, differential aperture photometry was performed using DAOPHOT package available in IRAF. The photometry is carried out using several aperture radii, ranging from 1 to 9 times the FWHM. The right size of the aperture is chosen keeping in mind the optimum value of S/N ratio and the prescription of Cellone et al. (2000) to avoid spurious variations. If the aperture is too large, nuclear emission is diluted by the contribution from the thermal emission of host galaxy leading to low S/N, while a very small aperture would lead to signal getting adversely affected by the seeing variations caused by atmospheric turbulence. Based on these criteria we use 4.5 arcsec as aperture radius for the target and other stars used in the differential photometry. We have used standard stars 6 (R=13.26 mag) & 5 (R=13.18 amg) from Villata et al. (1998), having apparent magnitudes close to that of the source to check the variability of the blazar. Such a choice of the

[1]IRAF is distributed by the NOAO, operated by the Association of Universities for Research in Astronomy, Inc., under cooperative agreement with the National Science Foundation

comparison and control stars is necessary to avoid any disparity in the measured dispersions of the target-comparison and comparison-control light curves (Howell et al., 1988) due to photon statistics. One star is used to correct the source magnitude and the other as a control star to check the stability.

To check the significance of intra-night variability, we performed the F-test incorporated in the R statistical package. The F-statistics is the ratio of the sample variances, or $F = S_B^2/S_C^2$ where S_B^2 is the variance in the blazar magnitude and S_C^2 is that in the standard stars during the whole night of observations. For all the five nights, the F-values are more than 9 with a significance level of 0.999995 or $\geq 5\sigma$. We have also calculated the intra-night variability amplitude which is given by

$$Amp = \sqrt{(A_{max} - A_{min})^2 - 2\sigma^2} \tag{3.1}$$

where A_{max} & A_{min} are the maximum and minimum values in the light curves and σ is given as follows

$$\sigma = \sqrt{\frac{\Sigma(m_i - \bar{m})^2}{N-1}} \tag{3.2}$$

where $m_i = (m_{S6} - m_{S5})_i$ is the differential magnitude of stars 6 and 5 for the i^{th} observation point while $\bar{m} = (m_{S6} - m_{S5})$ is their differential magnitudes averaged over the entire dataset, and N is the number of observation points obtained that night in a particular band. As the errors are subtracted from the total measured variability, Equ. 3.1 gives fairer estimate of the amplitude of variability in the source. The results from such analysis of our data for each night are discussed in next section.

3.3 Results & discussion

The light curves for the source were obtained by adopting above mentioned analysis procedure. The observed magnitudes of the source in B,V,R, & I bands are calculated with respect to the standard star 5 and nightly averaged values are plotted as a function of time in MJD in Fig 3.1 for 2010 March 8-10 and 19-20. In Fig 3.2, we plot R-band light curves showing intra-night variations during individual nights. The bottom curve in each panel shows differential light curve of the stars. The observational uncertainties are the *rms* errors of the nightly differential magnitudes of the calibration star 5 and check star 6 as given in Equ. 3.2. The typical *rms* errors for the R-band are less than 0.008 mag. These R-band magnitudes for S5 0716+71 for all the nights of observation are given in Table 2.

Table 3 lists the result of the F-test, giving the date of observation, F-value, standard deviation in the differential magnitudes of stars and the amplitude of variation in the source each night. On March 19, we have five data points at the beginning and 24 data points at the end of the night, covering about 3.5 hrs. The F-value for this night, therefore, is obtained from these limited measurements. The tabulated values for all the nights indicate that the source is significantly variable during present observing run, showing 100% duty cycle for variation. Similar result has been reported by other workers (e.g., Wagner and Witzel, 1995b) which emphasizes that S5 0716+714 is very active source, showing variations almost always. The F-test results are in very good agreement with the values obtained from the variability test (Jang and Miller, 1997). Here confidence level of variability is defined by the parameter C=σ_T/σ, where σ_T is the standard deviation in the differential light curve of the source and comparison star. The source is considered variable at 99% confidence level if $C \geq 2.576$. Our values for the variability parameter for 8, 9, 10 and 20 March are, 7.66, 3.35, 4.72 and 4.45, respectively, confirming significant variability in the source on all the nights. To further support the genuine nature of the microvaribility reported here, we note that the host galaxy is more than 4-magnitude fainter (at I= 17.5 mag) as compared to the source (Nilsson et al., 2008) ruling out any significant effect on the source variability. It adds credence to the intrinsic nature of variability in the source flux through out this observing epoch.

The variation rates (mag/hour) for various flares appearing in the light curves of each night of observation are calculated by fitting a straight line in the rising and falling segments using least square fitting algorithm. Nesci et al.

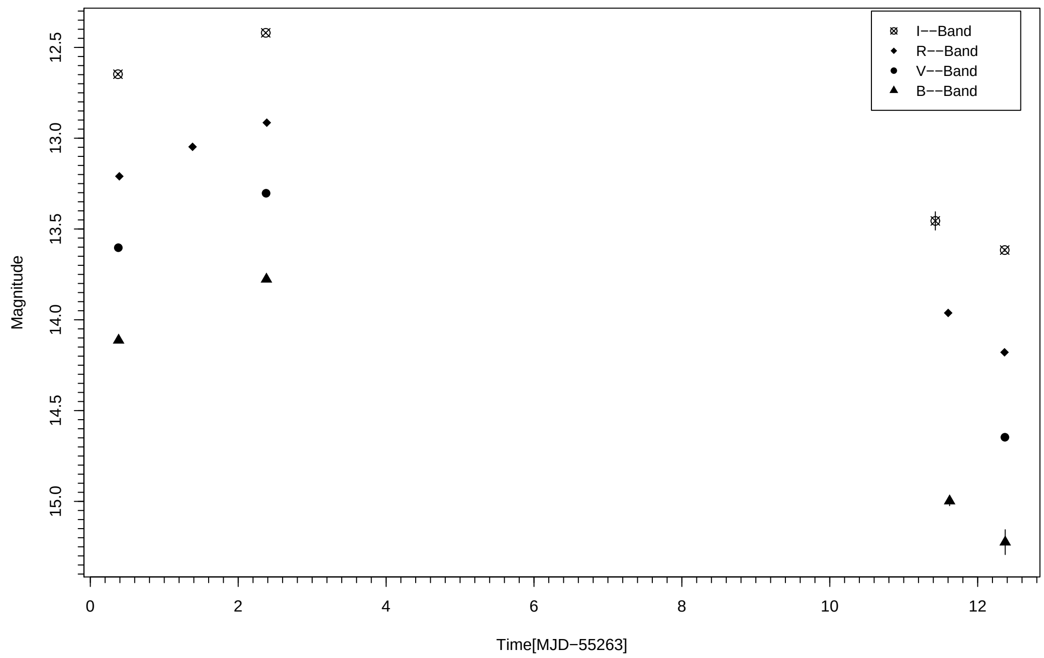

Figure 3.1 Nightly averaged B,V,R & I magnitudes for S5 0716+71 as a function of time during 2010 March 8-10 & 19-20. Most of the error bars ($\pm\sigma$) lie within the symbol.

(2002) studied intra-night variability of S5 0716+71 for 52 nights and claimed a variation rate of 0.02 mag/hour along with a maximum rising rate of 0.16 mag/hour while Montagni et al. (2006) reported equally fast variation rates of 0.1 - 0.16 mag/hour. In the following we discuss results obtained in the present study.

3.3.1 Inter-night variations

Fig.- 3.1 shows nightly averaged B, V, R & I magnitudes as a function of time (MJD) for all 5-nights. It is evident that S5 0716+71 brightens by 0.34, 0.3, 0.3 & 0.24 magnitudes in B, V, R and I bands, respectively, during 2010 March 8-10. During March 19-20, source decreases in brightness by 0.23, 0.22 and 0.21 mags in B, R and I bands, respectively. Evidently, during our

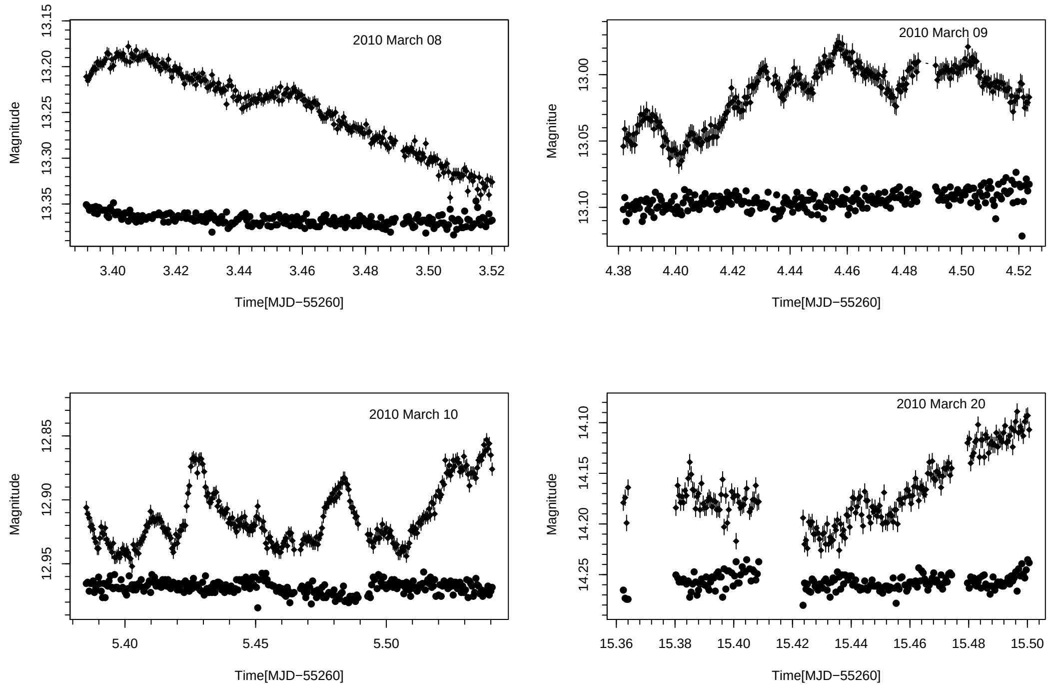

Figure 3.2 R-band light curves showing INOV for S5 0716+71 on 2010 March 08, 09, 10 and 20. Lower curve in each panel shows differential light curve for comparison and control stars plotted with appropriate offsets.

observations blazar S5 0716+71 was brightest on March 10 (R≈ 12.914 ± 0.008 mag) and faintest on March 20 (R≈ 14.179 ± 0.006 mag). The figure also gives clear indication that the source is mildly bluer when brighter and redder when fainter. During the period of eight days (March 11-18), when we do not have observations, S5 0716+71 became fainter by about 1.10 (R-band) and 1.49 (B-band) magnitudes, clearly showing increase in the amplitude of variation with the frequency during same period.

3.3.2 Intra-night variations (INOV)

From the light curves in Fig- 3.2, it is evident that the blazar S5 0716+71 is showing significant INOV on almost all the nights it was monitored. Here we discuss the variability behaviour night by night.

On 2010 March 8, the source brightens up to $R \sim 13.185$ mag at MJD = 55263.40. It then decays to $R \sim 13.335$ mag at MJD = 55263.52, a variation of 0.15 mag during 2.88 Hrs (decay rate $\approx$ 0.052 mag/hour). This smoothly falling curve is superposed by a flicker (between MJD55263.44 and MJD55263.465) brightening the source by more than 2σ within a time scale of about 15min.

The blazar S5 0716+71 appears to be very active during the 2010 March 9 night (cf Fig- 3.2). The source is in brightening phase with several rapid fluctuations modulating a smoothly varying intra-night light curve. During the first microvariability event of the night, source fades by 0.032 mag ($> 5\sigma$) with a time scale of $\approx$ 15 mins. It then brightens to its highest value (R=12.976 mag) at MJD=55264.456 within a time span of about 1.24 Hrs (rise rate 0.063 mag/hr). The source then decays by 0.05 mag within 0.48 hr towards the end of the observations.

Date	$F - Value$	σ(mag)	$Amp(\%)$
2010 March 08	38.82	0.006	16.8
09	11.27	0.006	9.1
10	20.51	0.005	9.9
19	98.54	0.004	12.8
20	19.73	0.008	14.4

Table 3.2: Intra-night variability results

The statistical analysis of the light curves shows fast variation rates (up to $\sim$ 0.38 mag/hour) for several segments on March 10. During this whole night, source remains in bright state with rapid fluctuations in the intensity. We have recorded most rapid fluctuation during this night. For the most significant peak we have calculated the rise and fall rates $\sim$ 0.38 mag/hour & $\sim$ 0.08 mag/hour, respectively. Towards the end (from MJD 55265.502 to MJD 55265.539), S5 0716+71 brightens by 0.09 mag in R-band within about 53 mins. The source also shows several microvariability events on a time scale of about 15 mins. On March 19, we have few observation points in the beginning and end of the night. However, the trend shows significant variation, about 0.1 mag in 3.5 hours of duration. The light curve for this night is not shown here. On March 20, source is initially stable but later (at MJD= 55275.43) starts brightening, changing by 0.12 mag in 1.68 hrs (0.07 mag/hr). Source is generally faint during these two nights and microvariability, if any, is washed out in the relatively large scatter (0.008 mag).

Let us now discuss our results in detail. The present observations reveal significant variability at intra-night (1.24 hr to 2.88 hrs), inter-night (night-to-night to 9 nights) time scales as well as microvariability (15 mins or more) or fast fluctuations. Similar behaviour for S5 0716+71 is reported by Carini et al. (2011) in their 2003 March 5-9 observations made in B and I bands. As mentioned above, to avoid the spurious variations caused by the variation in the seeing and/or contamination by the thermal emission from unresolved host galaxy, we have carefully chosen aperture and comparison/control stars. In order to delineate small scale fluctuations, we have used best temporal resolution ($\approx$ 45 seconds) ever used to detect micro-variations for any source. Many authors have reported INOV and microvariability for this source at similar time scales of variation (e.g., Quirrenbach et al., 1991; Villata et al., 2008b; Carini et al., 2011)) but with few minutes to tens of minutes temporal resolutions. Zhang et al. (2008) have reported fast variations with 6 minutes to 33 minutes time scales with unusually large (> 1 magnitude) amplitude of variations. They do not mention about the aperture size adopted but have used exposure times ranging from 4 minutes to 7 minutes and have calibrated the source magnitude with the brightest star in the field. Some of these are prescriptions for spurious variations as investigated by Cellone et al. (2000). Also, there is no report of such rapid (few minutes) variation with such high amplitude of variation for this source by any group to our knowledge. We have monitored this source for more than 200 hundred night during last seven years (as will be discussed in next chapter) and we have not detected such a high value of amplitude of variation in intra-night (many epochs with more than 4-hours of monitoring) observations. We, therefore, strongly feel that results reported by Zhang et al. (2008) are not correct.

3.3.3 Mechanisms for variability

The observed optical emission in blazars originates in a part of the accretion disk and the inner (pc-scale) regions of the jet. In the light of this, one can discuss the possible reasons behind the variations over various time scales. We should also keep in mind that optical variability time scales shorter than a few hours would imply emitting regions to be smaller than the Schwarzschild radius for certain objects, depending upon their mass. There are a host of models to explain extrinsic and intrinsic variability in blazars; microlensing effect (Chang and Refsdal, 1979), light house effect (Camenzind and Krockenberger, 1992), accretion disk models (Chakrabarti and Wiita, 1993; Mangalam and Wiita, 1993) and shock-in-jet model (Marscher and Gear, 1985b). So far as our observations presented here are concerned, we notice mild chromatic behaviour (bluer when brighter) in the inter-night light curves. Our intranight light curves do not show any symmetry or periodicity and the variability time scales are short, ranging from few tens of minutes to few hours. Such fast variations with amplitude of variations reported here are difficult to explain by the models invoking instability in the accretion disk. Since the blazar emission is dominated by the jet radiation, we concentrate on relativistic jet models. Also, since the flares/variations are aperiodic, chromatic and with asymmetrical shape, micro-lensing and light-house effects as causes of variation are ruled out.

A mild chromatic behaviour in the long term variation is explained by Villata et al. (2004b) and Papadakis et al. (2007) for BL Lacertae, using the data obtained during several WEBT (Whole Earth Blazar Telescope [2] campaigns covering the period from 1997 to 2002, by the variation in the Doppler factor due to the change in the viewing angle. They interpreted flux variability in terms of two components; long-term (few days time scale) variation component as a mildly chromatic event and a fast (intra-day) varying component

[2]www.to.astro.it/blazars/webt/

characterizing strong bluer when brighter chromatic behaviour. If the intrinsic source spectrum is well described by a power law, a Doppler factor variation does not imply a colour change. But a mildly chromatic behaviour could be due to Doppler factor variation on a spectrum slightly deviating from power law. A change in Doppler factor changes both, the flux ($F_\nu \; \alpha \; \delta^3$) and the frequency ($\nu \; \alpha \; \delta$) of emission. The inter-night variations reported here for S5 0716+71, which show mild chromatic behaviour, could be the result of the change in Doppler factor.

Rapid variability can be produced when a relativistic shock wave or a blob propagates down the jet with turbulent plasma (Marscher et al., 1992; Qian et al., 1991). Synchrotron emission gets enhanced when the shock encounters particle or magnetic field over-densities. The amplitude and the time scale of the variation depend on the turbulence and shock thickness. Fast variations, thus require shocks to be very thin and emission to originate from very close to the central engine. Based on our shortest intra-night variation time scale (t_v) of 1.24 hrs, the upper limit on the size of the emission region, with Doppler boosting and cosmological corrections, $R \leq t_v \delta c/(1+z)$ is $\approx 2 \times 10^{15}$ cm where c is the speed of light and δ be the Doppler factor (taken as 20 here). Considering this size as a bound on the Schwarzschild radius of the central engine, one can estimate its mass using $M \approx (c^2 R)/3G$, which comes out to be $\approx 1.1 \times 10^9 M_\odot$ which is in accord with values obtained by various other workers. However, estimation of black hole mass using such fast optical variations must be taken with caution (Quirrenbach et al., 1991). The variations shorter than INOV (microvariations) amounting to few tens of minutes as reported here and by many other authors can not possibly be explained by the shock-in-jet model. These are perhaps due to either small fluctuations intrinsic to the jet or imprinted by small fraction of black hole horizon (Begelman et al., 2008). Such fast variations may not represent linear dimension of an emission region.

3.4 Conclusions

Here we have reported intra-night variations and micro-variability in blazar S5 0716+71 as observed in the highest ever temporal resolution observations carried out during 2010 March 8-10 & 19-20. These high resolution observations with ≈ 45 second exposures are able to clearly de-lineate micro-variations. We note that the source was variable with 100% duty cycle at various time scales during whole observation epoch. Inter-night behaviour of the source appears to be bluer when brighter from the limited observations. It is evident that S5 0716+71 was highly active during 2010 March 9, 10 and 20 with rapid flickers superposed on the slowly varying intra-night light curves. On March 19 it shows substantial decay but we do not have full coverage of the night to comment on the nightly variation behaviour.

The source shows various time scales for the variation, ranging from close to two hours to 15 minutes. Since light curves show asymmetric and aperiodic flares, we rule out geometric effects as cause of variation. The inter-night variations showing mild bluer when brighter nature could be due to changes in the Doppler factor, or injection of higher energy population of electron compared to relatively cooler old population. While intra-night variations with few hours time scales are probably due to interaction of fast moving shocks in the jet with local small scale inhomogeneities, it is very difficult to associate faster variations with spatial extent of the emitting region. Perhaps these variations originate in a small region of the blob. Taking the shortest intra-night variability time scale of 1.24 hour, the linear size of the emitting region is estimated to be $\approx\ 10^{15}$ cm and with corresponding Schwarzschild radius, $\approx 1.1 \times 10^{9} M_{\odot}$ is mass of the black hole.

Chapter 4

Long term variability in BL Lac object *S5 0716+714*

4.1 Introduction

The variability has been one of the most powerful tools in revealing the nature of AGN, particularly when the inner-most regions of the central engine, where-from most emission processes are supposed to originate, are not resolvable by present day facilities. Blazars vary on diverse time-scales which can be, broadly, divided into three categories: intra-night variability (INV or IDV) or micro-variability, short-term (few days to few months) outbursts and long-term (months to several years) trends. While shortest variability (micro-variability) time-scales are important for understanding the geometry of the jet, mass of the black hole and magnetic field strengths based on emission zone size, physical processes in the jet and accretion disk manifest themselves in the long term variations. Some sources even show long-term quasi-periodic variations, sometimes explained by the binary black-hole models (e.g., 11.6 year periodicity in OJ287, (Sillanpaa et al., 1988)). The very long baseline interferometry (VLBI) maps are able to locate stationary radio core from which blobs (shocked regions) are being ejected and move away at apparent superluminal speeds. These shocks moving down the jet are thought to cause outbursts lasting several days to weeks (Marscher and Gear, 1985a; D'Arcangelo et al., 2009). The intra-night time-scale variability, though well established phenomenon in blazars, is less understood as is its relationship, if any, with the long-term variations. Clues to such relationship could possibly come from long-term monitoring of blazars which might also help discriminate among models proposed for flux variation.

BL Lac object S5 0716+714 is one of the optically brightest blazars which is also highly variable. It is one of the sources which are available in the sky for long hours to enable monitoring suitable for intra-night variability study. In earlier Chapter we discussed rapid variations in this source, reporting fastest rate of change during March 2010 which was used to estimate size of the emission region and related entities. However, there are several other questions we need to address: How frequent is intra-night variability in blazars in general and blazar S5 0716+714 in particular? What is the nature of variations when source is in bright/quiescent phase? Whether the source brightness shows any frequency dependence, particularly during variation? Whether faster variations have any relationship with long-term trends? Key to answer such questions perhaps lies in long-term monitoring of a sample of blazars. Blazar S5 0716+714 is a good candidate for such study. In the past, it has been used for such study, in limited way, by several workers (see,e.g., Zhang et al., 2012, and references there-in). Nesci et al. (2005a) reported extremely high duty cycle [>90 %] and a rate of magnitude variation as 0.11 mag per year during 1994 to 2003, while Zhang et al. (2012) reported $\approx$ 78% as duty cycle of variation. The duty cycle of variability of an object is the fraction of the total monitoring nights when source was reported be significantly active.

Here we use long term (2005 to 2012) monitoring data of S5 0716+714 obtained from Mt Abu Observatory to discuss nature of light curve and determine duty cycle of variation for this source while trying to address other relevant issues raised above.

4.2 Observations and data analysis

The optical monitoring of blazar S5 0716+714 was performed using liquid nitrogen cooled CCD camera [1296×1152 pixels] at the f/13 Cassegrain focus of 1.2m optical telescope installed at Mt. Abu Infrared Observatory (MIRO), Rajasthan, India. The altitude of the observatory site from sea level is ≈ 1680 meters. The weather and seeing at this site are good enough to accommodate approximately 180 photometric nights every year. However allocation of nights to blazar monitoring program is limited due to sharing of the telescope with other scientific programs. BL Lac object S5 0716+714 was observed for 162 nights in I, R, V and B optical bands [filters: Cousins & Johnsons] during the span of $\approx$ seven years from November 2005 to December 2012. The exposure times used for I,R,V & B bands are 30, 30, 30 & 50 seconds, respectively. Most of the monitoring was done in R band and we will use this band data for intra-night variability study while data through other bands will be used to address frequency dependence of variation and other issues. We, therefore, have very high temporal resolution (about 45 seconds) R-band data which should delineate microvariability structures in the intra-night light curves.

The differential photometry for all the 162 nights is performed using the standard procedures with the help of Image Reduction and Analysis Facility (IRAF) package provided by National Optical Astronomy Observatory (NOAO). The proper flat field and bias corrections are performed using the master flats and master bias frames generated from a large number of respective frames taken during individual nights. The field of view of our imaging system is large enough (6.5×5.5 arcmin) to accommodate at least four known comparison stars along with the source of interest, S5 0716+714. Therefore differential photometry provides the best option for generating the calibrated source lightcurves. An automated iraf script, using *WCSTools* and *Astrometry.net* packages for identifying the stars in the field, is used to perform the data reduction and photometry . We refer Chapter 2 and 3 of this thesis for detailed description of the imaging system and data analysis techniques used in this script. This script generates a text file containing the photometry of all the stars in the field for multiple apertures. The appropriate size of aperture for further analysis is determined by plotting the variation in the magnitudes of the stars in a single snapshot with increasing size of apertures. The one just before the approximate saturation is adopted as best aperture. This, in most of the cases, is roughly equal to the 2.35 $\times$ FWHM of the stars in the field. The magnitudes and photometric uncertainties for all the standard stars and source of interest corresponding to the best aperture are used for further analysis. The magnitudes for photometric standards i.e comparison stars are taken form Villata et al. (1998).

4.2.1 Sample of nights for duty cycle of variation

In order to determine how often the source shows intra-night variations during whole period of observation (duty cycle of variability), we set the following criteria for an observation night to qualify for its inclusion in the sample. Out of all the 162 nights during which the source was observed from MIRO during 2005 December to 2012 November, individual nights with a continuous monitoring of more than 2 hours qualify for investigating the intranight variability. The two hours time duration is chosen keeping in mind to include multiple peaks of short timescale fluctuations, if present, as reported in the literature with $\Delta t \sim 15 - 20$ minutes (Rani et al., 2009; Chandra et al., 2011a). The 78 nights of monitoring, performed at different epochs, qualify the above criteria. These 78 individual monitoring nights are then investigated for the possible contamination by spurious variations due to bad weather conditions during the observations. The nights reported having bad weather (high humidity, high wind speed and presence of moving thin clouds), resulting in extremely large fluctuations in both the comparison and control stars, are excluded from further analysis. After this filtration, 58 best quality monitoring nights are used for intranight variability studies. However, for long-term study of the source, all the nights, except those with very bad seeing, are used.

The estimation of variability amplitude and F-test is performed to statistically quantify the extent of variability during individual monitoring nights. The amplitude of variation is defined as:

$$A_{var} = \sqrt{(A_{max} - A_{min})^2 - 2\sigma^2}, \tag{4.1}$$

where A_{max} and A_{min} are the maximum and minimum values of magnitudes during the course of nightly observations. Whereas σ is given by

$$\sigma = \sqrt{\frac{\sum_{i=1}^{N}(m_i - \bar{m})^2}{N-1}}, \tag{4.2}$$

Where $m_i = (m_{c1} - m_{c2})_i$ is the differential magnitude of standard stars C1, & C2 in i^{th} image. While $\bar{m} = \overline{(m_{c1} - m_{c2})}$ is their differential magnitude averaged over the entire duration of particular monitoring night. N refers to the total number of images taken in that night. The significance of variability is also determined by performing the F-test incorporated in the R statistical package (R Development Core Team, 2008). The F-statistics is the ratio of the sample variances i.e. $F = \frac{S_B^2}{S_{CC}^2}$, where S_B^2 and S_{CC}^2 are the variance in the blazar magnitudes and differential magnitudes of standard stars for nightly observations, respectively. The value of F-statistics for all the nights alongwith the variability amplitude and σ are reported in Table-4.1. An F-value ≥ 3 indicates the variability with significance of more than 90 %. The F-value ≥ 5 corresponds to 99 % significance level. The Fig.- 4.5 shows the the variability parameters (Amplitude and F-value) for 58 monitoring nights. This cumulative distribution of parameters are used for determining the duty cycle of BL Lac object S5 0716+714. The details are discussed in section 3.2. The duty cycle of blazar is defined as the fraction of total number of nights during which the source shows significant activity.

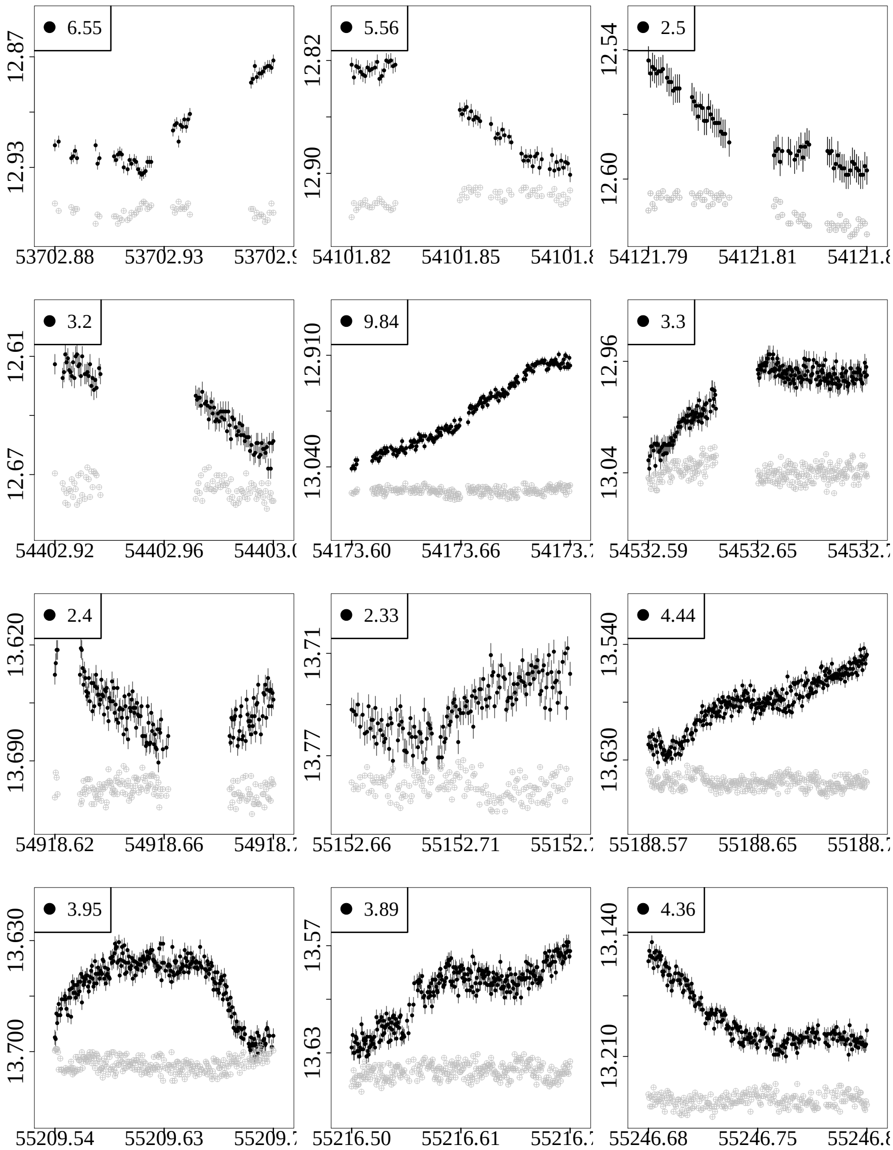

Figure 4.1 R band Intranight lightcurve S5 0716+714, X-axis gives the time in MJD.

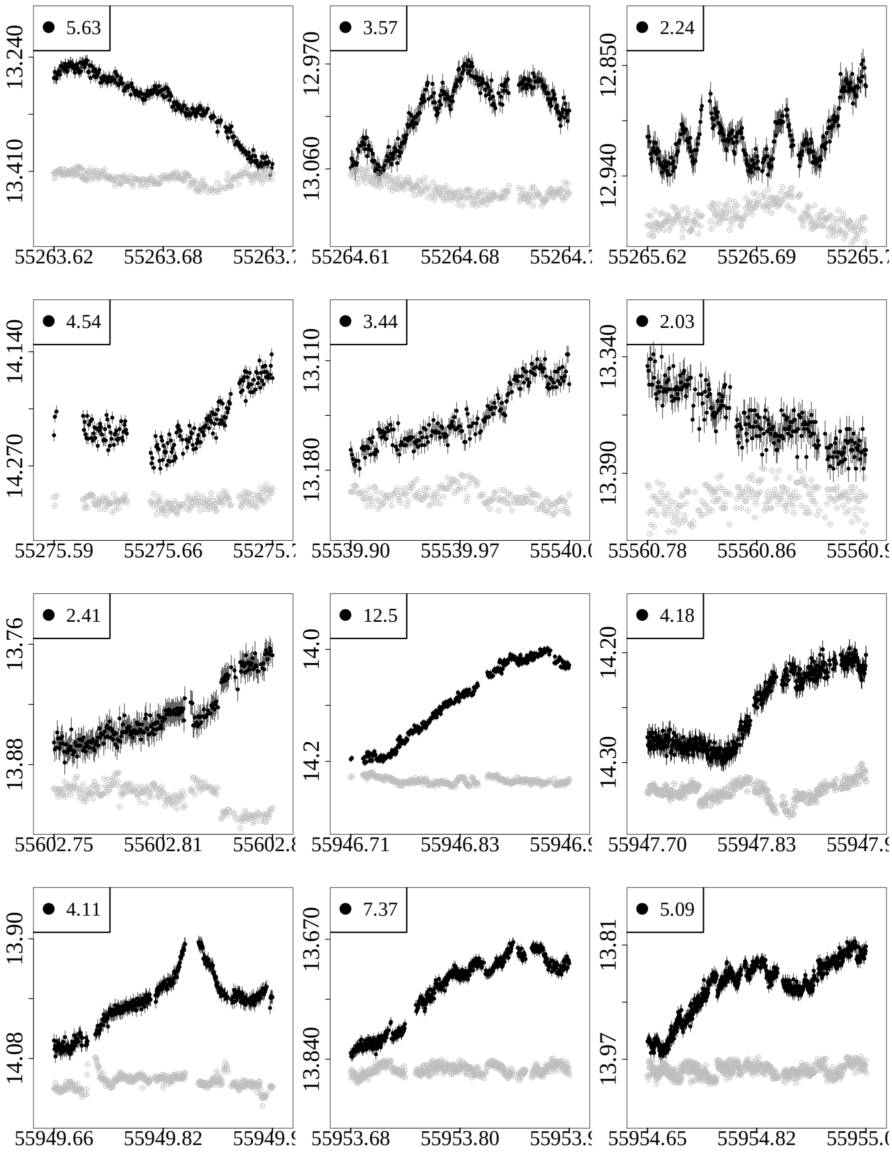

Figure 4.2 R band Intranight lightcurve S5 0716+714. X-axis refers the time in MJD.

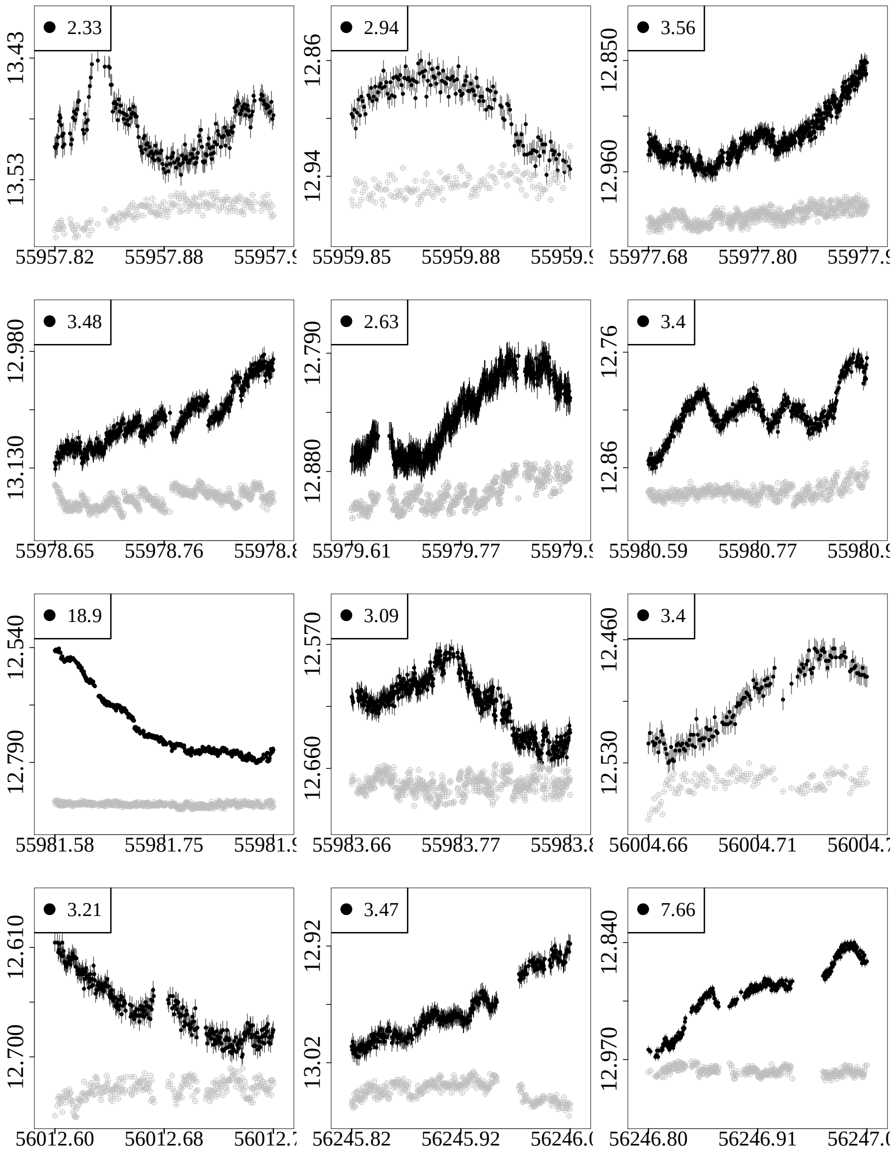

Figure 4.3 R band Intranight lightcurve S5 0716+714. X-axis refers the time in MJD.

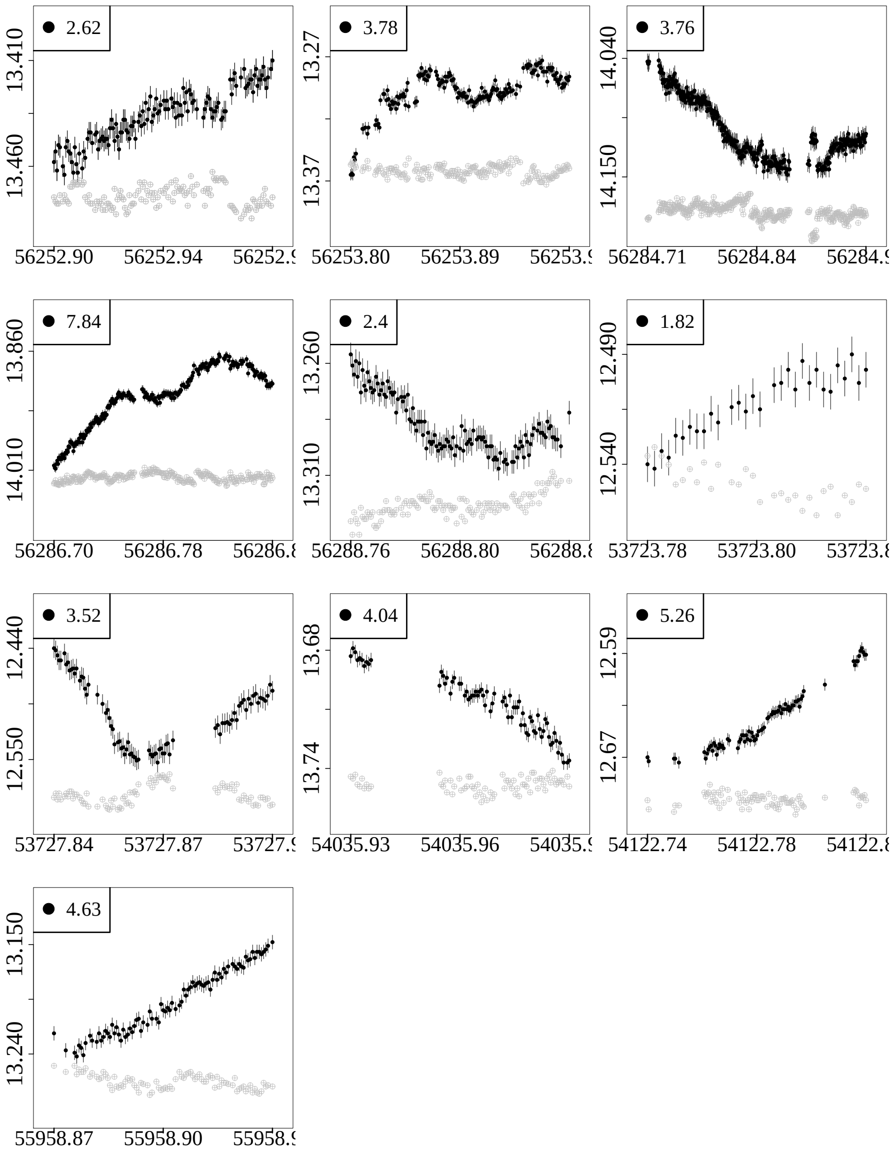

Figure 4.4 R band Intranight lightcurve S5 0716+714. X-axis refers the time in MJD.

4.3 Results and discussions

The intranight differential lightcurves are constructed from the data obtained during the period December 2005 to November 2012 for individual nights which qualify for intra-night variability. Some of these light curves showing intra-night variability, with calibrated source magnitudes are given in Fig.- 4.1-4.4. In total 44 out of 58 nights which qualified for intra-night variability are represented in these light curves. The x-axis refers to the time in MJD while y-axis is the source R-magnitude calibrated with the standard stars in the same field. The top curve in each panel refers to the blazar S5 0716+714 lightcurve. The lower, light grey, curve in each panel represents the differential lightcurves for comparison and control star (δ comparison), over-plotted with proper offset. All these light-curves represent highest temporal resolution photometric data ever used for blazar variability study. All the lightcurves shown in Fig.- 4.1-4.4 clearly exhibit intra-night variability (IDV or INV) observed at different epochs between 2005 - 2012. The numbers shown at top left corner in each panel are the ratio of standard deviations of source and δ comparison lightcurves which also reflect the extent of variability (variability parameter; C $\geq$ 2.75 for 99% confidence).

Fig.4.1 presents the lightcurves corresponding to the observations made during the period of 2005 November 28 - 2010 - February 19. The Fig.- 4.2 and Fig.- 4.3 comprise the lightcurves corresponding the epochs of 2010 March 08 - 2012 January 28 and 2012 January 28 - 2012 November 15, respectively. The first five blocks in Fig.- 4.4 are corresponding to the observations taken during 2012 November 21 to 2012 December 30. The rest 5 blocks in figure-4 are from those observations which do not follow the criteria of continuous monitoring of 2 hours or more but exhibit very prominent intranight/intraday variations. These lightcurves are not used for statistical distribution [Fig.- 4.5] for determining the duty cycle. These are shown for just an illustration of variations corresponding to the continuous monitoring of less than 2 hours. The data from all the 162 nights, averaged over the whole nights observation, are used to investigate long-term aspects of the source.

4.3.1 On the nature of intranight variability

The visual inspection of the lightcurves constructed for the different epochs show different nature of flux variations. In general we can broadly classify the observed behaviour in following subgroups 1.) a steady rise or fall in flux during overnight monitoring. 2.) A superposition of fast fluctuations over a slower change in flux and 3.) Very rapid change in flux during overnight monitoring. The above three kind of intranight flux variations reflect the possibility of intrinsic differences in the mechanisms responsible. The steady rise/fall for longer time [$\Delta t \sim$ few hours] may be due to the small scale steady acceleration/cooling of plasma in the shocked region. The very fast fluctuations in optical flux with a timescale shorter than few tens of minutes can not be associated with the size of emission region obtained using light time travel argument [R $\leq \frac{\gamma.c.\Delta t}{1+z}$] as it contradicts the simultaneity. These variations may be due to the small scale perturbations in the shock front or due to oscillations in the hotspot in the downstream jet. The lightcurves with overlapping fast and slow changes in flux indicate the violent and evolving nature of shock formed. The small timescale for all these variations suggest a possibility that the whole cross section of jet is not shocked all the time. Either a part of jet cross-section is affected by the instabilities or obliqueness of the shock is reflecting small size when projected in direction of observer. Any constraint on these possibilities can only be imposed using the simultaneous observations at different wavelengths which is beyond the scope of the present study.

Rise and fall rates

Intra-night light-curves shown in Fig.- 4.1-4.4 reflect smooth rise or fall in the source brightness over the night, as well as rise followed by fall or vice versa. Some of the nights show slowly rising/falling flux superposed by rapid fluctuations. In order to determine the rate of change of flux at different epochs, a line segment is fitted in the portion of lightcurves. The majority of observations show a steady rise/fall in flux for overnight observations with minor changes ($\frac{df}{dt} \leq 2\sigma$) in between. In such cases we fitted a single line for complete observations using least square algorithm. The significant number of lightcurves show a break in the trends in flux variations. In such cases multiple line segments are fitted. However there are some nights when very interesting trends in flux variations are seen. Rapid fluctuations are superimposed over the slower nightly change in the flux. In such cases a number of line segments, reflecting the rate at different components of light curve, are fitted. Table 2 presents the rates of change in brightness during different nightly observations shown in Fig.- 4.1-4.4. The first column in Table- 4.2 represents the date of observations while the second one is the mean time of the line segment used for estimating the rate of change in flux. The third columns gives the time duration in hours used for estimation of rate of flux change. The fourth and fifth columns of Table- 4.2 are the rate of flux change and associated uncertainty in the unit of mag per hours, respectively. The fastest rates of rise and fall in brightness are, respectively, 0.28 mag/her and 0.33 mag/hr as recorded on March 10, 2010 (MJD 55265.65 & 55265.66). These appear to be fastest rates of change in the brightness ever reported for S5 0716+714.

Nature of variations during flaring and quiescent phases

To study the nature of intra-day variability during different brightness phases of S5 0716+714, we grouped all the observed nights in three sets. From Table-4.1 it is evident that R band brightness of the source lies between approximately 12 to 13 for 19 nights, between 13 to 14 for 23 and during 5-nights source was observed to be fainter than 14 magnitude. Historically, blazar S5 0716+714 is reported to have 12.2, 13.5 and 15.5 R band magnitudes during its maximum, average and minimum brightness states. Therefore we can see that the source has witnessed variability in all the brightness phases during the reported period of observations, largely remaining in bright or in average brightness phase. Now, let us see how the variability activity shows up in different phases of brightness. To investigate this, we used variability amplitudes estimated for all individual nights showing intra-night variability and respective brightness magnitudes in R-band as a distribution. We performed the cluster analysis of this distribution using *Mclust* tool provided as contributory package for R statistical software. This performs mode-based clustering, classification, and density estimation based on finite normal mixture modelling. It provides functions for parameter estimation via the EM algorithm for normal mixture models with a variety of covariance structures, and functions for simulation from these models (Banfield and Raftery, 1993). The density contours over-plotted with the clustered points in different symbols and colors are shown in Fig.- 4.5.

Fig.- 4.5 shows three clusters, though the density contours show very weak significance for the second one. Basically we have two statistically significant clusters one which dominates when source is in brighter/flaring state while the other one dominates when source is relatively fainter.

Interestingly, the nature of micro-variations show very strange correlation with state of brightness in this source. The overall trend, though not very strong, shows larger intra-night variability amplitudes during the nights when the source is relatively fainter, relative to those during brighter phase. Normally, one would expect high variability activity with larger amplitude of variation during the bright, flaring phase when highly turbulent jet plasma is expected to interact with frequent shock formations leading to its rapid acceleration and subsequent radiative cooling. While during quiescent phase, the jet is relatively quiet and blazar emission is expected to have significant contribution from other components, for example accretion disk, BLR, and host galaxy thermal emission, just like radio-quiet sources. One would, therefore, not expect fast variations with large amplitude of variation during nights when source is in low phase. However, our observations for this source show very dramatic behaviour in nightly flux variations at different brightness states which can not be by chance.

The above results present a possibility of two different mechanisms respon-

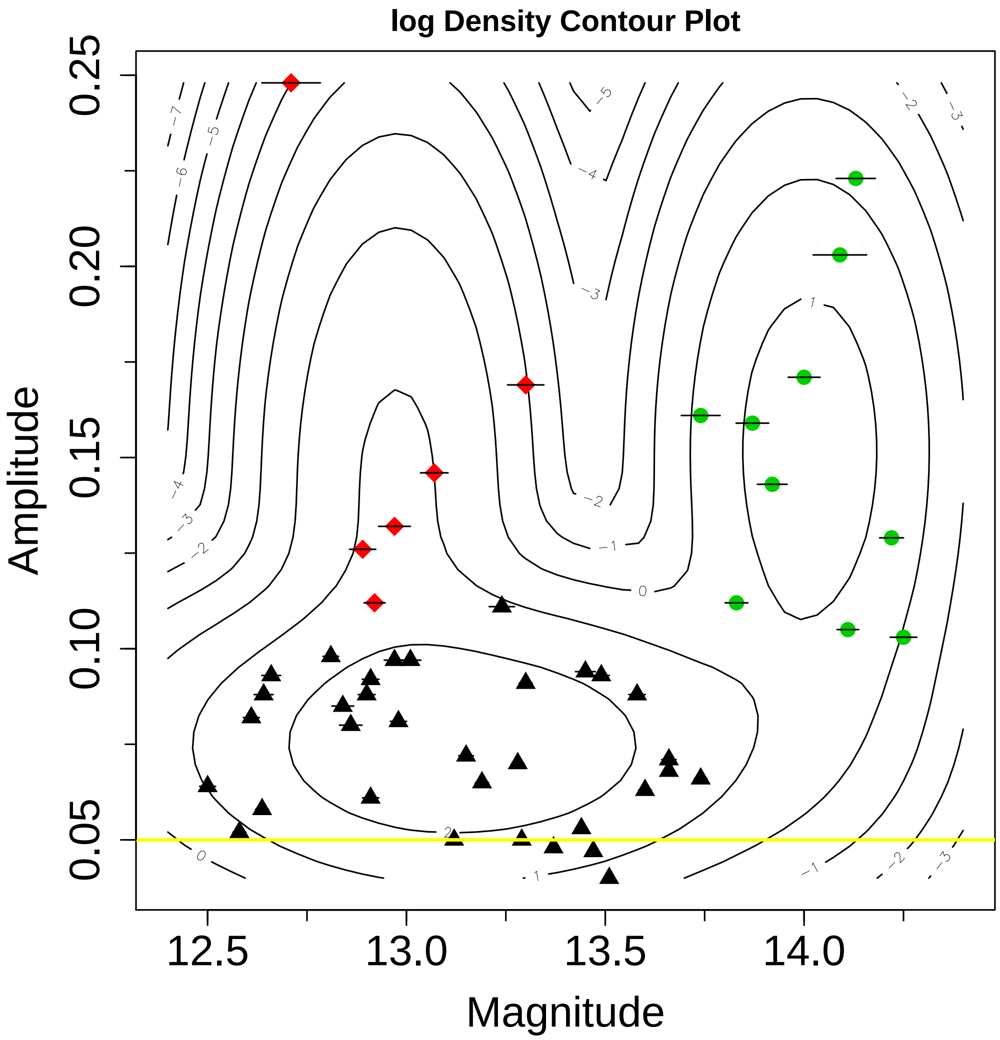

Figure 4.5 Amplitude of variability for different brightness state of BL Lac object S5 0716+714. Different symbols and colors show different clusters. The contours shown are the density plots showing the clustering.

sible for micro variability or IDV in the blazars emission. The first one is dominant when blazar emission is in overall high state i.e. in outburst state (blue circle). While the other component identified by red circle in Fig.- 4.5 indicate the short timescale activity even in relatively fainter state. Towards higher magnitude side the trend is not very clear. The intra-night longer-term variations [$\Delta t \sim$ few hours] during bright phase are then associated with the interaction of relativistic shock with the jet inhomogeneities or blobs of plasma passing through sub-mm core. Such variations have implications on the size of the emission region. The rapid fluctuations (with time-scales of few tens of minutes) superimposed over the smoother intra-night light-curves, when present, may be caused by the sites of emission within the the superluminal spiral knot passing through a cross section of the standing/moving mm-sub-mm core or just hitting the over-densities. Such emission sites are confined to much smaller size than the knot inside the jet. The second physical mechanism is dominant at relatively fainter state. In this case also the violent IDV or micro variations are witnessed which are similar in shape or trend as the one in bright state. The rapid variations seen in overall fainter state indicate the possibility of either presence of some kind of inhomogeneity in the jet or the amplification of emission from the hot spot in accretion disk. However the timescale of variation ($\Delta t \leq$ hours) rules out the disk origin. We propose that there could be another explanation in that during a flaring state, the average ambient flux is already so high that amplitude of variation due to rapid events, which are superposed on average flux, become subdued. On the other hand, during a quiet phase, any activity would lead to significant enhancement over and above quiescent jet emission, resulting in larger apparent variability amplitudes. However, this needs further, detailed study, with perhaps a larger sample of blazars.

Duty cycle of intra-night variability for S5 0716+714

In the earlier chapter, we have discussed in detail the rapid intra-night variability in S5 0716+714. Here we would like to know how often this source shows such variability behaviour. The duty cycle of variation is estimated by determining fraction of nights the source shows significant intra-night variation out of all the nights the source was monitored. As discussed above, the source was monitored for 162 nights during 2005 December to 2012 November and according to the criteria, 58 nights were qualified for the study of intra-night variability. Here we perform statistical analysis to estimate the duty cycle of variation.

Fig.- 4.6 presents the cumulative distribution of the variability parameters namely variability amplitude and F-test value. F-test value represents the ratio of variance of the source magnitude to the differential magnitude of standard stars. The nightly observations used for this analysis strictly qualify the criterion of continuous monitoring of 2 hours or more as already discussed earlier. Table- 4.1 presents the statistical results corresponding to each monitoring nights.

The above analysis clearly shows that more than 86 % of the IDV nights witnessed significant micro variability (F-value $\geq$ 3). If we tighten the condition of microvariability to be statistically significance i.e. F-value $\geq$ 5, then more than 74 % observations show microvariations. Therefore, we can safely state that the duty cycle of variation for this source is estimated to be 86 % with a corresponding 90 % confidence level. In another words, if one monitors BL Lac object S5 0716+714 continuously for a period of 2 hours or more, there is 86 % probability for the detection of micro-variations or short timescale flux variations during that night. This clearly establishes this source as an ideal candidate for studying the intra-night variability. Our results are in good agreement with those of Nesci et al. (2005a) [>90 %] and Zhang et al. (2012) ($\approx$ 78%).

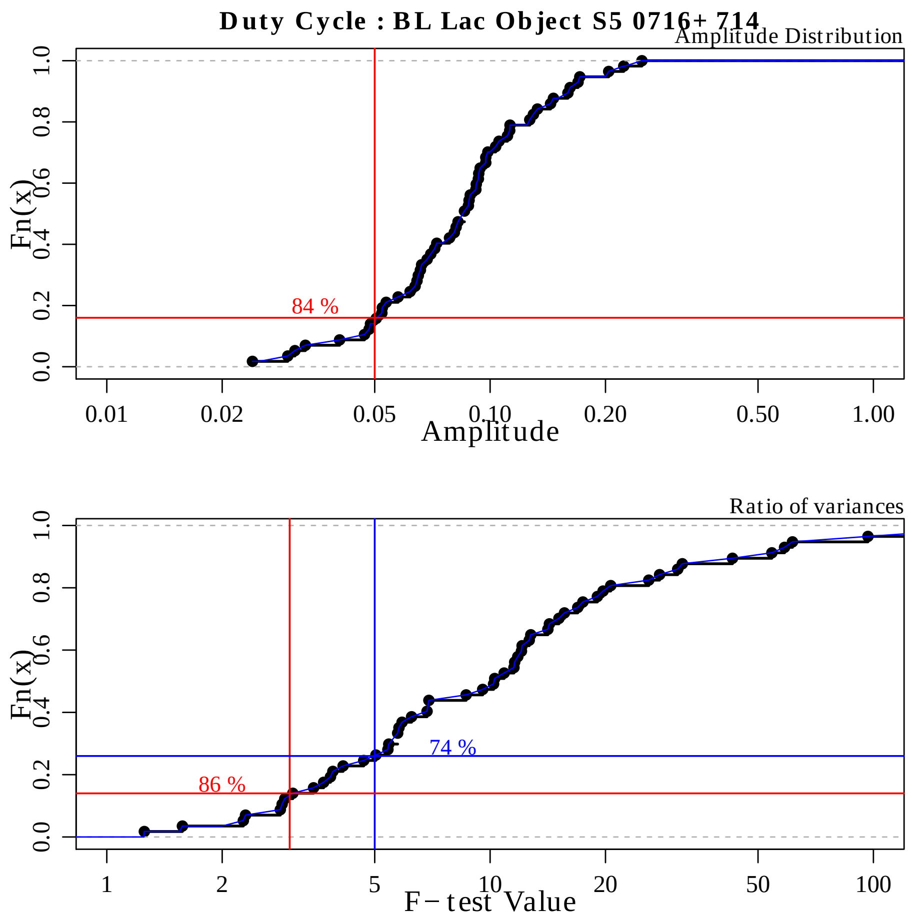

Figure 4.6 Statistical analysis of variability for determining the duty cycle of S5 0716+714. The above figure represents the statistical distribution of variability over the IDV nights [Table-1]. The top panel shows the cumulative distribution of Amplitude of variations while the bottom one is same for F-test value.

Table 4.1: The statistical parameters quantifying the intranight variability. The data is taken in R band using MIRO.

Date	***Time (MJD)***	***DelT***	***S***	σ_S	Δ_{CC}	σ	σ_S/σ_C	***Amp***	***F***
28nov05	53702.93142	2.36	12.91	0.0205	1.094	0.0031	6.549	0.061	42.89
22dec05	53726.868101	4.27	12.38	0.0096	0.1292	0.0063	1.507	0.029	2.271
24dec05	53728.874137	2.23	12.56	0.0074	1.115	0.0058	1.255	0.032	1.575
1jan07	54101.846571	3.18	12.86	0.0284	1.099	0.0051	5.555	0.080	30.86
20jan07	54120.779227	2.99	12.39	0.0086	1.115	0.0057	1.517	0.030	2.301
21jan07	54121.813355	2.35	12.58	0.0162	-1.1	0.0065	2.498	0.052	6.24
22jan07	54122.784082	1.99	12.641	0.0239	-0.578	0.0045	5.262	0.088	27.68
14mar07	54173.665743	2.93	12.97	0.0400	0.5336	0.0040	9.837	0.132	96.77
29Oct07	54402.970807	2.045	12.637	0.01622	0.091	0.0051	3.195	0.058	10.21
7mar08	54532.656387	3.06	12.98	0.0205	-0.052	0.0062	3.298	0.081	10.88
25mar09	54915.676753	2.32	13.51	0.0089	-1.217	0.0045	1.972	0.040	3.888
28mar09	54918.663004	2.28	13.66	0.0139	1.116	0.0058	2.396	0.068	5.739
17nov09	55152.709129	2.12	13.74	0.0161	1.18	0.0069	2.326	0.066	5.412

Table 4.1 – continued from previous page

Date	*Time (MJD)*	*DelT*	*S*	σ_S	Δ_{CC}	σ	σ_S/σ_C	*Amp*	*F*
23dec09	55188.648684	3.65	13.58	0.0206	1.169	0.0046	4.44	0.088	19.71
25dec09	55190.686317	3.45	13.08	0.0140	0.6073	0.0082	1.707	0.064	2.913
13jan10	55209.623254	4.31	13.66	0.0182	1.138	0.0046	3.954	0.071	15.63
16jan10	55212.663721	4.19	13.45	0.0250	0.0431	0.0130	1.918	0.094	3.679
20jan10	55216.608361	5.05	13.60	0.0162	1.69	0.0041	3.888	0.063	15.12
19feb10	55246.744141	3.09	13.19	0.0165	-1.114	0.0038	4.365	0.065	19.05
08march10	55263.674735	4.08	13.30	0.0458	1.14	0.0081	5.633	0.169	31.73
09mar10	55264.680729	3.40	13.01	0.0263	1.126	0.0073	3.574	0.097	12.77
10mar10	55265.69242	3.73	12.91	0.0212	-0.551	0.0094	2.244	0.092	5.036
19mar10	55274.665948	3.49	14.13	0.0493	1.624	0.0251	1.958	0.223	3.833
20mar10	55275.670723	3.31	14.22	0.0300	1.139	0.0066	4.543	0.129	20.64
07Dec10	55537.954931	4.16	13.24	0.0320	-1.712	0.0148	2.164	0.111	4.681
08DEc10	55538.935888	5.01	13.28	0.0154	1.159	0.0082	1.861	0.070	3.463
09dec10	55539.96905	6.37	13.15	0.0186	-1.079	0.0054	3.436	0.072	11.81
30dec10	55560.865563	5.76	13.37	0.0113	-1.091	0.0055	2.034	0.048	4.135
31dec10	55561.894627	4.21	13.47	0.0119	-0.588	0.0068	1.748	0.047	3.057

Table 4.1 – continued from previous page

Date	***Time (MJD)***	***DelT***	***S***	σ_S	Δ_{CC}	σ	σ_S/σ_C	***Amp***	***F***
10feb11	55602.801762	5.06	13.83	0.0288	0.6691	0.0119	2.405	0.112	5.784
29ma11	55649.694439	2.12	13.57	0.0055	0.0671	0.0049	1.119	0.023	1.253
20jan12	55946.832912	5.80	14.09	0.0674	1.091	0.0054	12.48	0.203	155.7
21jan12	55947.824985	6.41	14.25	0.0336	1.724	0.0080	4.179	0.103	17.46
23jan12	55949.813705	7.50	14.00	0.0401	-0.089	0.0097	4.115	0.171	16.93
27jan12	55953.799941	3.888	13.74	0.0489	-0.068	0.0066	7.371	0.161	54.33
28jan12	55954.810661	3.84	13.87	0.0411	-0.530	0.0080	5.093	0.159	25.94
31jan12	55957.884513	3.00	13.49	0.0203	-1.7	0.0087	2.333	0.093	5.441
02feb12	55959.880088	2.97	12.90	0.0213	1.71	0.0088	2.427	0.088	5.893
20feb12	55977.806917	6.04	12.92	0.0266	0.0787	0.0074	3.557	0.112	12.65
21feb12	55978.761959	6.90	13.07	0.0347	1.092	0.0099	3.481	0.146	12.12
22feb12	55979.773069	7.90	12.84	0.0276	0.0855	0.0105	2.631	0.085	6.923
23feb12	55980.760459	8.20	12.81	0.0197	1.175	0.0058	3.405	0.098	11.59
24feb12	55981.743233	8.13	12.71	0.0736	-1.182	0.0038	18.9	0.248	357.3
25feb12	55982.819163	6.88	12.69	0.0133	-0.557	0.0078	1.693	0.048	2.867
26feb12	55983.77463	5.74	12.61	0.0202	-1.088	0.0065	3.093	0.082	9.564

Table 4.1 – continued from previous page

Date	***Time (MJD)***	***DelT***	***S***	σ_S	Δ_{CC}	σ	σ_S/σ_C	***Amp***	***F***
18march12	56004.707386	2.53	12.50	0.0201	0.6197	0.0059	3.397	0.064	11.54
26march12	56012.681671	3.94	12.66	0.0237	1.158	0.0074	3.206	0.093	10.28
11nov12	56242.915194	4.72	13.30	0.0099	-0.084	0.0058	1.684	0.052	2.836
14nov12	56245.914294	5.10	12.97	0.0259	-1.101	0.0074	3.474	0.097	12.07
15nov12	56246.915332	5.71	12.89	0.0329	-1.085	0.0043	7.658	0.126	58.64
16nov12	56247.939711	4.08	13.12	0.0109	-1.728	0.0054	2.031	0.050	4.125
21nov12	56252.939049	4.76	13.44	0.0127	-1.088	0.0048	2.617	0.053	6.847
22Nov12	56253.894623	4.32	13.30	0.0166	1.709	0.0044	3.779	0.091	14.28
23dec12	56284.839984	6.33	14.11	0.0272	0.6276	0.0072	3.762	0.105	14.15
25Dec12	56286.781263	4.06	13.92	0.0373	1.089	0.0047	7.842	0.143	61.5
27dec12	56288.794495	2.78	13.29	0.0123	-1.101	0.0051	2.396	0.050	5.739

Table 4.2: This tables contains the rate of change of optical flux in various segments of the lightcurves shown in Figures 1-4.

Date	*Time [MJD]*	$\Delta T[hrs]$	$\frac{df}{dt}[mag/hr]$	*Unc* $\frac{df}{dt}[mag/hr]$
28 Nov 05	53702.95	1.4	-0.039	0.0014
19 Dec 05*	53723.8	0.98	-0.045	0.0034
23 Dec 05*	53727.85	0.53	0.22	0.0074
	53727.88	0.82	-0.082	0.0035
27 Oct 06*	54035.96	1.4	0.032	0.0015
01 Jan 07	54101.84	1.1	0.071	0.002
21 Jan 07	54121.79	2.3	0.034	0.0011
22 Jan 07*	54122.78	1.9	-0.05	0.0016
14 Mar 07	54173.66	2.7	-0.05	0.00068
29 Oct 07*	54402.96	2	0.021	0.00088
07 Mar 08	54532.62	1.8	-0.039	0.00093
	54532.69	1.1	0.0033	0.0014
28 Nov 08*	54798.63	0.63	-0.08	0.0028
28 Mar 09	54918.64	1.1	0.043	0.0035
17 Nov 09	55152.71	1.9	-0.023	0.0015
23 Dec 09	55188.6	1.3	-0.035	0.0016
	55188.67	2.2	-0.015	0.00073
13 Jan 10	55209.56	1.3	-0.029	0.0017
	55209.67	1.2	0.052	0.0021
20 Jan 10	55216.55	2.3	-0.021	0.00079
	55216.65	2.5	-0.003	0.00068
19 Feb 10	55246.72	1.7	0.033	0.00088
08 Mar 10	55263.69	2.9	0.048	0.00094
09 Mar 10	55264.62	0.24	0.13	——-
	55264.70	1.24	-0.06	——-

Continued on next page

Table 4.2 – continued from previous page

Date	*Time [MJD]*	$\Delta T[hrs]$	$\frac{df}{dt}[mag/hr]$	*Unc* $\frac{df}{dt}[mag/hr]$
	55264.74	0.48	-0.10	——-
10 Mar 10	55265.62	0.24	0.13	——-
	55265.63	0.24	-0.17	——-
	55265.64	0.24	0.13	——-
	55265.65	0.24	-0.33	——-
	55265.66	0.24	0.28	——-
	55265.70	0.24	-0.27	——-
	55265.71	0.24	0.24	——-
	55265.75	0.72	0.12	——-
20 Mar 10	55275.64	1.2	0.025	0.0033
	55275.69	1.5	-0.065	0.0025
09 Dec 10	55539.97	3	-0.018	0.00065
30 Dec 10	55560.86	3.8	0.0087	0.00033
10 Feb 11	55602.8	2.7	-0.032	9e-04
20 Jan 12	55946.83	4.6	-0.046	0.00041
21 Jan 12	55947.83	2.1	-0.044	0.0011
	55947.92	1.5	-0.012	0.0015
23 Jan 12	55949.73	3	-0.028	0.00063
	55949.82	1.3	-0.056	0.003
	55949.89	0.97	0.093	0.0027
27 Jan 12	55953.77	4.6	-0.036	0.00046
28 Jan 12	55954.72	3.1	-0.04	6e-04
	55954.86	1.6	0.025	0.0014
	55954.94	1.7	-0.031	0.0013
31 Jan 12	55957.83	0.58	-0.079	0.014
	55957.87	0.85	0.086	0.0044
	55957.91	1.3	-0.046	0.0025
01 Feb 12*	55958.9	1.1	-0.082	0.0016

Continued on next page

Table 4.2 – continued from previous page

Date	*Time [MJD]*	$\Delta T[hrs]$	$\frac{df}{dt}[mag/hr]$	$Unc\ \frac{df}{dt}[mag/hr]$
02 Feb 12	55959.86	0.62	-0.042	0.0048
	55959.89	1.1	0.067	0.0025
20 Feb 12	55977.71	1.7	0.014	0.00082
	55977.78	1.4	-0.026	0.001
	55977.88	2.5	-0.034	0.00059
21 Feb 12	55978.76	5.6	-0.02	0.00033
22 Feb 12	55979.78	3.4	-0.023	0.00035
	55979.92	0.93	0.03	0.0026
23 Feb 12	55980.64	1.8	-0.036	0.00063
	55980.69	0.62	0.049	0.0027
	55980.73	1.1	-0.02	0.0012
	55980.77	0.54	0.049	0.0053
	55980.8	0.58	-0.038	0.0041
	55980.83	1.1	0.023	0.0017
	55980.88	1.5	-0.044	0.0019
	55980.92	0.49	0.0094	0.0074
24 Feb 12	55981.68	4.8	0.049	0.00054
	55981.85	3.1	0.0071	0.00052
26 Feb 12	55983.72	2	-0.017	6e-04
	55983.82	2.6	0.027	7e-04
18 Mar 12	56004.7	1.7	-0.034	0.00094
26 Mar 12	56012.63	1.4	0.038	0.0012
	56012.72	1.7	0.016	0.0015
14 Nov 12	56245.92	5	-0.017	0.00025
15 Nov 12	56246.84	1.4	-0.056	0.0014
	56246.92	1.56	-0.012	0.0010
	56246.99	0.54	-0.067	0.0034
	56247.02	0.50	0.045	0.004

Continued on next page

Table 4.2 – continued from previous page

Date	*Time [MJD]*	$\Delta T[hrs]$	$\frac{df}{dt}[mag/hr]$	*Unc* $\frac{df}{dt}[mag/hr]$
21 Nov 12	56252.94	1.8	-0.021	0.00063
22 Nov 12	56253.83	1.4	-0.045	0.0032
	56253.88	0.97	0.026	0.0022
	56253.93	1.2	-0.022	0.002
	56253.96	0.56	0.028	0.0044
23 Dec 12	56284.79	3.7	0.027	0.00042
	56284.92	2.5	-0.011	0.001
25 Dec 12	56286.73	1.2	-0.072	0.0012
	56286.81	0.9	-0.058	0.0021
	56286.85	0.72	0.033	0.0034
27 Dec 12	56288.77	1.1	0.045	0.0015

4.3.2 Long-term study of S5 0716+714

Fig.- 4.7 shows the multi-frequency lightcurve of BL Lac object S5 0716+714 during the whole observation period considered here, including even those nights which did not qualify for intra-night variability. The magnitudes for S5 0716+714 for individual nights are averaged for the long-term light curves. In the composite light curve shown here, top to bottom panels refer to the long-term light-curves in I, R, V and B bands, respectively. A least square fitting algorithm is used to fit a line to the data to see any long-term trend, if present. The numbers in each panels show the slope of best fit line. The data tables corresponding to all the four filers and used for generating these lightcurves are present online [1].

Variability trend

Figure 4.1 shows the multi-frequency optical lightcurves of BL Lac object S5 0716+714 constructed using the nightly averaged magnitudes obtained from

[1] http://www.prl.res.in/ baliyan/download.html

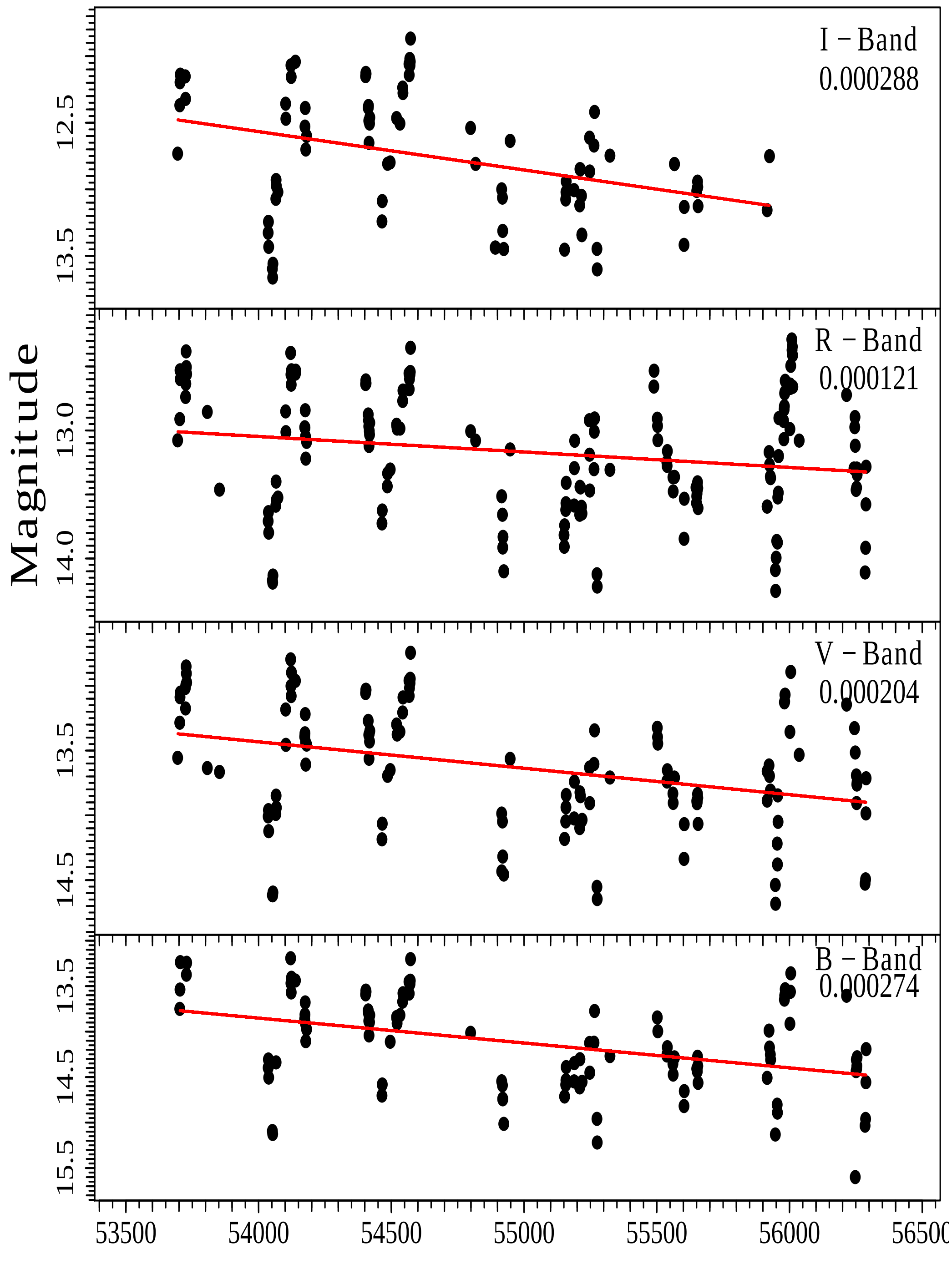

Figure 4.7 Multifrequency long-term lightcurves of BL Lac S5 0716+714 during the period from 2005 November 28 to 2012 December 27. The solid line shows least square fit.

all the observations over approximately past seven years of blazar monitoring program at MIRO. Let us discuss the broad features of the light curve. The best fit shows a global decrease in overall flux during the course of observations. The slow decay trend is traced nicely in all the observed wavelength bands. The limited number of observed points in I and B bands, alongwith larger photometric uncertainties in B band, however, give the feeling that the source decays faster in these bands, but that may be only due to sampling effect. The rate of change in I, R, V and B bands, as estimated from the slopes are 0.1, 0.04, 0.07 and 0.1 mag/year respectively. The time sampling in R and V band observations are much better with small uncertainties. If we focus on the R-band light-curve, it is very clear that during the span of about 7-years, notwithstanding the breaks in observations, there seems to be 9-instances when source shows peak brightness and 7 minima in the form of a series of highs and lows. Since our data from Mt Abu Observatory are not continuous as the telescope is not dedicated to this program only, we are not able to trace the complete outbursts. Also, there are large gaps due to closure of the observatory for about 3-months due to the onset of Monsoon.

From average value of the brightness level, these peaks of the outbursts are about one magnitude higher. We clearly see about 7 deepest points of varying extent with respect to average magnitude in the light curves. In general these dips are more than o.7 magnitude lower than average flux. The average span of these outbursts varies between 50 to 100 days but these do not appear to be periodic or quasi-periodic in nature reflecting their stochastic nature of variability which is well known for blazars. While maximum brightness of all the outbursts are similar, within the limits of observed sampling, there is mild trend of source going fainter with time. The average magnitude decreased from about 13 mag in R on 28 December 2005 to 13.4 on 27 November 2012, with linear slope of 0.04 magnitude per year. In our study the most dense observations are performed in 2011-2012, however, the brightest (R$\approx$ 12.25m) and faintest (R$\approx$ 14.2m) magnitudes for S5 0716+714 are recorded on 2010 March 10. It is interesting, but understandable, that on the same day, source undergoes through fastest rise (0.07mag) and fall (0.08mag) in brightness within less than 15 minutes.

It is worthwhile to report that Nesci et al. (2005a) detected much higher rate of magnitude variation, 0.11 mag per year, during 1994 to 2003, albeit towards brightening. It is possible that source brightened during 1994 to 2003 and then entered in slow decay phase. It should be noted that S5 0716+714 was in low decreasing phase during 1953 to 1985 and only after 1994, it started brightening. The reasons behind the slow trends of increase and decrease in flux of blazars are not clearly known but surely these changes relate to changes in the structure and/or direction of the jet or pattern of the injection of fresh plasma into the jet. The long-term trend of decreasing/increasing mean brightness in the source, on the time-scales of tens of years, underscores the need for preserving and organizing long term data encompassing several generations of the astronomers.

Long-term spectral behaviour

Blazars are known to exhibit different pattern when it comes to frequency dependence of brightness. Many blazars show well known bluer-when-brighter (BWB) behaviour while others show redder when brighter (RWB) pattern. However, it is also seen that same source exhibit different behaviour at different epochs. Truly achromatic behaviour is also reported at some occasions. Nonetheless, the colour information is important as it helps to discriminate among various physical processes responsible for variation. We have, therefore, used observed data in I,V,R,B bands for all the nights during 2005 December to 2012 November. Each nights data are averaged and colours (B-V, B-R, V-R) are determined. We have not used I-band data for this study as observations in I-band are for lesser epochs. We have plotted colour (B-V) as a function of average magnitude, (B+V)/2, in Fig.- 4.8 for whole duration. Other colour magnitude plots show very similar pattern. As is evident from the Fig.- 4.8, there is mild (with best fit slope $= 0.06 \pm 0.01$) bluer-when-brighter trend for this source. Similar behaviour for the blazar S5 0716+714 is reported by Wu

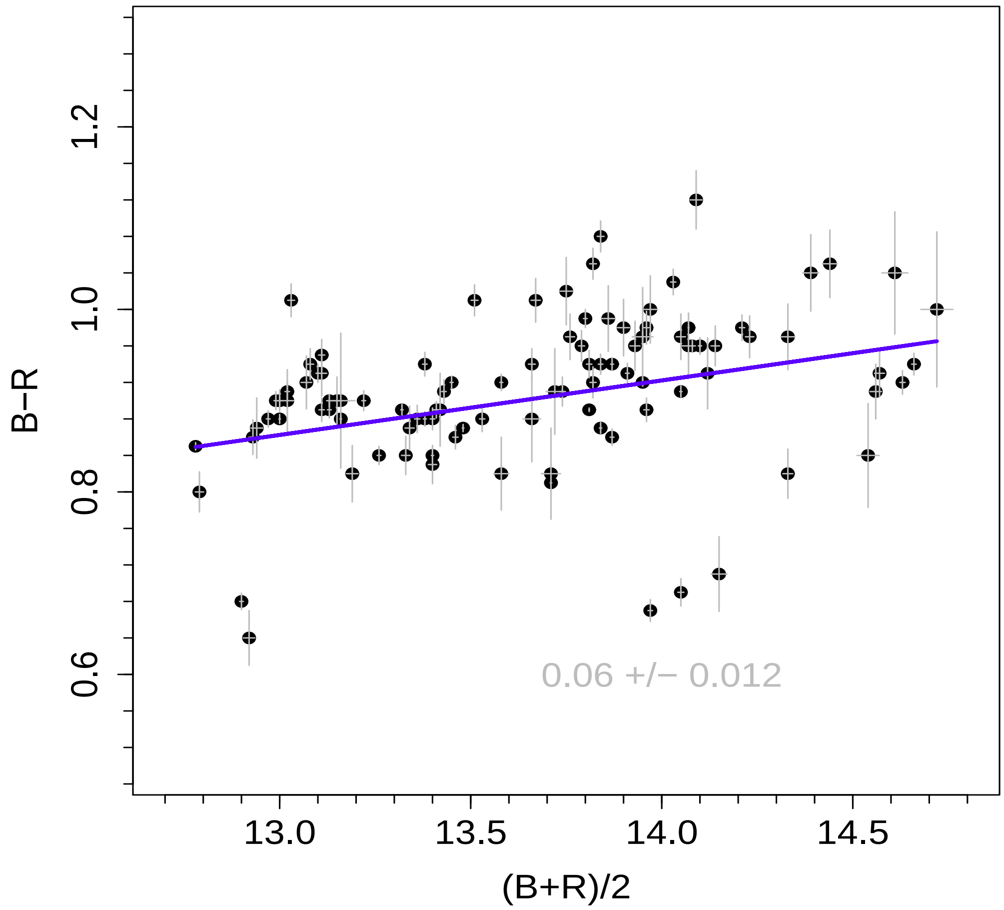

Figure 4.8 Colour-magnitude, (B-V) v/s (B+R)/2, plot for BL Lac S5 0716+714 for the period 2005 -2012

et al. (2005); Stalin et al. (2009); Raiteri et al. (2003), for both, intra-night and inter-night variations. However, Raiteri et al noted that on short time scales, the source shows all three patterns: BWB, RWB and achromatism. Dai et al. (2009) report that most of the Bl Lac sources show BWB while FSRQs exhibit redder when brighter pattern. It would be interesting to explore this aspect and look for physical reasons behind this.

The bluer when brighter trend in blazars could be explained based on shock-in-jet model (MarscherGear1985). Also, it can occur when an increase in luminosity of the blazar is caused by the injection of a population of fresh electrons/plasma with a harder energy distribution than the previously partially cooled ones (Mastichiadis and Kirk, 2002).

The change in spectral behaviour with brightness in S5 0716+714 has been noticed at other wavelengths as well. Raiteri et al. (2003) reported a flatter-when brighter trend in radio, Cappi et al. (1994) cited a steeper-when-fainter nature in x-ray, indicating that spectral changes with flux are rather common in blazars. It, therefore, may suggest a close relationship between the mechanisms responsible for the emission and variability in different wavebands. Such feature can be used to put strong constraints on the models proposed for these phenomena.

4.4 Conclusions

In this Chapter, we have used about 7-year (2005 December to 2012 November) optical data obtained with highest ever temporal resolution from Mt Abu IR Observatory. Such high temporal resolution data is very useful to delineate micro-fluctuations in the intra-night variability light-curve of violently variable blazars. The photometric data for all the nights for blazar S5 0716+714 was obtained in the differential photometry format to minimize the seeing effects. Such data is used to study intra-night variability and duty cycle of variation and also to address long-term variability in the source. While data for all the nights are used for long-term study, a proper sample is carved out of all the nights to qualify for intra-night variability study. Out of 162 nights, 58 nights qualify for such a study. Based on this study, following conclusions are drawn.

1. Blazar S5 0716+714 is highly variable on intra-night time-scale with duty cycle of variation more than 82%. This is in agreement with results obtained by Wu et al. (2005) (the reported duty cycle $\approx$ 78%) and others. These intra-night variations with time scales of few hours could be caused by a thin relativistic shock moving within a jet and encountering some feature such as particle or magnetic field over-density or a bend in the jet, leading to enhancement of observed flux.

2. Intra-night light curves show rise/fall in flux at varying rates on different nights. The fastest rising rate encountered in the present study being

0.33 mag hr^{-1} while most rapid rate of fall in flux is estimated as 0.28 mag hr^{-1}. Shape of the light-curves gives some idea about the tangled magnetic field in the jet's emission zone. Steep rise and fall in the light curve of flares reflect extent of the strength of magnetic field.

3. Contrary to the common belief, amplitudes of intra-night variation during the quiescent (fainter) phase of the source larger, as noticed during brighter/flaring phase. This phenomenon is not rare or by chance as it is observed for many nights in our study. Normally one would expect quiescent phase variations in blazar to be feeble, perhaps caused by disk instability or hot-spots. However, the nature of variation during this phase are quite similar, in time and shape to what are observed during relatively bright phase. Only probable explanation appears to be that in both states, the amplitude of variations are similar but they get pronounced due to overall low activity in the quiescent phase when average flux from jet emission is low.

4. In addition to variations with few hours time-scale during a night, the source shows vary rapid flux fluctuations with significant (more than 3 σ) amplitude of variation during some of the nights. Time-scales of such variations vary from 10 to 25 minutes and these structures are superposed over the relatively slow nightly variations. In some cases, these appear to be quasi-periodic but with asymmetric shaped sub-flares. These are too short to be associated with size of the emission region of a blazar.

5. On the long-term aspect, the source shows a slow rise/fall in the brightness incorporating many significant flares on intra-night time scales. The trend is similar in all bands (IRVB). Such long term variability trends are perhaps due to formation of shocks at the base of the jet and its evolution through its passage downstream. A mild 'bluer-when-brighter' (BWB) spectral trend is observed with a slope of about 0.05 in the long-term light-curve. BWB is explained by shock-in-jet model (Marscher and Gear, 1985b) in a natural way.

This study shows blazar S5 0716+714 exhibiting long-term variability trends, incorporating several flares/outbursts during 7-years of monitoring. This study also establishes, and confirms, very high ($\approx 82\%$) duty cycle of variation. The intra-night variations with few hours time-scales in S5 0716+714 could be caused by the interaction of shocks with jet inhomogeneities with implications on the size of the emission regions, while rapid fluctuations with few tens of minutes time-scales are very difficult to explain. The truly simultaneous multi frequency optical monitoring of a sample of blazars (Bl Lac Objects and FSRQs) is required to settle the issue of BWB and RWB trend, respectively, in BL Lacs and FSRQs whether it is true, and if so, what the processes are which cause such distinct behaviour. On the other hand, long-term variations, with time scales of several years are difficult to ascribe to a particular process as such study requires really long duration, good quality data on a sample of blazars. The limited data available on this source, including our observations, point to change in long-term behaviour of the source. It was decaying during 1953 to 1985 with very low mean brightness which increased during 1994-2003. Our data shows that perhaps after 2003, the source is slowly decaying again. However, our data sampling is not very dense and a more detailed study is needed to determine the trend. Such long-term trends, when mean brightness changes over tens or years, irrespective of short-long term outbursts with few days/months time scale, could be due to changes in the structure and/or jet direction or pattern of the plasma injection into the jet.

Chapter 5

Optical polarization study of BL Lac object *CGRaBSJ0211+1051*

5.1 Introduction

Polarization of light is the key to obtain a wealth of essential information which is encoded in the electromagnetic radiation reaching from distant astronomical sources. The technique of polarimetry provides unique information not available through photometry or spectroscopy, e.g., magnetic field prevalent in the source of study. AGN, particularly blazars, show appreciable linear optical and radio polarization, a characteristic of incoherent synchrotron emission (Rybicki & Lightman 1979, p. 180). At large scale (kpc) magnetic field is ordered and highly transverse, because the longitudinal component of magnetic field decays as $1/r^2$ while the transverse component decays as 1/r (r being radius of jet cross section). But at pc/sub-pc scale jet situation is much more complicated which manifests in varied nature of activities like, complex variation in flux and polarization. Study of variation in polarization, therefore, is an important tool to understand the nature of blazars. In this part of the thesis, we investigate polarization properties of blazar sub-classes and use this information to categorize blazar candidate CGRaBS J0211+1051.

CGRaBS J0211+1051 (RA. 02:11:13.2, Dec. 10:51:35, J2000) is also known as MG1 J021114+1051, 1FGL J0211.2+1049 and 87GB 020832.6+103726.

This object was first observed at high energies by Energetic Gamma-Ray Experiment Telescope (EGRET) instrument onboard Compton Gamma-Ray Observatory (CGRO). CGRaBS J0211+1051 was found to have a featureless optical spectrum and R-band magnitude of 15.42 in optical characterization of bright EGRET blazars in the uniform all-sky survey, CGRaBS (Healey et al., 2008). In previous studies based on radio observations at 8.4 GHz and 4775 MHz by Healey et al. (2007) and Lawrence et al. (1986), respectively, this object was identified as a possible radio source and/or BL Lac object. Later Snellen et al. (2002) performed optical identifications of radio sources from the Jodrell Bank Very Large Area Astrometric survey with $S_{6cm} \geq 200$ mJy and reported CGRaBS J0211+1051 to have an R-band magnitude of 15.41 alongwith 384 mJy and 314 mJy flux at 5 GHz and 1.4 GHz, respectively. The large area telescope (LAT) onboard Fermi space based Gamma-Ray observatory detected this source in $\gamma - Rays$ (E $\geq$ 100 MeV). This blazar candidate was included in first fermi catalog (Abdo et al., 2010b). The lack of significant line emission from this source makes the direct measurement of redshift very difficult. In a recent study by Meisner and Romani (2010), the redshift of CGRaBS J0211+1051 was estimated to be z = 0.20 $\pm$ 0.05 using optical photometry of host galaxy of this object.

The available history shows that the source was in low optical phase but had flaring activities from time to time. It had undergone multiple optical flaring episodes including a rise of $\sim$ 3.5 times of the average flux density within 100 days in 2006 December and again, during decline phase, rose by similar order of magnitude during the flare of 2007 October. The CRTS observations show a slow brightening of CGRaBS J0211+1050 since 2008 in the long term V band monitoring of this source (Djorgovski et al., 2011).

The longterm V-band lightcurve of this source observed from CRTS (Fig.-5.1) shows initially low optical flux but there is a clear evidence of brightening starting from 2008 February ($\sim$ MJD 54500) to 2011 February ($\sim$ MJD 55600). After the brightest optical flux (13.8 mJy) ever detected in 2011 February this source again entered in flux declining phase. The lightcurve clearly indicates

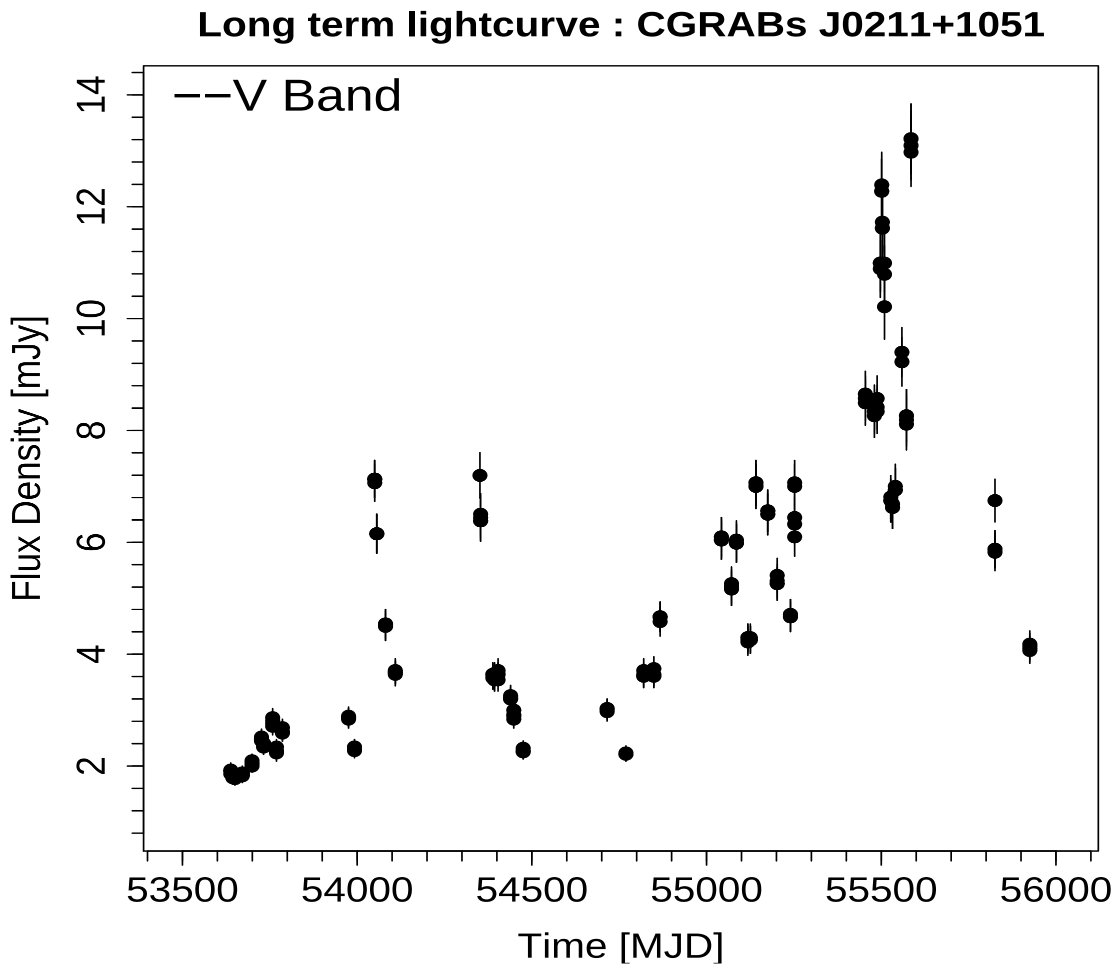

Figure 5.1 V-band CRTS observations showing slow increase in the flux during 2008-2011 (Courtesy Djorgovski et al. (2011))

the violent activity superposed on slow rising flux in this source. Since it's inclusion in the first LAT catalog, this source never showed very significant $\gamma - Ray$ activity. The daily averaged flux always showed upper-limit values. It was only in 2011 January when this blazar showed very violent Gamma-Ray activity.

On 2011 January 23 high activity in $\gamma - rays$ (E >100 MeV) was detected in CGRaBS J0211+1051 by LAT on board Fermi (D'Ammando, 2011). The measured flux of $1.0(\pm 0.3) \times 10^{-6}$ photon $cm^{-2}s^{-1}$, was 25 times more than the flux averaged over the previous 11 months (Abdo et al., 2010b). Following the report of this activity Swift monitored this source on 2011 January 25, under the scheme of target of opportunity (TOO) observations. The swift/UVOT observations showed that the source was about 1.3 and 1.4 magnitude brighter in U band (13.77$\pm$0.03 mag) and W2 band (14.44$\pm$0.04 mag), respectively, compared with their values on 2010 March 05 (D'Ammando et al., 2011b). These two reports attracted the attention of many ground based observatories to investigate this source in detail. On 2011 January 27, Nesci (2011) reported an R_c band magnitude of 13.37 for the source which is 1.74 mag brighter than the POSS-I red plate value and the Digitized First Byurakan Survey (DFBS) value of 15.1 as obtained in 1950 and 1971, respectively. In a telegram, Kudelina et al. (2011) used MASTER-net facility to report the source showing a continuous increase in brightness from 14.45 mag in white light on 2010 February 03 to 13.35 mag on 2011 January 24. All these reports, made by several observatories as mentioned above, suggest that CGRaBS J0211+1051 was brightening since last few years, having short variability timescales with 0.5-1.0 magnitude amplitude of variation. The observed insignificant flux measured by Swift (X-Ray) and Fermi (γ−ray) before 2010, indicates the flux increment at optical was not correlated with the flux at high energies. However, the blazar candidate CGRaBS J0211+1051 had undergone a violent state during 2011 January 03 - February 08 in almost all the wavebands. As there is very little informations available in literature on the nature of this source, characterised as a possible BL Lac object, it would be very interesting to study the behaviour of this source on short timescales using regular monitoring. During the 2011 flare of this source in $\gamma - Rays$, Gorbovskoy et al. (2011) made optical polarimetric measurements in the V-Band using MASTER-net facility at Tunka-Baykal and Amur-Blagoveschensk, and found the source showing 12% polarization on 2011 January 28. The corresponding V band magnitude was reported to be 13.65. Later on January 30, Chandra et al. (2011b) reported much higher (20.7%) degree of linear optical polarization.

Extreme variations in the flux and polarization at various time scales across the whole electromagnetic spectrum are the characteristics of the blazars (see Baliyan et al., 2001; Baliyan, 2001; Chandra et al., 2012, and references therein), a subclass of AGN seen at small angle ($\leq 10°$) to the jet emanating from very close to the black hole (Urry and Padovani, 1995; Blandford and Königl, 1979a). Such variations could be caused by the perturbations in accretion disk or relativistic jet as described by several models (e.g., Mangalam and Wiita, 1993; Marscher and Gear, 1985b; Qian et al., 1991; Marscher et al., 1992; Gopal-Krishna and Wiita, 1992). Since radio to X-ray emission in blazars can be associated with synchrotron radiation, systematic polarization measurements provide important tool to understand the nature of such variations and help to constrain the models of emission. A detailed review of polarization properties of the blazars is given by Angel and Stockman (1980). The study of variation in polarization is also useful in probing the structure of the jet and the nature of physical processes in AGN (Marscher, 2008; Andruchow et al., 2005).

Motivated by this, we decided to carry out a systematic study of polarization in AGN in general and blazars in particular as a part of this thesis. In the next section, we discuss optical polarization in blazars and perform a statistical investigation, using data available in literature and our own observations, on the nature of polarization in blazar sequence, that is, low and high energy peaked blazars and flat spectrum radio quasars. Subsequent part of the thesis deals with detailed optical polarization measurements, and results thereof, on the source CGRaBS J0211+1051 during 2011 January 30 to February 3. These observations were made using PRL made optical polarimeter as a back-end instrument on f/13 cassegrain focus of 1.2 m optical telescope at Mt. Abu Infrared Observatory (MIRO), Rajasthan. The main objective is to investigate the day-to-day variability in degree of polarization and position angle, and any possible intra-night activity in the source. These make first detailed and systematic polarization data on the CGRaBS J0211+1051 reported so far.

5.2 Statistical study of polarization in blazars

The blazars, a sub-class of AGN, comprise Flat Spectrum Quasars (FSRQs) and BL Lac Objects. These are seen at very small angles to the jet axis and hence their emission is dominated by jet, enhanced by Doppler boosting. The emission is the synchrotron radiation emitted by the relativistic electrons/positrons moving in magnetic field and hence is highly polarized (few % to as high as 70%) from radio to optical wavelengths, now observationally proven. The blazars are sub-classified into FSRQs, LBLs, IBLs and HBLs based on the positions of the synchrotron peak in their SEDs. The LBLs and FSRQs have their synchrotron peak lying somewhere below $10^{14} Hz$. The BL Lac objects with their synchrotron component of SED peaking above $10^{16} Hz$ are known as HBLs whereas the ones with same peaking in between $10^{14} - 10^{16} Hz$ are termed as IBLs. Such sub-classified objects show several properties in a distinct fashion. The FSRQ's are most luminous, have strongest jet power and both these properties decrease from FSRQ to HBL. However, the dominance of synchrotron component shows opposite trend with HBL showing larger synchrotron flux than FSRQ and LBLs. The FSRQs and LBLs also show higher $\gamma-$ray flux as compared to HBLs. Several researchers have studied their polarization properties but arrive at different conclusions, e.g., Andruchow et al. (2005) reported LBLs to show higher polarization than shown by HBLs, while Heidt and Nilsson (2011) found only marginal difference in their polarization properties. However, their sample of *blazar candidates* consisted of 37 HBLs and only 8 LBLs and hence their inference could be affected by the low statistics. We, therefore, decided to carry out a statistical study with a larger sample to investigate whether these sub-classes exhibit any difference in their polarization properties.

5.2.1 The sample of Blazars

Information on the optical polarization is not available for many known blazars due to very limited optical polarization studies. However, in order to settle the question of polarization nature of blazar sequence and to determine a reliable distribution of polarization (DP) for this purpose, we carried out a detailed study by significantly enlarging the sample of blazars with known/observed degree of polarization. Mt. Abu Infrared Observatory operates a photo-polarimeter built in-house. We have used polarimetric observations of 10 blazars monitored regularly during last five years. We also included data from Steward Observatory, University of Arizona which is regularly monitoring a set of 64 γ-ray bright blazars since mid of 2008, out of which 44 are FSRQs and 20 BL Lacs. The observation and analysis methodologies exercised at the Mt Abu Observatory are well described in chapter 2 of this dissertation. The details of observation criteria used will also be briefly described later in this chapter. Both the polarimeters, one being used at Steward Observatory and the one at MIRO, are exactly similar in their concept and functionality.

We constructed our sample by using above mentioned data on polarization from these two observatories and the samples used by Jannuzi et al. (1993); Visvanathan and Wills (1998); Andruchow et al. (2005, 2008). We, thus, have 93 blazars in our sample for which we have reliable and updated values of the degree of optical polarization. The sample is balanced in the sense that out of these 47 are LBLs/FSRQs and 46 HBLs(XBLs).

5.2.2 Sample analysis: Blazar sequence and polarization

In our sample, we have used the values showing maximum degree of observed polarization for individual sources. Tables 5.1 and 5.2 present the list of sources used in our sample with their values of DP for RBLs and XBLs, respectively. The first column of these tables show the names of the sources. Column 2 and column 3 are their corresponding RA (J2000) and Dec (J2000). Column 4 gives the maximum DP observed for these sources during the course of monitoring. The last two columns report synonyms from other catalogs. These two names were chosen for identification of type of sources from previous studies.

Table 5.1: Optical polarization for RBLs/LBLs. Courtesy: Steward Observatory, Arizona and MIRO, India.

S.No.	**Name**	***RA (J2000)***	***DEC (J2000)***	***DP***	**Few other popular names**	
1	0048-097	12.67	-9.48	27.1	PKS J0050-0929	1FGL J0050.6-0928
2	0109+224	18.02	22.74	13.4	S2 0109+22	1FGL J0112.0+2247
3	0118-272	20.13	-27.02	8.17	PKS J0120-2701	1FGL J0120.5-2700
4	0215+015	34.45	1.75	20	PKS J0217+0144	1FGL J0217.9+0144
5	3c66a	35.67	43.04	32.6	1ES 0219+428	1FGL J0222.6+4302
6	0219+428	35.67	43.04	15	1ES 0219+428	1FGL J0222.6+4302
7	0235+164	39.66	16.62	43.9	PKS J0238+1636	1FGL J0238.6+1637
8	0301-243	45.86	-24.12	11.7	PKS J0303-2407	1FGL J0303.5-2406
9	0300+471	45.9	47.27	24	4C+47.08	1FGL J0303.1+4711
10	0422+004	66.2	0.6	9.75	PKS J0424+0036	1FGL J0424.8+0036
11	0454+844	77.18	84.53	18.5	S5 0454+84	NVSS J050842+843204
12	0521-365	80.74	-36.46	9.4	PKS J0522-3627	1FGL J0522.8-3632
13	0537-441	84.71	-44.09	18.7	PKS J0538-4405	1FGL J0538.8-4405

DP shown in this table is maximum observed.

Table 5.1 – continued from previous page

S.No.	Name	*RA (J2000)*	*DEC (J2000)*	*DP*	Few other popular names	
14	0548-322	87.67	-32.27	2.4	PKS J0550-3216	SWIFT J0550.8-3215
15	0716+714	110.47	71.34	27.96	S5 0716+71	1FGL J0721.9+7120
16	0735+178	114.53	17.71	36	PKS J0738+1742	1FGL J0738.2+1741
17	0754+100	119.28	9.94	26	PKS J0757+0956	1FGL J0757.2+0956
18	0818-128	125.24	-12.98	18.2	PKS J0820-1258	2MASS J08205744-1258590
19	0823+033	126.46	3.16	22.9	PKS J0825+0309	1FGL J0825.9+0309
20	0823-223	126.51	-22.51	12.7	PKS J0826-2230	1FGL J0825.8-2230
21	0829+046	127.95	4.49	20.5	PKS J0831+0429	1FGL J0831.6+0429
22	0851+202	133.7	20.11	37.2	PKS J0854+2006	1FGL J0854.8+2006
23	0954+658	149.7	65.57	33.7	S4 0954+65	1FGL J1000.1+6539
24	1144-379	176.76	-38.2	3.36	PKS J1147-3812	1FGL J1146.9-3812
25	wcom	185.38	28.23	20.67	S3 1219+28	1FGL J1221.5+2814
26	1308+326	197.62	32.35	28	B2 1308+32	1FGL J1310.6+3222
27	1349-439	208.24	-44.21	21.5	PKS J1352-4412	2MASS J13525653-4412404
28	1400+16	210.69	16	16.2	PKS J1402+1600	2MASX J14024452+1559565

DP shown in this table is maximum observed.

Table 5.1 – continued from previous page

S.No.	Name	*RA (J2000)*	*DEC (J2000)*	*DP*	Few other popular names	
29	OQ530	214.94	54.39	6.4	S4 1418+54	BZB J1419+5423
30	1514+197	229.24	19.54	16.8	PKS J1516+1932	1FGL J1516.9+1928
31	1514-241	229.42	-24.37	8	PKS J1517-2422	1FGL J1517.8-2423
32	1519-273	230.66	-27.5	11.4	PKS J1522-2730	1FGL J1522.6-2732
33	1538+149	235.21	14.8	29.6	PKS J1540+1447	1RXS J154049.5+144739
34	1542.8+612	235.74	61.5	6.9	GB6 J1542+6129	1FGL J1542.9+6129
35	1749+701	267.14	70.1	20.3	S5 1749+70	1FGL J1748.5+7004
36	1749+096	267.89	9.65	32	PKS J1751+0939	1FGL J1751.5+0937
37	1803+784	270.19	78.47	35.2	S5 1803+78	1FGL J1800.4+7827
38	1807+698	271.71	69.82	12	S4 1807+69	1FGL J1807.0+6945
39	B1921-293	291.21	-29.24	20.9	PKS J1924-2914	1FGL J1925.2-2919
40	2007+777	301.38	77.88	15.1	S5 2007+77	1FGL J2006.0+7751
41	2005-489	302.36	-48.83	11.93	PKS J2009-4849	1FGL J2009.5-4849
42	2032+107	308.84	10.94	12	PKS J2035+1056	1FGL J2035.4+1100
43	2155-304	329.72	-30.23	6.1	PKS J2158-3013	1FGL J2158.8-3013

DP shown in this table is maximum observed.

Table 5.1 – continued from previous page

S.No.	**Name**	***RA (J2000)***	***DEC (J2000)***	***DP***	**Few other popular names**	
44	BLLac	330.68	42.28	26.08	B3 2200+420	1FGL J2202.8+4216
45	2233-148	339.14	-14.56	23.02	PKS J2236-1433	1FGL J2236.4-1432
46	2254+074	344.32	7.72	21	PKS J2257+0743	2MASS J22571731+0743122
47	2345-167	357.01	-16.52	19	PMN J2348-1631	1FGL J2348.0-1629

Table 5.2: Optical polarization for HBLs/XBLs. Courtesy: Steward Observatory, Arizona and MIRO, India. The data from Jazzuzi (1993) are also used.

S.No.	**Name**	***RA (J2000)***	***DEC (J2000)***	***DP***	**Few other popular names**	
1	0122.1+0903	21.18	9.32	3.5	MS 01221+0903	QSO B0122+090
2	0158.5+0019	30.28	0.57	6	BZB J0201+0034	NVSS J020106+003402
3	0205.7+3509	32.16	35.39	1.91	BZB J0208+3523	1FGL J0208.6+3522
4	0257.9+3429	45.27	34.68	6.25	BZB J0301+3441	1RXS J030103.8+344109
5	0317+185	49.97	18.76	5.2	BZB J0319+1845	1FGL J0319.7+1847
6	0323+022	51.56	2.42	10.37	BZB J0326+0225	1FGL J0326.2+0222
7	0419.3+1943	65.58	19.85	3.66	BZB J0422+1950	1RXS J042218.2+195047
8	0422+004	66.2	0.6	12.65	BZB J0424+0036	1FGL J0424.8+0036
9	0514+064	78.94	-45.95	6.91	BZQ J0515-4556	CRATES J051545.27-455643
10	0548-322	87.67	-32.27	1.48	BZB J0550-3216	1ES 0548-322
11	0607.9+7108	93.43	71.12	4.82	BZB J0613+7107	XBS J061342.7+710725
12	0647+250	102.69	25.05	3.8	BZB J0650+2503	1FGL J0650.7+2503

DP shown in this table is maximum observed.

Table 5.2 – continued from previous page

S.No.	Name	*RA (J2000)*	*DEC (J2000)*	*DP*	Few other popular names	
13	0737.9+7441	116.02	74.57	2.74	BZB J0744+7433	1FGL J0745.2+7438
14	0806+524	122.45	52.32	4.65	BZB J0809+5218	1FGL J0809.5+5219
15	0922.9+7459	142.01	74.79	6	BZB J0928+7447	RX J0928.0+7447
16	0950.9+4929	148.54	49.25	5.19	BZB J0954+4914	RX J0954.1+4914
17	1101-232	165.91	-23.49	2.68	BZB J1103-2329	1FGL J1103.7-2329
18	1101+384	166.11	38.21	7	BZB J1104+3812	1FGL J1104.4+3812
19	1133.7+1618	174.07	16.03	2.2	BZB J1136+1601	1RXS J113618.1+160148
20	1207.9+3945	182.64	39.41	4	NGC 4151	87GB 120800.7+394100
21	ON325	184.47	30.12	10.2	BZB J1217+3007	1FGL J1217.7+3007
22	1219+305	185.34	30.18	1.27	BZB J1221+3010	1FGL J1221.3+3008
23	1221.8+2452	186.1	24.61	12.3	BZB J1224+2436	MS 1221.8+2452
24	1229.2+6430	187.88	64.24	2.28	BZB J1231+6414	RGB J1231+642
25	1235.4+6315	189.41	62.98	2.62	BZB J1237+6258	NVSS J123739+625843
26	1258.4+6401	195.1	63.75	1.2	BZB J1300+6344	——
27	1402.3+0416	211.21	4.03	9.52	BZB J1404+0402	1E 1402.3+0416

DP shown in this table is maximum observed.

Table 5.2 – continued from previous page

S.No.	Name	*RA (J2000)*	*DEC (J2000)*	*DP*	Few other popular names	
28	1407.9+5954	212.35	59.66	8.64	BZB J1409+5939	MS 1407.9+5954
29	1415.6+2557	214.5	25.14	7.53	NGC 5548	RX J1417.9+2508
30	1426+428	217.14	42.67	2.48	BZB J1428+4240	1FGL J1428.7+4239
31	1440+122	220.7	12.01	3.36	BZB J1442+1200	1FGL J1442.8+1158
32	1458.8+2249	225.26	22.64	7.03	BZB J1501+2238	1FGL J1501.1+2237
33	1534.2+0148	234.19	1.63	3.73	BZB J1536+0137	MS 1534.2+0148
34	1552.1+2020	238.6	20.19	5.95	BZB J1554+2011	1ES 1552+203
35	1553+113	238.93	11.19	3.7	BZB J1555+1111	1FGL J1555.7+1111
36	1652+398	253.47	39.76	4.6	BZB J1653+3945	1FGL J1653.9+3945
37	1704.9+6046	256.4	60.7	7.48	BZB J1705+6042	1E 1704.9+6047
38	1722+119	261.27	11.87	6.1	BZB J1725+1152	1FGL J1725.0+1151
39	1757.7+7034	269.3	70.56	3.7	BZB J1757+7033	MS 1757.7+7034
40	1959+650	300	65.15	6.4	BZB J1959+6508	1FGL J2000.0+6508
41	2155-304	329.72	-30.23	4.99	BZB J2158-3013	1FGL J2158.8-3013
42	1652+398	329.72	-30.23	2.42	BZB J1653+3945	1FGL J2158.8-3013

DP shown in this table is maximum observed.

Table 5.2 – continued from previous page

S.No.	Name	*RA (J2000)*	*DEC (J2000)*	*DP*	Few other popular names	
43	2336.5+0517	354.78	5.57	5.13	BZB J2339+0534	MS 2336.5+0517
44	2342.7-1531	356.34	-15.25	7.87	BZU J2345-1515	MS 2342.7-1531
45	2344+514	356.77	51.7	3.05	BZB J2347+5142	1FGL J2347.1+5142
46	2347.4+1924	357.5	19.69	3.09	BZB J2350+1941	MS 2347.4+1924

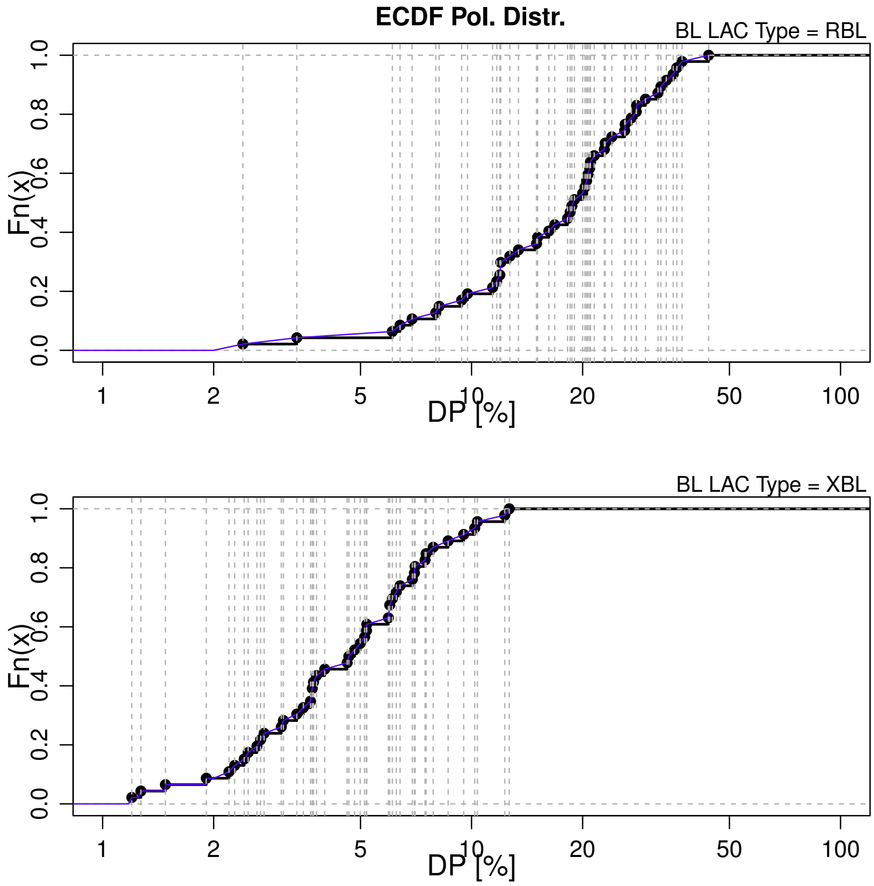

Figure 5.2 The cumulative distribution of RBLs and XBLs. The top panel shows the distribution of DP for a sample of LBLs and the bottom one for HBLs.

For a better presentation of the findings of the statistical study, we plot the cumulative distribution of degree of polarization over the samples of blazars. The figure 5.2 presents the results of the study mentioned above. The two panels show the cumulative plots of the distribution of DP for the RBLs (upper) and XBLs (lower), respectively. Fig.- 5.2 clearly indicates that most of the RBLs show the degree of polarization (DP) as high as more than 15 %. While the lower panel indicates that most of the XBLs are seen to show lower DP as less than 10 %. This result is consistent with the previous studies (Antonucci, 2002; Wills et al., 1992). The present statistical analysis confirms that the LBL and HBLs show distinct polarization property which can be used to tentatively classify blazars. We have grouped LBLs and FSRQs together in this study. Here we clearly see that LBL (RBLs) in general show much higher degree of polarization as compared to HBLs. The exact reason behind this behaviour is not clearly known but either LBLs have stronger and/or more highly aligned magnetic field as compared to HBLs or perhaps they differ in particle and magnetic energy densities. We know that HBL have their synchrotron peak at very high energies, meaning either they have very high and/or aligned magnetic field or larger number of energetic particles than LBL. But since they have low optical polarization, as per present study, they are not expected to have stronger magnetic field. They therefore have systematically more energetic particles, with higher Lorentz factors, in their jet that cool down radiating high energy emission. The LBLs are known to have higher macroscopic bulk motion (Fan et al., 1997) hence displaying higher duty cycle of variation.

This study could be used as a tool to determine the nature of a source for which information related to its other properties are not known. We however, feel that this gives only a tentative clue whether the blazar candidate was LBL or HBL, while true test remains spectral energy distribution of the source. Nonetheless, in the next section We will show how we can use the result of this study in order to characterize blazar candidate.

5.3 Linear optical polarization study of source CGRaBS J0211+1051

The detection of high polarization in this possible BL Lac object during the decay phase of a γ-ray flare motivated us to carry out a detailed polarization study of this source when it was still in optically flaring phase, precisely from 2011 January 29 to 2011 February 03. The main aim of this part of the study is to determine the polarization properties of CGRaBS J0211+1051 and the nature of this source.

5.3.1 Observations and data analysis

We monitored this source during it's outburst phase in 2011 for consecutive five nights. The PRL made photo-polarimeter (PRLPOL) was used as a backend instrument on 1.2 m telescope at Mt. Abu Infrared Observatory Rajasthan, operated by Physical Research laboratory, Ahmedabad. This is a rotating half-wave plate polarimeter with two identical PMTs used a detectors. The PRLPOL, described in detail by Deshpande et al. (1985), was recently fully refurbished and automated (Ganesh et al., 2009). A detail description of present design and working of PRLPOL is given in chapter 2 (section 2.2.2) of this document. It works on the principle of rapid modulation with a fast-rotating, super-achromatic half-wave plate, completing one physical rotation in 96 steps (3.75°per step). The rapid modulation using rotating halfwave plate is used to avoid the uncertainties incorporated by atmospheric scintillation, seeing and by inaccurate telescope guiding. These are the main sources of error in polarization measurements of a bright star. The rapid modulation technique makes the polarization measurements feasible with a precision even better than $\pm 0.01\%$. In our setup at MIRO four modulation cycles are completed in one full rotation of the half-wave plate with 24 steps per modulation cycle. The Wollaston prism divides the incident light beam into two orthogonally polarized components, each one directed to separate identical detectors, here photomultiplier tube (PMT). The instrument has a UBVRI-system filter slide and a second slide with diaphragms of differently sized apertures. A glan prism is used on the top for calibration of the instrument for 100% and 0% polarized light. In the following text we describe the details of strategies and methods used for observing this source.

This blazar is relatively faint in optical band. Therefore the observations were carried out mostly in the white light to maximize the signal. For white light, the effective wavelength is determined by the sensitivity of the detector, here PMT (EMI 9863B), which peaks at $\sim \lambda = 400$ nm. Apart from white light monitoring, some measurements were also made with B, V, and R filters to investigate the wavelength dependence of polarization (WDP), if any. We used same exposure time and aperture to snap the nearby star free area to get the sky or background, contribution. In order to avoid the change in polarization because of changes in background the alternative exposures of source and sky are performed. This way we are incorporating the most recent status of background polarization. The centring of source in aperture diaphragm was cross checked after each exposure to avoid any spurious effect because of scattering from edges of diaphragm. The source was re-centred whenever a small drift was noticed during the observation. In the present case the part of sky in the direction of source is rare enough to provide nearby source free region. Therefore sky measurements were taken about 30 arcsec away from the target source. The exposure time for white light and different filters are decided on the basis of counts obtained from PMTs. This in present case for both the sky and the source was kept at 40 seconds during all five nights for unfiltered white light observations and 120 s for observations in the B, V, and R bands. The selection of appropriate size of aperture is very important decision for such polarimeters. The smaller ($\sim FWHM$) aperture may introduce spurious variations caused by the slight change in atmospheric conditions. On the other hand, bigger size of aperture includes a larger sky background which increases the uncertainties in measurement leading to low S/N. The larger aperture also includes the larger contribution of thermal emission from host galaxy which further dilutes the intrinsic polarized flux from the nucleus. Therefore one need to choose some criteria for optimizing the size of aperture. In the present case host galaxy is more than 3 mag fainter than the nucleus (Meisner and Romani, 2010). Weather conditions were photometric with a moonless sky, which was always more than 2 mag fainter than the source. Keeping all this in mind and using the prescriptions by Andruchow et al. (2008) for avoiding spurious variations caused by any possible change in the seeing and the contamination by the thermal emission from the host galaxy, 10 arcsec aperture is chosen for the target and other observed stars used for calibrations. For the duration of integration on the sky or the source, counts are accumulated in 24 array locations corresponding to the half-wave plate positions with a 2 ms sampling time. The degree of polarization (DP), error of polarization and the polarization position angle (PA) for the source are then calculated by the control program after each integration, subtracting the previously observed sky counts. The computation is performed using a least-squares fit to the counts from the two PMTs to determine the stokes parameters. The stokes parameter are then used to determine the DP and PA using equation 2.2 (chapter 2). The mean error in the DP is estimated from the deviation of the actual counts from the fitted curve. Standard stars were observed every night to determine the zero point for the P.A. and the instrumental polarization, which was found to be negligibly small (<0.02%).

5.3.2 Results and discussions

The zero point for P.A. of polarization for the source was corrected using measurements on the polarization standard 9-Gem and error in P.A. was estimated using the following expression by Serkowski (1974).

$$e_{PA} = \frac{e_{DP} \times 28.6}{DP} \tag{5.1}$$

The observations described in previous section are performed with utmost care of all the possible source of errors in polarization. The polarimeter setup is enabled with rapidly modulated rotating super achromatic retarder (half-wave plate) which itself takes care of systematics errors mainly because of scintillation and seeing effects. A possible source of error in the measurement of polarization parameters lies in dealing with the sky background. It could be particularly serious when the sky is close to the source brightness and has large and variable polarization due to, for example, the presence of Moon. Since such a large, variable polarization affects both the source and the sky, therefore, this systematic effect can be effectively removed if the sky measurements are made close in position and time to the source observations. In the present case, we have taken the above precaution in the sky measurement adapting sky-source-sky strategy. Also the moonless, dark ($\sim$ 2 mag fainter than source) and stable sky (maximum 6%) during the course of monitoring made our life very simple.

Date	MJD	$\Delta T[hr]$	DP [%]	σ_{DP}	P.A. $[Deg.]$	$\sigma_{P.A.}$
2011 Jan 30	55591.3796	0.336	21.052	0.295	42.771	0.634
2011 Jan 31	55592.4665	0.864	12.871	0.489	28.963	0.758
2011 Feb 01	55593.4352	2.498	10.643	0.493	30.679	1.373
2011 Feb 02	55594.4362	2.112	12.629	0.981	52.982	1.412
2011 Feb 03	55595.4308	1.920	15.481	1.412	43.578	1.762

Note: Entries are the dates of observation, MJD, duration of observation, DP, σ_{DP} , P.A., and $\sigma_{P.A.}$.

Table 5.3: Nightly Averaged Polarization Data for CGRaBS J0211+1051

Any change in the DP of the sky on any particular night remained well within the measurement errors. We, therefore, do not expect any significant spurious effect on the source polarization due to the sky fluctuations.

In the Table 5.3, we report the polarization data during the given observing run giving date, MJD, the duration of observation in hours, nightly averaged values of the DP, P.A., and their respective standard deviations. The polarization data reported here are obtained through a 10 arcsec aperture as mentioned in the previous section. A larger aperture might result in a significant reduction in the DP due to thermal emission from the host galaxy contaminating the nonthermal emission from the nucleus, particularly when the host galaxy is bright. CGRaBS J0211+1051 and its host galaxy had I -band magnitudes of 15.32 and 16.91, respectively, as reported by Meisner and Romani (2010) during their 2008 October 31 to November 2 observations. Since galaxy light peaks in the near-infrared band and has a reduced brightness at a shorter wavelength, the effect of galaxy light contaminating the nuclear emission will be reduced in the optical B, V, and R bands. Also, the source was in a fairly bright phase, brighter than 13.5 in R (Nesci, 2011; Kudelina et al., 2011), during our polarimetric observations, making it more than 3 mag brighter than the host galaxy. Therefore, there should not be any significant contamination of the nuclear light by the host. Nevertheless, the polarization values reported here should be marginally lower than their intrinsic values.

Intra-night and inter-night variation in polarization

The blazars are known to show rapid, large-amplitude variations in flux and polarization at various timescales. The nature of such variations can be used to infer the physical processes at work in these sources. The intra-night variations in DP and P.A. are investigated using the data collected during the five night of monitoring. Figures 5.3(a)-5.3(e) demonstrate the curves of representation. The upper panel of each plot shows the variation of DP with time. The reference of time is taken as MJD 55590 (2011 January 29). For the observations made during the course of 2011 January 30 to 2011 February 01, the monitoring was done in white light only while B, V and R band monitoring was also performed during February 02 and 03. The main aim of using other bands was to know color dependence in polarization, if any. The error bars in plots indicate the uncertainties (including the uncertainty in the background determination) in the individual measurement of DP and P.A. In the following, we present polarization results from these nightly polarization curves.

On 2011 January 30, the source was highly polarized at more than 21% level during our 20 minute observations (Figure 5.3(a)). The P.A. was $\sim 43^\circ$. We do not note any significant variation in DP or P.A. during the course of our observations on that night. However, this value of DP is much higher than the value reported by Gorbovskoy et al. (2011) on 2011 January 28 (DP = 12%), just two days prior to our measurements. This indicates that the source has increased it's polarization by about 9% within only two days. This source was monitored only for 0.7 hours during the 2011 January 31 with only 14 data points. At the onset of observations, DP is about 13%, increasing to 13.81($\pm$0.35)% before falling by 2.7% (5σ) to 11.10($\pm$0.41)% within about 20 minutes (decay rate, $\sim 8\%\ hr^{-1}$). The DP starts increasing again and reaches about a 13.2% level in 18 minutes (rising rate, $7\%\ hr^{-1}$) with a 2.1% (4σ) amplitude of variation. The visual inspection, therefore, shows rapid variation in DP with significant ($4\sigma - 5\sigma$) amplitude of variation on 2011 January 31 (see Figure 5.3(b)). The P.A., however, remains well behaved without any significant variation. During the course of February

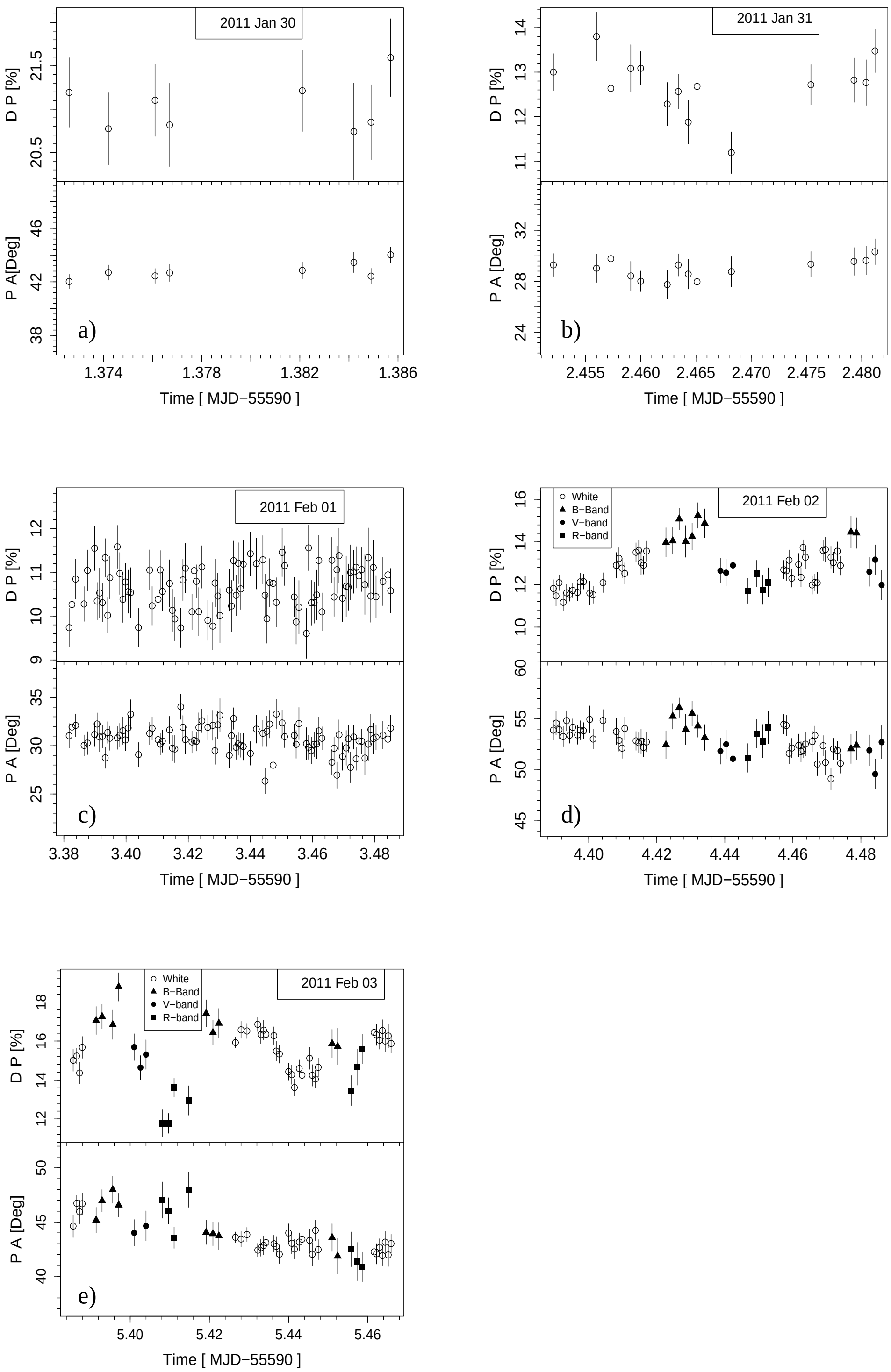

Figure 5.3 Intra-night variation in D.P. and P.A for all the five nights from January 30 to 2011 February 03. The open circle represents the measurements taken in white light. The different symbols in the curves dated 02 & 03 February 2011 are used for observations in other filters.

01 this source was monitored for comparatively longer duration ($\sim$ 2.4 hrs). Several micro-variability events appear to be superimposed over a non-varying component [Figure 5.3(c)]. However, except for the two events beginning at MJD 55593.424 and MJD 55593.446 with more than 3σ amplitude of variation in DP, other variations are within 2σ . The P.A. stays within $31° \pm 3°$ without any significant change.

The temporal behaviour of the polarization of the blazar CGRaBS J0211+1051 on 2011 February 02 and 03 is shown in Figures 5.3(d) and (e). During these two nights, in addition to the white light, observations were also made in the B, V, and R filter bands to observe any wavelength dependence in the DP and P.A. Let us first look at the behaviour of the source in the white light only. On 2011 February 02, beginning and ending segments (from time 4.388 to 4.418 and 4.456 to 4.476) of the curve display white light measurements [cf. Figure 5.3(d)]. The visual inspection of the plot clearly shows an increase in DP by 2.2% (close to 3σ) during $\sim$ 32 minutes (rate of increase in DP, $4\% hr^{-1}$). The measurements in the white light toward the end also give an indication of a change (at 2σ level) in DP. On 2011 February 03, DP decreases from 16.8% at time $\sim$ 5.432 to $\sim$ 13.8% at time 5.442 (cf. Figure 5.3(e)), with an amplitude of variation of about 3% (3σ). This drop is then followed by an increase in DP by about 2.6% within a span of 35 minutes at the rate of 4.5% hr^{-1} toward the end of the observations. The source, therefore, undergoes rapid intra-night variations in the DP on 2011 January 31, and February 02 and 03, as reflected in the white light polarization curves.

Considering the observations made through the B, V, and R filters in addition to the white light ones, we now discuss Figure 5.3(d) & (e) again. On 2011 February 02, DP rises from 11.5% (at time 4.392) to 13.5% (at time 4.416, cf. Figure 2(a)) in white light. The rise continues in the B-band observations reaching more than 15% at MJD = 55594.43. Beyond that, DP decreases in V and R bands partly due perhaps to the increase in wavelength and partly due to the intrinsic variation in the polarization of the source. The rates of decay in DP from the B to V bands and the V to R bands are approximately 22% hr^{-1}

and 11% hr^{-1}, respectively. Toward the end, observations in the white light show an increasing trend with DP peaking in the B band ($\sim$ 14.3%) before dropping to $\sim$ 12.2% in the V band (DP decay rate from the B to V bands was 14% hr^{-1}). The P.A. largely remains within the $\pm 3°$ range. Figure 5.3(e) shows polarization behaviour of CGRaBS J0211+1051 during 2011 February 03. Interestingly, the composite curve shows three quasi-periodic polarization flashes with a significant amplitude of variation (up to 4%). These events have fast rise and fall timescales, ranging from 17 to 35 minutes. It is important to note that DP changes at a rate of about 31%, 35%, and 40% hr^{-1} from B to V, V to R, and R to B bands, respectively, as estimated from the polarization curve for 2011 February 03. The P.A. varies between 41° and 46° during the course of observations and can be considered as only mildly variable.

The blazars are known to show wavelength dependent polarization (WDP). Any WDP in the jet-dominated blazars is known to be due to the source geometry and/or due to the contamination of the nuclear non-thermal radiation by the thermal unpolarized emission from the host galaxy (Brindle et al., 1986; Angel and Stockman, 1980). In many cases, DP is noticed to increase with frequency (e.g., Sitko et al., 1985; Holmes et al., 1984; Angel and Stockman, 1980) in the optical region. However, decrease in DP with frequency is also detected in several cases. For example, Tommasi et al. (2001) observed several blazars simultaneously in UBVRI optical bands. While they found DP to increase with frequency in many sources, OJ287 and the BL Lac object were noticed to show a decrease in DP with frequency.

In the present case, 2011 February 2 and 3 measurements with B, V, and R filters appear to support the trend that the DP increases with frequency in Bl Lac objects. The DP in the B band shows an increase over R- and V-band values (Figure 2), which cannot only be due to the intrinsic variation because variation timescales are expected to be longer than the temporal resolution (about 5 minutes) used here. A careful examination of the variation pattern in DP shows that while the rate of change in DP obtained in white light is, on average, about 4% - 8% hr^{-1} (except for a segment in the polarization curve

on 2011 February 03 when it is about 11% hr^{-1}), it is as high as 12% - 40% hr^{-1} in the values obtained using different bands. The significant increase in the rate of change in DP with time when observed through the B, V, and R bands, is, perhaps, partly due to WDP. However, from the present data, it is not possible to clearly establish the extent to which WDP contributes to the observed polarization variability. For this, simultaneous observations in different optical bands are needed.
Now, let us look at the inter-night variations during 2011 January 30 to February 03. Table 5.3 and Figure 5.4 represents the averaged DP and P.A. for all five nights. The uncertainties plotted in Figure 5.4 are the spread (1σ) of to intra-night variations in addition to the measurement errors. It is evident from the figure 5.4 that the source was highly polarized on 2011 January 30 with DP at about 21%, which decreased by 9% and 11% on 2011 January 31 and February 01, respectively. A flip in behaviour in DP is seen in between February 01 -02 as clear from the curve (cf. Figure 5.4). After the decrease upto January 01 DP increased again reaching 15.5% on 2011 February 03. The P.A. is also seen to change significantly from night to night, initially following the trend in the DP but dropping to 45° on the last night while DP increased to a 15% level. We note changes in the P.A. by $2° - 22°$ while remaining within the $28° - 53°$ range during our observations.

Apart from above simple analysis of the polarization curves to look for variations, we also carried out a statistical parametrization to detect and quantify the variations using the criterion of Kesteven et al. (1976) and applied by several authors for variability studies (e.g., Romero et al., 1994; Andruchow et al., 2005). Here, the variability in DP and P.A. during individual night are described by the fluctuation index μ and the fractional variability index FV of the source. The corresponding expressions for both the quantities are given as below:

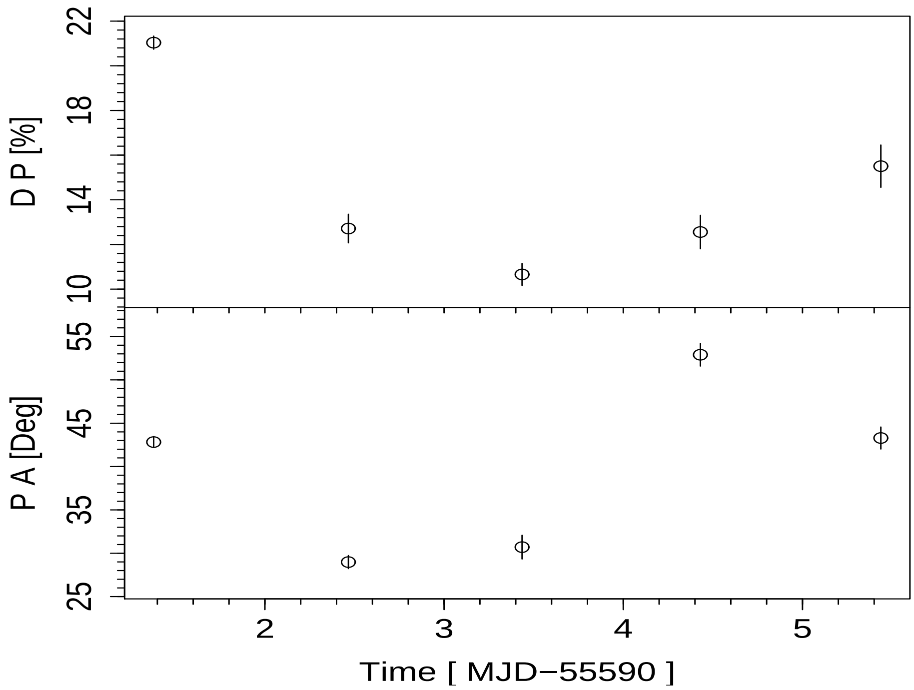

Figure 5.4 Intra-night variation in nightly averaged D.P. and P.A for all the five nights from January 30 to 2011 February 03. The error bars are the standard deviations in overnight measurements.

$$\mu = 100\frac{\sigma_S}{\langle S\rangle}\% \tag{5.2}$$

$$FV = \frac{S_{max} - S_{min}}{S_{max} + S_{min}} \tag{5.3}$$

Where σ_S is the standard deviation and $\langle S\rangle$ is the mean value of the DP and P.A. obtained during a particular night, S_{max} ans S_{min} are the, respectively, the maximum and minimum values of the DP or P.A. Furthermore, the source is classified to be variable if the probability of exceeding the observed value of

$$\chi^2 = \sum_{i=1}^{n} \epsilon_i^{-2}(S_i - \langle S\rangle)^2 \tag{5.4}$$

by chance is $< 0.1\%$, non-variable if $> 0.5\%$ and possibly variable for in-between values. In the above expression ϵ_i are uncertainties in the individual measurements, S_i. The values in above expression will be following χ^2 distribution with n - 1 degree of freedom (dof) for random values of ϵ_i, where n is total number of data points in the distribution. Since variability in the polarization parameters (DP and P.A.) due to the WDP and intrinsic variations cannot be separated, the statistical analysis is performed only using white light data. Table 5.4 summarizes the results of above analysis. Columns 1 and 2 represents the date and number of observation points in white light. Columns 3-6 presents the values of μ, FV, χ^2 for DP and status of source (V,NV and PV) inferred using χ^2 values. The remaining four columns represents the same parameters for P.A. The results listed in Table 5.4 quantitatively substantiate the significance of Intra-night variability in both DP and P.A. during the observations of February 02 and 03. According to this analysis the source DP was seen to be non variable during January 30 and February 01 while the P.A. values show a possibly variable status. On January 31 the DP was possibly variable while the P.A. was not varying. It is, however, to be noted that when the number of measurements during a night is not large enough, the above test may not be very suitable. Perhaps that is why the test gives a PV status for DP on 2011 January 31 when we only had 14 data points, while visual inspection shows noticeable variability.

Let us now discuss physics possibly responsible for these observational findings. The optical emission observed in the AGN may be generated mainly in the accretion disk and inner (parsec-scale) regions of the relativistic jet. The disk emission is in general thermal in nature and the polarization is caused by the scattering of disk emission with electrons or dust. The resulting polarization is usually very small ($\leq few\%$). The blazar CGRaBS J0211+1051 is reported in flaring state in $\gamma Rays$ few days prior to our observations. The observations at other wavebands also indicate enhanced emission at lower energies. This perhaps indicate to multi-wavelength emission due to some event in the jet. Also, the high degree of polarization (10 % - 21 %) as observed by us confirm the emission to be dominated by the relativistic jet, aligned at a small angle to the line of sight. The emission in jet at lower frequencies ($\leq 10^{18} Hz$) is mainly due to synchrotron radiation from the relativistically moving electrons in the jet and is highly polarized (>70%) if the magnetic field is uniformly aligned. A reduced observed DP indicates a chaotic magnetic field, which can be described in terms of N cells with a uniform but randomly oriented magnetic field (Marscher, 2008). The DP could also be reduced by geometrical depolarization due to variation in the magnetic field orientation along the line of sight and the contamination by the thermal emission from the host galaxy. In the present case, the depolarization caused by host galaxy is negligible as host galaxy is about 3 mag fainter than the nuclear source.

The P.A. is supposed to be orthogonal to the projected direction of the magnetic field. However, relativistic motion may cause aberrations in the angle resulting in a P.A. that is more aligned with the jet direction. In BL Lac objects, the parsec-scale magnetic field in the jet is tangled and shocks moving down the jet compress the magnetic fields, aligning it perpendicular to the flow direction (Marscher and Gear, 1985b). The interaction of relativistic shocks with features in the parsec-scale jet results in rapid variations in the flux and polarization (Marscher and Bloom, 1992; Qian et al., 1991). Such features are varied in nature and generally are sub-parsec in size. Macroscopic Kelvin-Helmholtz instabilities are capable of producing such features in the inner beam. Quasi-periodic variations could be caused by the regularly spaced obstacles in the path of the jet. The high and variable degree of polarization observed here could be indicative of formation of the shock in the jet and its interaction with the plasma inhomogeneities as discussed in above mentioned models. This mechanism can successfully explain the variations with timescales of weeks to few days. Faster variation down to sub-hour timescales cannot be explained by these models due to limited thickness of the shocks. Such intra-night quasi-periodic flashes observed during February 02 and 03, 2011 are perhaps caused by the turbulence in the post-shock region. In order to characterize such events the variability at other frequencies may play very important role.

The $\geq$ 9% change in DP during 2011 January 28 [DP 12% as reported by Gorbovskoy et al. (2011)] and January 30 (21%, our observations) may be due to compression of plasma by shock as we expect rise in polarization with alignment of magnetic field. Also, sudden changes in DP and PA as observed during Jan 30 & 31, and Feb 1 - 3, 2011, could be indicative of the fresh injection of the plasma at the base of the jet (Andruchow et al., 2003). The mild bluer when brighter nature of flux variation substantiates the fresh injection scenario. The P.A. shows about 25° rise between February 01 - 02 and then decreases by 10° on February 03. The sudden change in the behaviour of P.A. exclude the geometry dependence as we expect the smooth rise or fall over relatively larger timescales. Detailed multi-wavelength, simultaneous observations in flux and polarization are required to have a better understanding of the physical processes at work in these type of enigmatic sources.

.

Date	n	D.P				P.A.			
		μ[%]	FV	χ^2	status	μ[%]	FV	χ^2	status
2011 Jan 30	8	1.403	0.021	2.942	NV	1.482	0.023	8.215	PV
2011 Jan 31	14	3.799	0.075	13.341	PV	2.618	0.044	7.573	NV
2011 Feb 01	87	4.639	0.093	84.610	NV	4.475	0.127	89.691	PV
2011 Feb 02	39	6.153	0.103	128.810	V	2.473	0.056	61.825	V
2011 Feb 03	30	6.121	0.107	121.733	V	2.944	0.054	60.086	V

Note: μ and FV represents the fluctuation index, the fractional variability index for the source using individual night data. The status of the variability is also determined using χ^2 test.

Table 5.4: Variability Test Results for CGRaBS J0211+1051 Using White Light Data Only

5.3.3 CGRaBS J0211+1051: A probable Low-energy peaked BLazar (LBL)

Depending upon their discovery in either radio or X-Ray surveys blazars were broadly classified as radio selected blazars (RBLs) and X-ray selected blazar (XBLs). The later studies carried out by several authors confirmed that they not only differ in wavelength of discovery but also in many of the observational properties like characteristic variability timescale, polarization etc (Urry and Padovani, 1995; Kollgaard, 1994; Fan et al., 1997; Heidt and Nilsson, 2011). Position of the peak of synchrotron component in blazars SEDs classifies them as FSRQs, low-energy peaked BL Lac objects (LBLs) and high-energy peaked BL Lac objects (HBLs). These subclasses are known to have some very distinct properties. For example, their bolometric luminosity decreases from FSRQ to XBL as does the dominance of γ -ray emission (Sambruna, 2007; Fossati et al., 1998). Similarly, RBLs/LBLs are reported to have, on average, much higher DP and amplitude of variation than XBLs (e.g., Andruchow et al., 2005; Tommasi et al., 2001; Fan et al., 1997; Jannuzi et al., 1993). Fan et al. (1997) have ascribed this difference in the DP to the difference in their beaming effect: RBLs show stronger beaming. Ghisellini et al. (1998) confirms the decreasing jet power from FSRQs to XBLs by fitting the SEDs of a sample of blazars which was first suggested by (Fossati et al., 1998). This further supports the stronger beaming in LBLs as compared to HBLs. We discussed deficiencies in the blazar samples used in the past for studying their polarization properties in the preceding section where we put-together a more complete, balanced sample for LBLs and HBLs for such study demonstrating that LBLs are normally more highly polarized than HBLs.

As described in this chapter, CGRaBS J0211+1051 shows rapid, large-amplitude variations in the degree of optical polarization. It also indicates a high duty cycle of variation in polarized flux, showing variability on three (including a borderline variation on 2011 January 31) out of five nights of observation. The DP for this source is always greater than 10% throughout the monitoring period with a maximum value of $\sim 21\%$. As already discussed high DP is characteristic property of RBLs. We can also detect high DP in case of FSRQs. Previous studies suggests this source to be a BL Lac object. Therefore the extent and nature of the linear polarization exhibited by CGRaBS J0211+1051 during 2011 January 30 to February 3 led us to infer that the source probably belongs to the low-energy peaked BL Lac objects (RBLs). Multi-frequency observations covering the radio to γ -ray region, however, are required to study its spectral energy distribution to determine the location of the two peaks and confirm its status in the blazar sequence.

5.4 Conclusions

The present work is the first detailed study of optical polarization measurements for this source. The study is performed based on the linear polarization measurements performed during the multi-frequency flaring of CGRaBS J0211+1051 during 2011 January 30 to 2011 February 03. The source showed a high and variable DP (21% - 10 %) during the course of monitoring. Substantial intra-night variability in DP was observed during February 02 and 03 while the source DP was possibly variable for January 31 as inferred by statistical analysis. The significant variation in P.A. is also observed during

February 02 and 03 while this was seen to be within 2σ during the nights of January 30 and February 01. The P.A. was not variable during February 01. Significant inter-night variations in the DP and P.A. are also noticed. The first rise in DP observed during January 28 (Gorbovskoy et al., 2011) and January 30 could be indicative of the formation of shock in jet. Further decrease in DP and PA between January 30 to February 01 may be the effect of evolution of shock. The second rise in DP and PA around February 01 may be due to the formation of the secondary shock or the oblique nature of shock is responsible for this. The sudden flip in behaviour observed in DP and PA on February 02 is somewhat unclear. This sudden change in PA over-rule the possibility of obliqueness or geometry of shock as it indicates smooth variation in both PA and DP. The exact nature can only be understood after comparing this with the flux variation at other wavelengths. The intra-night variation observed during February 02 and 03 may be the effect of small turbulence or perturbations in the after shock region.

We conducted a statistical study on blazars with a large, balanced sample of LBLs and HBLs to determine whether these sub-classes show any distinct behaviour with respect to degree of optical polarization. Our study clearly establishes that LBLs in general show much higher degree of polarization than HBLs. It indicates that LBLs have stronger magnetic fields, higher macroscopic bulk motion while HBLs have larger number of energetic particles with higher microscopic Lorentz factors in their jet. It is possible that HBLs also have stronger field albeit less homogeneous.

Based on the average high degree polarization (DP) observed during all the five nights we suggest this source to be a LBL. The exact nature can be confirmed by constructing the SED of the source using observations at other wavebands. This source was also observed by many other facilities. In the next chapter we will investigate the SED and multi-frequency lightcurve to confirm the predictions based on optical polarization data only.

Chapter 6

Multi-wavelength study of BL Lac *CGRaBSJ0211+1051*

6.1 Introduction

In the previous Chapter, we reported the detection of high and variable optical linear polarization in the source CGRaBS J0211+1051 in a first detailed polarization study of this source. Based on such high degree of polarization, we also claimed that the source belonged to the sub-class of blazars, called LBL, for which the low energy (synchrotron) part of SED peaks at low frequencies ($\leq 10^{15}$ Hz). However, the confirmation of such a claim, and of the idea that blazars can be classified based on their polarization properties, calls for the determination of the synchrotron peak frequency for this source by constructing its spectral energy distribution. It requires a multi-wavelength study, from radio to gamma-rays to be carried out for CGRaBS J0211+1051. In this part of thesis, we report the outcome of such a study by discussing its SED and light curves.

Blazars are the extreme class of Active Galactic Nuclei (AGN) with variable continuum emission spread over the whole energy spectrum. They are also known to show high ($\geq 3\%$) and variable radio and optical polarization. These sources are characterized by a relativistic jet of plasma emanating from very close to the central black hole and perpendicular to the accretion disk, which is seen at a very small angle ($\lesssim 10°$) (Urry and Padovani, 1995; Urry, 2000) to the line of sight. This implies the emission from these objects are dominated by the jet emission which is highly boosted due to the effects of special relativity. The very fact that such emission is generated from very close to the central source makes variability in blazar emission an important tool to study the central engine in AGN. The timescales observed could give us clues about emission regions and physical processes responsible for such emission.

The spectral energy distribution (SEDs) of blazars have a characteristic double-peaked shape with a low frequency component peaking somewhere in sub-mm to X-Rays energy band, and a high frequency component peaking at MeV-TeV energies. The low energy component of SED is well explained by synchrotron emission from relativistic electrons in the jet (Urry et al., 1986), while the physics behind high energy component is not yet very well understood. Two approaches are suggested for its explanation. In the hadronic model, the protons accelerated to very high energies in the jet give rise to the gamma-ray emission from neutral pion decay, proton synchrotron emission and synchrotron emission from pair production (Marscher, 1980; Marscher et al., 2006; Muecke, 1999; Müecke and Pohl, 1999; Böttcher, 2005). In the leptonic approach, the high energy flux is produced by inverse Compton up-scattering of low energy seed photons. The origin of these seed photons can either be the synchrotron emission itself (Synchrotron self Compton, SSC; (Ghisellini et al., 1985; Bloom and Marscher, 1996; Sokolov et al., 2004)) or photons from sources external to the emission region e.g accretion disk, broad line region, torus etc (External Compton, EC). Several models have been proposed explaining different external sources of photons taking part in high energy generation in blazars (Dermer et al., 1992; Sikora et al., 1994; Błażejowski et al., 2000; Sikora et al., 2009; Agudo et al., 2011). In order to pin point the physical processes responsible for the energy generation in blazars, study of both light-curve and SED is needed which requires a long term simultaneous multi-wavelength monitoring of a sample of blazars.

As discussed earlier, position of the synchrotron peak in the spectral energy distribution (SEDs) of blazars classifies them into blazar sequence; flat spectrum radio quasars (FSRQ), low energy peaked BL Lacs (LBL), and high energy peaked BL Lac objects (HBL) (Urry and Padovani, 1995; Fan et al., 1997; Heidt and Nilsson, 2011, and references therein). These subclasses are known to have intrinsic differences in several of their properties. For example, their bolometric luminosity decreases from FSRQ to HBL as does the dominance of γ -ray emission (Fossati et al., 1998; Sambruna et al., 2009). Similarly, LBLs are reported to have, on average, higher degree of polarization (DP) and amplitude of variation than HBLs (e.g., Andruchow et al., 2005; Tommasi et al., 2001; Fan et al., 1997; Jannuzi et al., 1993, and references therein). Based upon our earlier study with much larger sample, we have shown that LBLs indeed show significantly higher degree of optical polarization and in the event of lack of other information, can be used to tentatively classify them.

The object CGRaBS J0211+1051 was first observed by EGRET on-board Compton Gamma Ray Observatory (CGRO) and later found to show featureless optical spectrum (Healey et al., 2008). Previous studies (Healey et al., 2007; Lawrence et al., 1986; Snellen et al., 2002) showed it to be a BL Lac object. During 2011 January 30-February 3, Chandra et al. (2012) found that the source showed significant variations with time-scales of hours with degree of polarization varying between $9\% - 21\%$. Based on that, which is already discussed in last chapter, this source was proposed to be a LBL or RBL. However a true test of such classification is the position of synchrotron peak in SED. Here in this chapter, we aim to confirm this proposition in this study by using multi-wavelength data from radio to gamma-rays in addition to determining other properties of the source. The SED of CGRaBSJ0211+1051 is constructed using multi-wavelength data during 2011 January 24 to February 03 and the nature of the source is discussed accordingly. The next section discusses the observations and analysis of the data.

6.2 Observations and data analysis

In order to study the behaviour of blazar *CGRABsJ0211+1051*, we generated the light-curve and SED using quasi-simultaneous data in all available energy bands, e.g., radio, IR, NIR/optical, UV, X-ray and γ-rays. For SED, excluding few points in radio, all the data used are almost simultaneous. The high energy γ- and X-ray data are taken from Large Area Telescope (Atwood et al., 2009) on-board *Fermi* and XRT on-board *Swift* space based observatories respectively. Recent version of ScienceTools (version v9r27) are used to analyse LAT data. The data from the X-ray telescope (XRT; Burrows et al. (2005)), and the optical/ultraviolet monitor (UVOT; Roming et al. (2005)) are processed and analysed using HEASOFT version 6.12 with calibration database as updated on 2011 Aug 25. For constructing SED the flux at radio frequencies (8.4 GHz, 4.85 GHz, 4.775 GHz and 1.4 GHz) are retrieved from NASA Extragalactic Database (NED). For the completeness we have also used the flux observed by Wide Field Infrared Survey Explorer (WISE) and Plank mission. WISE has provided the averaged flux as observed throughout the one year life time of this mission in four Infrared bands W1, W2, W3 and W4 centred at 3.4, 4.6, 12 and 22 μ, respectively (Wright et al., 2010). ERCSC catalogs (30, 100, 217, 353 GHz) (Planck Collaboration et al., 2011b) provided the flux in sub-mm regime observed by Planck mission (Planck Collaboration et al., 2011a). Some older observations are also imported to compare the SED in the flaring state. These observations are not of same epoch. The 2cm flux from MOJAVE database (Lister et al., 2009), observed on 2011, February 27, is also used. In the following, we summarize the various analysis techniques used for data from different instruments.

6.2.1 Optical polarization and R-band observations from MIRO

The photopolarimetric observations for this source were carried out using PRL made optical polarimeter (PRLPOL) as a backend instrument at f/13

Cassegrain focus of 1.2 m optical telescope at Mt. Abu Infrared Observatory (MIRO). The detailed information about the observations during 2011 January 30-February 3 are given in Chandra et al. (2012) and Chapter 5. We refer to (Deshpande et al., 1985; Ganesh et al., 2009) for the details of the instrument and working methodology. The instrument electronics enables the online data reduction and provides the degree of polarization (DP), error in DP, position angle (PA) of polarization and other parameters, as output. The uncertainty in PA was calculated using the following expression (Serkowski, 1974):

$$e_{PA} = \frac{e_{DP} \times 28.6}{DP} \tag{6.1}$$

where e_{DP} is the error in DP. The nightly averaged values of DP and PA along with their respective standard deviations as reported in Tables in preceding chapter. Here some details about the R-band photometric observations carried using 0.5m telescope are given.

The R band optical photometric observations were performed using recently installed 0.5 m aperture optical telescope ATVS-MIRO (for details, refer to Chapter 2). It is equipped with 1024×1024 ANDOR EMCCD camera, as a backend instrument at its f/6.8 Cassegrain focus. The thermoelectric cooling is capable of achieving detector temperature of about $-80°$C, good enough to keep dark current negligible. The telescope system is made automated for remote operations. The field of view and plate scale of the system are $12'.5 \times 12'.5$ and 0.79 arcsec/pixel respectively.

The Automated Telescope for Variability Studies (ATVS), described above, was used to monitor blazar CGRaBS J0211+1051 during 2011 Jan 30-31 and 2011 Feb 01 and 03. Due to some technical problems, observations could not be made on February 2. The large field of view of the CCD is good enough to accommodate a number of comparison stars in the source field. The standard Image Reduction and Analysis Facility (IRAF) software has been used for reduction and differential photometry of the observed data. In the vicinity of source there are no known standard stars which can be used for calibration. We, therefore, performed aperture photometry on all the stars present in the field. The photometry of all the stars along with the source lying in same field, was performed using the automated photometric pipeline. This pipeline uses the WCSTools and Astrometry.net packages to identify the required sources and IRAF for reduction and photometry. The observed magnitudes of these stars are corrected with web based SIMBAD application having several catalogs [USNO, AAVSO etc]. The proper filter transformations were performed wherever needed. Three out of ten stars are found appropriate for use as standard comparison stars for present analysis. We used one of the three, close in brightness to the source as comparison star and rest as control stars for calibration (Table 6.1). The calibrated magnitudes were then corrected for foreground galactic absorption as prescribed by Cardelli et al. (1989). The conversion of magnitude to energy flux was performed using appropriate factors and zero point flux as described in Bessell (1979). The resulting flux values are then plotted in lightcurves shown in Fig.- 6.1-d.

Date 2011	Time (MJD)	S	σ_S	σ_S	C1	σ_{C1}	C2	σ_{C2}	C3	σ_{C3}
Jan 29	55591.47	13.23	0.005	0.039	13.54	0.037	12.10	0.033	12.29	0.039
Jan 31	55592.45	13.32	0.004	0.030	13.54	0.051	12.09	0.043	12.28	0.046
Feb 02	55594.44	13.31	0.005	0.063	13.53	0.059	12.08	0.059	12.27	0.063
Feb 03	55595.44	13.41	0.003	0.036	13.53	0.041	12.09	0.037	12.28	0.038

Table 6.1: Internight Optical Variability in CGRABsJ0211+1051

6.2.2 Swift observations

The X-ray and UV archival data from HEASARC, observed using XRT and UVOT instruments onboard Swift space laboratory, are analysed to investigate the higher energy counterpart of the optical observations made during the 2011 January flaring event. The observation Ids used for present analysis alongwith the respective exposure times are listed in Table-1. *Swift* started following object CGRaBS J0211+1051 just after the report of an intense flaring activity in γ-rays by LAT onboard *Fermi* (D'Ammando et al., 2011a) on January 25,

2011. The data observed by both the instruments was downloaded for analysis. The standard data reduction and analysis procedures as provided by respective instrument teams are used. The latest version of HEASOFT package (v6.12) with recently updated calibration database (updated on august 25, 2011) is employed for the analysis.

Obsid	XRT		UVOT : U band	
	Date & Time	Exp(s)	Time	Exp(s)
00039111003	2011-01-25 20:16:26	3919.53	20:17:02	16.52
00039111004	2011-01-28 23:10:23	3864.32	23:12:41	65.72
00039111005	2011-01-31 15:41:59	3449.26	15:45:42	107.05
00039111006	2011-02-03 17:34:17	3932.49	17:36:27	60.80

Table 6.2: Details of the Swift Observations

The above table contains the details of pointed observations of this source taken by XRT and UVOT onboard Swift. The columns are self explanatory. In the following sub-sections we describe details of analysis method adopted for the data from various detectors on-board *Swift*.

XRT

For the analysis of the XRT data, *xrtpipeline* script, a part of HEASOFT package, is used to generate the level-2 cleaned event file. This script makes use of default screening parameters as input. Though the pipeline provides spectrum and lightcurves as products, we performed proper grade and region filtering to generate the lightcurve and spectrum using these level-2 cleaned event files. The grades 0-12 and 0-2 are selected for *pc* and *wt* modes of XRT, respectively using Ftool *xselect*. The 15° circular area centred at source position was used as source region. While the background light curve and spectrum are generated after using the four source free circular regions (each with radius of 50 pixels) near the source as background region. The required ancillary response matrix is generated by using task *xrtmkarf* followed by *xrtcentroid*. The response matrix file provided with the CALDB distribution is used for further analysis.

The spectral fitting was done in the energy band between 0.2 to 10.0 keV using XSPEC (version 12.7.0) package distributed with HEASOFT 6.12. The *simple power* law along with the warm absorption (*wabs*) gives the best fit for almost all the observations of interest. The model parameter $N_{\rm H}$ (the galactic column density) is kept fixed at a value of 5.5×10^{22} cm^{-2} (Kalberla et al., 2005). Table 6.3 summarizes the best fit results for all the observation Ids. We do not see any significant variation in photon index for the different observations (perhaps because of poor statistics) implying that the source remains in same spectral state during the course of monitoring. We, however, notice variations in flux as indicated by the light-curve [Fig.- 6.1b].

ObsID 000..	Start Time 2011 (UT)	Exp. (ks)	α	σ_α $\times10^{-2}$	Norm. $\times10^{-3}$	σ_{Norm} $\times10^{-5}$	χ^2/ν	ν
39111003	Jan 25 20:16:26	3.92	2.39	9.92	1.08	5.51	1.08	17
39111004	Jan 28 23:10:23	3.88	2.38	7.45	1.61	6.67	1.03	25
39111005	Jan 31 15:41:59	3.45	2.27	9.32	1.31	6.57	1.34	18
39111006	Feb 03 17:34:17	3.93	2.29	7.19	1.43	6.19	0.98	25

Table 6.3: Results from fitting the Swift XRT-PCA data. The parameters are calculated after fitting the power law to respective data set using XSPEC 12.04. The fitting was performed with a fixed value of nH (nH = $5.5 \times 10^{20} cm^{-3}$) particular to the source direction.

For constructing SED, we estimated the photon flux in several small energy bins using interactive plotting utility (IPLOT), a part of PGPLOT, while fitting with XSPEC. The Galactic extinction correction is done by using unabsorbed flux in the following manner. First of all, modelled photon flux is calculated for all small energy bands using IPL with an appropriate value of parameter nH for that direction (as already discussed above). Then the same is repeated using $N_{\rm H} = 0$ which assumes no absorbing material in that particular line of sight. The ratio between absorbed and unabsorbed model photon fluxes gives the absorption factor. This factor is then used to correct the observed photon flux calculated by IPL in order to get intrinsic photon flux. The galactic extinction corrected photon flux respective to different energy bins are then converted into energy flux and used to construct SED [Fig.- 6.2].

UVOT

UVOT instrument onboard *Swift* provides simultaneous observation in optical (V) and several ultra-violet bands. UVOT snapshots with all the six available filters, V (5468 $\mathring{A}$), B (4392 $\mathring{A}$), U (3465 $\mathring{A}$), UVW1 (2600 $\mathring{A}$), UVM2(2246 $\mathring{A}$) and UVW2 (1928 $\mathring{A}$) for all the obsIds (Table 6.2), were integrated with the *uvotimsum* task and analysed by using *uvotsource* task, with a source region of 5 arcsec, while the background was extracted from an annular region centred on the blazar with external radius of 40" and internal radii of 7 arcsec Foschini et al. (2010). The observed magnitudes from all obsId are then corrected for extinction according to the model described in Cardelli et al. (1989). The magnitudes thus obtained are converted to energy flux (erg^2 cm^{-2} s^{-1} Å^{-1}) using following equation:

$$F_\lambda = FCF \times 10^{(ZPT-m)/2.5} \tag{6.2}$$

where ZPT is zero point flux, FCF is the flux conversion factor [erg^2 cm^{-2} count^{-1} Å^{-1}] and m is the observed magnitude in a particular filter. These values are taken from instruments calibration database (CALDB, Poole et al. (2008)). The light-curves are then constructed by using flux values in filters V, B, U, UVW1, UVM2, and UVW2 for different ObsIds(Fig.- 6.1c). The UVOT flux averaged over whole observing period, are used to construct the Spectral Energy Distribution (SED) of the source (in Fig.- 6.2).

6.2.3 Fermi/LAT observations

The energy coverage of LAT on-board *Fermi* Gamma-ray observatory is broad (30 MeV - 300 GeV) enough to cover the part of blazar SED which is assumed to be mainly contributed by inverse Compton processes in the jet. Source CGRABs J0211+1051 was first reported in outburst state in 0.1-100 GeV by D'Ammando (2011). In order to investigate the high energy emission before and after the flaring period along with the outburst state, we analysed the data ranging from MJD 55548 to MJD 55610 (approximately 2 month). Only a part of this, coinciding with the Swfit observations (MJD 55586-95) is shown in Fig.- 1-a.

The PASS7 photon dataset with a region of interest of 15° for CGRaBS J0211+1051 was obtained from Fermi data archive for the present investigation. The latest version of ScienceTool (v9r27) and calibration files are used. The part of data with zenith angle $\geq 100°$ are discarded in order to avoid the contributions from earth albedo. The unbinned likelihood analysis method is used to reconstruct the source energy spectrum. For this, first of all coordinate, time, energy and region selection are performed on the raw event file to avoid unwanted contributions. The output file of previous step is again corrected for detector live time. A source model is constructed using the contributory python script *make2FGLxml* incorporating the latest *Fermi*-LAT catalog *gll_psc_v07.fit*, diffuse background components *gal_2yearp7v6_v0.fits* and extra-galactic background *iso_p7v6source.txt*. The Galactic diffuse emission model is generated using the GALPROP package and available online as a contributory file, while the extra-galactic one is described by a simple power law (Abdo et al., 2009).

The light-curve and SED are generated using likelihood analysis. Aperture photometry was also performed to cross check the trends observed in lightcurves. We have adopted the similar methodology as used by Foschini et al. (2010); Foschini (2011) and discussed here briefly. First, the complete data are used for likelihood analysis using energy band of 0.1 to 100 GeV in order to determine the best fit source model. We found that *powerlaw2* model is the best fit source model as indicated by high test statistics (530.9). The powerlaw index value for the present fit is 2.03 ± 0.06. The same source model with this power law index is used for constructing light curve. The one day and three day time bins are used when generating light-curve. The flux with TS ≥ 9, equivalent to $\sigma \sim 3$, are used for constructing lightcurve.

For constructing SED, the event file is binned in several energy bins (*100MeV - 500MeV, 500MeV - 1GeV, 1GeV - 5GeV and 5GeV - 50GeV, 50GeV - 100 GeV and 100GeV - 200GeV*) and likelihood analysis is performed for each energy bin, to get energy flux for respective energy bands. The data between MJD 55580 to MJD 55596 are used to construct SED. The source model used for this step is similar to that used for complete energy band. For each energy bin the source under investigation and all nearby sources in the region of interest (ROI) are described by one parameter representing the integral flux in that energy bin. The diffuse background components are modelled with one single parameter, describing the normalization. The upper-limit estimation is done for last two energy bins as TS is always less than 9 for these bins.

The following tools provided as a part of software distributions are used for the analysis carries out here. The *gtselect* and *gtmktime* are used for event selection and live time correction, respectively. The *gtltcube*, *gtdiffrsp* and *gtexpmap* are used for generating livetime cube, Galactic diffuse response, and exposure map respectively. Last tool which is used for final likelihood analysis is *gtlike*. It provides the test statistics for source model fit along with the other model parameters.

Additional data from other facilities.

When constructing the SED of this source we have made use of data provided by several other facilities at many frequencies. The mid IR average flux values are taken from Infrared Processing and Analysis Center (IPAC) observed by Wide Field Infrared Survey Explorer (WISE) (Wright et al., 2010). WISE is a medium class explorer mission by NASA, launched on 2009 December 14, aimed to survey the sky simultaneously in four Infrared bands W1, W2, W3 and W4 centred at 3.4, 4.6, 12 and 22 μ respectively during the course of one year period from its launching date. The magnitudes provided by IPAC for year 2010 were converted into flux using the zero-point flux in Wright et al. (2010). The sub-millimetre data points are taken from Planck ERCSC catalogs (30, 100, 217, 353 GHz) (Planck Collaboration et al., 2011b). The Planck flux values correspond to observations after the flaring episode in 2011 January. The optical/IR magnitudes observed by GROND system (Greiner et al., 2008) and published in Rau et al. (2012) are also used for SED construction. GROND enables simultaneous monitoring in four optical (U, B, V and R) and three near IR bands (J, H and K) and also belong to pre-flare era when source was in low phase. The CRTS V-band flux corresponding to different observation epochs are used in SED. MOJAVE 2-cm flux observed during different epochs for the period 2010 and 2012 are also used. We have also used several other radio (8.4 GHz, 4.85 GHz, 4.775 GHz and 1.4 GHz) and optical data points taken from the NASA Extra-galactic Database (NED) though these observations are relatively older. The γ-Ray flux from LAT 1st and 2nd catalog values along with those analysed by us for comparison are also used. Several other observations in X-Ray by XMM are also imported from catalogs. In order to compare the Swift XRT flux before and after the flaring period we have also analysed three more observation Ids dated on 2010-03-05, 2010-06-13 and 2011-11-21 respectively. The source was faint in X-ray in 2010 March and an increasing trend was seen in 2010 March-June. The source is found to be too faint to give significant counts during Swift observations in 2011 November. The resulting SED using the data discussed here and in last few subsections as well is shown in Figure-6.2.

6.3 Results and discussion

The blazar CGRaBSJ0211+1051 is an interesting source which has been brightening since 2005 (Chandra et al., 2012) from the levels of 15.5 mag in V band (Djorgovski et al., 2011) and had undergone a strong flaring activity during

2011 January 25 - February 3. It was reported to show bright state in almost all wave-bands and *Fermi* γ-ray photon flux rose by 25 times compared to the yearly averaged values (D'Ammando, 2011). We used the available data on the source along with our own observations to produce light curves and spectral energy distribution to understand the nature of the source and to ascertain its actual classification. In the following we discuss the results obtained from this study and available information from the literature.

6.3.1 Multi-wavelength lightcurve and polarization

Fig.- 6.1 shows the multi-wavelength light curve for the blazar CGRABsJ0211 + 1051. The panels a and b show the γ -Ray and X-Ray flux variations observed by LAT and *Swift* respectively. The panel c contains UV/Optical light-curves as obtained from UVOT on-board *Swift*. The panel d shows the R band light-curve obtained using EMCCD mounted at ATVS. The last two panels e and f, show the variations in nightly averaged degree of polarization and position angle as discussed in Chandra et al. (2012). In the following we discuss each component individually in connection with source behaviour in other wavebands.

First of all, let us discuss variation of polarization and position angle with time during 2011 January 30 to February 3 when CGRaBSJ0211+1051 was in flaring state. The intranight variations are already discussed in detail by Chandra et al. (2012) and in earlier chapter. Here, we are mainly interested in inter-night behaviour in order to compare with light-curve features in other bands. The visual inspection of Fig.- 6.1(f) clearly shows that emission was highly polarized ($DP \sim 21.05\%$) on MJD 55591.38 (2011 January 30). High DP indicates highly aligned distribution of magnetic field in the emission region. The DP then gradually decreased to a value of 10.63% on 2011 February 1 (MJD 55593.44) at a rate of 5% per day. After this fall, DP again started increasing at a relatively slower rate (2.42% per day) over next two days. Similar

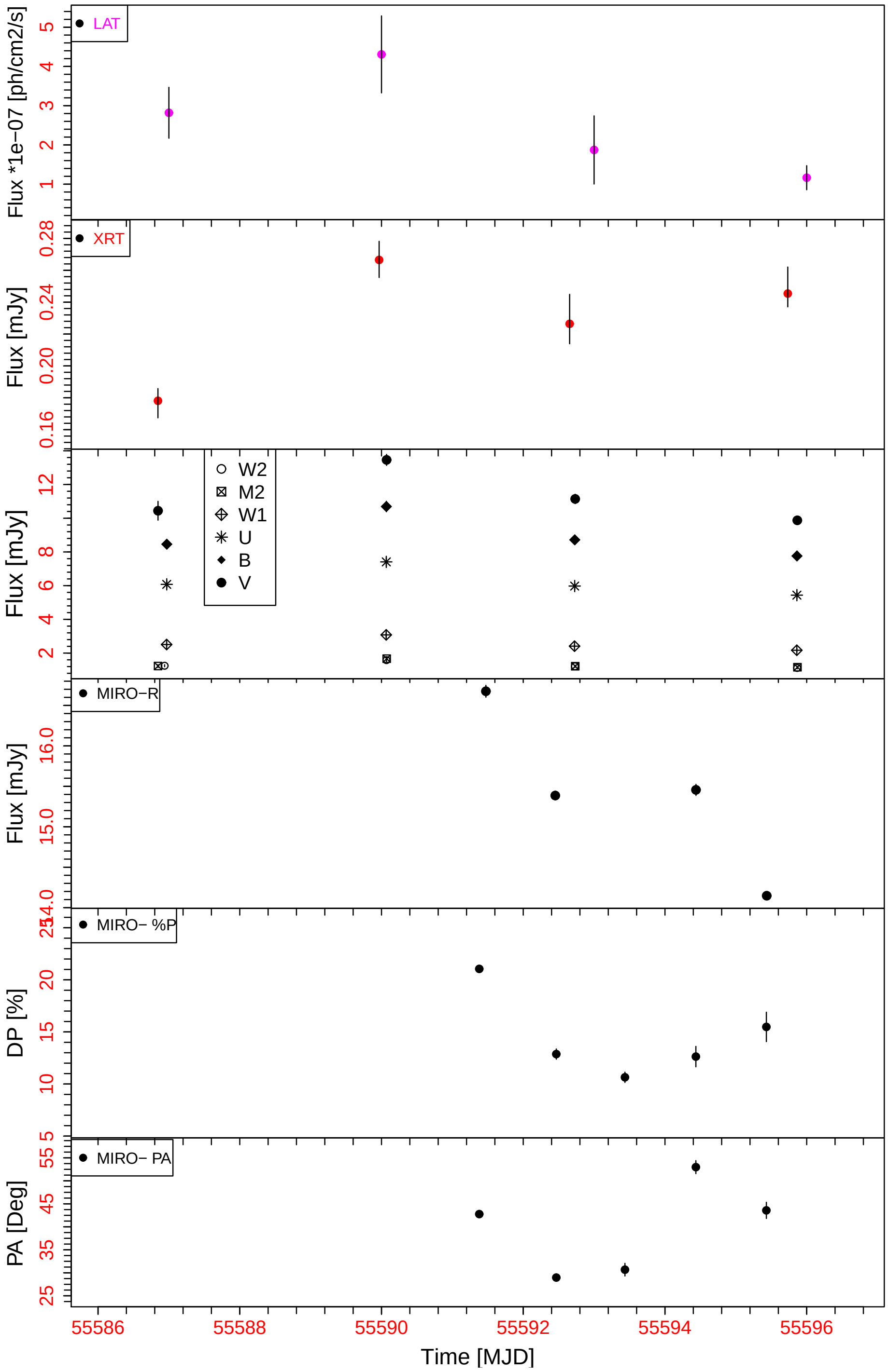

Figure 6.1 Multi-wavelength light curve for blazar CGRABsJ0211+1051. (a) γ -ray flux from *Fermi*/LAT, averaged over 3-days, (b) Swift-XRT x-ray integrated flux between 2 to 10 keV, (c) UVOT fluxes in various bands as measured by UVOT on-board Swift., (d) daily averaged R-band flux from the ATVS-MIRO measurements, (e) & f) Degree of polarization & position angle during 2011 Jan 30 to Feb 3 (Chandra et al., 2012).

temporal behaviour is also seen in position angle (PA) with a difference that it shows downturn during the last day (2011 February 3) of observation. First it decreased by 13.8° (from 42.77° to 28.96°) between MJD 55591.38 and MJD 55592.47 and then started rising, reaching to 52.98° on MJD 55594.44. The variations in DP can be explained using several intrinsic models like shock in jet model, fresh injection of matter in the jet etc., depending on the time-scale and nature of changes observed. The sudden change in PA during 2011 January 30-31 perhaps indicates to injection of fresh plasma (shock) into the jet, which is substantiated by mild BWB trend in colour. The shock compresses the tangled magnetic field parallel to the shock front resulting in sudden change in the PA of the polarised synchrotron emission. The drop in total intensity (R-band, cf next para) leads to drop in the DP. However, the new shock should have caused flux to increase afterwards (eg. Feb 1) but we do not have R-band data to confirm that, although we see a hint of enhanced flux on February 2. Subsequent behaviour of DP and PA, which vary on internight scale, could be due to passage of this short-lived relativistic shock that results in mild variation in the viewing angle.

The R band light curve (Fig.- 6.1(d)) indicates that the source must have seen its brightest moments before 2011 January 30 exhibiting an overall decrease in flux starting from our observations during 2011 January 30 - February 3, which is in agreement with the trend reported by Nesci (2011) showing the source at $R_c \sim 13.37$ level on 2011 January 27 whereas ATVS R-band flux is much higher (about 17.5 mJy) with decreasing trend. History of the source brightness is detailed by Chandra et al. (2012) mentioning its steady enhancement over the years. Apart from a global decreasing trend, present R band light-curve also indicates a small rise in flux between MJD 55592.4 and MJD 55595.4 around which DP and PA are showing opposite behaviour. This might be indicative of a small flaring activity around that time, enhancing the R-band flux and DP followed by a change in PA as discussed above.

The UV-Opt light-curves (Fig.- 6.1(c)) as plotted with Swift data show almost similar behaviour in all bands albeit with a weak colour dependence. The source appears to show mild bluer when brighter and redder when fainter behaviour which is consistent with shock-in-jet model. We notice about 20% increase in U-band energy flux during MJD 55586.8 to MJD 55590.4(2011 January 26 to 29). In all optical and UV bands, the source had maxima and minima around MJD 55590 and MJD 55595.5 with values in U,B,V bands as 9.58, 11.2, 14.3 mJy and 7.02, 8.1, 10.4 mJy, respectively. R-band flux peaked on MJD 55591.4 (16.67mJy) while source was faintest in R-band on MJD 55595.4 (14.14mJy). The delay of about one day in the maximum and minimum as seen in R-band vis-a-vis U,V,B Swift bands is possibly due only to difference in time of observations or binning effect. As shown in Fig.- 6.1(b), XRT-Swift X-ray energy flux goes up by about 50% (from 0.18 to 0.27 mJy) within approximately 4 days (MJD 55586.4 to 55590.4) and then drops by 0.04 mJy within next 2.8 days. Therefore evolution of flux in flare is not due to light crossing time but injection/acceleration or/and the cooling time scales must be affecting flux variation. The X-Ray (0.2-10.0 keV) lightcurve also follows the similar trend as seen in UV bands except that X-ray lightcurve registers an increase in the flux towards the end while fluxes in other bands decrease. The maximum (0.28 mJy) and minimum (0.16mJy) in the X-ray lightcurve occur on MJD 55590.08 and MJD 55587.02, respectively.

In an Astronomers telegram on 2011 Jan 25 (D'Ammando, 2011), the source is reported to have highest γ-Ray flux on 2011 January 23 observed till date. The $\gamma-$ray lightcurves are obtained from LAT data with inclusion of flux corresponding to TS $\geq$ 9 ($\sigma \sim 9$). Here one point represents the photon flux averaged over 3 days. The $\gamma-$ray light curve clearly indicates significant rise in flux around 2011 January 23, and again on 2011 January 29. For better visualization of quasi-simultaneous data available at other wavebands, we present Gamma-ray lightcurve in Fig.- 6.1(a) only after 2011 January 25. The γ -ray lightcurve shows a peak in flux centred on January 29 and then it decays slowly with time with a mild hump around MJD 55595. At the time of this 'mild' hump, X-ray and UV flux show significant enhancement as discussed above. This flare appears to be different from the one which took place around 2011 January 23, decaying part of which might have overlapped with rising part of the second (January 29) flare. The peak photon flux ($4.3\times10^{-7} phtons/cm^2/sec$) in this flare is almost at the same level as that of January 23 flare.

Now, analysing the composite light-curve in the context of discussion of the individual components, it is clear that the source CGRaBS J0211+1051 has undergone through a significant bright phase during 2011 January - February. Additionally, observational data on 2 cm from MOJAVE showing higher flux on January 27 supports the multi-energy flaring activity. Fig.- 6.1 shows that γ -ray, $X-ray$, UV and optical fluxes vary largely in unison during 2011 January 25 to February 2. If one looks at carefully, all the light-curves appear to peak somewhere near January 29. Now, considering polarization behaviour, we have observations during January 30 to February 03. Though there are no polarimetric observations on 29 January, a polarization value of 12% on 2011 January 28 was reported by Gorbovskoy et al. (2011), followed by our measurements of $\sim$ 21% degree of polarization two days later on January 30. Therefore, the trend in polarization shows a rapid increase in DP during January 28 - 30 and then equally rapid drop with January 31 recording a value of 12.8%, indicating degree of polarization to peak sometime on January 29 where all multi-wavelength fluxes also appear to peak. While PA follows DP during January 30-Feb 02, we do not know how it behaved near the peak as there are no measurements of PA on January 28. As mentioned earlier, from 2011 February 1 (MJD 55593.4) DP increases slowly while PA shows an increase upto February 2 and then decreases. Interestingly, flux in the R-band also shows a mild rise on February 2 and then a sharp fall of about 10%, almost like PA. A slight increase in X-ray light curve is also noticeable at this epoch. Also, one day averaged *Fermi*/LAT flux shows an enhancement on February 2 (MJD 55594). It might be indicative of a flicker at around MJD 55594.4 caused by inhomogeneity in the jet, leading to enhancement in flux and polarization accompanied with change in PA. However, in the absence of UVOT pointed observations at this epoch, nothing can be said of UVOT fluxes. Quasi-simultaneous high activity in broadly all the energy regimes indicates to a relativistic shock passing through a moving or standing core/knot out side the BLR region ($R_{BLR} \leq 1$ parsec) where emission is transparent at almost all the frequencies.

We, therefore, conclude that in totality, variations in fluxes at all the bands appear to be simultaneous in nature, indicating co-spatiality of the emission at all these wavebands. However, one can not miss differences in the nature of short term fluctuations at different wavebands, implying the presence of small scale inhomogeneities in the physical conditions across the source.

6.3.2 Spectral Energy Distribution (SED)

In order to confirm the classification of this source suggested in earlier chapter and by Chandra et al. (2012) based on polarization studies, we constructed the spectral energy distribution (SED) using the multi-epoch data from various resources ranging from radio to Gamma-ray frequencies. Fig.- 6.2 shows the SED of CGRaBS J0211+1051. In the figure, the data shown in dark black represent values during the flaring period (sometime averaged over several days) at various frequencies. The flux values shown in grey (Radio-NED, WISE, Fermi) are for pre-flare period when source was in relatively fainter phase. The points in blue show the observations (Plank and Swift) after 2011 February and relate to the post flaring period. All the flux values used in Fig.- 6.2 are galactic extinction corrected. The filled diamonds represent the UVOT and ATVS-R band flux while the filled-black triangles are 0.3-10KeV flux observed by XRT and averaged over whole observing period. The last two points in high energy component of SED are upper-limits on Gamma-ray flux with the corresponding TS values less than 9 ($\sim 3\ \sigma$). The spectral energy distribution for blazars consists of continuum emission from nuclear source (accretion disk + jet) and thermal emission from the host galaxy. Sometimes, particularly with resolved host galaxy having non-negligible contribution, it

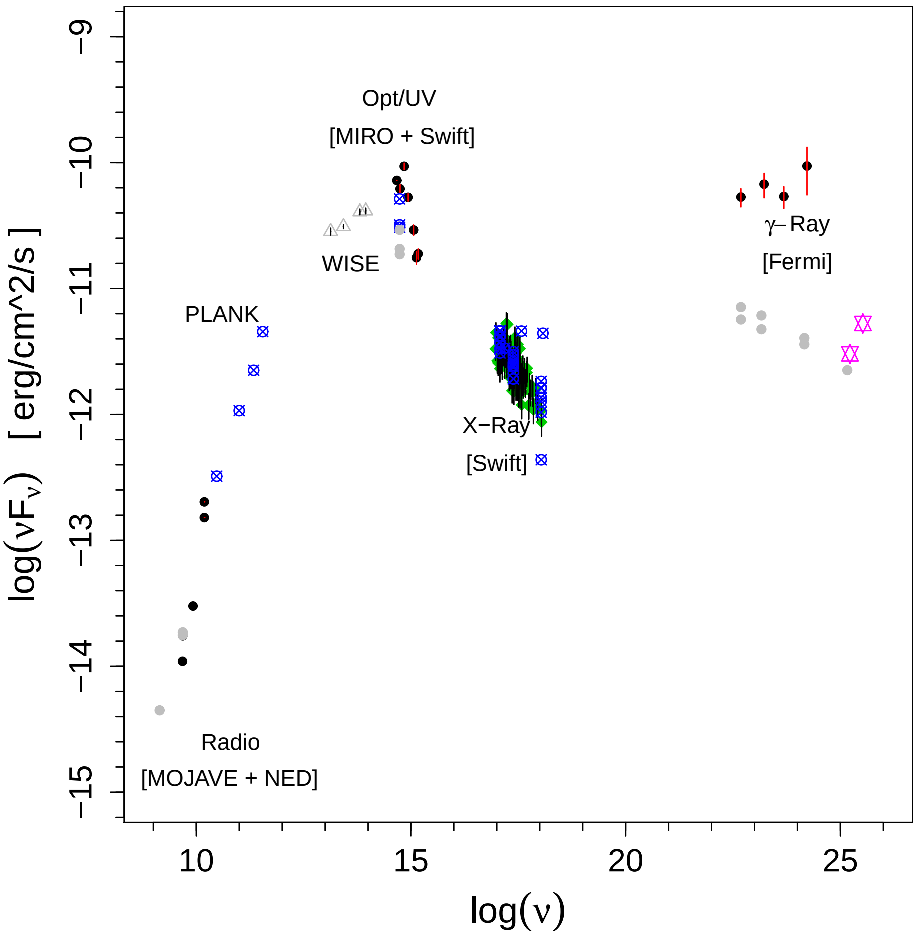

Figure 6.2 Broadband spectral Energy Distribution (SED) of CGRABsJ0211+1051 during flaring phase. The legends describe the sources of data used in generating SED. All fluxes are corrected for Galactic extinction. Data shown for other epochs are described in the text

becomes necessary to subtract the host contribution to arrive at blazar SED. In the present case, though host galaxy is fainter by more than two magnitudes as compared to the central source, still we would like to check if its contribution is significant.

Correction for host galaxy emission

The SED as displayed in Fig.- 6.2 is corrected for possible contributions from it's host galaxy. The procedures used for estimating host galaxy contribution to SED are as follows:

The template SED for an elliptical galaxy (type E0) as provided by Mannucci et al. (2001) is used to construct the expected SED for host galaxy. The E0 template is chosen as the host of blazars are mostly elliptical galaxies. The template contains two columns. The first column represents the wavelength in μm and second one the flux at respective wavelengths normalized to flux in Johnson V-band. In order to construct the expected SED for host, V-band observed flux of host galaxy is multiplied by the normalized flux of template spectrum. The computed host SED then needs to be transformed to the source frame of reference of SED for comparison. The K-correction can be used to transform SED to the rest frame. The simulated host galaxy spectrum then can be integrated over the profiles of different filters to give rise to the estimated effective host flux for those filters. The resulting flux then needs to be subtracted from the source flux in respective bands if found significant.

Above general procedure is to be used if one is interested to correct the source SED for host galaxy contribution. For this we have used Sloan I-band observations of the host galaxy by Meisner and Romani (2010). This magnitude is then converted into Johnson V-band magnitude using the filter transformation equations as prescribed in Blanton and Roweis (2007). As we do not have any color information for CGRaBS J0211+1051 host, we have used the template colors which might, however, introduce some uncertainties in the measurements. The colors used for this analysis are as follow:

U-B=0.50, B-V =0.99

V-R=0.59, V-I=1.22

The galactic absorption corrected V-band flux is used to generate the simulated SED for the host galaxy of CGRaBS J0211+1051. The inverse K-correction is used to get the host SED in observer's frame of reference. The resulting host SED is over-plotted with the observed source SED for the observations during 2011 January (Fig.- 6.3) . The yellow points in Fig.- 6.3 represent the host contributions at different energies. This clearly establishes

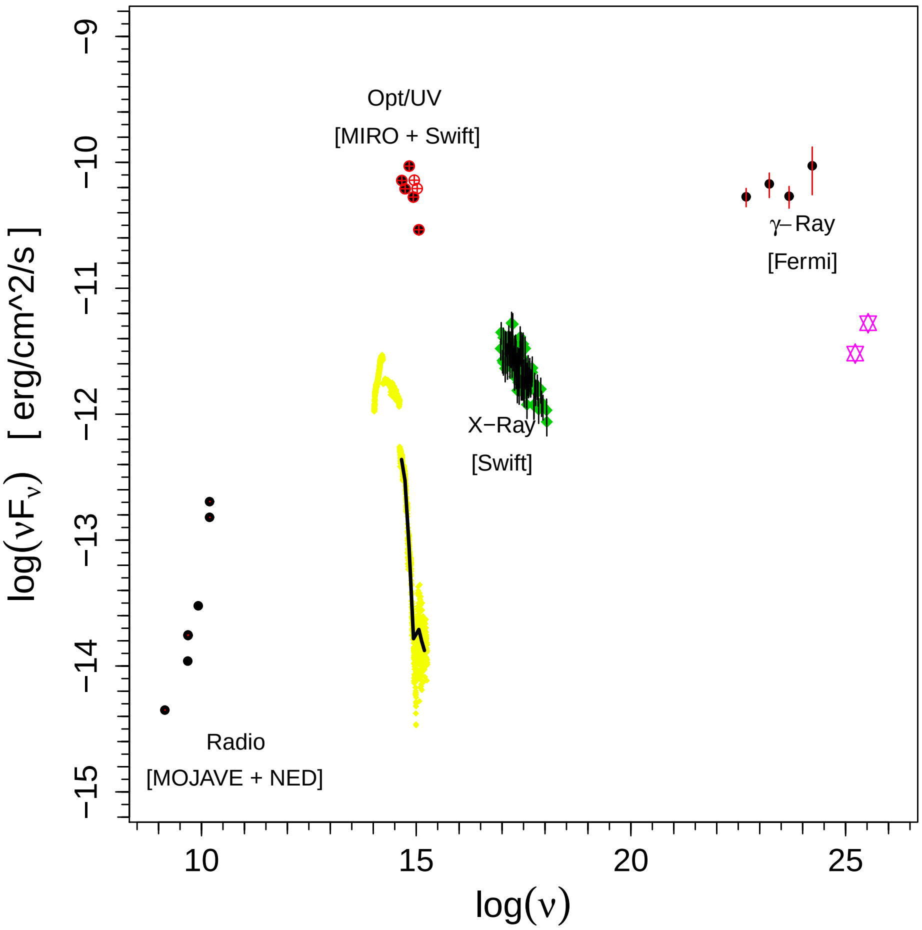

Figure 6.3 Yellow curve in the SED of CGRaBS J0211+1051 represents the simulated host contribution.

about two orders of magnitude difference between the nuclear (source) flux and host galaxy contributed flux. As is evident from the Fig.- 6.3, the contribution of the host galaxy is really insignificant as inferred by us from its relative faint brightness as compared to the nuclear source. However, the analysis gives us confidence to use the source SED obtained for flaring period for further analysis without any correction.

Discussion of the CGRaBS J0211+1051 SED

Fig.- 6.2 shows SEDs at, in limited way, different epochs. A careful inspection makes it clear that the source flux varies from epoch to epoch. The SED shown in dark black is largely for the period when the source underwent very bright state during 2011 Jan 25 - 2011 Feb 03 while the one in grey belong to pre-flare era. If one compares the $\gamma - rays$ flux densities during two epochs, it is very evident that $\gamma - rays$ flux went up by order of magnitude during the flare period as compared to quiescent one. We also see significant changes in flux during two epochs at other frequencies as well - for example, in optical and UV. However, it is interesting to notice that soft X-ray flux almost overlaps in both phases. Also, high energy X-ray flux appears to show quite different behaviour, showing a mild increase with energy. It is possible that there is minor change at low energies (radio) while significant changes are seen at high energy gamma-ray flux. There is a clear indication of significant shift in the position of IC component of SED with a change in the trend. The $\gamma - rays$ flux softens with frequency during low phase while it shows clear hardening during flaring period, that is spectra hardens with intensity Baliyan (2001). It appears that particles are accelerated to higher energies before they start emitting- cooling rate is slow. During the low phase, high energy particles slowly accelerate and seem to cool faster before leaving the emission region. It leads to spectral softening. As discussed in the last chapter in detail, we have claimed CGRaBS J0211+1051 to belong to low frequency peak BL Lac (LBL) based on the high degree of linear optical polarization. However, a true test for such classification is the position of the synchrotron peak in the SED. In order to determine the position of synchrotron peak, ν_{SyP}, and peak flux of synchrotron component in SED a n-degree polynomial (see. Equ. 6.3) is fitted to the synchrotron component using nonlinear least square regression techniques. The polynomial with n=5 provides the best fit. The Fig.- 6.4 shows the synchrotron component of SED along with the fitted polynomial. The lower panel of Figure-6.4 presents the residual obtained from observed and fitted data. The position of the synchrotron peak and peak flux obtained from this fit are $\nu_{SyP} = 1.35 \times 10^{14}$ Hz and $F_{Sy} = 5.21 \times 10^{-11}$ $erg/cm^2/s$, respectively.

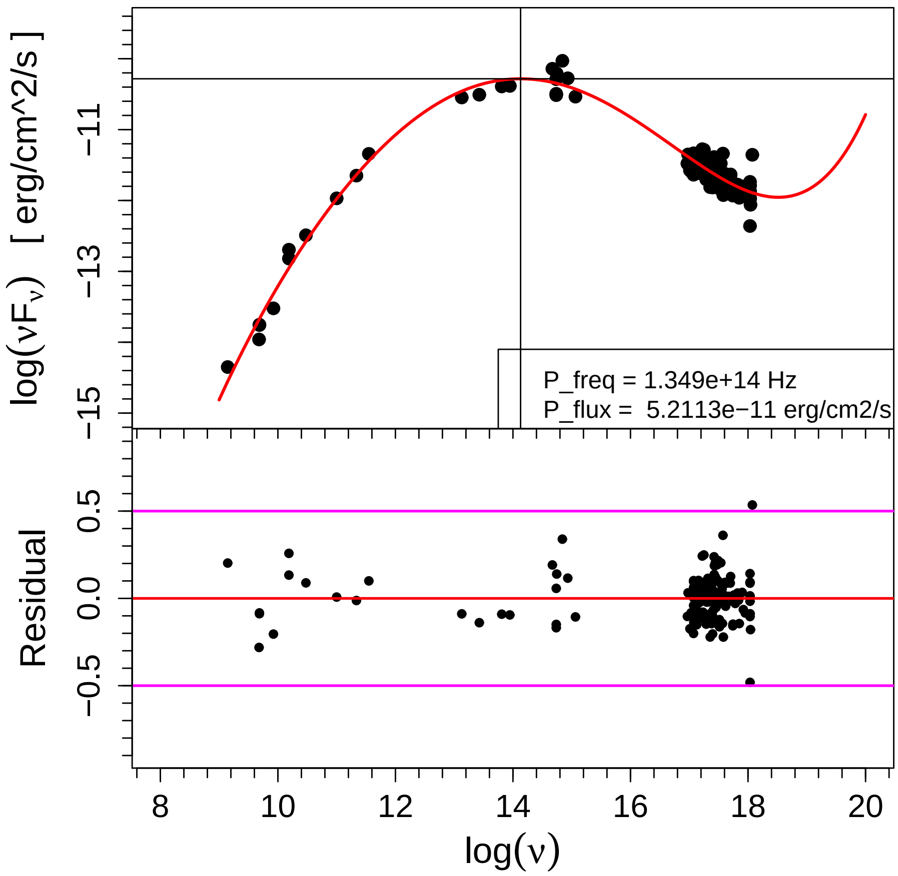

Figure 6.4 Synchrotron component of CGRaBS J0211+1051 SED with best fit polynomial for the frequency range 10^8 to $10^{18.5}$ Hz.

$$log(\nu L_\nu) = A_n \times [log(\nu)]^n + A_{n-1} \times log(\nu)^{n-1} + ... + A_1 \times log(\nu) + A_0 \quad (6.3)$$

where $A_n's$ are the coefficients of the nth terms of the polynomial. The generalized non-linear model (gnlm) package available in R is used for above analysis.

The above values show that the position of the peak of the low energy component (synchrotron) of SED for this blazar lies in near Infrared region. According to the blazar classification/sequence, the blazars with the position of low energy component of SED or synchrotron peak in near-IR/optical frequency range are termed as "low energy peaked (LBL)" (or RBL) and those for which this peak falls in UV/X-ray are known as "high energy peaked (HBL)" (or XBL). Therefore above results clearly support the suggestion made by us in previous chapter using polarization observations that CGRaBS J0211+1051 belongs to the class of low energy peak blazar (LBL). The present study, also, gives credence to the idea that blazars can broadly be classified based on their polarization properties.

6.3.3 Estimation of jet parameters

In case of blazars, emission from the relativistic electrons in the jet dominate the overall emission. Thus jet plays an important role. It is therefore, quite relevant to understand the structure of jet and the emission processes that lead to such emission. In this section, we determine upper limit to the size of emission region, value of the co-moving magnetic field, black hole mass and Jet Power.

Using the shortest variability timescales, position and peak flux of synchrotron component of SED, a rough estimate of several other parameters can be determined. We have estimated the size of emission region using the shortest variability timescale as given in the equations below:

$$R_B \sim \frac{\delta}{1+z} \times c\Delta t \tag{6.4}$$

where δ and Δt are the Doppler boosting factor and shortest variability timescale respectively.

The shortest variability timescale is obtained from optical observations (Fig.- 6.1) using following criteria. If the lightcurve is long enough to cover at least two consecutive maxima or minima with a change in the flux by more than 30 %, we take the half of the total time duration between two consecutive maxima or minima as shortest variability timescale. While in other cases we use the time duration corresponding to a rise or fall in flux by 40 %. In our case the optical flux has increased by approximately 33% within two observations 3 days apart. In the next observation it is again seen in lower state by approximately same amount in flux. Therefore, according to above assumptions $\Delta t \sim 3$ days . The corresponding size of emission region (R_B), estimated using equation 6.4, is $\sim (6.48 \pm 0.57) \times 10^{16}$cm.

The position of synchrotron peak (ν_{sy}) and peak flux (f_{sy}) along with size of emission region (R_B) are used to estimate the co-moving magnetic field in the emission region. According to the expression derived by Böttcher (2007):

$$B_{eB} = 9D_1^{-1}\left[\frac{d_{27}^4 f_{-10}^2 e_B^2}{(1+z)^4\epsilon_{sy,-6}R_{15}^6(p-2)}\right]^{1/7} G \qquad (6.5)$$

where synchrotron peak flux;

$$f_{-10} = \frac{f_\epsilon^{sy}}{10^{-10}} erg/cm^2/s$$

syncrotron peak frequency and Size of emission region

$$\epsilon_{sy,-6} = \frac{\epsilon_{sy}}{10^{-6}}, \epsilon_{sy} = \frac{h\nu_{sy}}{m_e c^2}, R_{15} = \frac{R_B}{10^{15}} cm$$

and luminosity distance

$$d_{27} = \frac{d_L}{10^{27}} cm$$

The luminosity distance of this source corresponding to the red-shift (z) 0.2 ± 0.05 (Meisner and Romani, 2010) is estimated using online cosmology calculator (Wright, 2006). For a given cosmological constants $\Lambda_M = 0.27$, $\Lambda_\nu = 0.73$ and $H_0 = 72 km/s/Mpc$ the luminosity distance d_L comes out to be 957.1 Mpc or 2.953 $\times 10^{27}$ cm.

From equation 6.5 the co-moving magnetic field (B) in the emission region is $\sim 27.38\ \delta^{-13/7} e_B^{2/7}$. Assuming the equipartition of energy and Doppler boosting factor equal to 10, the co-moving magnetic field becomes ~ 0.4 Gauss. Similar values have been obtained by other workers, e.g., 0.93 Gauss for OJ287 by Baliyan et al. (1996) but typically higher ($\sim$ few Gauss) of magnetic field are also reported for BL Lac objects.

An alternative method for the estimation of co-moving magnetic field is also performed using the prescription given in Joshi and Boettcher (2007),

$$t_{sy}^{cool} = t_{sy}^{var} \approx 2.8 \times 10^3 (\frac{\delta}{15(1+z)})^{-1/2} (\frac{B}{2.9G})^{-3/2} \nu_{15,sy}^{-1/2} s \tag{6.6}$$

where t_{sy}^{cool} and t_{sy}^{var} refer to the synchrotron cooling timescales and variability timescales in synchrotron regimes, respectively. B is the co-moving magnetic field. $\nu_{15,sy}^{-1/2} = \nu_{Opt}/10^{15}$ i.e. peak frequency in terms of 10^{15} Hz. The resulting magnetic field using equation 6.5 is ≈ 0.3 Gauss. The magnetic field estimates using both the methods described here are in good agreement.

Assuming that this event is triggered by instabilities very near to the central engine and using the assumptions and prescriptions by (Abramowicz and Nobili, 1982), a crude estimation of the black hole mass can be presented. The black hole mass (M_{BH}) is estimated using the formula $\sim \frac{c^2 \times R_B}{3G}$. The resulting value of M_{BH} is $2 \times 10^{10} M_{\odot}$. This value is very high for a typical BL Lac object. The more accurate estimate can be obtained by fitting the overall SED. The long term multi-wavelength monitoring is needed for more accurate characterization of this blazar.

The total jet power (P_j) (kinetic + poynting) is estimated using single frequency luminosity at 15 GHz (L_{15GHz}) in the following analytical relation as derived by Foschini (2011).

$$logP_j = (11 \pm 3) + (0.81 \pm 0.06) logL_{15GHz} \tag{6.7}$$

The resulting total jet power thus estimated is $\approx 5 \times 10^{48}$ erg/s. All the above estimations are performed using the information out of the limited observations. For better estimates of these parameters and putting stringent constraints on the model of emission, extensive study of blazar CGRaBS J0211+1051 is needed at all the wavelengths. Thus this particular study underscores the need for a detailed study of this source.

6.4 Conclusions

In this chapter, we have used multi-wavelength observation data for blazar candidate CGRaBSJ021+1051 to understand its behaviour when it was undergoing a strong flare. The data on this source are very scanty which makes any significant conclusion a difficult proposition. Nonetheless, we have used whatever data was available in various energy regime and our own observations to make some useful conclusions.

First of all, from this first of its kind study on this source, we would like to confirm that blazar belongs to low energy peaked BL Lac (LBL) sub-class of blazars as its synchrotron SED component peaks at 1.34×10^{14} Hz. It verifies the claim made with our polarization based study in which it shows high polarization.

Based on the multi-wavelength light curves, we notice presence of another flare peaking sometime on 2011 January 29, with almost similar *Fermi*/LAT photon flux as reported for the 2011 January 23 flare. It appears a double flare when the decaying part of the first flare overlaps the rising part of the second flare. The nature of the multi-wavelength light curves presented here shows that flux at all wavelengths vary in unison with time, perhaps peaking some time on January 29, with minor delays. Such quasi-simultaneous trend suggests that the emissions in all the energy bands are being generated in the same part of the jet, though emission sizes might differ with frequencies. The fact that the jet emission dominates is also confirmed from it's high degree of polarization observed.

Spectral energy distribution of the source, generated during pre- and post flaring epochs provides interesting information. It shows that source shows significant variation in flux at high energies during flaring epochs. Also, the peak frequencies shift to higher values as source brightens. The $\gamma - ray$ flux shows order of magnitude enhancement during flaring epoch alongwith a trend for bluer when brighter. It seems that particles are being continuously accelerated before they leave the emission region. During low phase, however, the high energy particles lose their energy in rapid cooling. X-ray flux hardly shows any change in two phases. The trend shows that soft x-rays are partly form tail of synchrotron emission while some contribution could be from disk corona where UV photons are up-scattered to soft x-rays. Higher energy X-ray appear to be of Inverse Compton origin. It is very strange that during flaring period, SED resembles to LBL with quite significant IC component while during quiet phase, it gives impression of an HBL. This and other enigmatic features (eg, X-ray flux) make this source good candidate for further detailed study.

Synchrotron self Compton (SSC) processes can be used to explain SED and determine various properties of the jet emission in this source. Several parameters are estimated using canonical jet model, indicating mild co-moving magnetic field (0.3- 0.4 G) in the region. We estimate the mass of black hole to be $\approx 2 \times 10^{10} M_{\odot}$. The assumption that UV emission is mainly contributed by disk gives us the estimation of the size of BLR which comes almost equal to the size of emission region. A long duration multiwavelength, simultaneous monitoring is emphasized by the present study.

Chapter 7

Long term multi-wavelength study of FSRQ *PKS 1510-089*

7.1 Introduction

We know that blazars are highly energetic with apparent luminosity exceeding $10^{48} erg\ s^{-1}$ during flaring, understood due to Doppler boosting of the non-thermal emission from relativistic jet pointed close to our line of sight (LOS), which also shortens the observed time scales. The emission is synchrotron radiation from radio to UV and sometimes upto X-ray energies. The electron population giving rise to such emission is also responsible for high energy X-rays and gamma-rays through inverse Compton scattering. The seed photons for up-scattering may come from synchrotron emission itself or from the components near nuclear source. However, neither the source of seed photons, nor the exact nature of processes that energize the radiating electrons are clearly known. Similarly, the size and location of the various emission regions are ambiguous. The radio morphological studies can reveal many of the jet properties which are directly linked with either the environment of the jet surroundings or the central engine, responsible for launching and powering the jet. The study of proper motion and ejection of new structures along with the polarization information can be used successfully to map the processes in the jet. A promising method is to have long-term multi-wavelength observations covering various stages of source brightness to determine correlated variations in different energy regimes from the light-curves.

PKS 1510-089 is among the well studied flat spectrum quasars (FSRQs). This is one of the very active objects where quiescent periods are interspersed with high activity states when flux density abruptly increases at almost all wavebands (Tornikoski et al., 1994b,a; Jorstad and Marscher, 2001; Venturi et al., 2001). This source was first observed as $\gamma - Ray$ source by EGRET instrument onboard Compton Gamma-Ray observatory. PKS 1510-089 is also observed at very high energies ($\sim$ TeV) by MAGIC and HESS (Wagner et al., 2010; Wagner and Hauser, 2010; Cortina, 2012). It was detected with an average flux (E$\geq$ 100MeV) $2.70 \pm 0.65 \times 10^{-6} ph/cm^2/s$ by AGILE (Pucella et al., 2008) during 2007 August 23-27. However, flux variability in this source was not well observed before 2008, with only a mild variation reported in EGRET observations (Hartman, 1999). However, with the advancement of space based instruments like LAT/Fermi and XRT-UVOT(Swift) for observations in Gamma-Ray, X-ray and UV alongwith availability of co-ordinated observations with ground based optical and radio facilities, study for the flux variations in this source has been addressed by many workers (Marscher et al., 2010; Orienti et al., 2011; Chatterjee et al., 2012; Nalewajko, 2012). The observations reveal intense activity over complete electromagnetic spectrum (Pucella et al., 2008; D'Ammando et al., 2009, 2011a; Abdo et al., 2010c).

7.1.1 Overview of PKS 1510-089

Marscher et al. (2010) studied this source using multi-wavelength data observed during the major gamma ray flare during 2008-2009. During the first half of 2009 only, the authors reported eight major $\gamma - Ray$ flares, many of them were found associated with the activity at other wavelengths. They noticed two radio knots crossing the core at $MJD54674.5 \pm 20$ and $MJD54958.5 \pm 4$, respectively. The first event corresponds to a major rise in X-Ray flux with steady optical emission. However, after a delay of about one month, a mild $\gamma - Ray$ flare was detected following a mild optical flare. This delayed outburst were seen to follow the frequency dependent delay. This follows the idea that high energy $\gamma - Ray$ emission often coincides with superluminal knot passing through a sub-mm- core (Jorstad and Marscher, 2001; Lähteenmäki and Valtaoja, 2003).

The second $\gamma - ray$ outburst in 2009 is explained by Marscher et al. (2010) as accompanied by enhancement in X-rays, Optical, Radio fluxes and ejection of a feature from the core. A major rotation in position angle was also observed before the flare indicating possibility of helical trajectory of the emitting blob down the jet. The $\gamma - ray$ enhancements unassociated with the significant change in optical continuum was inferred to be indicative of increase in seed photon density, instead of increase in the kinetic energy of electrons/positrons, to produce enhanced high energy flux. However the $\gamma - ray$ flares associated with simultaneous high X-ray, Optical and Radio states could be indicative of the SSC dominance. This emphasizes how multi-wavelength variability study can enrich the knowledge about the blazars jet and energetics. However, the non-availability of simultaneous data except for only few blazars does not allow to draw generalized conclusions. Also there are inherent complications such as the same source at different epochs behaving differently. Here, in this study we aim to investigate this source for flux variability during one of the historic high $\gamma - ray$ state observed in second half of 2011 and another one during early 2012, in order to understand the energy generation processes responsible for flaring.

7.2 Observations and data analysis

For this study we have made use of the archival data from instruments on-board Fermi and Swift along with the optical monitoring data obtained from our MIRO observatory and CRTS [1]. We have also made use of 43 GHz VLBA data from the Boston University gamma-ray blazar monitoring program [2],

[1] http://crts.caltech.edu/

[2] http://www.bu.edu/blazars/VLBA project.html

funded by NASA through the Fermi Guest Investigator Program. The 2 cm (15 GHz) radio data are taken from MOJAVE data base [3]. The additional optical/IR data are borrowed from SMARTS project at Yale University [4] (Bonning et al., 2012). This group is monitoring this object, alongwith other sources, since 2008 in optical (B, V and R) and IR (J, H and K) bands on regular basis using two telescopes at Cerro Tololo International Observatory (CTIO) in Chile. This program is dedicated to carry out coordinated observation with Gamma-ray observation by Fermi space based observatory. The optical polarization measurements are taken from MIRO, Physical Research Laboratory and Steward Observatory, University of Arizona, USA [5]. The data taken from other sources except Swift and Fermi observational data, are already reduced and directly usable. The data obtained from MIRO, Swift and Fermi are analysed using standard procedures. It is described in the following sections.

7.2.1 Optical photometry and polarization measurements: MIRO

The Mt. Abu Infrared Observatory is engaged in monitoring a sample of bright blazars on a regular basis using 1.2 m and 0.5m optical telescope. FSRQ PKS 1510-089 is also monitored from MIRO using CCD and Optical Polarimeter since 2005. The optical photometric monitoring is performed using CCD camera equipped with Johnson & Cousins filters I, R , V and B. The observation strategy is to observe few frames in all the bands and then monitor for longer time in R band. The bias and twilight flat field frames are taken during every night of observations. The CCD chip is cooled enough ($-120°$) to respond with negligible dark current. The analysis of optical images are done using the IRAF and script developed in-house, as already discussed in section 4.2, performing the source identification, flat field/bias correction and aperture differential photometry. The resulting magnitudes are then calibrated using the

[3]http://www.physics.purdue.edu/MOJAVE
[4]http://www.astro.yale.edu/smarts/glast/home.php
[5]http://james.as.arizona.edu/ psmith/Fermi/

photometric standards from Raiteri et al. (1998); Villata et al. (1997b); Smith and Balonek (1998). The reduction of optical polarization are done by on chip program. The position angle is corrected using polarization standards observed during every observational night. The resulting magnitudes and fractional polarization are used along with the data from Yale and Steward Observatory.

7.2.2 Swift observations

The instruments on-board swift have observed this source many times since 2008 in UV and X-rays. The data from XRT for the duration between 2011 June 27 to 2012 February are analysed using xrtpipeline, using standard procedures suggested by instrument team, with default input parameters (see section 6.2.2 for details). The resulting level 2 event files are then used to generate lightcurve and spectrum using source region with radius $15°$ centred on source position. The source lightcurve and spectrum are then corrected for background using the similar procedure constructing four source free background regions with radius of 50 pixels around the source region. The individual lightcurves are combined after proper time stamping to present the lightcurve used in this study.

The UVOT data are analysed using the same procedure as used in section 6.2.2. The snapshots taken in UVOT filters are integrated using *uvotimsum* task and analysed by *uvotsource* task, with a source region of 5 arcsec, while the background was extracted from an annular region centred on the blazar with an external radius of $40 arcsec$ and internal radius of $7 arcsec$. The galactic extinction correction for resulting magnitudes are performed using the prescription in Cardelli et al. (1989).

7.2.3 Fermi observations

The LAT onboard Fermi is scanning whole sky at $\gamma Rays$ (E: 0.1 - 300 GeV) every 3 hours. This is producing wealth of well sampled data for bright $\gamma - Ray$ sources. PKS 1510-089 is one of the very bright and active blazar regularly observed by Fermi. PASS 7 photon data for the period from June 27, 211 to February 27, 2012 for this source, obtained from Fermi data archive, are analysed using standard procedures with the help of software ScientceTool (v9r27) provided by LAT team. The standard data, time, energy and region cuts are performed before using unbinned likelihood analysis in order to obtain source lightcurve and spectral energy distribution. For this an xml model file constructed using python script *make2FGLxml* incorporating latest Fermi-LAT catalog (*gll_psc_v07.fit*), diffuse background *gal_2yearp7v6_vo.fit* and extra galactic background *iso_p7v6source.txt*. All these files are distributed as part of ScienceTools. The Galactic diffuse model is generated using the GALPROP package while the extragalactic background is described by a simple power law. The input model used for likelihood analysis comprises all the sources in 20° field of view. The model parameters for model sources within 10° are kept free while the ones related to beyond this region are frozen to default catalog values. The *logparabola* model is used for PKS 1510-089. The flux corresponding to the TS values greater than 25 ($\sigma \sim 25$) are adopted as statistically significant and for the rest an upper limit is estimated. The time bin used for present analysis is 3 days. The tools used to perform the filtering and performing unbinned likelihood analysis are provided as a part of the ScienceTools package. The input parameters for individual steps are decided as standard values suggested by the instrument team.

7.3 Results and discussions

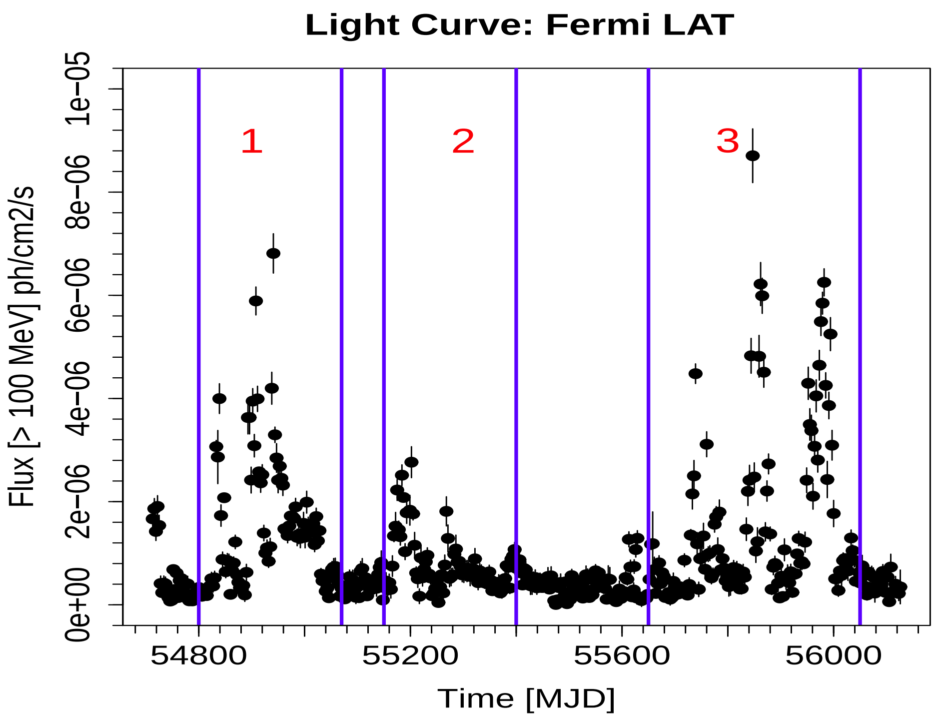

Figure 7.1 Three day averaged Fermi-LAT γ-ray lightcurve of PKS 1510-089 for the duration of 2008.5 to 2012.5 showing 3 setsb of flares.

FSRQ PKS 1510-089 is well known to show peculiar activity throughout the energy spectrum. Fig.- 7.1 shows the $\gamma-ray$ (0.1-100 GeV) light curve observed by LAT onboard Fermi space based observatory. The X-axis gives the time in MJD while the Y-axis shows the $\gamma - ray$ photon flux estimated in the energy band 0.1-100 GeV during the period from June 2008 to June 2012. This lightcurve clearly illustrates intense activity in this source at high energies. The prominent fast rises in the flux or outbursts are interspersed between the quiescent phases. We see three sets of Gamma-Ray flaring activities, or outbursts indicated by numbers 1, 2 and 3 spread over the period from 2008 June to 2012 June. This source has shown historical high energy flux during 2011 flares. The event number 1 and 2 are already discussed in great detail by

Marscher et al. (2010); Orienti et al. (2011). Here, in our study we will discuss the flaring event numbered as 3 in Fig.- 7.1.

The multi-wavelength lightcurves are analysed for probing the possible energy mechanism responsible for this event during the period MJD 55600 to 56100 (2011 June -2012 February). For clarity, in Fig.- 7.2 we plot the multi-wavelength lightcurve generated for the time domain covered by two vertical lines defining the event number 3 in Fig.- 7.1. Interestingly, this time domain also contains three main flares in Gamma-ray flux, as shown in the top panel of Fig.- 7.2, in the units of photon cm^{-2} s^{-1} $\times 10^{6}$ binned over 3-days, as a function of time in MJD. The three vertical lines indicate the time of highest observed flux for three sub-flares. The second panel shows the variation in X-ray count rates (F_X) with time as observed by XRT onboard Swift. The third panel from the top displays the variations in UV flux (F_{UV}) in different filters as observed at different epochs by UVOT instrument onboard Swift. The UVOT observes the source in six filters but for the convenience and clarity we have plotted only three filters (W2:black, U:red, V:green). The fourth panel from top is Opt/IR magnitudes in different bands as observed by MIRO, and SMARTS project. The different colors are chosen for magnitudes in different filters (B:black, V:red, R:Green, J:blue, K:pink). We have not included H band data as it shows the trend similar to J band flux. The fifth and sixth panel from top refer to the Optical fractional polarization and Position angles as a function of time in MJD. The data shown here are related to the observations taken from MIRO and University of Arizona, respectively. The polarisation angle (PA) is normalized to the range 0 to 180 degree. The seventh and eighth panels from top are the VLBA observations at 43 GHz by Blazar monitoring group at Yale University. The vertical line in this panel marks the time of maximum flux observed at 43 GHz. The last bottom panel shows the VLBI flux at 15 GHz taken from MOJAVE data base. The X axis is time in MJD common to all panels. Fig.- 7.2 displays the source showing complex nature of variability in multi-wavelength flux as well as significant variations in degree of polarization and position angle of polarization with time.

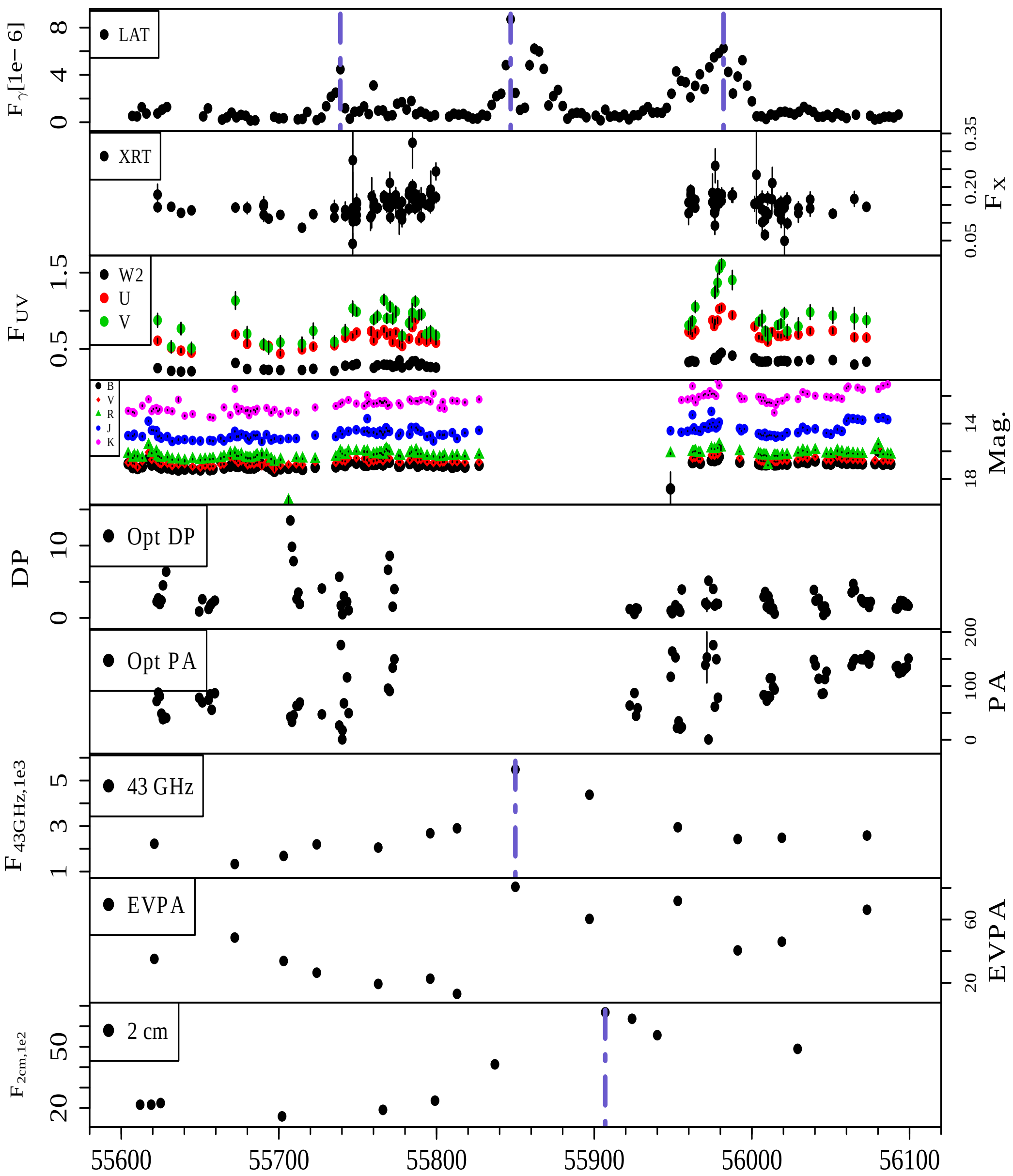

Figure 7.2 Multi-wavelength lightcurve for FSRQ PKS 1510-089 during 2011 to 2013.3, shoing $\gamma - ray$, X-ray, UV, Optical/IR, Optical polarization and PA, 43 GHz, EVPA, and 2cm flux.

In the following we discuss various features in the light-curves in different energy regimes.

7.3.1 Gamma-Ray lightcurve

In this chapter we are studying the 2011 γ-ray flaring event for PKS 1510-089 [# 3 in Fig.- 7.1]. As mentioned, this outburst state comprises of 3-main flares in the flux which have been zoomed in Fig.- 7.3, 7.4 & 7.5. The first event, shown in Fig.- 7.3, covers the time span of 100 days ranging from MJD 55700 to MJD 55800 and comprises of a series of three consecutive bright sub-flares peaking at MJD 55739, MJD 55760 and MJD 55784, separated by 21 and 24 days respectively. The peak flux for subsequent sub-flares is decreasing with time. The doubling timescale corresponding to this event is 2.7 days. The second Gamma Ray high state, shown by Fig.- 7.4, lasts approximately 70 days. This event also consists of three consecutive sub-flares peaking on MJD 55847, MJD 55862 and 55877 respectively i.e. at a difference of 15 days from each other. The first peak marks the historical high $\gamma - ray$ flare for this source as the three day averaged flux reached to 8.8 $\times 10^{-6}$ ph $cm^{-2}s^{-1}$. Around the highest peak the source flux increased by 2 times within approximately 3 days. While during it's decreasing phase the source flux fell by 4 times during next 3 days.Therefore the rise and fall episode lasts only 12 days. The three day averaged source flux was at 6.2 $\times 10^{-6}$ photon cm^{-2} s^{-1}. The second sub-flare lasts for longer duration ($\sim$ 15 days). After this second flare we also witness a third prominent increase around MJD 55877. However, the overall flux is only 2.8 $\times 10^{-6}$ photon $cm^{-2}s^{-1}$. The rise during this peak is slower while a fast decrease is seen in the flux. The third and last outburst episode of gamma-ray high states is shown in Fig.- 7.5. The individual points in this lightcurve are averaged over three day bins. We see prolonged high state which lasts for 50 days and peaks at MJD 55982.

We, thus, notice different type of variations at high energies [$\gamma - rays$]

during different phases of this source. The fastest $\gamma - ray$ variability observed is of the order of 2.7 days. This is the minimum doubling/halving timescale observed during the course of this study. A single $\gamma - ray$ high state comprises multiple short time scale flares.

7.3.2 Discussion of multi-wavelength lightcurves

In this section we will discuss γ ray flaring activities as shown in the light-curves in the context of multi-wavelength observations in radio, optical, UV and X-rays. From Fig.- 7.2 we can see three major *gamma* ray outbursts peaking around MJD 55739 (2011 June 27), MJD 55847 (2011 October 13) and MJD 55982 (2012 February 25), respectively. All the three outbursts maintain high brightness status for approximately 50 days. The first two outbursts contain significantly distinguished multiple γ ray flares separated by approximately 15-20 days while the third outburst has preceding and following sub-flares overlapping with main flare. It is worth mention that the 2011 October outburst records a historical $\gamma - ray$ high state.

Period of first $\gamma-$ray outburst

During 2011 June, γ-ray shows enhanced flux with three distinct flares. The source flux, averaged over three days, reached approximately 4.6×10^-6 photon $cm^{-2}s^{-1}$ which was about 4 times the yearly averaged flux. The X-ray flux starts increasing but gets subdued showing a plateau during the $\gamma-$ray burst. A clear rise in Optical/UV flux density measured by UVOT instrument onboard Swift (3rd panel from top) is seen which appears to peak with a delay of about 8 days with respect to the first γ-ray peak and remains in high state with mild fluctuation. The BVRJK band brightness as measured by MIRO and SMARTS facilities almost follow the same pattern as shown by UV- but there is no clear peak, just a plateau of enhanced brightness. Source brightness in these optical/NIR and UV bands drops slightly where 2nd $\gamma-$ray flare peaks and increases again peaking somewhere between 2nd and 3rd $\gamma-$ray flare peaks (8-days delay with respect to 2nd $\gamma-$ray peak flux). Flux in UV/optical/NIR bands drops again but gives a third peak about 4-days after the 3rd peak in $\gamma-$rays light-curve. The second and third optical flares are symmetrical in shape. This clearly establishes the delay observed between different $\gamma-$rays and Optical/uv emissions during the 2011 June outburst. The Optical polarimetric observations are very limited and do not trace the complete outburst period. The degree of polarization (DP) drops sharply (14 % on MJD 55707 to $\sim$ 2% on MJD 55713.5, 12% decrease in less than 7-days) on the onset of $\gamma-$ray flare while PA starts increasing (30° to 70°). During the gamma-ray peak, DP drops from 6% to about 1% where PA is undefined. Just after the peak, PA increases from 10° to 70° within 5-days. Next epoch for DP/PA measurements (8 days after the second gamma-ray peak) shows high but decreasing DP and moderate increase in PA with no clear pattern. The 43 GHz radio observations in nearby epochs indicate a mild enhancement in the flux which drops near the 3rd gamma-ray peak while the 15 GHz flux shows very low flux with almost no change (perhaps optically thick region for 2-cm emission) during whole period of γ ray enhancements. The amplitude of variation in optical is approximately proportional to $\gamma - ray$ amplitude of variation, indicating to high energy emission dominated by external inverse Compton-seed photons, perhaps, coming from accretion disk and/or BLR region.

Period of second $\gamma-$ray outburst

Second outburst, centred on October 2011 [MJD 55847] is historically largest γ-ray outburst. Unfortunately, we do not have any optical or X-Ray observations during this epoch. The 43 GHz flux density shows a peak almost simultaneous to the γ ray peak. The peak flux at 15 GHz appears to delay by approximately 47 days with respect to the 43 GHz peak. The EVPA at 43 GHz also follow the similar trend as total flux, changing from 15° to 70° during the peak flux period.

Simultaneity of millimetre-γ-ray outburst and frequency dependent delayed flares at lower energies confirms the applicability of shock in jet scenario for energy generation in the jet of PKS 1510-089 (Valtaoja and Valtonen, 1992).

This indicates the co-spatiality of emission region for both the high energy and mm-radiation. According to shock in jet model the formation of shock take place because of interaction of two components with differing propagation velocities. The opacity of the emission region governs the observability of the particular frequency. The high energy radio emission will be detected first (sub-mm/mm) followed by a time delay at other lower frequencies as the emission region propagate through the jet. During the second flare the frequency dependence in radio frequencies are seen. The higher frequency peaks earlier and the higher frequency peaks follow them with delay in time. Orienti et al. (2013) have also witnessed the frequency dependent delay in peak flux at different radio frequency. They represents very dense sampled data at several frequencies ranging from 142 GHz to 2.6 GHz. Figure 7.2 clearly illustrates the frequency dependence of peak radio flux. Two vertical dotted lines shows the first two major γ ray flares occurred in 2011, June and 2011, October respectively. They have observed the radio frequency 142 GHz peaked first and the lower frequencies followed that peak. The flux density at 142 and 86 GHz reaches it's maximum almost simultaneously at the end of September. The time delay increases with the wavelengths, from about one months at 32 GHz and 22 GHz, upto several months at centimetre regimes.

The statistical studies of the lightcurves of blazars, performed by several authors time to time, shows that during an outburst, the time at which peak flux is observed depends upon the frequency of observations (Hovatta et al., 2008; Hughes et al., 2011). In the shock in the jet scenario one expects the peaks to occur at millimetre frequencies followed by the peaks at longer wavelengths with some time delay, as a consequence of change in opacity of medium as emission region propagate through jet. Therefore the time delay in different frequencies are very important to constrain the jet properties of the shock and it's evolution during the observed outburst. The peak of 2011, October Gamma ray outburst seems to occur almost simultaneously to the one observed at 43 GHz. However the lightcurve (Fig.- 7.6) shows that the 86 and 142 GHz peaks seem to precede the high γ-ray flare detected in 2011, October.

The actual peak time cannot be determined because of poor time sampling at those frequencies. Therefore we can not deny those to be simultaneous. The starting of rise in flux at millimetre wavelengths (43 GHz) may be related to the high energy outburst in 2011, June. However, flares at millimetre wavelengths often peak simultaneously with the γ-ray flare (Abdo et al., 2010b), and a delay of more than three month (115 days in this case) is unusual. The Orienti et al. (2013) has also discussed the study of evolution of parsec scale features in the jet. The Fig.- 7.7 is taken from Orienti et al. (2013) illustrating the results of this study. There have observed evolution of two components with respective separation velocities of 1.5 $\pm$ 0.1 mas yr^{-1} [$V_{app} \sim$ (33.4 $\pm$ 2.2)c] and 0.92 $\pm$ 0.35 mas yr^{-1} [$V_{app} \sim$ (20.5 $\pm$ 7.8)c]. The ejection time of both the components are 2010.8 $\pm$ 0.05 and 2011.83, respectively. This clearly indicates that the γ-ray flare observed in 2011, June is not related to any new ejection of parsec scale features while the second γ-ray outburst observed in 2011, October is very closely related to the ejection of a new feature from core around 2011, October 26.

An estimation of location of emission region responsible for this outburst was performed by Orienti et al. (2013) using their better sampled radio data. The following expression was used to the required estimation

$$\Delta r = \frac{\beta_{app} c}{sin\theta} \times \frac{\Delta t_{obs}}{(1+z)} \tag{7.1}$$

where β_{app} is the apparent jet velocity, c speed of light, Δt_{obs} is the time elapsed between the onset of the millimetre outburst and γ-ray in observer's reference frame, and θ is the viewing angle (Pushkarev et al., 2010). Using above formula and Δt_{obs} computed from 22 GHz observations as the time between the epochs when flux density doubled it's value (2011, September 09) and epoch of the detection of γ-ray. The resulting value of Δr in de-projected plane comes to 10 parsec which is beyond the BLR region ($<$ 1 parsec). Therefore this outburst presents an evidence of phenomenon about the major dissipation occurring beyond the BLR region whereas majority of blazar dissipation occurs within the BLR regions (Ghisellini et al., 1998).

Period of third $\gamma-$ray outburst

During the third episode of $\gamma-$ray outbursts in 2012 February the three day averaged GeV ($>$ 100MeV) photon flux density reached upto [6.4 $\times$ 10$^-$6 ph $cm^{-2}s^{-1}$] at MJD 55982. A minor sub-flare precedes the main one, decaying part of which overlaps with its rising phase. Similarly, a rapid decay in the main flare appears to be overlapping with a rising third sub-flare. It is difficult to completely resolve these in 3-day averaged data and perhaps it is worthwhile to look at features in the smaller binned light curves. The slow rise and rapid fall in the flux during this asymmetrical flare indicates to the slow acceleration of electrons which attain higher energy and cool rapidly before escaping the emission region.

The X-ray count rate observed at same epoch as the complete outburst, shows mild increase with slight delay. Part of it could be contributed by disk UV photons up-scattered from the corona- hence the delay. The UV band flux from Swift, in all the bands, appears to be peaking with main peak in the γ-ray flux. Unfortunately, there are no data in optical and NIR bands for the duration MJD 55980 (two days prior to γ-ray peak) to MJD 55990 to ascertain the peak flux in the optical-NIR. However, the V-band flux observed by Swift peaks almost simultaneously with γ-ray (main peak). That means that emissions at the γ-ray, Optical/UV and near-IR from Fermi, Swift/SMARTS+MIRO are simultaneous, with, if at all, a minor lag/delay (cf, Fig.- 7.2 & 7.7). The optical polarization starts increasing with onset of outburst in γ-ray, reaching maximum (5%) just before the main peak in Gamma-ray and then falling rapidly to minimum at MJD 55982. It appears to increase again (no data) with decrease with quenching of the outburst. The optical polarization PA undergoes continuous change, rapidly during the main Gamma-ray peak, remaining within 20° - 180°. After the main γ-ray peak, the limited observations show rapid change in PA from 150° to 100°. The radio flux, however, at 43 and 15 GHz do not appear to show any significant simultaneous change, albeit these are larger compared to their pre-outburst epoch values. It could be due to the lack of observations (as we saw in case of near IR/Optical) with good sampling during/after the peak in γ-ray flux. The origin of $\gamma-$ray, IR/optical, UV and substantial X-ray emission appears to be co-spatial due to interaction/ejection of shock/new-knot with/from standing or moving core further down-stream the jet. The one of the most important part of this outburst is enhancement in optical flux with hump in γ-ray flux because the polarization observations reveal a sudden flip in PA just before the peak in γ-rays. The sudden change in PA is not expected in the case of normal cooling of shocked region, if the particular outburst is manifestation of superposition of two emission regions in shocks/shells with accidental coincidence of magnetic vectors in two regions. But if variation is caused by compact blob with different magnetic fields than the magnetic field in underlying region, a sudden change in PA may occur. Another possibility for such change in PA is the possibility of sudden change in Doppler factor due to the presence of local bending in the jet or change in the trajectory of moving emission region. The 2012, February outbursts will be very close in time to the second parsec scale ejection if we consider the other end of uncertainty box but the observations in past for this source and others show that γ-ray either precedes the core, crosses or is simultaneous in time (Abdo et al., 2010b; Orienti et al., 2011; Marscher et al., 2010). Therefore 2012 February outburst is unlikely to be related to any core passing event.

If we look at the amplitude of variation in optical, it changes by a factor of 2 while the change in the amplitude, during this period, in gamma-ray flux is more than 6 times. Since synchrotron electrons in the jet play important role in both, synchrotron and IC flux (by up-scattering the seed photons) we expect external IC component to vary in proportion to variation in synchrotron flux, while SSC flux will change as square of the change in synchrotron flux. It is because SSC flux is proportional to the electron density as well as synchrotron photon density. Here since γ-ray flux changes by more than a factor of 4, perhaps it has significant contribution from external Compton as well. The seed photons might come from reflected torus emission.

After the major flare in 2012 February, minor fluctuations in γ-ray flux are seen around MJD 56030 with a simultaneous flux enhancements in NIR, Optical, UV bands and perhaps with a delay in X-ray flux. The polarization measurements only available during the decay part of $\gamma-$ray flare show rapid decrease in DP accompanied by a sudden change in PA. The PA drops by 70° (from 150° to 80°) and then rapidly increases towards the end of observations (Fig.- 7.5). Such a sudden flip in PA during the mild change in flux at high energies, accompanied with significant uv/Optical/IR flux enhancements is intriguing. The γ ray emission with a simultaneous or delayed emission in optical bands in the case of other blazars are also reported (Jorstad et al., 2013; Wehrle et al., 2012; Vercellone et al., 2011; Chatterjee, 2010; Abdo et al., 2010d; Ackermann et al., 2012; Raiteri et al., 2008; Hagen-Thorn et al., 2008; Larionov et al., 2008).

The high energy emission in blazars are mainly generated because of inverse compton processes in the jet. Therefore flux enhancements at high energies indicate either the formation of shock because of interaction of two ejected components differing in velocity or due to compression of emission regions by the presence of some stationary core. The re-confinement and acceleration zones in the relativistic jet can also be responsible for flux enhancements (Nalewajko et al., 2011; Nalewajko, 2012; Nalewajko and Sikora, 2008, 2010). There are also few studies done using the older data for this source and in some cases authors have reported the close association of ejection of radio features from the core (Marscher et al., 2010; Orienti et al., 2011) into the jet. The change in DP observed with the association of high energy emission can be understood on the basis of normal shock formation scenario while the change in PA is not expected in the case of compression of emission region because of shock compression in the case of axially symmetric, matter dominated jet (Abdo et al., 2010d). Therefore the observed large change in PA at least for one case indicates either the geometry dependence of emission or emission is following curved trajectory causing change in Doppler factor (δ) resulting in change in total flux and position angle (PA). However, the nature of flux change resulted due to the change in Doppler boosting factor (δ) is completely achromatic i.e. no frequency dependence is expected. As an alternative process, if the small-scale variation is generated by very compact blob that is different from the larger emission region responsible for the underlying larger time-scale variation, a sudden change of PA may occur because the magnetic field direction inside the compact blob does not need to be the same as exists for larger emission region in the jet.

7.4 Conclusion

In this chapter we discussed the results obtained from the multi-wavelength study of FSRQ PKS 1510-089 when it underwent the set of three major γ outbursts during 2011.5-2012.4. Such a multi-wavelength study is very useful to understand the mechanism and location of emission in the jet. Our study highlights the nature of emissions at different wavelengths during different episodes of outbursts. The one of the most striking observation is that almost all the γ-ray outbursts comprise the multiple γ-ray flares. The very first outburst in June-July, 2011 is related to the delayed NIR/optical/UV flux enhancements. The absence of any significant flux enhancements at cm wavelength indicates the origin of emission from a region very close to the central engine where the radiation is opaque at the radio frequencies.

On the other hand the historically strong $\gamma-$ray outburst in 2011, October seems to be related to a huge radio flux detected since the beginning of the 2011 September. The enhancement in flux at higher radio frequencies is followed, with a time delay, rise at lower frequencies indicating to frequency stratification in flux. The possible coincidence of γ-ray and radio outbursts indicates the possibility of γ-ray emission region located further downstream the jet where emission at radio frequencies is transparent. Though, we do not have data on optical/X-ray frequencies for this time domain but the site of emission region as estimated by (Orienti et al., 2013) [10 pc] shows that the most of the emission occurs beyond the BLR region, a very rare observation. This strong

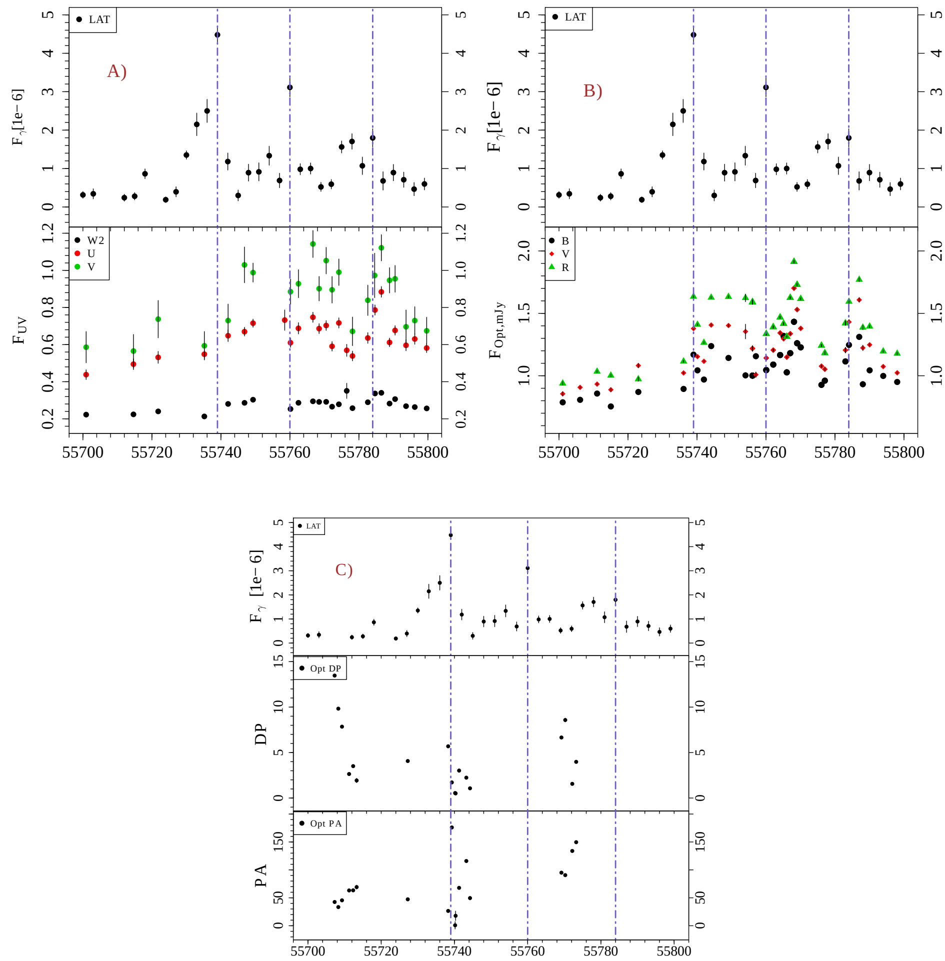

Figure 7.3 The three day averaged γ-ray lightcurve enlarged to show the first γ-ray outburst in peaking around 2011, June 27. In addition to main first flare, two sub-flare are clearly seen in γ-ray , similar trends, albeit subdued, are seen in UV/Optical fluxes.

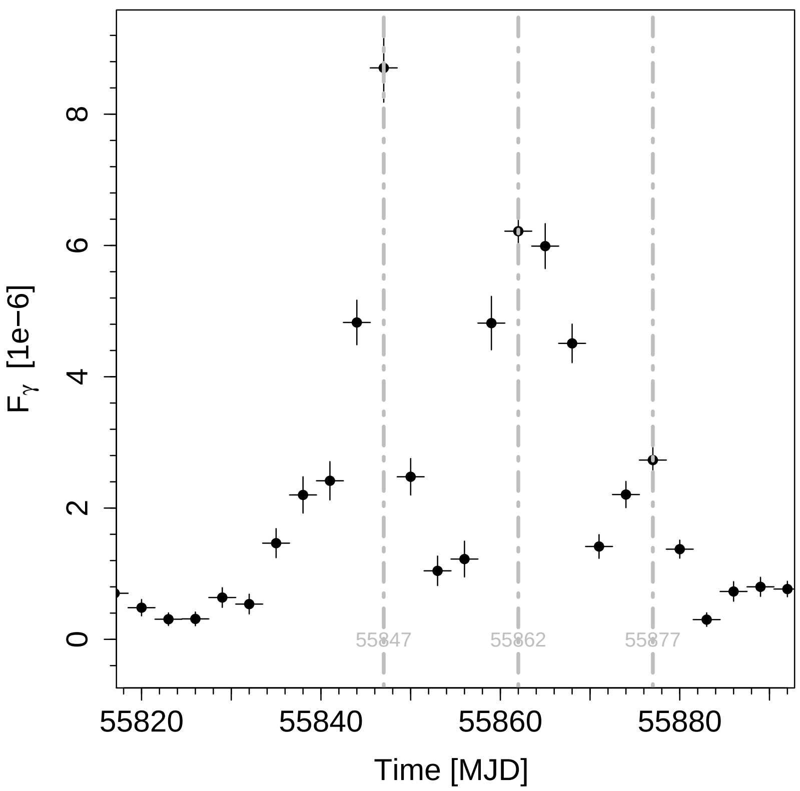

Figure 7.4 The three day averaged γ-ray lightcurve enlarged to show the second episodes of γ-ray outbursts peaking around 2011, October 13. Two more sub-flares are seen along with prominent high γ-ray state.

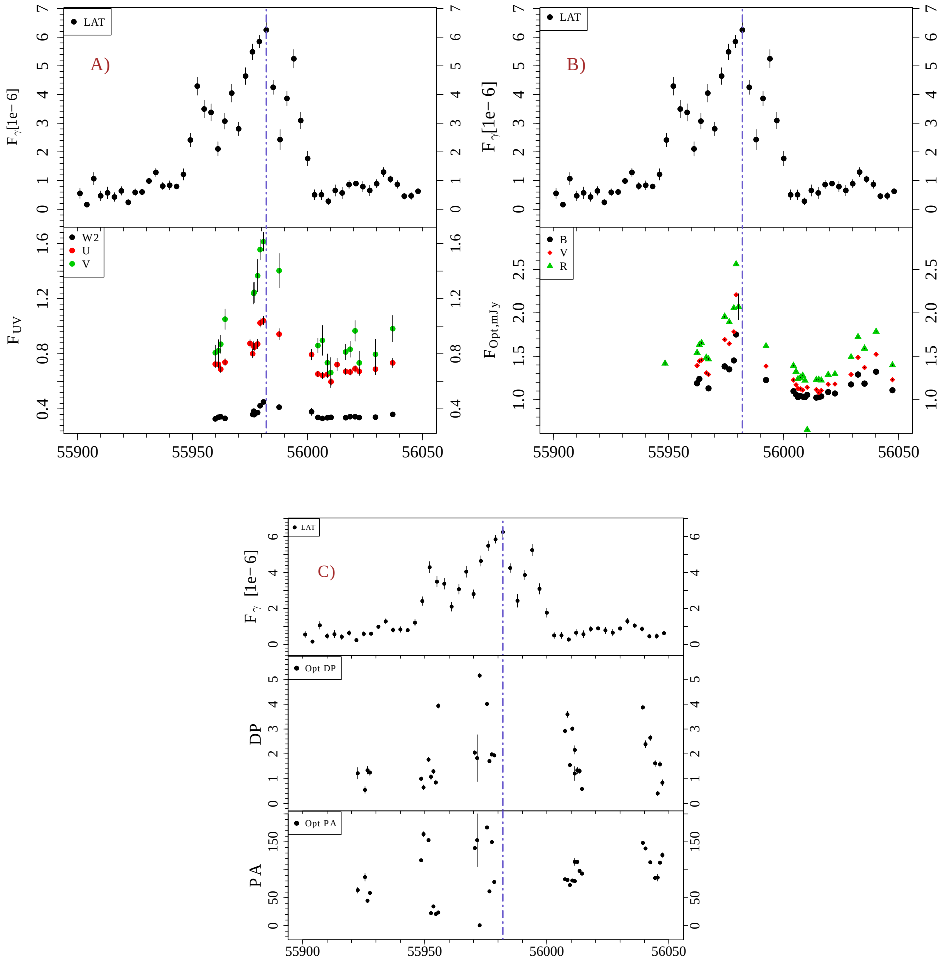

Figure 7.5 Third set of γ-ray flares peaking around 2012, February 25. Two more sub-flares are seen in the light-curve. Also shown, in separate panels, are flux in optical and polarization curves.

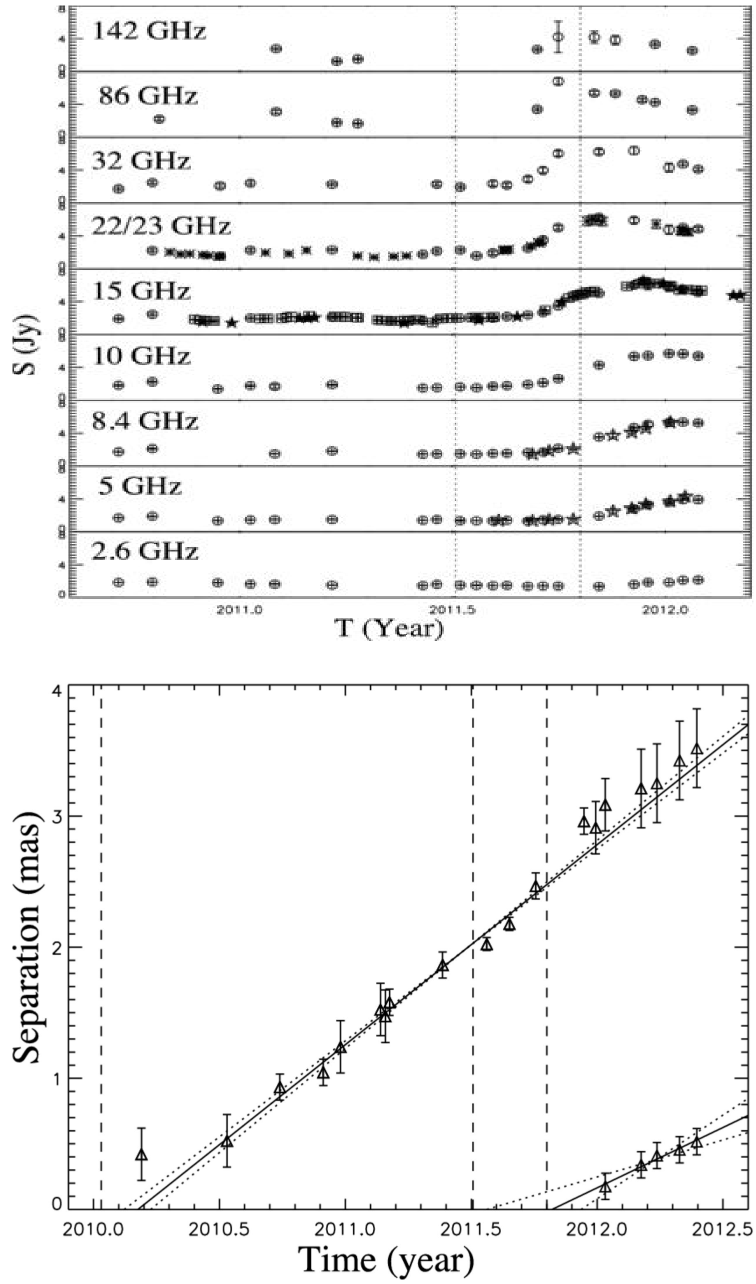

Figure 7.6 The upper panel shows the multi-frequency radio lightcurve borrowed from Orienti et al. (2013) showing the time delay in peaks at different frequencies. The lower panel illustrates the ejection and evolution of parsec scale radio features borrowed from same article.

flare is likely to be related to the ejection of a new superluminal component from the radio core.

The third and last episode of γ-ray outbursts, observed in the course of study, coincides with the second highest near IR, optical and UV emissions emitted from this source. This γ-ray outburst is again a set of three sub-flares but the three day averaged lightcurve is very difficult to separate the individual flares. The unavailability of any significant change in the under-sampled cm flux connected with this event makes it difficult to ascertain the location of such emission: whether close to the central region where radio emission is not able to escape the medium. However significant change in EVPA measurements at 43 GHz occurred during same time dilutes above inference. A second optical outburst after 50 days the February 2012 major flare accompanied with a small hump in γ-ray low level flux state and association with a sudden change in PA makes it interesting. The second optical flare may be because of the cooling trail of γ-ray photons but the change in PA indicate geometry dependent. The composite picture of the third $\gamma-ray$ outburst epoch is that though we do not have sufficient information at radio side, all other emissions appear to be quasi-simultaneous. The change in amplitude of variations at $\gamma-ray$ energies is more than square of such change at lower frequencies (tail of synchrotron emission). That shows that significant contribution to high energy flux comes from SSC emission in addition to substantial EIC. It might indicate the generation of multi-frequency emissions from a region far away from BLR region where seed photons from torus plays a role.

The broad picture of flux variability study carried out in this chapter shows that first two set of outburst may be explained assuming to be originated because of the propagation of same disturbance downstream the jet. The first outburst occur very near to the central engine i.e. in the initial part of the jet just prior to sum-mm conical shock, which was opaque to the radio frequencies. As the disturbance propagates down the jet the opacity decreases and other energy emission become visible. As the disturbance passed through some oblique standing shock the second high energy flare is seen. The low energy photons intrinsically from the same region or exterior are up-scattered to the high energies due to Inverse Compton processes in the shocked region. The frequency dependent response of peaks at longer radio wavelengths confirms the shock formation downstream the jet (Orienti et al., 2013). Further propagation of this emission region downstream the jet, a superluminal component becomes visible at parsec scale observations using VLBI techniques. However, the third γ-ray outburst seems to be independent as inferred from the absence of no radio flux enhancements. The location of this emission may be again the close environment of central region but beyond the BLR, else high energy gamma-ray emission will be absorbed. The simultaneous optical and γ-ray enhancements indicate the SSC origin of high energy photons which indicates to another possibility of emission at all the wavelengths, considering we do not have well sampled data at lower, radio frequencies, to be simultaneous caused by interaction of a shock/new knot with standing/moving shocked region. The seed photons might be coming from torus for up-scattering, in addition to significant SSC emission as reflected by large ratio of optical to γ-ray changes in amplitudes. The second flare seen after 50 days of this event may be because of change in Doppler factor, inferred from the sudden change in optical position angle observations. Perhaps new simultaneous observations at all wavebands might be able to provide a clear picture of violent activity in this source.

Chapter 8

Summary and outlook

In spite of considerable amount of work done to understand the high energy ($\sim 10^{48-50}$ erg s^{-1}) output from AGNs and their detailed structure, progress in this direction has been far from satisfactory. Main reason being their compact nature and large distances which make them difficult to be resolved with present day and near future facilities. The variability in blazars- a subclass of AGNs, which are seen at small angles to the relativistic jet direction, provides an important tool to probe the deepest regions of central engine. Their multi-wavelength flux variability indirectly provides insight of intrinsic properties of the regions and their surroundings where these are produced. The observations at multiple energy bands taken almost simultaneously can be used to understand the complete picture of energy generation processes. The variability time scales, their relative correlations among different energy bands, amplitudes of variations, shapes of the flares coupled with polarization and its variability provide host of information on the size, location, local magnetic field configuration and probable physical processes occurring in the emission regions. In the present work reported in this thesis, we have used these techniques in an attempt to reveal the complex processes responsible for variability in blazars and deduced important physical quantities related to these complex sources. In the following a brief summary and conclusions drawn from this work are mentioned.

8.1 Summary and conclusions

In this dissertation the flux and polarization variability are investigated in order to study the physical processes responsible for emission and nature of emission regions in blazars. Optical observations reported here are obtained mostly from Mt Abu IR Observatory while data from other facilities, such as SWIFT, Fermi etc., are analysed and used. First two chapters introduce the subject and the facilities used, methodology adopted. Remaining part of the thesis presents the main part of the work carried out and is briefed in the following.

- The microvariation or intranight variability (INV), an interesting aspect of blazars, is investigated in Chapters 3 & 4. A sample of blazars are regularly monitored in four optical bands (BVRI) using MIRO. BL Lac S5 0716+714 is one of the optically bright blazar monitored extensively during the last seven years of blazar monitoring program at MIRO. During 2010, March the source underwent a significant optically bright phase. The rapid intranight variations were recorded during the course of monitoring period. The object had shown the fastest ever reported flux variations [0.33 mag hr^{-1}] during the monitoring of 2010, March 10. The high temporal resolution [effective exposure $\sim$ 45 sec] was able to delineate rapid asymmetric variability patterns very well. Shortest intra-night timescale of 1.42 hrs is used to estimate the size of emission region (2×10^{15} cm) and associated black-hole mass (about a billion solar mas). The five nights of monitoring of this source are used to infer the possible physical processes responsible for variation. The asymmetric nature of INV features rules out the geometric or propagation dependent models for variability. A significant change in nightly averaged flux is also seen during the course of monitoring period. The mild color dependence observed between different nights supports their intrinsic origin. The inter-night variations, variations in nightly averaged flux, showing mild bluer when brighter nature could be due either to changes in the

Doppler factor or faster acceleration of higher energy electrons relative to their cooling time scales. While intra-night variations with few hours time scales are probably due to interaction of fast moving shocks in the jet with local small scale inhomogeneities, it is very difficult to associate faster variations with spatial extent of the emitting region. Chapter 3 covers a detailed discussion about this study.

- To ascertain how frequent is intra-night variability in Bl Lac S5 0716+714, we used long term monitored data from Mt Abu observatory and plotted nightly light-curves. The pattern of INVs during different nights appear quite different indicating to their origin to turbulence in the jet. There are many epochs when rapid flickering are superimposed onto slowly varying intra-night flux whereas many INVs just show consistent rise/fall in the flux level during overnight monitoring. The rapid acceleration and cooling in the turbulent shock regions may be responsible for such short timescale variations. The 58 best photometric nights each with a continuous monitoring of 2 hours or more are used to study the long term behaviour of the BL Lac object S5 0716+714. From the study we established very high duty cycle of variation for this object [84%] which is in agreement with older results. The amplitude of variations during various brightness states of the source gives interesting scenario. The amplitude of variations during relatively low brightness phases are in general larger than those during the brighter phases. Normally one would expect a contrary result- larger amplitude of variations during bright phase as source is undergoing violent activity. We propose that varibility amplitudes are perhaps similar but they get pronounced due to low mean flux during quiescent phase. The longterm (about seven years) light-curves show several outbursts superposed on the mean value of source brightness. Since the data is rather sparse, it is difficult to comment on the existence of any quasi-periodicity. It is interesting to note a slow decrease in mean brightness of the source with time. A mild bluer-when-brighter (BWB) spectral trend is observed with a slope of about 0.05 in the long-term light-curve which clearly favours the formations of internal shocks in the jet responsible for variability.

- We investigated polarization nature of an interesting source, CGRaBS J0211+1051, which was detected undergoing a flaring activity in Gamma-rays on 2011 January 23. High temporal observational study for intra-night as well as inter-night variations in degree of polarization (DP) and position angle (PA) for this possible blazar candidate is performed during January 30-February 3, 2011. The rapid variations [$\Delta t \sim$ 15-20 minutes] in DP and PA are seen during at least three nights indicating to turbulent plasma in the jet. The source also shows very high and variable (9-20%) inter-night degree of polarization with significant change in PA. Many workers associate high degree of polarization with the low energy peaked blazars(LBLs), while others believe that there is no significant difference between the two (LBL and HBL) sub-classes as regards to polarization property. In order to investigate this aspect, and also to characterize this source, we used a large sample of bright blazars from literature for which polarization data was available along-with our own observations. With this sample, we carried out a statistical study which clearly establishes that the low energy peaked blazars (LBLs) show, with few exceptions, distinctively much higher degree of polarization than HBLs. Based on the high degree of polarization observed, we, therefore, suggested this source to be a low energy peaked BL Lac object (LBL). However, the true test comes from position of synchrotron peak in the SED. For this We carried out a multi-wavelength study of the source in Chapter 6, generating its lightcurve and spectral energy distribution. The SED shows the synchrotron peak falling at 10^{14} Hz, confirming CGRaBS J0211+1051 an LBL. From its SED, we also notice somewhat intriguing behaviour in this source. During low phase, IC component of SED does not show a dominant behaviour expected of LBLs. Also the peak shifts to lower energies. X-ray emission, at least partly, appears to be tail part of synchrotron emission. Several parameters are estimated, eg, luminosity distance d_L

for source (957.1 Mpc or 2.953 $\times 10^{27}$ cm), co-moving magnetic field ($\sim$ 0.4 Gauss) and jet power.

- Long-term multi-wavelength light-curves are instrumental for understanding the physical processes at work in a source and to infer relative locations of the emission regions. A long-term multi-wavelength variability study of PKS 1510-089 is performed covering the period of mid 2011 to early 2013. This source showed three episodes of major γ-ray outbursts each consisting of multiple flares. The response of individual outburst at different wavelengths are analysed in great detail. One interesting result from this study is different natures of multi-wavelength emissions during three outbursts. The absence of no prominent variations at mm/cm and a possible lag at optical/UV frequencies during it's first outburst [2011, June-July], indicate that this may be associated with a shock formation in a region of the jet close to the central engine which is opaque to the low energy emission. The second episode of outbursts show a historic γ-ray flux approximately simultaneous to the peak at radio frequencies. The frequency dependent radio observations confirm the ejection of a knot responsible for this. For this outburst Orienti et al. (2013) estimated the location of emission region to be around 10 pc which is far away from BLR region. This result establishes the dissipation region to lie downstream the jet. The third outburst episode [2012 February] shows similar gamma-ray activity almost coinciding the optical flare. The under-sampled radio flux and EVPA restrict us to make any firm conclusion about the location of the emission region. However, the amplitude of variation in gamma-ray flare is more than the square of the amplitude of variation at optical wavelengths, signifying the contribution of EC processes in addition to the SSC for high energy emission. Such high energy gamma-ray emission, quasi-simultaneous with optical, UV and x-ray flaring, indicates to a region of origin beyond BLR to avoid significant absorption.

Implications of the present study:

Our study underscores the importance of high temporal resolution multi-wavelength light-curves for the better understanding of emission processes in AGNs.

It confirms very high duty cycle of variations in blazars.

That blazar S5 0716+714 shows larger amplitude of variation when in relatively fainter state, a result which needs to be explored further for this source and many others.

That LBLs show, in general, distinctly higher degree of polarization than HBLs and therefore, when other properties are not known, can be used to classify blazars.

That source CGRaBS J0211+1051 is an LBL but needs further study to understand its high energy IC component.

That simultaneous multi-wavelength light-curves help locate the regions of emission.

8.2 Future projections

Significant progress has been made over several decades in our understanding of the AGNs. The availability of high quality data from larger ground based telescopes and space based facilities over the entire range of frequencies has made it possible to discuss much finer aspects of their energy processes and structures than was possible earlier. Multi-wavelength observing campaigns, such as whole earth blazar telescope (WEBT), have been able to generate episodic light-curves on several sources to enable better modelling of their energy processes. The study of correlated variations among different energy regimes in association with VLBI imaging of the sub-parsec level jet has been able to at least indicate the location of various emission regions in some sources. While recent studies have answered some questions, these have also raised new ones. Many a times, correlations between two energy bands lead to entirely opposite result for the same source but at different epochs. Study of variations in various energy regimes indicates to very complex behaviour. Complex behaviour indicates to complex sources which require comprehensive study of individual source at one hand and of a large sample of such sources on the other to come to a general understanding of their nature. Therefore, a lot more needs to be done to understand these enigmatic sources. In near future, larger optical ground based telescope (30-40m) should be available along with more powerful space based observatories to provide much better quality data to meet the challenges thrown by these enigmatic sources and perhaps be done with *enigma*.

While carrying out the present study, we felt the need to explore further several issues. In case of S5 0716+714, our statistical study for the amplitude of variation as a function of brightness resulted in very interesting result-that variability amplitudes are larger when source is relatively fainter. That is contrary to common notion that source is expected to show larger variability amplitudes when it is in flaring, violent phase. We would like to explore it further with larger data and by carrying out similar study on other sources. From a sizeable sample of LBLs and HBLs, we inferred that LBLs show much higher degree of optical polarization and the polarization nature can be used for classification of blazars. It would be worthwhile to make this finding robust by carrying out such study with much larger sample as polarization measurements are being made on more and more blazars. In order to locate the locations of high energy emission, study of blazars undergoing flaring activity in different energy regimes will be done by looking at delays between various emissions. It should provide information about the scattering regions, where photons are getting up-scattered, either in the vicinity of accretion disk, within the inner parsec or further out down the stream. This information coupled with VLBI imaging and optical polarization will help constrain the models of emission describing physical conditions in the jet (magnetic field, electron energy density, energy gains and losses of relativistic electrons etc.)

Appendix A

Tables with filter information

A.1 Information about Optical Filters Used.

Filters are very important component of any imaging instrument. As clear from name itself, they transmit only a particular waveband depending upon the filter. There are plenty of optical filters available in the market. The specifications of these filters depend the kind of use. Filters are characterized by the effective wavelength, bandwidth and transmittance. Many observatories have their specific filters. Mt. Abu Infrared Observatory is using standard Johnson & Cousins optical filters as a part of two optical imaging instruments (CCD-Camera & ATVS) and PRL made optical polarimeter (PRLPOL). The NICMOS is using standard JHK filters. We have also made use of optical data from UVOT instrument onboard Swift. The UVOT is having seven filters including white light. The table A-2 presents the information about UVOT filters. The following equation is used to covert the UVOT magnitude into flux using the filter characteristics shown in Table A.2.

$$F_\lambda = FCF \times 10^{-\frac{(m-ZPT)}{2.5}} \tag{A.1}$$

Where m is the observed apparent magnitude of object. FCF and ZPT can be obtained from above table. FCF & ZPT stand for Flux conversion factor and Zero Point, respectively.

S.No.	Filter	λ_{eff} (μm)	$\Delta\lambda_{fwhm}$ (μm)	Absolute Flux Density (w $m^{-2}hz^{-1}$)
1	U	0.36	0.065	1.81×10^{-23}
2	B	0.44	0.089	4.26×10^{-23}
3	V	0.55	0.084	3.64×10^{-23}
4	R_C	0.64	0.16	3.08×10^{-23}
5	I_C	0.79	0.22	2.55×10^{-23}
6	J	1.25	0.30	1.67×10^{-23}
7	H	1.65	0.29	9.80×10^{-24}
8	K	2.2	0.41	6.49×10^{-24}

Table A.1: Standard Optical (UBVRI: Johnson & Cousins) and Near IR (JHK: NICMOS) filter being used at MIRO

S.No.	Filter	λ_{eff} ($\mathring{A}$)	FCF $\pm\ \sigma_{FCF}$ $\times\ 10^{-16}$ (erg $cm^{-2}\mathring{A}^{-1}c^{-1}$)	ZPT $\pm\ \sigma_{ZPT}$ mag
1	U	3501	1.62 ± 0.025	18.34 ± 0.02
2	B	4329	1.47 ± 0.0056	19.11 ± 0.02
3	V	5402	2.63 ± 0.0087	17.89 ± 0.02
4	UVW1	2591	4.21 ± 0.130	17.44 ± 0.02
5	UVW2	2033	5.97 ± 0.130	17.38 ± 0.02
6	UVM2	2229	8.44 ± 0.053	16.85 ± 0.02
7	White	3470	0.37 ± 0.049	20.89 ± 0.02

Table A.2: *Swift* UVOT filters and related information (Poole et al., 2008)

Appendix B

Filter Characteristics

B.1 Filter Transmission Curves

The transmittance of the optical filters decay with time. Therefore a regular check-up of the transmittance are essential. The filter characterization is performed using spectrophotometer, emitting a continuous spectrum between 0.3 μm - 3 μm, every year before the start of observing session (Every September). Following curves are shown for an example of the transmittance of three set of optical filters used in various instruments being used at MIRO. The analysis was performed in September 2011. All the figures are self explanatory. For completeness, the X-axis represents the wavelength in $\AA$. Y-axis is transmittance which defines the quality of filters.

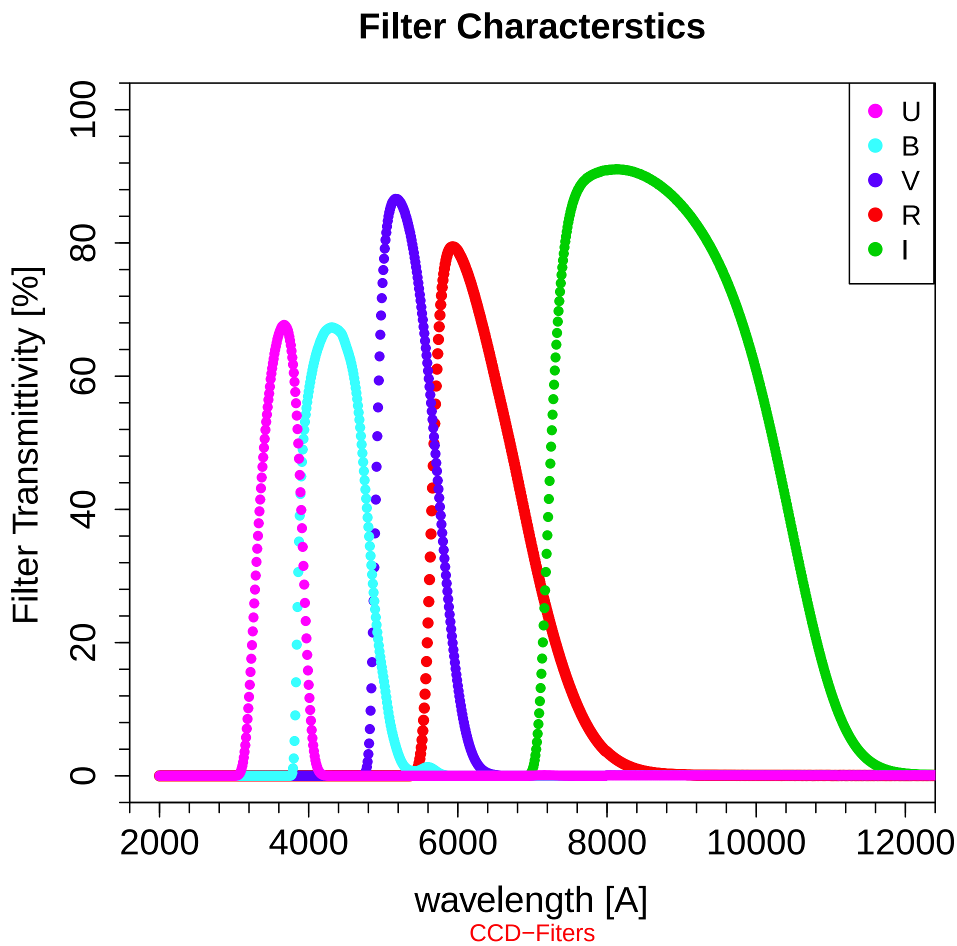

Figure B.1 Filter transmission curve for the filters (UBVRI) used in CCD Camera at MIRO.

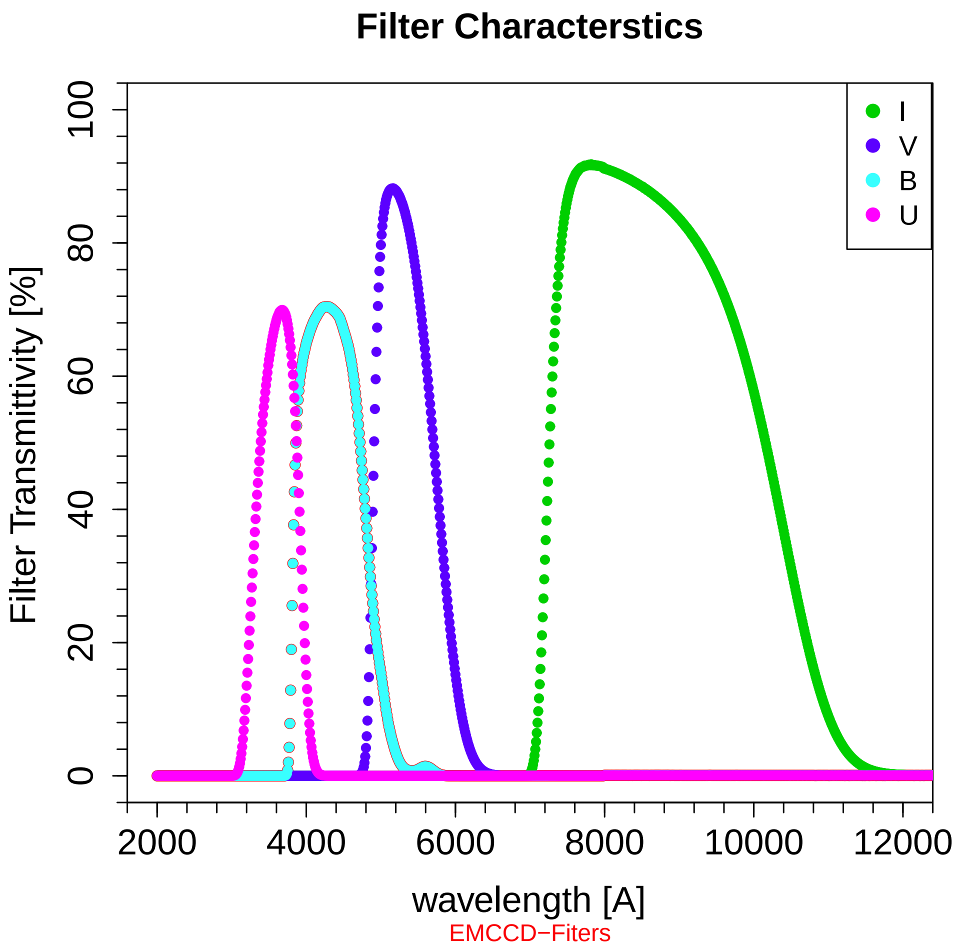

Figure B.2 Filter transmission curve for the filters (UBVI) used in EMCCD CCD Camera at the backend of ATVS at MIRO.

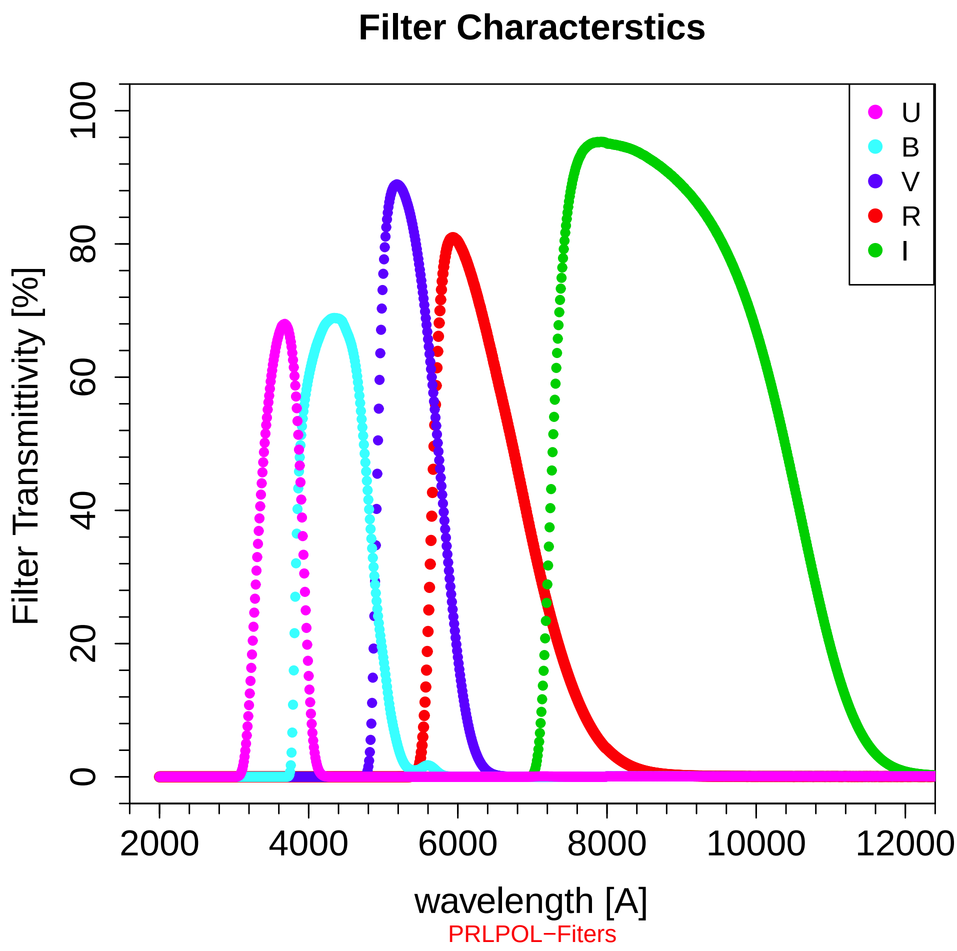

Figure B.3 Filter transmission curve for the filters (UBVRI) used in PRL made Optical Polarimeter (PRLPOL).

Bibliography

Abdo, A. A., Ackermann, M., Ajello, M., Baldini, L., et al. Radio-Loud Narrow-Line Seyfert 1 as a New Class of Gamma-Ray Active Galactic Nuclei. *ApJ* , 707:L142–L147, December 2009.

Abdo, A. A., Ackermann, M., Agudo, I., Ajello, M., et al. The Spectral Energy Distribution of Fermi Bright Blazars. *ApJ*, 716:30–70, June 2010a.

Abdo, A. A., Ackermann, M., Ajello, M., Allafort, A., et al. Fermi Large Area Telescope First Source Catalog. *ApJS*, 188:405–436, June 2010b.

Abdo, A. A., Ackermann, M., Ajello, M., Antolini, E., et al. Gamma-ray Light Curves and Variability of Bright Fermi-detected Blazars. *ApJ*, 722:520–542, October 2010c.

Abdo, A. A., Ackermann, M., Ajello, M., Axelsson, M., et al. A change in the optical polarization associated with a γ-ray flare in the blazar 3C279. *Nature*, 463:919–923, February 2010d.

Abramowicz, M. A. & Nobili, L. Are there black holes in quasars. *Nature*, 300:506, December 1982.

Ackermann, M., Ajello, M., Ballet, J., Barbiellini, G., et al. Multi-wavelength Observations of Blazar AO 0235+164 in the 2008-2009 Flaring State. *ApJ*, 751:159, June 2012.

Agudo, I., Jorstad, S. G., Marscher, A. P., Larionov, V. M., et al. Location of γ-ray Flare Emission in the Jet of the BL Lacertae Object OJ287 More than 14 pc from the Central Engine. *ApJ* , 726:L13, January 2011.

Andrews, P. J., Glass, I. S., & Hawarden, T. G. Photometry of AP Lib and PKS 0521-36. *MNRAS* , 168:7P–11P, July 1974.

Andruchow, I., Cellone, S. A., Romero, G. E., Dominici, T. P., & Abraham, Z. Microvariability in the optical polarization of 3C 279. *A&A* , 409:857–865, October 2003.

Andruchow, I., Romero, G. E., & Cellone, S. A. Polarization microvariability of BL Lacertae objects. *A&A* , 442:97–107, October 2005.

Andruchow, I., Cellone, S. A., & Romero, G. E. Incidence of the host galaxy on the measured optical linear polarization of blazars. *MNRAS* , 388:1766–1774, August 2008.

Angel, J. R. P. & Stockman, H. S. Optical and infrared polarization of active extragalactic objects. *ARA&A*, 18:321–361, 1980.

Antonucci, R. Polarization insights for active galactic nuclei. In Trujillo-Bueno, J., Moreno-Insertis, F., & Sánchez, F., editors, *Astrophysical Spectropolarimetry*, pages 151–175, 2002.

Antonucci, R. R. J. Deep radio maps of BL Lacertae and 3C 446. *ApJ*, 304: 634–636, May 1986.

Atwood, W. B., Bagagli, R., Baldini, L., Bellazzini, R., et al. Design and initial tests of the Tracker-converter of the Gamma-ray Large Area Space Telescope. *Astroparticle Physics*, 28:422–434, December 2007.

Atwood, W. B., Abdo, A. A., Ackermann, M., Althouse, W., et al. The Large Area Telescope on the Fermi Gamma-Ray Space Telescope Mission. *ApJ*, 697:1071–1102, June 2009.

Bach, U., Krichbaum, T. P., Ros, E., Britzen, S., Witzel, A., & Zensus, J. A. Is 0716+714 a superluminal blazar? In Ros, E., Porcas, R. W., Lobanov, A. P., & Zensus, J. A., editors, *Proceedings of the 6th EVN Symposium*, page 119, June 2002.

Bai, J. M., Xie, G. Z., Li, K. H., Zhang, X., & Liu, W. W. The intraday variability in the radio-selected and X-ray-selected BL Lacertae objects. *A&AS* , 132:83–92, October 1998.

Baliyan, K. S. Multiwavelength study of the variability in blazars. *Bulletin of the Astronomical Society of India*, 29:397–405, September 2001.

Baliyan, K. S., Joshi, U. C., & Deshpande, M. R. On the variability timescales and magnetic field in OJ 287. *Ap&SS*, 240:195–204, September 1996.

Baliyan, K. S., Ganesh, S., Joshi, U. C., Shah, C. R., Vadher, N. M., & Deshpande, M. R. Study of variability in BL Lac objects. *Bulletin of the Astronomical Society of India*, 29:421–424, September 2001.

Baliyan, K. S., Joshi, U. C., & Ganesh, S. Monitoring of AGNs for variability from MIRO. *Bulletin of the Astronomical Society of India*, 33:181, June 2005.

Ballard, K. R., Mead, A. R. G., Brand, P. W. J. L., & Hough, J. H. The optical and infrared emission of blazars. *MNRAS* , 243:640–655, April 1990.

Banfield, J. D. & Raftery, A. E. Model-Based Guassian and Non-Gaussian Clustering. *Biometrics*, 49:803–821, September 1993.

Barthelmy, S. D. Burst Alert Telescope (BAT) on the Swift MIDEX mission. In Flanagan, K. A. & Siegmund, O. H. W., editors, *Society of Photo-Optical Instrumentation Engineers (SPIE) Conference Series*, volume 5165 of *Society of Photo-Optical Instrumentation Engineers (SPIE) Conference Series*, pages 175–189, February 2004.

Beall, J. H. & Bednarek, W. On the Hadronic Beam Model for Gamma-Ray Production in Blazars. *ApJ*, 510:188–196, January 1999.

Begelman, M. C., Fabian, A. C., & Rees, M. J. Implications of very rapid TeV variability in blazars. *MNRAS* , 384:L19–L23, February 2008.

Berriman, G., Schmidt, G. D., West, S. C., & Stockman, H. S. An optical polarization survey of the Palomar-Green bright quasar sample. *ApJS*, 74: 869–883, December 1990.

Bertaud, C., Wlerick, G., Veron, P., Dumortier, B., et al. Etude photometrique de BL Lacertae. *A&A* , 24:357, 1973.

Bessell, M. S. UBVRI photometry. II - The Cousins VRI system, its temperature and absolute flux calibration, and relevance for two-dimensional photometry. *PASP*, 91:589–607, October 1979.

Bessell, M. S. UBVRI passbands. *PASP*, 102:1181–1199, October 1990.

Bessell, M. S. UBVRI Filters for CCD Photometry. *CCD Astronomy*, 2:20, 1995.

Bessell, M. S. & Brett, J. M. JHKLM photometry - Standard systems, passbands, and intrinsic colors. *PASP*, 100:1134–1151, September 1988.

Bjornsson, C.-I. Frequency-dependent polarization in blazars. *MNRAS* , 216: 241–253, September 1985.

Blandford, R. D. & Königl, A. Relativistic jets as compact radio sources. *ApJ*, 232:34–48, August 1979a.

Blandford, R. D. & Königl, A. Relativistic jets as compact radio sources. *ApJ*, 232:34–48, August 1979b.

Blandford, R. D. & Levinson, A. Pair cascades in extragalactic jets. 1: Gamma rays. *ApJ*, 441:79–95, March 1995.

Blandford, R. D. & Rees, M. J. Extended and compact extragalactic radio sources - Interpretation and theory. *Phys. Scr*, 17:265–274, March 1978.

Blandford, R. D. & Rees, M. J. The standard model and some new directions. In Holt, S. S., Neff, S. G., & Urry, C. M., editors, *American Institute of Physics Conference Series*, volume 254 of *American Institute of Physics Conference Series*, pages 3–19, 1992.

Blanton, M. R. & Roweis, S. K-Corrections and Filter Transformations in the Ultraviolet, Optical, and Near-Infrared. *AJ*, 133:734–754, February 2007.

Błażejowski, M., Sikora, M., Moderski, R., & Madejski, G. M. Comptonization of Infrared Radiation from Hot Dust by Relativistic Jets in Quasars. *ApJ*, 545:107–116, December 2000.

Bloom, S. D. & Marscher, A. P. An Analysis of the Synchrotron Self-Compton Model for the Multi–Wave Band Spectra of Blazars. *ApJ*, 461:657, April 1996.

Bonning, E., Urry, C. M., Bailyn, C., Buxton, M., et al. SMARTS Optical and Infrared Monitoring of 12 Gamma-Ray Bright Blazars. *ApJ*, 756:13, September 2012.

Böttcher, M. A Hadronic Synchrotron Mirror Model for the "Orphan" TeV Flare in 1ES 1959+650. *ApJ*, 621:176–180, March 2005.

Böttcher, M. Modeling the emission processes in blazars. *Ap&SS*, 309:95–104, June 2007.

Böttcher, M., Marscher, A. P., Ravasio, M., Villata, M., et al. Coordinated Multiwavelength Observations of BL Lacertae in 2000. *ApJ*, 596:847–859, October 2003.

Bridle, A. H. & Perley, R. A. Extragalactic Radio Jets. *ARA&A*, 22:319–358, 1984.

Brindle, C. The internight variability of the optical to near-infrared flux density and polarization of the blazars 0215+015 and 0851+202 during outbursts. *MNRAS* , 282:788–796, October 1996.

Brindle, C., Hough, J. H., Bailey, J. A., Axon, D. J., & Hyland, A. R. Simultaneous optical and infrared polarization measurements of blazars. *MNRAS* , 221:739–768, August 1986.

Burrows, D. N., Hill, J. E., Nousek, J. A., Kennea, J. A., et al. The Swift X-Ray Telescope. *Space Sci. Rev.*, 120:165–195, October 2005.

Camenzind, M. & Krockenberger, M. The lighthouse effect of relativistic jets in blazars - A geometric origin of intraday variability. *A&A* , 255:59–62, February 1992.

Cappi, M., Comastri, A., Molendi, S., Palumbo, G. G. C., Della Ceca, R., & Maccacaro, T. The variable ROSAT X-ray spectrum of the BL Lac 0716+714. *MNRAS* , 271:438–448, November 1994.

Cardelli, J. A., Clayton, G. C., & Mathis, J. S. The relationship between infrared, optical, and ultraviolet extinction. *ApJ*, 345:245–256, October 1989.

Carini, M. T., Miller, H. R., & Goodrich, B. D. The timescales of the optical variability of blazars. I - OQ 530. *AJ*, 100:347–355, August 1990.

Carini, M. T., Walters, R., & Hopper, L. Multicolor Optical Microvariability in S5 0716+714. *AJ*, 141:49, February 2011.

Cellone, S. A., Romero, G. E., & Combi, J. A. The Incidence of the Host Galaxy in Microvariability Observations of Quasars. *AJ*, 119:1534–1541, April 2000.

Celotti, A. & Ghisellini, G. The power of blazar jets. *MNRAS* , 385:283–300, March 2008.

Chakrabarti, S. K. & Wiita, P. J. Spiral shocks in accretion disks as a contributor to variability in active galactic nuclei. *ApJ*, 411:602–609, July 1993.

Chandra, S., Baliyan, K. S., Ganesh, S., & Joshi, U. C. Rapid Optical Variability in Blazar S5 0716+71 During 2010 March. *ApJ*, 731:118, April 2011a.

Chandra, S., Baliyan, K. S., Ganesh, S., Joshi, U. C., & Foschini, L. Fast optical variability in blazar S5 0716+714. In *Astronomical Society of India Conference Series*, volume 3 of *Astronomical Society of India Conference Series*, page 152, 2011b.

Chandra, S., Baliyan, K. S., Ganesh, S., & Joshi, U. C. Optical Polarimetry of the Blazar CGRaBS J0211+1051 from Mount Abu Infrared Observatory. *ApJ*, 746:92, February 2012.

Chang, K. & Refsdal, S. Flux variations of QSO 0957+561 A, B and image splitting by stars near the light path. *Nature*, 282:561–564, December 1979.

Chatterjee, R. *Multi-frequency time variability of active galactic nuclei*. PhD thesis, Boston University, 2010.

Chatterjee, R., Jorstad, S. G., Marscher, A. P., Oh, H., et al. Correlated Multi-Wave Band Variability in the Blazar 3C 279 from 1996 to 2007. *ApJ*, 689:79–94, December 2008.

Chatterjee, R., Bailyn, C. D., Bonning, E. W., Buxton, M., et al. Similarity of the Optical-Infrared and γ-Ray Time Variability of Fermi Blazars. *ApJ*, 749:191, April 2012.

Cortina, J. MAGIC detects very high energy gamma-ray emission from the FSRQ PKS 1510-089. *The Astronomer's Telegram*, 3965:1, March 2012.

Courvoisier, T. J.-L., Blecha, A., Bouchet, P., Bratschi, P., et al. Multiwavelength monitoring of the BL Lacertae object PKS 2155-304. 3: Ground-based observations in 1991 November. *ApJ*, 438:108–119, January 1995.

Dai, B. Z., Li, X. H., Liu, Z. M., Zhang, B. K., et al. The long-term multiband optical observations and colour index for the quasar 3C 273. *MNRAS* , 392: 1181–1192, January 2009.

Dai, Y., Wu, J., Zhu, Z.-H., Zhou, X., et al. Seven-year Multi-color Optical Monitoring of BL Lacertae Object S5 0716+714. *ApJS*, 204:22, February 2013.

D'Ammando, F. Fermi LAT detection of a gamma-ray flare from CGRaBS J0211+1051. *The Astronomer's Telegram*, 3120:1, January 2011.

D'Ammando, F., Pucella, G., Raiteri, C. M., Villata, M., et al. AGILE detection of a rapid γ-ray flare from the blazar PKS 1510-089 during the GASP-WEBT monitoring. *A&A* , 508:181–189, December 2009.

D'Ammando, F., Raiteri, C. M., Villata, M., Romano, P., et al. AGILE detection of extreme γ-ray activity from the blazar PKS 1510-089 during March 2009. Multifrequency analysis. *A&A* , 529:A145, May 2011a.

D'Ammando, F., Sokolovsky, K. V., & Hoversten, E. Swift follow-up of the gamma-ray flaring BL Lac CGRaBS J0211+1051. *The Astronomer's Telegram*, 3129:1, January 2011b.

D'Arcangelo, F. D., Marscher, A. P., Jorstad, S. G., Smith, P. S., et al. Correlated Multiwavelength Polarization in Blazar Cores. In *American Astronomical Society Meeting Abstracts #213*, volume 41 of *Bulletin of the American Astronomical Society*, page 326.01, January 2009.

de Bruyn, A. G. WSRT Observations of Hourly Flux Variations in OJ287 at 6 CM Wavelength. In Reid, M. J. & Moran, J. M., editors, *The Impact of VLBI on Astrophysics and Geophysics*, volume 129 of *IAU Symposium*, page 97, 1988.

Dent, W. A. Variation in the Radio Emission of 3C273 and Other Quasi-Stellar Sources. *AJ*, 70:672, November 1965.

Dermer, C. D. & Schlickeiser, R. Model for the High-Energy Emission from Blazars. *ApJ*, 416:458, October 1993.

Dermer, C. D., Schlickeiser, R., & Mastichiadis, A. High-energy gamma radiation from extragalactic radio sources. *A&A* , 256:L27–L30, March 1992.

Dermer, C. D., Sturner, S. J., & Schlickeiser, R. Nonthermal Compton and Synchrotron Processes in the Jets of Active Galactic Nuclei. *ApJS*, 109:103, March 1997.

Deshpande, M. R., Joshi, U. C., Kulshrestha, A. K., Banshidhar, & Vadher, N. M. An astronomical polarimeter. *Bulletin of the Astronomical Society of India*, 13:157–161, June 1985.

Djorgovski, S. G., Drake, A. J., Mahabal, A. A., Graham, M. J., et al. CRTS Observations of the Gamma-Ray Flaring Blazar CGRaBS J0211+1051. *The Astronomer's Telegram*, 3133:1, January 2011.

Dominici, T. P., Abraham, Z., Pereyra, A., & Magalhães, A. M. Characterization of the optical polarimetric variability in a sample of blazars. In Storchi-Bergmann, T., Ho, L. C., & Schmitt, H. R., editors, *The Interplay Among Black Holes, Stars and ISM in Galactic Nuclei*, volume 222 of *IAU Symposium*, pages 89–90, November 2004.

Dreher, J. W., Roberts, D. H., & Lehar, J. Very large array observations of rapid non-periodic variations in OJ 287. *Nature*, 320:239–242, March 1986.

Dussault, D. & Hoess, P. Noise performance comparison of ICCD with CCD and EMCCD cameras. In Dereniak, E. L., Sampson, R. E., & Johnson, C. B., editors, *Society of Photo-Optical Instrumentation Engineers (SPIE) Conference Series*, volume 5563 of *Society of Photo-Optical Instrumentation Engineers (SPIE) Conference Series*, pages 195–204, October 2004.

Efanov, V. A., Moiseev, I. G., Nesterov, N. S., & Shakhovskoi, N. M. Rapid fluctuations of radio flux and polarisation in quasar 3C273. *Nature*, 269:493, October 1977.

Epstein, E. E., Fogarty, W. G., Hackney, K. R., Hackney, R. L., et al. 3C 120, BL Lacertae, and OJ 287: Coordinated Optical, Infrared, and Radio Observations of Intraday Variability. *ApJ* , 178:L51, December 1972.

Fan, J. H., Cheng, K. S., Zhang, L., & Liu, C. H. Polarization and beaming effect for BL Lacertae objects. *A&A* , 327:947–951, November 1997.

Fan, J. H., Lin, R. G., Xie, G. Z., Zhang, L., et al. Optical periodicity analysis for radio selected BL Lacertae objects (RBLs). *A&A* , 381:1–5, January 2002.

Fan, J.-H., Tao, J., Qian, B.-C., Liu, Y., et al. Rapid variability in S5 0716+714. *Research in Astronomy and Astrophysics*, 11:1311–1316, November 2011.

Fanaroff, B. L. & Riley, J. M. The morphology of extragalactic radio sources of high and low luminosity. *MNRAS* , 167:31P–36P, May 1974.

Flix, J. & MAGIC Collaboration. The MAGIC Cherenkov Telescope for Gamma-Ray Astronomy. In Prada, F., Martinez Delgado, D., & Mahoney, T. J., editors, *Satellites and Tidal Streams*, volume 327 of *Astronomical Society of the Pacific Conference Series*, page 52, December 2004.

Foschini, L. Accretion and jet power in active galactic nuclei. *Research in Astronomy and Astrophysics*, 11:1266–1278, November 2011.

Foschini, L., Tagliaferri, G., Pian, E., Ghisellini, G., et al. Simultaneous X-ray and optical observations of S5 0716+714 after the outburst of March 2004. *A&A* , 455:871–877, September 2006.

Foschini, L., Maraschi, L., Tavecchio, F., Ghisellini, G., Gliozzi, M., & Sambruna, R. M. Blazar nuclei in radio-loud narrow-line Seyfert 1? *Advances in Space Research*, 43:889–894, March 2009.

Foschini, L., Tagliaferri, G., Ghisellini, G., Ghirlanda, G., Tavecchio, F., & Bonnoli, G. Does the gamma-ray flux of the blazar 3C454.3 vary on subhour time-scales? *MNRAS* , 408:448–451, October 2010.

Foschini, L., Ghisellini, G., Kovalev, Y. Y., Lister, M. L., et al. The first gamma-ray outburst of a narrow-line Seyfert 1 galaxy: the case of PMN J0948+0022 in 2010 July. *MNRAS* , 413:1671–1677, May 2011a.

Foschini, L., Ghisellini, G., Kovalev, Y. Y., Lister, M. L., et al. The first gamma-ray outburst of a narrow-line Seyfert 1 galaxy: the case of PMN J0948+0022 in 2010 July. *MNRAS* , 413:1671–1677, May 2011b.

Foschini, L., Ghisellini, G., Tavecchio, F., Bonnoli, G., & Stamerra, A. Search for the shortest variability at gamma rays in flat-spectrum radio quasars. *A&A* , 530:A77, June 2011c.

Fossati, G., Maraschi, L., Celotti, A., Comastri, A., & Ghisellini, G. A unifying view of the spectral energy distributions of blazars. *MNRAS* , 299:433–448, September 1998.

Frank, J., King, A., & Raine, D. J. *Accretion Power in Astrophysics: Third Edition*. January 2002.

Frecker, J. E. & Serkowski, K. Linear polarimeter with rapid modulation, achromatic in the 0.3-1.1-micron range. *Appl. Opt.*, 15:605, March 1976.

Gabuzda, D. C., Wardle, J. F. C., & Roberts, D. H. Linear polarization structure of the BL Lacertae object 0735+178 at milliarcsecond resolution. *ApJ*, 338:743–751, March 1989.

Gabuzda, D. C., Kovalev, Y. Y., Krichbaum, T. P., Alef, W., et al. VLBI polarization observations of the rapidly variable BL Lacertae object BL 0716+714. *A&A* , 333:445–451, May 1998.

Gabuzda, D. C., Kochenov, P. Y., & Cawthorne, T. V. Serendipitous VLBI observations of polarization intraday variability in three BL Lacertae objects. *MNRAS* , 319:1125–1135, December 2000a.

Gabuzda, D. C., Kochenov, P. Y., Cawthorne, T. V., & Kollgaard, R. I. Intraday polarization variability outside the VLBI core of the active galactic nucleus 0716+714. *MNRAS* , 313:627–636, April 2000b.

Gabuzda, D. C., Rastorgueva, E. A., Smith, P. S., & O'Sullivan, S. P. Evidence for cospatial optical and radio polarized emission in active galactic nuclei. *MNRAS* , 369:1596–1602, July 2006.

Ganesh, S., Joshi, U. C., Baliyan, K. S., Mathur, S. N., Patwal, P. S., & Shah, R. R. Automation of PRL's Astronomical Optical Polarimeter with a GNU/Linux based distributed control system. *ArXiv e-prints*, December 2009.

Georganopoulos, M. & Kazanas, D. Decelerating Flows in TeV Blazars: A Resolution to the BL Lacertae-FR I Unification Problem. *ApJ* , 594:L27–L30, September 2003a.

Georganopoulos, M. & Kazanas, D. Relativistic and Slowing Down: The Flow in the Hot Spots of Powerful Radio Galaxies and Quasars. *ApJ* , 589:L5–L8, May 2003b.

Ghisellini, G. & Madau, P. On the origin of the gamma-ray emission in blazars. *MNRAS* , 280:67–76, May 1996.

Ghisellini, G. & Tavecchio, F. The blazar sequence: a new perspective. *MNRAS* , 387:1669–1680, July 2008.

Ghisellini, G. & Tavecchio, F. Canonical high-power blazars. *MNRAS* , 397:985–1002, August 2009.

Ghisellini, G., Maraschi, L., & Treves, A. Inhomogeneous synchrotron-self-Compton models and the problem of relativistic beaming of BL Lac objects. *A&A* , 146:204–212, May 1985.

Ghisellini, G., Celotti, A., Fossati, G., Maraschi, L., & Comastri, A. A theoretical unifying scheme for gamma-ray bright blazars. *MNRAS* , 301:451–468, December 1998.

Ghisellini, G., Tagliaferri, G., Foschini, L., Ghirlanda, G., et al. High-redshift Fermi blazars. *MNRAS* , 411:901–914, February 2011.

Gierliński, M., Middleton, M., Ward, M., & Done, C. A periodicity of ˜1hour in X-ray emission from the active galaxy RE J1034+396. *Nature*, 455:369–371, September 2008.

Giltinan, A., Loughnan, D., Collins, A., & Smith, N. Using EMCCD's to improve the photometric precision of ground-based astronomical observations. *Journal of Physics Conference Series*, 307(1):012010, August 2011.

Giommi, P., Barr, P., Pollock, A. M. T., Garilli, B., & Maccagni, D. A study of BL Lacertae-type objects with Exosat. I - Flux correlations, luminosity variability, and spectral variability. *ApJ*, 356:432–455, June 1990.

Goodrich, R. W. Spectropolarimetry of 'narrow-line' Seyfert 1 galaxies. *ApJ*, 342:224–234, July 1989.

Gopal-Krishna & Subramanian, K. Gravitational micro-lensing of the relativistic jets of quasars. *Nature*, 349:766–768, February 1991.

Gopal-Krishna & Wiita, P. J. Swinging jets and the variability of active galactic nuclei. *A&A* , 259:109–117, June 1992.

Gorbovskoy, E., Balanutsa, P., Lipunov, V., Kornilov, V., et al. MASTER discovery of the 12% optical polarization of the gamma-ray flaring BL Lac CGRaBS J0211+1051. *The Astronomer's Telegram*, 3134:1, January 2011.

Grauer, A. D. Evidence for rapid optical variations of the quasi-stellar radio source 4C 29.45. *ApJ*, 277:77–81, February 1984.

Greiner, J., Bornemann, W., Clemens, C., Deuter, M., et al. GROND—a 7-Channel Imager. *PASP*, 120:405–424, April 2008.

Grove, J. E., Johnson, W. N., Strickman, M. S., Fewtrell, Z., Chekhtman, A., & Piron, F. The Calorimeter for the GLAST Large Area Telescope. In Ritz, S., Michelson, P., & Meegan, C. A., editors, *The First GLAST Symposium*, volume 921 of *American Institute of Physics Conference Series*, pages 550–551, July 2007.

Gupta, A. C., Cha, S.-M., Lee, S., Jin, H., et al. Multicolor Near-Infrared Intra-Day and Short-Term Variability of the Blazar S5 0716+714. *AJ*, 136: 2359–2366, December 2008.

Hackney, R. L., Hackney, K. R., Smith, A. G., Folsom, G. H., et al. Optical and Radio Flares in BL Lacerta (VRO 42.22.01). *Astrophys. Lett.*, 12:147, September 1972.

Hagen-Thorn, V. A., Larionov, V. M., Jorstad, S. G., Arkharov, A. A., et al. The Outburst of the Blazar AO 0235+164 in 2006 December: Shock-in-Jet Interpretation. *ApJ*, 672:40–47, January 2008.

Hartman, R. C. CGRO Observations of BL Lac Objects and Other Blazars. In Takalo, L. O. & Sillanpää, A., editors, *BL Lac Phenomenon*, volume 159 of *Astronomical Society of the Pacific Conference Series*, page 199, 1999.

Hartman, R. C., Bertsch, D. L., Dingus, B. L., Fichtel, C. E., et al. EGRET detection of high-energy gamma radiation from the OVV quasar 3C 454.3. *ApJ* , 407:L41–L44, April 1993.

Harvey, G. A., Andrew, B. H., Macleod, J. M., & Medd, W. K. A Search for Rapidly Varying Radio Sources. *Astrophys. Lett.*, 11:147, May 1972.

Healey, S. E., Romani, R. W., Taylor, G. B., Sadler, E. M., et al. CRATES: An All-Sky Survey of Flat-Spectrum Radio Sources. *ApJS*, 171:61–71, July 2007.

Healey, S. E., Romani, R. W., Cotter, G., Michelson, P. F., et al. CGRaBS: An All-Sky Survey of Gamma-Ray Blazar Candidates. *ApJS*, 175:97–104, March 2008.

Heckman, T. M., Miley, G. K., van Breugel, W. J. M., & Butcher, H. R. Narrow-Line Profiles in Active Nuclei. In *Bulletin of the American Astronomical Society*, volume 12 of *Bulletin of the American Astronomical Society*, page 809, September 1980.

Heeschen, D. S. & Rickett, B. J. The Galactic latitude dependence of centimeter-wavelength flicker. *AJ*, 93:589–591, March 1987.

Heidt, J. & Nilsson, K. Polarimetry of optically selected BL Lacertae candidates from the SDSS. *A&A* , 529:A162, May 2011.

Heidt, J. & Wagner, S. J. Statistics of optical intraday variability in a complete sample of radio-selected BL Lacertae objects. *A&A* , 305:42, January 1996.

Hoffmeister, C., Richter, G., Wenzel, W., Dunlop, S., & Andrews, A. D. Book-Review - Variable Stars. *Irish Astronomical Journal*, 20:306, September 1992.

Holmes, P. A., Brand, P. W. J. L., Impey, C. D., Williams, P. M., et al. A polarization flare in OJ 287. *MNRAS* , 211:497–506, December 1984.

Hovatta, T., Nieppola, E., Tornikoski, M., Valtaoja, E., Aller, M. F., & Aller, H. D. Long-term radio variability of AGN: flare characteristics. *A&A* , 485: 51–61, July 2008.

Howell, S. B. *Handbook of CCD Astronomy*. March 2006.

Howell, S. B., Warnock, III, A., & Mitchell, K. J. Statistical error analysis in CCD time-resolved photometry with applications to variable stars and quasars. *AJ*, 95:247–256, January 1988.

Hughes, P. A. *Beams and jets in astrophysics*. 1991.

Hughes, P. A., Aller, H. D., & Aller, M. F. Synchrotron emission from shocked relativistic jets. I - The theory of radio-wavelength variability and its relation to superluminal motion. *ApJ*, 341:54–79, June 1989.

Hughes, P. A., Aller, M. F., & Aller, H. D. Oblique Shocks as the Origin of Radio to Gamma-ray Variability in Active Galactic Nuclei. *ApJ*, 735:81, July 2011.

Hunter, S. D., Bertsch, D. L., Dingus, B. L., Fichtel, C. E., et al. Detection of high-energy gamma rays from quasar PKS 0528 + 134 by EGRET on the Compton Gamma Ray Observatory. *ApJ*, 409:134–138, May 1993.

Ikejiri, Y., Uemura, M., Sasada, M., Sakimoto, K., et al. Photopolarimetric monitoring of 41 blazars in the optical and near-infrared bands with the Kanata telescope. *ArXiv e-prints*, December 2009.

Impey, C. D., Malkan, M. A., & Tapia, S. The miniblazar in 3C 273. *ApJ*, 347:96–111, December 1989.

Impey, C. D., Bychkov, V., Tapia, S., Gnedin, Y., & Pustilnik, S. Rapid Polarization Variability in the BL Lacertae Object S5 0716+714. *AJ*, 119: 1542–1561, April 2000.

Jang, M. & Miller, H. R. The Microvariability of Selected Radio-Quiet and Radio-Loud QSOs. *AJ*, 114:565–574, August 1997.

Jannuzi, B. T., Green, R. F., & French, H. An optical polarization survey for BL Lacertae objects and highly polarized quasars. *ApJ*, 404:100–111, February 1993.

Jorstad, S. G. & Marscher, A. P. Connection Between Parsec-Scale Jet Properties and Gamma-Ray Emission of Blazars. In Peterson, B. M., Pogge, R. W., & Polidan, R. S., editors, *Probing the Physics of Active Galactic Nuclei*, volume 224 of *Astronomical Society of the Pacific Conference Series*, page 255, 2001.

Jorstad, S. G., Marscher, A. P., Smith, P. S., Larionov, V. M., et al. A Tight Connection between Gamma-Ray Outbursts and Parsec-scale Jet Activity in the Quasar 3C 454.3. *ApJ*, 773:147, August 2013.

Joshi, M. & Boettcher, M. Time-dependent Radiation Transfer in the Internal Shock Model for Blazars Jets. In *American Astronomical Society Meeting Abstracts*, volume 39 of *Bulletin of the American Astronomical Society*, page 784, December 2007.

Joshi, U. C., Deshpande, M. R., Sen, A. K., & Kulshrestha, A. Polarization investigations in four peculiar supergiants with high IR excess. *A&A* , 181: 31–33, July 1987.

Kalberla, P. M. W., Burton, W. B., Hartmann, D., Arnal, E. M., et al. The Leiden/Argentine/Bonn (LAB) Survey of Galactic HI. Final data release of the combined LDS and IAR surveys with improved stray-radiation corrections. *A&A* , 440:775–782, September 2005.

Kataoka, J., Takahashi, T., Wagner, S. J., Iyomoto, N., et al. Characteristic X-Ray Variability of TeV Blazars: Probing the Link between the Jet and the Central Engine. *ApJ*, 560:659–674, October 2001.

Kellermann, K. I. Detection of a Strong and Possibly Variable Compact Millimeter Wave Component in Centaurus a. *ApJ* , 194:L135–L137, December 1974.

Kerrick, A. D., Akerlof, C. W., Biller, S. D., Buckley, J. H., et al. Outburst of TeV photons from Markarian 421. *ApJ* , 438:L59–L62, January 1995.

Kesteven, M. J. L., Bridle, A. H., & Brandie, G. W. Variability of extragalactic sources at 2.7 GHz. I - Results of a 2-yr monitoring program. *AJ*, 81:919–932, November 1976.

Khachikian, E. Y. & Weedman, D. W. An atlas of Seyfert galaxies. *ApJ*, 192: 581–589, September 1974.

Kikuchi, S., Tabara, H., Mikami, Y., Kawano, N., et al. Simultaneous Radio and Optical Observations of OJ 287. *PASJ*, 25:555, 1973.

Kinman, T. D. & Conklin, E. K. Observations of OJ 287 at Optical and Millimeter Wavelengths. *Astrophys. Lett.*, 9:147–149, August 1971.

Kniffen, D. A., Bertsch, D. L., Fichtel, C. E., Hartman, R. C., et al. Time variability in the gamma-ray emission of 3C 279. *ApJ*, 411:133–136, July 1993.

Kohnle, A. HESS - The High Energy Stereoscopic System. In *International Cosmic Ray Conference*, volume 5 of *International Cosmic Ray Conference*, page 239, 1999.

Kollgaard, R. I. Relativistic jets and the nature of BL Lacertae objects. *Vistas in Astronomy*, 38:29–75, 1994.

Komossa, S., Voges, W., Xu, D., Mathur, S., et al. Radio-loud Narrow-Line Type 1 Quasars. *AJ*, 132:531–545, August 2006.

Konigl, A. Relativistic jets as X-ray and gamma-ray sources. *ApJ*, 243:700–709, February 1981.

Koul, R., Bhat, C. L., Tickoo, A. K., Kaul, I. K., et al. Detector instrumentation and drive system for TACTIC gamma-ray telescope. *Bulletin of the Astronomical Society of India*, 21:503–506, September 1993.

Kudelina, I., Gorbovskoy, E., Balanutsa, P., Lipunov, V., et al. MASTER serendipitous observations of the gamma-ray flaring BL Lac CGRaBS J0211+1051. *The Astronomer's Telegram*, 3131:1, January 2011.

Kuehr, H., Pauliny-Toth, I. I. K., Witzel, A., & Schmidt, J. The 5-GHz strong source surveys. V - Survey of the area between declinations 70 and 90 deg. *AJ*, 86:854–863, June 1981.

Kuehr, H., Johnston, K. J., Odenwald, S., & Adlhoch, J. Optical identifications and radio morphology of the complete 5 GHz S5 survey. *A&AS* , 71:493–523, December 1987.

Kulshrestha, A., Deshpande, M. R., & Joshi, U. C. The optical polarization properties of blazars. *A&AS* , 71:565–568, December 1987.

Lähteenmäki, A. & Valtaoja, E. Testing of Inverse Compton Models for Active Galactic Nuclei with Gamma-Ray and Radio Observations. *ApJ*, 590:95–108, June 2003.

Larionov, V. M., Jorstad, S. G., Marscher, A. P., Raiteri, C. M., et al. Results of WEBT, VLBA and RXTE monitoring of 3C 279 during 2006-2007. *A&A* , 492:389–400, December 2008.

Larionov, V. M., Jorstad, S. G., Marscher, A. P., Morozova, D. A., et al. The Outburst of the Blazar S5 0716+71 in 2011 October: Shock in a Helical Jet. *ApJ*, 768:40, May 2013.

Lawrence, C. R., Bennett, C. L., Hewitt, J. N., Langston, G. I., et al. 5 GHz radio structure and optical identifications of sources from the MG survey. II - Maps and finding charts. *ApJS*, 61:105–157, May 1986.

Learned, J. G. & Mannheim, K. High-Energy Neutrino Astrophysics. *Annual Review of Nuclear and Particle Science*, 50:679–749, 2000.

Lister, M. L., Cohen, M. H., Homan, D. C., Kadler, M., et al. MOJAVE: Monitoring of Jets in Active Galactic Nuclei with VLBA Experiments. VI. Kinematics Analysis of a Complete Sample of Blazar Jets. *AJ*, 138:1874–1892, December 2009.

Longair, M. S. *High energy astrophysics. Volume 2. Stars, the Galaxy and the interstellar medium.* 1994.

MacLeod, J. M., Andrew, B. H., Medd, W. J., & Olsen, E. T. Comprehensive Observations of the Rapidly Varying Radio Source VRO 42.22.01 (BL Lac). *Astrophys. Lett.*, 9:19, August 1971.

Maesano, M., Montagni, F., Massaro, E., & Nesci, R. BVRI photometry of BL Lacertae in 1993-1995. *A&AS* , 122:267–270, April 1997.

Mangalam, A. V. & Wiita, P. J. Accretion disk models for optical and ultraviolet microvariability in active galactic nuclei. *ApJ*, 406:420–429, April 1993.

Mannheim, K. & Biermann, P. L. Photomeson production in active galactic nuclei. *A&A* , 221:211–220, September 1989.

Mannucci, F., Basile, F., Poggianti, B. M., Cimatti, A., et al. Near-infrared template spectra of normal galaxies: k-corrections, galaxy models and stellar populations. *MNRAS* , 326:745–758, September 2001.

Maraschi, L., Treves, A., Tagliaferri, G., & Tanzi, E. G. Variability of the BL Lacertae objects PKS 2155 - 304 and OJ 287 in the far-ultraviolet. *ApJ*, 304:637–645, May 1986.

Maraschi, L., Ghisellini, G., & Celotti, A. A jet model for the gamma-ray emitting blazar 3C 279. *ApJ* , 397:L5–L9, September 1992.

Marscher, A. P. Spontaneous formation of knots in relativistic flows - A model for variability in compact synchrotron sources. *ApJ*, 239:296–304, July 1980.

Marscher, A. P. Variability of the Non-thermal Emission in the Jets of Blazars. In Miller, H. R., Webb, J. R., & Noble, J. C., editors, *Blazar Continuum Variability*, volume 110 of *Astronomical Society of the Pacific Conference Series*, page 248, 1996a.

Marscher, A. P. The Inner Jets of Blazars. In Hardee, P. E., Bridle, A. H., & Zensus, J. A., editors, *Energy Transport in Radio Galaxies and Quasars*, volume 100 of *Astronomical Society of the Pacific Conference Series*, page 45, 1996b.

Marscher, A. P. Frequency Stratification of the Nonthermal Emission in Blazars. *NASA STI/Recon Technical Report N*, 1:54791, January 2001.

Marscher, A. P. The Core of a Blazar Jet. In Rector, T. A. & De Young, D. S., editors, *Extragalactic Jets: Theory and Observation from Radio to Gamma Ray*, volume 386 of *Astronomical Society of the Pacific Conference Series*, page 437, June 2008.

Marscher, A. P. & Bloom, S. D. Hard gamma ray emission from blazars. In Shrader, C. R., Gehrels, N., & Dennis, B., editors, *NASA Conference Publication*, volume 3137 of *NASA Conference Publication*, pages 346–353, February 1992.

Marscher, A. P. & Gear, W. K. Models for high-frequency radio outbursts in extragalactic sources, with application to the early 1983 millimeter-to-infrared flare of 3C 273. *ApJ*, 298:114–127, November 1985a.

Marscher, A. P. & Gear, W. K. Models for high-frequency radio outbursts in extragalactic sources, with application to the early 1983 millimeter-to-infrared flare of 3C 273. *ApJ*, 298:114–127, November 1985b.

Marscher, A. P., Gear, W. K., & Travis, J. P. Variability of Nonthermal Continuum Emission in Blazars. In Valtaoja, E. & Valtonen, M., editors, *Variability of Blazars*, page 85, 1992.

Marscher, A. P., Jorstad, S. G., Gomez, J. L., McHardy, I. M., Krichbaum, T. P., & Agudo, I. Limit to the Positron Content of the Jet in 3C 120 from INTEGRAL and mm-Wave VLBI Observations. In *American Astronomical Society Meeting Abstracts*, volume 38 of *Bulletin of the American Astronomical Society*, page 239.05, December 2006.

Marscher, A. P., Jorstad, S. G., Larionov, V. M., Aller, M. F., et al. Probing the Inner Jet of the Quasar PKS 1510-089 with Multi-Waveband Monitoring During Strong Gamma-Ray Activity. *ApJ* , 710:L126–L131, February 2010.

Marshall, H. L., Carone, T. E., & Fruscione, A. Observations of PKS 2155-304 with the Extreme Ultraviolet Explorer. *ApJ* , 414:L53–L56, September 1993.

Mastichiadis, A. & Kirk, J. G. Models of Variability in Blazar Jets. *PASA*, 19:138–142, 2002.

Matthews, T. A. & Sandage, A. R. Optical Identification of 3c 48, 3c 196, and 3c 286 with Stellar Objects. *ApJ*, 138:30, July 1963.

Meisner, A. M. & Romani, R. W. Imaging Redshift Estimates for BL Lacertae Objects. *ApJ*, 712:14–25, March 2010.

Michelson, P. F., Bertsch, D. L., Brazier, K., Chiang, J., et al. EGRET upper limits to the high-energy gamma-ray emission from the millisecond pulsars in nearby globular clusters. *ApJ*, 435:218–224, November 1994.

Miller, H. R. B2 1101+38: a BL Lacertae object. *ApJ* , 201:L109–L111, November 1975.

Miller, H. R. The recent optical variability of 3C 446. *ApJ*, 244:426–428, March 1981.

Miller, H. R., Carini, M. T., & Goodrich, B. D. Detection of microvariability for BL Lacertae objects. *Nature*, 337:627–629, February 1989.

Miller, H. R., Ferrara, E. C., McFarland, J. P., Williams, A. M., Wilson, J. W., & Noble, J. C. Blazar Microvariability. In Peterson, B. M., Pogge, R. W., & Polidan, R. S., editors, *Probing the Physics of Active Galactic Nuclei*, volume 224 of *Astronomical Society of the Pacific Conference Series*, page 63, 2001.

Montagni, F., Maselli, A., Massaro, E., Nesci, R., Sclavi, S., & Maesano, M. The intra-night optical variability of the bright BL Lacertae object S5 0716+714. *A&A* , 451:435–442, May 2006.

Mücke, A. & Protheroe, R. J. A proton synchrotron blazar model for flaring in Markarian 501. *Astroparticle Physics*, 15:121–136, March 2001.

Mücke, A., Protheroe, R. J., Engel, R., Rachen, J. P., & Stanev, T. BL Lac objects in the synchrotron proton blazar model. *Astroparticle Physics*, 18: 593–613, March 2003.

Muecke, A. Proton energy loss in photohadronic interactions on the microwave nackground. In *International Cosmic Ray Conference*, volume 2 of *International Cosmic Ray Conference*, page 240, 1999.

Müecke, A. & Pohl, M. On the Contribution of Unresolved Blazars to the Extragalactic γ-ray Background. In Takalo, L. O. & Sillanpää, A., editors, *BL Lac Phenomenon*, volume 159 of *Astronomical Society of the Pacific Conference Series*, page 217, 1999.

Nalewajko, K. Dissipation efficiency of reconfinement shocks in relativistic jets. *MNRAS* , 420:L48–L52, February 2012.

Nalewajko, K. & Sikora, M. Reconfinement shocks in relativistic AGN jets. In Aharonian, F. A., Hofmann, W., & Rieger, F., editors, *American Institute of Physics Conference Series*, volume 1085 of *American Institute of Physics Conference Series*, pages 483–485, December 2008.

Nalewajko, K. & Sikora, M. Polarization of Synchrotron Emission from Relativistic Reconfinement Shocks. In Maraschi, L., Ghisellini, G., Della Ceca, R., & Tavecchio, F., editors, *Accretion and Ejection in AGN: a Global View*, volume 427 of *Astronomical Society of the Pacific Conference Series*, page 205, October 2010.

Nalewajko, K., Giannios, D., Begelman, M. C., Uzdensky, D. A., & Sikora, M. Radiative properties of reconnection-powered minijets in blazars. *MNRAS* , 413:333–346, May 2011.

Nesci, R. Optical follow-up of 1FGL J0211.2+1049. *The Astronomer's Telegram*, 3127:1, January 2011.

Nesci, R., Massaro, E., & Montagni, F. Intraday Optical Variability of S5 0716+714. *PASA*, 19:143–146, 2002.

Nesci, R., Sclavi, S., Maesano, M., Massaro, E., Dolci, M., & D'Alessio, F. Simultaneous optical-NIR observations of four BL Lacertae objects. *Mem. Soc. Astron. Italiana*, 74:169, 2003.

Nesci, R., Massaro, E., Rossi, C., Sclavi, S., Maesano, M., & Montagni, F. The Long-Term Optical Variability of the BL Lacertae Object S5 0716+714: Evidence for a Precessing Jet. *AJ*, 130:1466–1471, October 2005a.

Nesci, R., Massaro, E., Rossi, C., Sclavi, S., Maesano, M., & Montagni, F. The Long-Term Optical Variability of the BL Lacertae Object S5 0716+714: Evidence for a Precessing Jet. *AJ*, 130:1466–1471, October 2005b.

Nilsson, K., Charles, P. A., Pursimo, T., Takalo, L. O., Sillanpaeae, A., & Teerikorpi, P. The complex environment of AO 0235+164. *A&A* , 314: 754–762, October 1996.

Nilsson, K., Pursimo, T., Sillanpää, A., Takalo, L. O., & Lindfors, E. Detection of the host galaxy of S5 0716+714. *A&A* , 487:L29–L32, August 2008.

Oke, J. B. Spectrophotometric Observations of Rapid Variability in 3c 279 and 3c 446. *ApJ*, 147:901, March 1967.

Orienti, M., Venturi, T., Dallacasa, D., D'Ammando, F., et al. Multi-epoch parsec-scale observations of the blazar PKS 1510-089. *MNRAS* , 417:359–369, October 2011.

Orienti, M., Koyama, S., D'Ammando, F., Giroletti, M., et al. Radio and γ-ray follow-up of the exceptionally high-activity state of PKS 1510-089 in 2011. *MNRAS* , 428:2418–2429, January 2013.

Osterbrock, D. E. & Pogge, R. W. The spectra of narrow-line Seyfert 1 galaxies. *ApJ*, 297:166–176, October 1985.

Papadakis, I. E., Villata, M., & Raiteri, C. M. The long-term optical spectral variability of BL Lacertae. *A&A* , 470:857–863, August 2007.

Peterson, B. M. *An Introduction to Active Galactic Nuclei.* February 1997.

Pian, E. X-ray Variability of Blazars. *PASA*, 19:49–54, 2002.

Pihajoki, P., Valtonen, M., Zola, S., Liakos, A., et al. Precursor Flares in OJ 287. *ApJ*, 764:5, February 2013.

Planck Collaboration, Ade, P. A. R., Aghanim, N., Arnaud, M., et al. Planck early results. I. The Planck mission. *A&A* , 536:A1, December 2011a.

Planck Collaboration, Ade, P. A. R., Aghanim, N., Arnaud, M., et al. Planck early results. VII. The Early Release Compact Source Catalogue. *A&A* , 536:A7, December 2011b.

Pogge, R. W., Garnavich, P., & Pedani, M. Supernova 2011ay in NGC 2315 = PSN J07023406+5035250. *Central Bureau Electronic Telegrams*, 2678:2, March 2011.

Pollock, J. T., Webb, J. R., & Azarnia, G. Simultaneous Microvariability Observations of 0716+71. *AJ*, 133:487–488, February 2007.

Poole, T. S., Breeveld, A. A., Page, M. J., Landsman, W., et al. Photometric calibration of the Swift ultraviolet/optical telescope. *MNRAS* , 383:627–645, January 2008.

Poon, H., Fan, J. H., & Fu, J. N. The Optical Microvariability and Spectral Changes of the BL Lacertae Object S5 0716+714. *ApJS*, 185:511–525, December 2009.

Pucella, G., Vittorini, V., D'Ammando, F., Tavani, M., et al. AGILE detection of intense gamma-ray emission from the blazar PKS 1510-089. *A&A* , 491: L21–L24, November 2008.

Pushkarev, A. B., Kovalev, Y. Y., & Lister, M. L. Radio/Gamma-ray Time Delay in the Parsec-scale Cores of Active Galactic Nuclei. *ApJ* , 722:L7–L11, October 2010.

Qian, S. J., Quirrenbach, A., Witzel, A., Krichbaum, T. P., Hummel, C. A., & Zensus, J. A. A model for the rapid radio variability in the quasar 0917 + 624. *A&A* , 241:15–21, January 1991.

Quirrenbach, A., Witzel, A., Wagner, S., Sanchez-Pons, F., et al. Correlated radio and optical variability in the BL Lacertae object 0716 + 714. *ApJ* , 372:L71–L74, May 1991.

Quirrenbach, A., Kraus, A., Witzel, A., Zensus, J. A., et al. Intraday variability in compact extragalactic radio sources. I. VLA observations. *A&AS* , 141: 221–256, January 2000.

R Development Core Team. *R: A Language and Environment for Statistical Computing*. R Foundation for Statistical Computing, Vienna, Austria, 2008. URL `http://www.R-project.org`. ISBN 3-900051-07-0.

Racine, R. Photometry of BL Lacertae with a Time Resolution of 15 Seconds. *ApJ* , 159:L99, February 1970.

Raiteri, C. M., Villata, M., Lanteri, L., Cavallone, M., & Sobrito, G. BVR photometry of comparison stars in selected blazar fields. II. Photometric sequences for 9 quasars. *A&AS* , 130:495–500, June 1998.

Raiteri, C. M., Villata, M., Tosti, G., Nesci, R., et al. Optical and radio behaviour of the BL Lacertae object ¡ASTROBJ¿0716+714¡/ASTROBJ¿. *A&A* , 402:151–169, April 2003.

Raiteri, C. M., Villata, M., Larionov, V. M., Aller, M. F., et al. Radio-to-UV monitoring of ¡ASTROBJ¿AO 0235+164¡/ASTROBJ¿ by the WEBT and Swift during the 2006-2007 outburst. *A&A* , 480:339–347, March 2008.

Raiteri, C. M., Villata, M., Capetti, A., Aller, M. F., et al. WEBT multiwavelength monitoring and XMM-Newton observations of ¡ASTROBJ¿BL Lacertae¡/ASTROBJ¿ in 2007-2008. Unveiling different emission components. *A&A* , 507:769–779, November 2009.

Rani, B., Wiita, P. J., & Gupta, A. C. Nearly Periodic Fluctuations in the Long-term X-Ray Light Curves of the Blazars AO 0235+164 and 1ES 2321+419. *ApJ*, 696:2170–2178, May 2009.

Rani, B., Gupta, A. C., Joshi, U. C., Ganesh, S., & Wiita, P. J. Quasi-periodic Oscillations of ˜15 Minutes in the Optical Light Curve of the BL Lac S5 0716+714. *ApJ* , 719:L153–L157, August 2010.

Rau, A., Schady, P., Greiner, J., Salvato, M., et al. BL Lacertae objects beyond redshift 1.3 - UV-to-NIR photometry and photometric redshift for Fermi/LAT blazars. *A&A* , 538:A26, February 2012.

Rector, T. A. & Stocke, J. T. The Properties of the Radio-Selected 1 Jy Sample of BL Lacertae Objects. *AJ*, 122:565–584, August 2001.

Reynolds, S. P. Theoretical studies of compact radio sources. I - Synchrotron radiation from relativistic flows. *ApJ*, 256:13–37, May 1982.

Rieke, G. H., Lebofsky, M. J., Tapia, S., Kemp, J. C., & Coyne, G. V. Infrared and visible polarimetry and photometry of highly variable quasi-stellar sources. *ApJ* , 218:L37–L41, December 1977.

Robson, E. I., Gear, W. K., Clegg, P. E., Ade, P. A. R., et al. A flare in the millimetre to IR spectrum of 3C273. *Nature*, 305:194–196, September 1983.

Romero, G. E. Fine-Scale Structure in Relativistic Jets and Rapid Variability in Blazars. *Ap&SS*, 234:49–55, December 1995.

Romero, G. E., Combi, J. A., & Colomb, F. R. Strong intraday variability in the southern blazar PKS 0537-441 at 1.42 GHz. *A&A* , 288:731–737, August 1994.

Romero, G. E., Cellone, S. A., Combi, J. A., & Andruchow, I. Optical microvariability of EGRET blazars. *A&A* , 390:431–438, August 2002.

Roming, P. W. A., Kennedy, T. E., Mason, K. O., Nousek, J. A., et al. The Swift Ultra-Violet/Optical Telescope. *Space Sci. Rev.*, 120:95–142, October 2005.

Ryle, M. & Sandage, A. The Optical Identification of Three New Radio Objects of the 3c 48 Class. *ApJ*, 139:419, January 1964.

Sagar, R., Stalin, C. S., Gopal-Krishna, & Wiita, P. J. Intranight optical variability of blazars. *MNRAS* , 348:176–186, February 2004.

Sambruna, R. M. Multiwavelength observations of blazars: a summary. *Ap&SS*, 311:241–246, October 2007.

Sambruna, R. M., Barr, P., Maraschi, L., Tagliaferri, G., & Treves, A. A spectral study of four X-ray-selected BL Lacertae objects with EXOSAT. *ApJ*, 408:452–459, May 1993.

Sambruna, R. M., Reeves, J. N., Braito, V., Lewis, K. T., et al. Structure of the Accretion Flow in Broad-Line Radio Galaxies: The Case of 3C 390.3. *ApJ*, 700:1473–1487, August 2009.

Schmitt, J. L. BL Lac identified as a Radio Source. *Nature*, 218:663, May 1968.

Sembay, S., Warwick, R. S., Urry, C. M., Sokoloski, J., et al. The X-ray spectral variability of the BL Lacertae type object PKS 2155-304. *ApJ*, 404: 112–123, February 1993.

Serkowski, K. Polarimeters for Optical Astronomy. In Gehrels, T., editor, *IAU Colloq. 23: Planets, Stars, and Nebulae: Studied with Photopolarimetry*, page 135, 1974.

Seyfert, C. K. Nuclear Emission in Spiral Nebulae. *ApJ*, 97:28, January 1943.

Shi, W., Liu, X., & Song, H. A new model for the periodic outbursts of the BL Lac object OJ287. *Ap&SS*, 310:59–63, July 2007.

Sholomitskii, G. B. Fluctuations in the 32.5-cm Flux of CTA 102. *Soviet Ast.*, 9:516, December 1965.

Sikora, M., Begelman, M. C., & Rees, M. J. Comptonization of diffuse ambient radiation by a relativistic jet: The source of gamma rays from blazars? *ApJ*, 421:153–162, January 1994.

Sikora, M., Stawarz, Ł., Moderski, R., Nalewajko, K., & Madejski, G. M. Constraining Emission Models of Luminous Blazar Sources. *ApJ*, 704:38–50, October 2009.

Sillanpaa, A. Simultaneous optical and radio polarization rotation in OJ287. *A&A* , 247:11–14, July 1991.

Sillanpaa, A., Haarala, S., Valtonen, M. J., Sundelius, B., & Byrd, G. G. OJ 287 - Binary pair of supermassive black holes. *ApJ*, 325:628–634, February 1988.

Sitko, M. L., Schmidt, G. D., & Stein, W. A. Optical polarimetry of BL Lacertae objects and violent variable quasars. *ApJS*, 59:323–342, November 1985.

Smith, N., Coates, C., Giltinan, A., Howard, J., et al. EMCCD technology and its impact on rapid low-light photometry. In Garnett, J. D. & Beletic, J. W., editors, *Society of Photo-Optical Instrumentation Engineers (SPIE) Conference Series*, volume 5499 of *Society of Photo-Optical Instrumentation Engineers (SPIE) Conference Series*, pages 162–172, September 2004.

Smith, N., Giltinan, A., O'Connor, A., O'Driscoll, S., et al. EMCCD Technology in High Precision Photometry on Short Timescales. In Phelan, D., Ryan, O., & Shearer, A., editors, *Astrophysics and Space Science Library*, volume 351 of *Astrophysics and Space Science Library*, page 257, 2008.

Smith, P. S. & Balonek, T. J. Photometric Calibration of Stars in the Fields of Selected BL Lacertae Objects and Quasars. *PASP*, 110:1164–1171, October 1998.

Smith, P. S., Hall, P. B., Allen, R. G., & Sitko, M. L. Intensive optical monitoring of the BL Lacertae object PKS 2155-304. *ApJ*, 400:115–126, November 1992.

Snellen, I. A. G., McMahon, R. G., Hook, I. M., & Browne, I. W. A. Automated optical identification of a large complete northern hemisphere sample of flat-spectrum radio sources with [formmu1]$S_{6cm}\geq$200 mJy. *MNRAS* , 329:700–746, February 2002.

Snyder, W. A., Davidsen, A. F., Wood, K., Kinzer, R., et al. Rapid X-ray variability of PKS 2155-304. *ApJ* , 237:L11–L14, April 1980.

Sokolov, A., Marscher, A. P., & McHardy, I. M. Synchrotron Self-Compton Model for Rapid Nonthermal Flares in Blazars with Frequency-dependent Time Lags. *ApJ*, 613:725–746, October 2004.

Spada, M., Ghisellini, G., Lazzati, D., & Celotti, A. Internal shocks in the jets of radio-loud quasars. *MNRAS* , 325:1559–1570, August 2001.

Stalin, C. S., Kawabata, K. S., Uemura, M., Yoshida, M., et al. Simultaneous MITSuME g'$R_C I_C$ monitoring of S5 0716+714. *MNRAS* , 399:1357–1366, November 2009.

Stickel, M. The Optical and Radio Spectrum of the Radio-Selected High Redshift Quasar S4:1745+624. *A&A* , 275:49, August 1993.

Stickel, M., Padovani, P., Urry, C. M., Fried, J. W., & Kuehr, H. The complete sample of 1 Jansky BL Lacertae objects. I - Summary properties. *ApJ*, 374: 431–439, June 1991.

Takalo, L. O., Sillanpaa, A., Nilsson, K., Kidger, M., de Diego, J. A., & Piirola, V. Simultaneous UBVRI photopolarimetric observations of blazars. II. *A&AS* , 94:37–42, July 1992.

Takalo, L. O., Sillanpaeae, A., Nilsson, K., Kidger, M., & de Diego, J. A. Intense blazar activity in the photopolarimetric light curve of OJ 287. *A&AS* , 104:115–120, April 1994.

Tashiro, M., Ueda, Y., Kii, T., Makino, F., et al. ASCA Observations of Blazars. In Makino, F. & Ohashi, T., editors, *New Horizon of X-Ray Astronomy. First Results from ASCA*, page 343, January 1994.

Thomas, H.-C. & Fink, H. H. ROSAT spectra and lightcurves of bright BL Lacertae objects at low interstellar absorption. In Courvoisier, T. & Blecha, A., editors, *Multi-Wavelength Continuum Emission of AGN*, volume 159 of *IAU Symposium*, page 384, 1994.

Tommasi, L., Palazzi, E., Pian, E., Piirola, V., et al. Multiband optical polarimetry of BL Lacertae objects with the Nordic Optical Telescope. *A&A* , 376:51–58, September 2001.

Tornikoski, M., Valtaoja, E., Teraesranta, H., & Okyudo, M. A simultaneous radio-optical flare in BL Lacertae. *A&A* , 286:80–83, June 1994a.

Tornikoski, M., Valtaoja, E., Terasranta, H., Smith, A. G., et al. Correlated radio and optical variations in a sample of active galactic nuclei. *A&A* , 289: 673–710, September 1994b.

Türler, M., Chernyakova, M., Courvoisier, T. J.-L., Foellmi, C., et al. A historic jet-emission minimum reveals hidden spectral features in 3C 273. *A&A* , 451:L1–L4, May 2006.

Urry, C. M. Blazars, jets, and the unification of AGN. In Holt, S. S. & Zhang, W. W., editors, *American Institute of Physics Conference Series*, volume 522 of *American Institute of Physics Conference Series*, pages 299–306, June 2000.

Urry, C. M. & Padovani, P. Unified Schemes for Radio-Loud Active Galactic Nuclei. *PASP*, 107:803, September 1995.

Urry, C. M., Mushotzky, R. F., & Holt, S. S. X-ray spectroscopy of five BL Lacertae objects. *ApJ*, 305:369–398, June 1986.

Valtaoja, E. & Valtonen, M., editors. *Variability of blazars. Conference in honour of the 100th anniversary of the birth of Yrjö Väisälä. Proceedings.*, 1992.

Valtaoja, L., Sillanpaa, A., Valtaoja, E., Shakhovskoi, N. M., & Efimov, I. S. UBVRI photopolarimetry of BL Lac objects - The connection between frequency-dependent polarization and growing radio shocks. *AJ*, 101: 78–87, January 1991.

Valtonen, M. J., Lehto, H. J., & Pietilä, H. Probing the jet in the binary black hole model of the quasar OJ287. *A&A* , 342:L29–L31, February 1999.

Valtonen, M. J., Lehto, H. J., Nilsson, K., Heidt, J., et al. A massive binary black-hole system in OJ287 and a test of general relativity. *Nature*, 452: 851–853, April 2008.

Valtonen, M. J., Mikkola, S., Lehto, H. J., Hyvönen, T., et al. Measuring black hole spin in OJ287. *Celestial Mechanics and Dynamical Astronomy*, 106:235–243, March 2010a.

Valtonen, M. J., Mikkola, S., Merritt, D., Gopakumar, A., et al. Measuring the Spin of the Primary Black Hole in OJ287. *ApJ*, 709:725–732, February 2010b.

Valtonen, M. J., Savolainen, T., Wiik, K., Nilsson, K., et al. Variation of the Jet Angle of OJ287 in the Binary Black Hole Model. In *American Astronomical Society Meeting Abstracts #216*, volume 216 of *American Astronomical Society Meeting Abstracts*, page 304.07, May 2010c.

Venturi, T., Dallacasa, D., Orfei, A., Bondi, M., et al. Radio monitoring of a sample of X- and gamma-ray loud blazars. *A&A* , 379:755–766, December 2001.

Vercellone, S., D'Ammando, F., Vittorini, V., Donnarumma, I., et al. Multi-wavelength Observations of 3C 454.3. III. Eighteen Months of Agile Monitoring of the "Crazy Diamond". *ApJ*, 712:405–420, March 2010.

Vercellone, S., Striani, E., Vittorini, V., Donnarumma, I., et al. The Brightest Gamma-Ray Flaring Blazar in the Sky: AGILE and Multi-wavelength Observations of 3C 454.3 During 2010 November. *ApJ* , 736:L38, August 2011.

Villata, M., Raiteri, C. M., Ghisellini, G., de Francesco, G., et al. Optical photometric monitoring of gamma-ray loud blazars. *A&AS* , 121:119–138, January 1997a.

Villata, M., Raiteri, C. M., Ghisellini, G., de Francesco, G., et al. Optical photometric monitoring of gamma-ray loud blazars. *A&AS* , 121:119–138, January 1997b.

Villata, M., Raiteri, C. M., Lanteri, L., Sobrito, G., & Cavallone, M. BVR photometry of comparison stars in selected blazar fields. I. Photometric sequences for 10 BL Lacertae objects. *A&AS* , 130:305–310, June 1998.

Villata, M., Mattox, J. R., Massaro, E., Nesci, R., et al. The 0716+714 WEBT campaign of February 1999. *A&A* , 363:108–116, November 2000.

Villata, M., Raiteri, C. M., Kurtanidze, O. M., Nikolashvili, M. G., et al. The WEBT ¡ASTROBJ¿BL Lacertae¡/ASTROBJ¿ Campaign 2001 and its extension. Optical light curves and colour analysis 1994-2002. *A&A* , 421: 103–114, July 2004a.

Villata, M., Raiteri, C. M., Kurtanidze, O. M., Nikolashvili, M. G., et al. The WEBT ¡ASTROBJ¿BL Lacertae¡/ASTROBJ¿ Campaign 2001 and its extension. Optical light curves and colour analysis 1994-2002. *A&A* , 421: 103–114, July 2004b.

Villata, M., Raiteri, C. M., Balonek, T. J., Aller, M. F., et al. The unprecedented optical outburst of the quasar ¡ASTROBJ¿3C 454.3¡/ASTROBJ¿. The WEBT campaign of 2004-2005. *A&A* , 453:817–822, July 2006.

Villata, M., Raiteri, C. M., Aller, M. F., Bach, U., et al. The radio delay of the exceptional ¡ASTROBJ¿3C 454.3¡/ASTROBJ¿ outburst. Follow-up WEBT observations in 2005-2006. *A&A* , 464:L5–L9, March 2007.

Villata, M., Raiteri, C. M., Larionov, V. M., Kurtanidze, O. M., et al. Multifrequency monitoring of the blazar ¡ASTROBJ¿0716+714¡/ASTROBJ¿ during the GASP-WEBT-AGILE campaign of 2007. *A&A* , 481:L79–L82, April 2008a.

Villata, M., Raiteri, C. M., Larionov, V. M., Kurtanidze, O. M., et al. Multifrequency monitoring of the blazar ¡ASTROBJ¿0716+714¡/ASTROBJ¿ during the GASP-WEBT-AGILE campaign of 2007. *A&A* , 481:L79–L82, April 2008b.

Villata, M., Raiteri, C. M., Gurwell, M. A., Larionov, V. M., et al. The GASP-WEBT monitoring of ¡ASTROBJ¿3C 454.3¡/ASTROBJ¿ during the 2008 optical-to-radio and γ-ray outburst. *A&A* , 504:L9–L12, September 2009a.

Villata, M., Raiteri, C. M., Larionov, V. M., Nikolashvili, M. G., et al. The correlated optical and radio variability of ¡ASTROBJ¿BL Lacertae¡/ASTROBJ¿. WEBT data analysis 1994-2005. *A&A* , 501:455–460, July 2009b.

Visvanathan, N. & Wills, B. J. Optical Polarization of 52 Radio-loud QSOS and BL Lacertae Objects. *AJ*, 116:2119–2122, November 1998.

Wagner, S. & Hauser, M. Relations between optical synchrotron and gamma-ray variability. In *38th COSPAR Scientific Assembly*, volume 38 of *COSPAR Meeting*, page 2258, 2010.

Wagner, S. J. Fast flares of blazars during gamma-ray observations. Optical - gamma-ray correlations. *A&AS* , 120:C495, December 1996.

Wagner, S. J. & Witzel, A. Intraday Variability In Quasars and BL Lac Objects. *ARA&A*, 33:163–198, 1995a.

Wagner, S. J. & Witzel, A. Intraday Variability In Quasars and BL Lac Objects. *ARA&A*, 33:163–198, 1995b.

Wagner, S. J., Witzel, A., Krichbaum, T. P., Wegner, R., et al. Intraday variability in the BL Lac object 0954 + 658. *A&A* , 271:344, April 1993.

Wagner, S. J., Behera, B., & H.E.S.S. Collaboration. Hess Observations Of Quasars. In *AAS/High Energy Astrophysics Division #11*, volume 42 of *Bulletin of the American Astronomical Society*, page 660, February 2010.

Webb, J. R., Smith, A. G., Leacock, R. J., Fitzgibbons, G. L., Gombola, P. P., & Shepherd, D. W. Optical observations of 22 violently variable extragalactic sources - 1968-1986. *AJ*, 95:374–397, February 1988.

Weekes, T. C., Akerlof, C., Biller, S., Breslin, A. C., et al. VERITAS: The Very Energetic Radiation Imaging Telescope Array System. In *International Cosmic Ray Conference*, volume 5 of *International Cosmic Ray Conference*, page 173, 1997.

Wehrle, A. E., Marscher, A. P., Jorstad, S. G., Gurwell, M. A., et al. Multi-wavelength Variations of 3C 454.3 during the 2010 November to 2011 January Outburst. *ApJ*, 758:72, October 2012.

Wills, B. J., Wills, D., Breger, M., Antonucci, R. R. J., & Barvainis, R. A survey for high optical polarization in quasars with core-dominant radio structure - Is there a beamed optical continuum? *ApJ*, 398:454–475, October 1992.

Witzel, A. Superluminal motion and other indications of bulk relativistic motion in a complete sample of radio sources from the S5 survey. In Zensus, J. A. & Pearson, T. J., editors, *Superluminal Radio Sources*, pages 83–93, 1987.

Witzel, A., Heeschen, D. S., Schalinski, C., & Krichbaum, T. Kurzzeit-Variabilität extragalaktischer Radioquellen. *Mitteilungen der Astronomischen Gesellschaft Hamburg*, 65:239, 1986.

Witzel, A., Schalinski, C. J., Johnston, K. J., Biermann, P. L., et al. The occurrence of bulk relativistic motion in compact radio sources. *A&A* , 206: 245–252, November 1988.

Wright, E. L. A Cosmology Calculator for the World Wide Web. *PASP*, 118: 1711–1715, December 2006.

Wright, E. L., Eisenhardt, P. R. M., Mainzer, A. K., Ressler, M. E., et al. The Wide-field Infrared Survey Explorer (WISE): Mission Description and Initial On-orbit Performance. *AJ*, 140:1868, December 2010.

Wu, J., Peng, B., Zhou, X., Ma, J., Jiang, Z., & Chen, J. Optical Monitoring of BL Lacertae Object S5 0716+714 with High Temporal Resolution. *AJ*, 129:1818–1826, April 2005.

Xie, G. Z., Li, K. H., Bai, J. M., Dai, B. Z., et al. Search for Short Variability Timescale of the GEV Gamma-Ray-Loud Blazars. *ApJ*, 548:200–212, February 2001.

Xie, G. Z., Zhou, S. B., Dai, B. Z., Liang, E. W., et al. Photometric monitoring of 12 BL Lacertae objects. *MNRAS* , 329:689–699, February 2002.

Xie, G. Z., Zhou, S. B., Li, K. H., Dai, H., Chen, L. E., & Ma, L. CCD photometric studies of rapid variability in eight blazars. *MNRAS* , 348: 831–845, March 2004.

Young, A. T., Genet, R. M., Boyd, L. J., Borucki, W. J., et al. Precise automatic differential stellar photometry. *PASP*, 103:221–242, February 1991.

Zhang, B. K., Dai, B. Z., Wang, L. P., Zhao, M., Zhang, L., & Cao, Z. Intraday optical variability of the BL Lacertae object S5 0716+714. *MNRAS* , 421: 3111–3115, April 2012.

Zhang, X., Zheng, Y. G., Zhang, H. J., Liu, Y., Wen, Y. B., & Wang, W. CCD Photometric Monitoring of the BL Lacertae Object s5 0716+714 from 2001 TO 2006. *AJ*, 136:1846–1851, November 2008.

THE ASTROPHYSICAL JOURNAL, 746:92 (6pp), 2012 February 10 doi:10.1088/0004-637X/746/1/92

OPTICAL POLARIMETRY OF THE BLAZAR CGRaBS J0211+1051 FROM MOUNT ABU INFRARED OBSERVATORY

SUNIL CHANDRA, KIRAN S. BALIYAN, SHASHIKIRAN GANESH, AND UMESH C. JOSHI
Astronomy & Astrophysics Division, Physical Research Laboratory, Ahmedabad 380009, India; baliyan@prl.res.in
Received 2011 April 22; accepted 2011 November 23; published 2012 January 27

ABSTRACT

We report the detection of high polarization in the first detailed optical linear polarization measurements on the BL Lac object CGRaBS J0211+1051, which flared in γ-rays on 2011 January 23 as reported by *Fermi*. The observations were made during 2011 January 30–February 3 using a photo-polarimeter mounted at the 1.2 m telescope of Mount Abu Infrared Observatory. CGRaBS J0211+1051 was detected to have a $\sim$21.05% $\pm$ 0.41% degree of polarization (DP) with a steady position angle (P.A.) at 43° on 2011 January 30. During January 31 and February 1, while polarization shows some variation, the P.A. remained steady through the night. Several polarization flashes occurred during February 2 and 3 resulting in changes in the DP by more than 4% at short timescales ($\sim$17–45 minutes). The intra-night variability shown by the source appears to be related to the turbulence in the relativistic jet. A mild wavelength dependence of polarization is not ruled out during the nights of February 2 and 3. The source exhibited significant inter-night variations in the DP (changing by about 2%–9%) and P.A. (changing by 2°–22°) during the five nights of observations. A sudden change in the P.A. accompanied by a rise in the DP could be indicative of the fresh injection of plasma in the jet. The detection of a high and variable DP suggests that the source is a low-energy peaked blazar.

Key words: BL Lacertae objects: individual (CGRaBS J0211+1051) – galaxies: active – galaxies: nuclei – methods: observational – techniques: polarimetric

1. INTRODUCTION

CGRaBS J0211+1051, also known as MG1 J021114+1051, 1FGL J0211.2+1049, 87GB 020832.6+103726, etc. (R.A. 02:11:13.2, decl. 10:51:35, J2000), was found to have a featureless optical spectrum and R-band magnitude of 15.42 in optical characterization of bright blazars in the uniform all-sky survey, CGRaBS (Healey et al. 2008). It was identified as a radio source and/or BL Lac object in a 8.4 GHz survey of bright, flat-spectrum radio sources (Healey et al. 2007) and in several other surveys, including the 4775 MHz survey (Lawrence et al. 1986). Snellen et al. (2002) performed optical identification of the radio sources from the Jodrell Bank Very Large Area astrometric survey with $S_{6\,\mathrm{cm}} > 200$ mJy and reported CGRaBS J0211+1051 to have an R-band magnitude of 15.41 along with 384 mJy and 318 mJy flux values at 5 GHz and 1.4 GHz, respectively. The source was detected in γ-rays ($E > 100$ MeV) by the Large Area Telescope (LAT) on board *Fermi* and is listed in the first Fermi catalog (Abdo et al. 2010). Recently, the redshift of CGRaBS J0211+1051 was estimated to be $z = 0.20 \pm 0.05$ from its host galaxy observations (Meisner & Romani 2010).

On 2011 January 23, flaring activity in γ-rays ($E > 100$ MeV) was detected in CGRaBS J0211+1051 by LAT on board *Fermi* (D'Ammando et al. 2011a). The measured flux at the level of $1.0(\pm 0.3) \times 10^{-6}$ photon cm^{-2} s^{-1} was 25 times the flux averaged over the previous 11 months (Abdo et al. 2010). *Swift*/UVOT Target of Opportunity observations (D'Ammando et al. 2011b) on 2011 January 25 found that CGRaBS J0211+1051 was about 1.3 and 1.4 mag brighter in the U band (13.77 ± 0.03 mag) and $W2$ band (14.44 ± 0.04 mag), respectively, compared with their values on 2010 March 5. *Swift* also observed CGRaBS J0211+1051 in V band with 14.00 $\pm$ 0.08 mag. On 2011 January 27, Nesci (2011) reported an R_c-band magnitude of 13.37 for the source showing it to be 1.74 mag brighter than the POSS-I red plate value and the Digitized First Byurakan Survey value of $R = 15.1$ as obtained in 1950 and 1971, respectively. Based on their past observations made with MASTER-net (Lipunov et al. 2004), Kudelina et al. (2011) found the source to have continuously increased in brightness from 14.45 mag in white light on 2010 February 3 to 13.35 mag on 2011 January 24. Djorgovski et al. (2011) reported a steady rise in the source brightness from $\sim$15.6 mag in 2008 to about 13.5 mag in V band on 2011 January 24.

All of these reports suggest that CGRaBS J0211+1051 has been in a brightening phase for the last several years, having short (months) variability timescales with 0.5–1 mag amplitude of variation. Such variations indicate strong activity in the optical while the source flared at high-energy γ-rays. It would be interesting to see the behavior of this source on intra-night timescales with continuous monitoring. Following the flaring of the source in γ-rays, Gorbovskoy et al. (2011) made optical polarimetric measurements in the V band using MASTER-net observational sites at Tunka-Baykal and Amur-Blagoveschensk and found the source to have a 12% polarization on 2011 January 28. The corresponding V-band brightness magnitude of the source was about 13.65 mag. Chandra et al. (2011b) detected an even higher degree of polarization (DP; > 20.7%) in white light during their observations from Mount Abu Infrared Observatory (MIRO) on 2011 January 30.

Extreme variations in the flux and polarization at various timescales across the whole electromagnetic spectrum are the characteristics of blazars, a subclass of active galactic nuclei (AGNs) seen at a small angle ($\leqslant 10°$) to the jet emanating from very close to the black hole (Urry & Padovani 1995; Blandford & Konigl 1979; Chandra et al. 2011a). Such variations could be caused by the perturbations in the accretion disk or the relativistic jet as described by several models (e.g., Mangalam & Wiita 1993; Marscher & Gear 1985; Qian et al. 1991; Marscher et al. 1992; Gopal-Krishna & Wiita 1992).

Since radio to X-ray emission in blazars is normally associated with the synchrotron radiation from the relativistic electrons moving in the magnetic field, systematic polarization measurements provide an important tool to understand the nature of such variations and help constrain the models of emission. However, very limited observations have been reported that deal with intra-night and night-to-night variations in blazars (e.g., Andruchow et al. 2003; Villforth et al. 2009; Heidt & Nilsson 2011, and references therein). The DP and its variation have been used by many workers as a tool for detecting or confirming BL Lac candidates (e.g., Smith et al. 2007; Jannuzi et al. 1993, and references therein). A detailed review of polarization properties of the blazars is given by Angel & Stockman (1980). The study of the variations in polarization is also useful in probing the structure of the jet and the nature of the physical processes in AGNs (Marscher 2008; Andruchow et al. 2005). Motivated by this, we made detailed optical polarization measurements from MIRO during 2011 January 30 to February 3. The main objective was to investigate the night-to-night variability in polarization and position angle (P.A.) and any possible intra-night activity in the source. These are, we believe, the first detailed and systematic polarization data reported so far on the blazar CGRaBS J0211+1051.

2. OBSERVATIONS AND DATA ANALYSIS

The observations were made using the two-channel Physical Research Laboratory Photo-polarimeter (PRLPOL) mounted on the Cassegrain focus of the 1.2 m telescope of MIRO, operated by the Physical Research Laboratory, Ahmedabad, India, during five consecutive nights, 2011 January 30 to February 3. The PRLPOL, described in detail by Deshpande et al. (1985), was recently fully refurbished and automated (Ganesh et al. 2009). It works on the principle of rapid modulation with a fast-rotating, super-achromatic half-wave plate, completing one physical rotation in 96 steps ($3^{\circ}\!.75$ per step). The four modulation cycles are thus completed in one full rotation of the half-wave plate with 24 steps per modulation cycle. A Wollaston prism divides the incident light beam into two orthogonally polarized components, each one directed to a separate photomultiplier tube (PMT). The rapid modulation of the incident light and simultaneous measurement of the two polarized components take care of the atmospheric scintillation effects. The instrument has a *UBVRI*-system filter slide and a second slide with diaphragms of differently sized apertures. The observations were carried out mostly in the white light to maximize the signal. For white light, the effective wavelength is determined by the sensitivity of the detector, here PMT (EMI 9863B), which peaks at $\sim\lambda = 400$ nm. Some measurements were made with *B*, *V*, and *R* filters to investigate any wavelength dependence of polarization (WDP). We adopted a sky–source–sky observation strategy for the observations where, alternately, sky and source were kept at the center of the aperture. The source was recentered whenever a drift was noticed during the observation. The sky measurements were taken about $30''$ away from the source. The exposure time for both the sky and the source was kept at 40 s during all five nights for unfiltered white light observations and 120 s for observations in the *B*, *V*, and *R* bands. The appropriate size of the aperture is chosen by keeping in mind the optimum value of the signal-to-noise ratio and the prescription of Andruchow et al. (2008) for avoiding spurious variations caused by any possible change in the seeing and the contamination by the thermal emission from the host galaxy, which tends to decrease the value of intrinsic polarization. Too small ($\sim$ FWHM) an aperture might introduce spurious variations if the seeing changes under unstable sky conditions, while a large one would result in the suppression of any intrinsic variation and extent of the polarization of the source. In the present case, the host galaxy was more than 3 mag fainter than the source (Meisner & Romani 2010) as the source was in a relatively brighter phase (Nesci 2011; Kudelina et al. 2011). Based on these criteria, we use a 10 arcsec aperture for the target and other observed stars used for the calibration. Weather conditions were photometric with a moonless sky, which was more than 2 mag fainter than the source.

For the duration of integration on the sky or the source, counts are accumulated in 24 array locations corresponding to the half-wave plate positions with a 2 ms sampling time. The DP and the P.A. for the source are then calculated by the control program after each integration, subtracting the previously observed sky counts. The computation is performed using a least-squares fit to the counts from the two PMTs. The mean error in the DP is estimated from the deviation of the actual counts from the fitted curve. Standard stars were observed every night to determine the zero point for the P.A. and the instrumental polarization, which was found to be negligibly small ($<0.02\%$).

Table 1
Nightly Averaged Polarization Data for CGRaBS J0211+1051

Date	MJD	Δ_T (hr)	DP (%)	σ_{DP} (%)	P.A. (°)	$\sigma_{\mathrm{P.A.}}$ (°)
2011 Jan 30	55591.3796	0.336	21.052	0.295	42.771	0.634
2011 Jan 31	55592.4665	0.864	12.871	0.489	28.963	0.758
2011 Feb 1	55593.4352	2.498	10.643	0.493	30.679	1.373
2011 Feb 2	55594.4362	2.112	12.629	0.981	52.982	1.412
2011 Feb 3	55595.4308	1.920	15.481	1.412	43.578	1.762

Note. Entries are the dates of observation, MJD, duration of observation, DP, σ_{DP}, P.A., and $\sigma_{\mathrm{P.A.}}$.

3. RESULTS AND DISCUSSION

The P.A. of polarization for the source was corrected using measurements on the 9-Gem and error in P.A. was calculated using the expression by Serkowski (1974). A possible source of error in the measurement of polarization parameters lies in dealing with the sky background. It could be particularly serious when the sky is close to the source in brightness and has large and variable polarization due to, for example, the presence of Moon. Such large, variable polarization affects both the source and the sky, and, therefore, this systematic error should be removed when the data are reduced if the sky measurements are made close (both in time and position) to the source observations. In the present case, we have taken the above precaution in the sky measurement. In addition, the observations were made in moonless sky conditions and the source was more than 2 mag brighter than the sky. Also, the sky was fairly stable with DP remaining low (maximum 6%) during 2011 January 30 to February 3. Any change in the DP of the sky on any particular night remained well within the measurement errors. We, therefore, do not expect any significant spurious effect on the source polarization due to the sky.

The nightly averaged values of the DP and the P.A. were calculated and their standard deviations were obtained. In Table 1, we report polarization data during the given observing run date, MJD, duration of observation in hours, nightly averaged values of the DP, P.A., and their respective standard deviations. The polarization data reported here are obtained through a 10 arcsec aperture as mentioned in the previous section. A larger aperture might result in a significant reduction in the DP due to thermal emission from the host galaxy contaminating the nonthermal emission from the nucleus, particularly when the host galaxy is bright. CGRaBS J0211+1051 and its host galaxy had I'-band magnitudes of 15.32 and 16.91, respectively, as reported by Meisner & Romani (2010) during their 2008 October 31 to November 2 observations. Since galaxy light peaks in the near-infrared band and has a reduced brightness at a shorter wavelength, the effect of galaxy light contaminating the nuclear emission will be reduced in the optical B, V, and R bands. Also, the source was in a fairly bright phase, brighter than 13.5 in R (Nesci 2011; Kudelina et al. 2011), during our polarimetric observations, making it more than 3 mag brighter than the host galaxy. Therefore, there should not be any significant contamination of the nuclear light by the host. Nevertheless, the polarization values reported here should be marginally lower than their intrinsic values.

3.1. Intra-night and Inter-night Variation in Polarization

The blazars are known to show rapid, large-amplitude variations in flux and polarization at various timescales. The nature of such variations can be used to infer the physical processes at work in these sources. To investigate the intra-night polarization behavior of CGRaBS J0211+1051, DP and P.A. are plotted as a function of time (MJD) in Figures 1(a)–(c) and 2(a) and (b) for the observations made during 2011 January 30 to February 1 (in white light) and February 2 and 3 (in B, V, R bands and white light), respectively. The error bars indicate the uncertainties (including the uncertainty in the background determination) in the individual measurement of DP and P.A. In the following, we present polarization results from our nightly observations.

On 2011 January 30, the source was highly polarized at more than a 21% level during our 20 minute observations (Figure 1(a)). The P.A. was $\sim 43°$. We do not note any significant variation in DP or P.A. during this night. However, this value of DP is much higher than the value reported by Gorbovskoy et al. (2011) on 2011 January 28 (DP = 12%), just two days prior to our measurements. We have 14 data points on 2011 January 31 obtained within 0.7 hr of observation. At the onset of observations, DP is about 13%, increasing to 13.81($\pm$0.35)% before falling by 2.7% ($>5\sigma$) to 11.10($\pm$0.41)% within about 20 minutes (decay rate, $\sim$8% hr^{-1}). The DP starts increasing again and reaches about a 13.2% level in 18 minutes (rising rate, 7% hr^{-1}) with a 2.1% ($>4\sigma$) amplitude of variation. The visual inspection, therefore, shows rapid variation in DP with significant (4σ–5σ) amplitude of variation on 2011 January 31. The P.A., however, remains well behaved without any appreciable variation. 2011 February 1 has a large number of observational points (87) obtained during 2.4 hr of monitoring. Several microvariability events appear to be superimposed over a nonvarying component (Figure 1(c)). However, except for the two events beginning at MJD 55593.424 and MJD 55593.446 with more than 3σ amplitude of variation in DP, other variations are within 2σ. The P.A. stays within $31° \pm 3°$ without any structures.

The temporal behavior of the polarization of the blazar CGRaBS J0211+1051 on 2011 February 2 and 3 is shown in Figures 2(a) and (b). During these two nights, in addition to the white light, we also made observations in the B, V, and R filter bands to observe any wavelength dependence in the DP and P.A. Let us first look at the behavior of the source in the

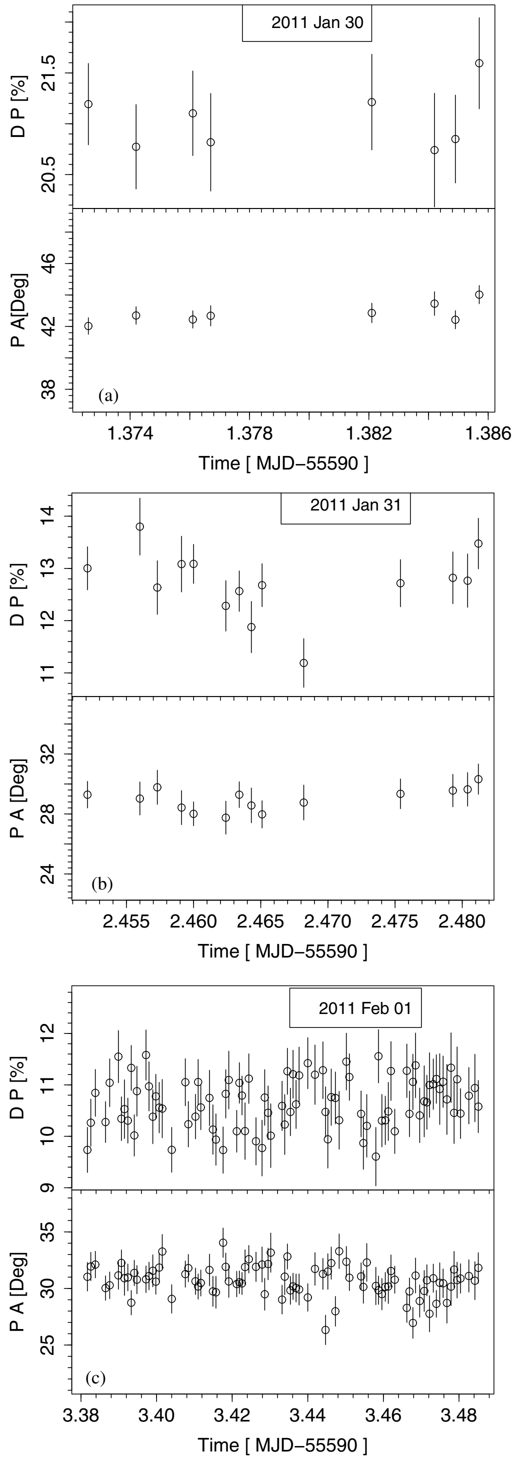

Figure 1. Intra-night variations in the DP and P.A. during 2011 January 30 to February 1 for CGRaBS J0 211+1051 in white light. The error bars show uncertainties in the individual measurements.

white light only. On 2011 February 2, beginning and ending segments (from time 4.388 to 4.418 and 4.456 to 4.476) of the

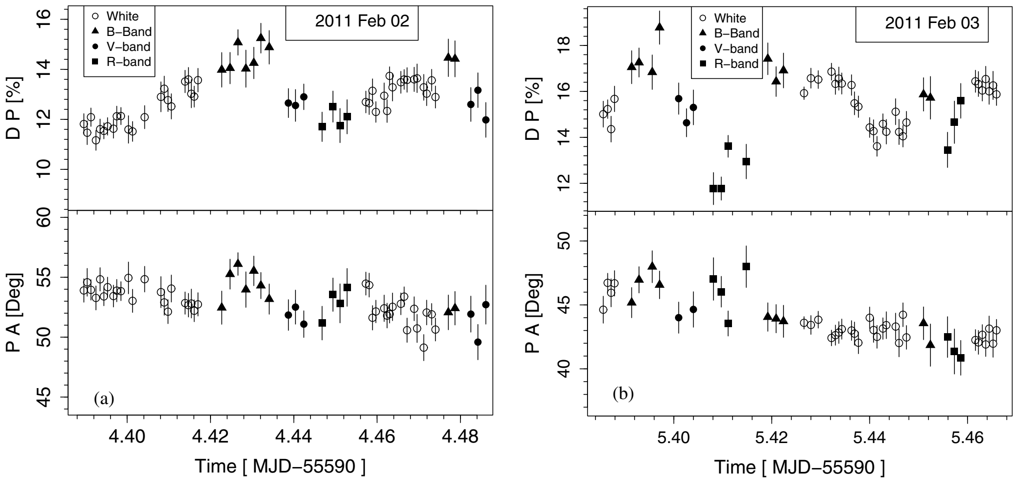

Figure 2. Same as Figure 1 but for 2011 February 2 and 3 in the *B*, *V*, and *R* bands and white light.

curve display white light measurements (cf. Figure 2(a)). The visual inspection of the plot clearly shows an increase in DP by 2.2% (close to 3σ) during ≈32 minutes (rate of increase in DP, 4% hr^{-1}). The measurements in the white light toward the end also give an indication of a change (at 2σ level) in DP. On 2011 February 3, DP decreases from 16.8% at time ∼5.432 to ≈13.8% at time 5.442 (cf. Figure 2(b)), with an amplitude of variation of about 3% ($> 3\sigma$). This drop is then followed by an increase in DP by about 2.6% within a span of 35 minutes at the rate of 4.5% hr^{-1} toward the end of the observations. The source, therefore, undergoes rapid intra-night variations in the DP on 2011 January 31, and February 2 and 3, as reflected in the white light polarization curves.

Considering the observations made through the *B*, *V*, and *R* filters in addition to the white light ones, we now discuss Figure 2 again. On 2011 February 2, DP rises from 11.5% (at time 4.392) to 13.5% (at time 4.416, cf. Figure 2(a)) in white light. The rise continues in the *B*-band observations reaching more than 15% at MJD = 55594.43. Beyond that, DP decreases in *V* and *R* bands partly due perhaps to the increase in wavelength and partly due to the intrinsic variation in the polarization of the source. The rates of decay in DP from the *B* to *V* bands and the *V* to *R* bands are approximately 22% hr^{-1} and 11% hr^{-1}, respectively. Toward the end, observations in the white light show an increasing trend with DP peaking in the *B* band (∼14.3%) before dropping to ∼12.2% in the *V* band (DP decay rate from the *B* to *V* bands was 14% hr^{-1}). The P.A. largely remains within the ±3° range. Figure 2(b) shows polarization behavior of CGRaBS J0211+1051 during 2011 February 3. Interestingly, the composite curve shows three quasiperiodic polarization flashes with a significant amplitude of variation (up to 4%). These events have fast rise and fall timescales, ranging from 17 to 35 minutes. It is important to note that DP changes at a rate of about 31%, 35%, and 40% hr^{-1} from *B* to *V*, *V* to *R*, and *R* to *B* bands, respectively, as estimated from the polarization curve for 2011 February 3. The P.A. varies between 41° and 46° during the course of observations and can be considered as mildly variable.

The blazars are known to show WDP. Any WDP in the jet-dominated blazars is known to be due to the source geometry and/or due to the contamination of the nuclear nonthermal radiation by the thermal unpolarized emission from the host galaxy (Brindle et al. 1986; Angel & Stockman 1980). In many cases, DP is noticed to increase with frequency (e.g., Sitko et al. 1985; Holmes et al. 1984; Angel & Stockman 1980, and references therein) in the optical region. However, decrease in DP with frequency is also detected in several cases. For example, Tommasi et al. (2001) observed several blazars simultaneously in *UBVRI* optical bands. While they found DP to increase with frequency in many sources, OJ287 and the BL Lac object were noticed to show a decrease in DP with frequency.

In the present case, 2011 February 2 and 3 measurements with *B*, *V*, and *R* filters appear to support the trend that the DP increases with frequency in Bl Lac objects. The DP in the *B* band shows an increase over *R*- and *V*-band values (Figure 2), which cannot only be due to the intrinsic variation because variation timescales are expected to be longer than the temporal resolution (about 5 minutes) used here. A careful examination of the variation pattern in DP shows that while the rate of change in DP obtained in white light is, on average, about 4%–8% hr^{-1} (except for a segment in the polarization curve on 2011 February 3 when it is about 11% per Hr), it is as high as 12%–40% per Hr in the values obtained using different bands. The significant increase in the rate of change in DP with time when observed through the *B*, *V*, and *R* bands, is, perhaps, partly due to WDP. However, from the present data, it is not possible to clearly establish the extent to which WDP contributes to the observed polarization variability. For this, simultaneous observations in different optical bands are needed.

Now, let us look at the inter-night variations during 2011 January 30 to February 3. Table 1 and Figure 3 show averaged DP and P.A. for these nights. The error bars in the figure reflect the spread (1σ) due to intra-night variations in addition to the measurement errors. It is evident from the observed data that the source was highly polarized on 2011 January 30 with DP at about 21%, which decreased by 9% and 11% on 2011 January 31 and February 1, respectively. The DP increased again reaching 15.5% on 2011 February 3. The P.A. also changed significantly from night to night, initially following the trend in the DP but dropping to 45° on the last night while DP increased to a 15% level. We note changes in the P.A. by 2°–22° while remaining within the 28°–53° range during our observations.

Apart from visual inspection of the polarization curves to look for variations, we also carried out a statistical analysis to

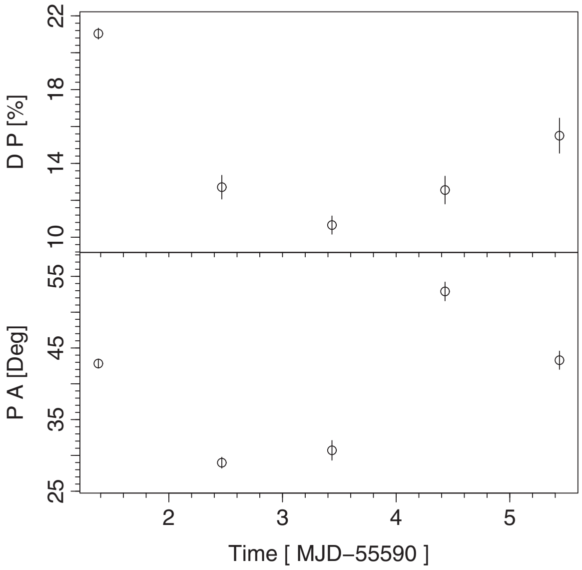

Figure 3. Night-to-night variation in the DP and P.A. during 2011 January 30 to February 3. The error bars reflect the spread ($\pm\sigma$) due to intra-night variations.

detect and quantify the variation parameters using the criterion of Kesteven et al. (1976) applied by several authors to the variability studies (e.g., Romero et al. 1994; Andruchow et al. 2005). Here, the variability in DP and P.A. is described by the fluctuation index μ and the fractional variability index FV of the source obtained from each individual night's data. The corresponding expressions are

$$\mu = 100\frac{\sigma_S}{\langle S\rangle}\ \%, \tag{1}$$

$$\mathrm{FV} = \frac{S_{\max} - S_{\min}}{S_{\max} + S_{\min}}, \tag{2}$$

where σ_S is the standard deviation, $\langle S\rangle$ is the mean value of the DP or the P.A. obtained during a particular night, $S_{\max}$ and $S_{\min}$ are, respectively, the maximum and minimum values for the DP or P.A. The source is classified as variable (V) if the probability of exceeding the observed value of

$$x^2 = \sum_{i=1}^{n} \epsilon_i^{-2} (S_i - \langle S\rangle)^2 \tag{3}$$

by chance is $<0.1\%$, nonvariable (NV) if $> 0.5\%$, and possibly variable (PV) for in-between values. In the above expression, ϵ_i are the uncertainties in the individual measurements. If the errors are random, x^2 is distributed as χ^2 with $n-1$ degrees of freedom, where n is the number of points in the distribution.

Since variability in the polarization parameters (DP and P.A.) due to the WDP and intrinsic variation cannot be separated, a statistical analysis is performed using only the white light data. Table 2 shows the values of the variability parameters for the DP and P.A. Columns 1 and 2 give the date and the number of observation points, Columns 3–6 present the values of μ, FV, and χ^2 for DP, and the status of the source (V, NV, and PV). The remaining four columns give these values for the P.A. These results quantitatively substantiate significant intra-night variability during 2011 February 2 and 3 in the polarization behavior of

Table 2
Variability Test Results for CGRaBS J0211+1051 Using White Light Data Only

Date	n	DP				P.A.			
		$\mu(\%)$	FV	χ^2	Status	$\mu(\%)$	FV	χ^2	Status
2011 Jan 30	8	1.403	0.021	2.942	NV	1.482	0.023	8.215	PV
2011 Jan 31	14	3.799	0.075	13.341	PV	2.618	0.044	7.573	NV
2011 Feb 1	87	4.639	0.093	84.610	NV	4.475	0.127	89.691	PV
2011 Feb 2	39	6.153	0.103	128.810	V	2.473	0.056	61.825	V
2011 Feb 3	30	6.121	0.107	121.733	V	2.944	0.054	60.086	V

the source as noticed in the visual inspection of the respective figures. It is, however, to be noted that when the number of measurements during a night is not large enough, the above test may not be very suitable. Perhaps that is why the test gives a PV status for DP on 2011 January 31 when we only had 14 data points, while visual inspection shows noticeable variability.

Let us briefly discuss these results. The observed optical emission in the blazars originates in a part of the accretion disk and the inner (parsec-scale) regions of the jet. The polarization caused by the electron or dust scattering in the accretion disk is usually low (a few percent). Since CGRaBS J0211+1051 shows a high DP (10%–21%) during the present observations, the emission must be dominated by the relativistic jet, aligned at a small angle to the line of sight. This emission is mostly synchrotron radiation from the relativistically moving electrons in the jet and is highly polarized ($>70\%$) if the magnetic field is uniformly aligned. A reduced observed DP indicates a chaotic magnetic field, which can be described in terms of N cells with a uniform but randomly oriented magnetic field (Marscher 2008). The DP could also be reduced by geometrical depolarization due to variation in the magnetic field orientation along the line of sight and the contamination by the thermal emission from the host galaxy. The P.A. is orthogonal to the projected direction of the magnetic field. However, relativistic motion aberrates the angle resulting in a P.A. that is more aligned with the jet direction. In BL Lac objects, the parsec-scale magnetic field in the jet is tangled and shocks moving down the jet compress the magnetic fields, aligning it perpendicular to the flow direction (Marscher & Gear 1985). The interaction of relativistic shocks with features in the parsec-scale jet results in rapid variations in the flux and polarization (Marscher et al. 1992; Qian et al. 1991). The features are varied in nature depending on the model and they are generally subparsec in size. Macroscopic Kelvin–Helmholtz instabilities are capable of producing such features in the inner beam. Quasiperiodic variations could be caused by the regularly spaced obstacles in the path of the jet.

These models can explain variations with timescales of weeks to days. Faster variations down to the subhour timescales cannot be explained by these models due to the limited thickness of the shocks. The rapid, intra-night flickerings in the DP as observed during 2011 January 31 to February 3 could be the effect of turbulence in the postshock region of the jet. The P.A. of polarization suffered drastic changes between the nights of 2011 January 30 and 31, February 2 and 3 by more than 8° and 10°, respectively, while the DP underwent an 8% and 3% change during these periods. The DP changed by more than 9% during 2011 January 28 (DP 12% as reported by Gorbovskoy et al. 2011) and January 30 (21%, our value). These sudden changes in the P.A. and DP, as noticed in other BL Lac objects, for example, 3C279 (Andruchow et al. 2003), are perhaps caused by the fresh injection of the plasma blobs in the jet on 2011

January 28 and February 2. Shocks thus formed compress and enhance the magnetic field parallel to the shock front, giving rise to sudden changes in the P.A. and DP.

3.2. CGRaBS J0211+1051: A Probable Low-energy Peaked Blazar

Depending on the position of the synchrotron peak in the spectral energy distribution of the blazars, they are subclassified into blazar sequence, flat spectrum radio quasars (FSRQ), radio-selected BL Lac objects (RBL), and X-ray-selected BL Lac objects (XBL) (Urry & Padovani 1995; Fan et al. 1997; Heidt & Nilsson 2011, and references therein). These subclasses are known to have some very distinct properties. For example, their bolometric luminosity decreases from FSRQ to XBL as does the dominance of γ-ray emission (Sambruna 2007; Fossati et al. 1998). Similarly, RBLs are reported to have, on average, much higher DP and amplitude of variation than XBLs (e.g., Andruchow et al. 2005; Tommasi et al. 2001; Fan et al. 1997; Jannuzi et al. 1993, and references therein). Fan et al. (1997) ascribe this difference in the DP to the difference in their beaming effect: RBLs show stronger beaming. Recently, Heidt & Nilsson (2011) found only a marginal difference in the polarization behavior of the RBLs and the XBLs as inferred from their sample of probable blazar candidates taken from the Sloan Digital Sky Survey. However, their inference could be affected by low statistics because they only have 8 RBLs and 37 XBLs in their sample. On the other hand, Andruchow et al. (2005) and Ikejiri et al. (2009) report, based on the studies of their samples, that RBLs generally have a higher DP compared with XBLs.

As described in the present work, CGRaBS J0211+1051 shows rapid, large-amplitude variations in the degree of optical polarization. It also indicates a high duty cycle of variation in polarization, showing variability on three (including a borderline variation on 2011 January 31) out of five nights of observation. The extent and nature of the linear polarization exhibited by CGRaBS J0211+1051 during 2011 January 30 to February 3 led us to infer that the source probably belongs to the low-energy peaked BL Lac objects (RBLs). Multifrequency observations covering the radio to γ-ray region, however, are required to study its spectral energy distribution to determine the location of the two peaks and confirm its status in the blazar sequence.

4. CONCLUSIONS

The first detailed optical polarization measurements performed during 2011 January 30 to February 3 are reported for the blazar CGRaBS J0211+1051. The source shows a high and variable (10%–21%) DP during this period. While the source is possibly variable on 2011 January 31, substantial intra-night variability is noticed on 2011 February 2 and 3 with DP changing by as much as 4%. The P.A. remains within 2σ during the individual nights but changes significantly from night to night. Significant inter-night variations in the DP are also noticed. The sudden changes in the P.A. accompanied by increased DP could be indicative of the fresh injection of the plasma in the jet. The rapid intra-night flickerings in the polarization appear to be due to small-scale turbulence in the postshock region of the jet.

There are no other polarization results in the literature for this source except for a report of 12% polarization on 2011 January 28 by Gorbovskoy et al. (2011). The present results show a variation in DP from about 21% to 10% during 2011 January 30–February 3; therefore, their value is in agreement with ours. The high value of polarization is perhaps indicative of the source being a low-energy peaked BL Lac object. More multiwavelength observations, along with very long baseline interferometry imaging, are needed to study the structure and spectral energy distribution of the source to constrain the models of variability.

The authors thank the anonymous referee for constructive comments and suggestions. This work is supported by the Department of Space, Government of India.

Facility: MIRO:1.2m (PRLPOL)

REFERENCES

Abdo, A. A., Ackermann, M., Ajello, M., et al. 2010, ApJS, 188, 405
Andruchow, I., Cellone, S., & Romero, G. E. 2008, MNRAS, 388, 1766
Andruchow, I., Cellone, S., Romero, G. E., Dominici, T. P., & Abraham, Z. 2003, A&A, 409, 857
Andruchow, I., Romero, G. E., & Cellone, S. 2005, A&A, 442, 97
Angel, J. R. P., & Stockman, H. S. 1980, ARA&A, 18, 321
Blandford, R. D., & Konigl, A. 1979, ApJ, 232, 34
Brindle, C., Hough, J. H., Bailey, J. A., Axon, D. J., & Hyland, A. R. 1986, MNRAS, 221, 739
Chandra, S., Baliyan, K. S., Ganesh, S., & Joshi, U. C. 2011a, ApJ, 731, 118
Chandra, S., Ganesh, S., Baliyan, K. S., & Joshi, U. C. 2011b, ATel, 3136, 1
D'Ammando, F., & Fermi-LAT Collaboration. 2011a, ATel, 3120, 1
D'Ammando, F., & Fermi-LAT Collaboration. 2011b, ATel, 3129, 1
Deshpande, M. R., Joshi, U. C., Kulshrestha, A. K., Banshidhar, & Vadher, N. M. 1985, Bull. Astron. Soc. India, 13, 157
Djorgovski, S. G., Drake, A. J., Mahabal, A. A., et al. 2011, ATel, 3133, 1
Fan, J. H., Cheng, K. S., Zhang, L., & Liu, C. H. 1997, A&A, 327, 947
Fossati, G., Maraschi, L., Celotti, A., Comastri, A., & Ghisellini, G. 1998, MNRAS, 299, 433
Ganesh, S., Joshi, U. C., Baliyan, K. S., et al. 2009, PRL Technical Report PRL-TN-2008-93 (arXiv:0912.0076)
Gopal-Krishna, & Wiita, P. J. 1992, A&A, 259, 109
Gorbovskoy, E., Balanutsa, P., Lipunov, V., et al. 2011, ATel, 3134, 1
Healey, S. E., Romani, R. W., Cotter, G., et al. 2008, ApJS, 175, 97
Healey, S. E., Romani, R. W., Taylor, G. B., et al. 2007, ApJS, 171, 61
Heidt, J., & Nilsson, K. 2011, A&A, 529, A162
Holmes, P. A., Brand, P. W. J. L., Impey, C. D., et al. 1984, MNRAS, 211, 497
Ikejiri, Y., Uemura, M., Sasada, M., et al. 2009, also, Fermi Symposium 2009 (Washington, DC), arXiv:0912.3664
Jannuzi, B. T., Green, R. F., & French, H. 1993, ApJ, 404, 100
Kesteven, M. J. L., Bridle, A. H., & Brandie, G. W. 1976, AJ, 81, 919
Kudelina, I., Gorbovskoy, E., Balanutsa, P., et al. 2011, ATel, 3131, 1
Lawrence, C. R., et al. 1986, ApJS, 61, 105
Lipunov, V. M., Krylov, A. V., Kornilov, V. G., et al. 2004, Astron. Nachr., 325, 580
Mangalam, A. V., & Wiita, P. J. 1993, ApJ, 406, 420
Marscher, A. P. 2008, in Proc. Workshop on Blazar Variability across the Electromagnetic Spectrum, POS(BLAZARS2008)010, 1
Marscher, A. P., & Gear, W. K. 1985, ApJ, 298, 114
Marscher, A. P., Gear, W. K., & Travis, J. P. 1992, in Variability of Blazars, ed. E. Valtaoja & M. Valtonen (Cambridge: Cambridge Univ. Press), 85
Meisner, A. M., & Romani, R. W. 2010, ApJ, 712, 14
Nesci, R. 2011, ATel, 3127, 1
Qian, S. J., Quirrenbach, A., Witzel, A., et al. 1991, A&A, 241, 15
Romero, G. E., Combi, J. A., & Colomb, F. R. 1994, A&A, 288, 731
Sambruna, M. 2007, Ap&SS, 311, 241
Serkowski, K. 1974, in IAU Colloq. 23, Planets, Stars and Nebulae, Polarimetry for Optical Astronomy, ed. T. Gehrels (Tucson, AZ: Univ. Arizona Press), 135
Sitko, M., Schmidt, G. D., & Stein, W. A. 1985, ApJS, 59, 323
Smith, P. S., Williams, G. G., Schmidt, G. D., Diamond-Stanic, A. M., & Means, D. L. 2007, AJ, 663, 118
Snellen, I. A. G., McMahon, R. G., Hook, I. M. F., & Browne, I. W. A. 2002, MNRAS, 329, 700
Tommasi, L., Palazzi, E., Pian, E., et al. 2001, A&A, 376, 51
Urry, C. M., & Padovani, P. 1995, PASP, 107, 803
Villforth, C., Nilsson, K., Ostensen, R., et al. 2009, MNRAS, 397, 1893

The Astrophysical Journal, 731:118 (5pp), 2011 April 20 doi:10.1088/0004-637X/731/2/118

RAPID OPTICAL VARIABILITY IN BLAZAR S5 0716+71 DURING 2010 MARCH

S. Chandra, K. S. Baliyan, S. Ganesh, and U. C. Joshi
Astronomy & Astrophysics Division, Physical Research Laboratory, Ahmedabad-380009, India; sunilc@prl.res.in
Received 2011 February 2; accepted 2011 February 22; published 2011 March 31

ABSTRACT

We report rapid optical variability for the blazar S5 0716+71 during 2010 March 8–10 and 19–20 in the CCD observations made from Mt. Abu Infrared Observatory. The light curves are constructed for a duration longer than 3 hr each night, with very high temporal resolution (≈45 s in the *R* band). During 2010 March 8, the source smoothly decayed by about 0.15 mag in 2.88 hr, apart from a fast flicker lasting about 30 minutes. S5 0716+71 brightened during March 9 and 10, showing high activity, while it was relatively faint (>14 mag in the *R* band) albeit variable during March 19–20. During March 9 and 10, rapid flickers in the intensity modulated the long-term intra-night (∼3 hr) variations. The present observations suggest that the blazar S5 0716+71 showed night-to-night and intra-night variability at various timescales with a 100% duty cycle for variation along with microvariability at significant levels. On a night-to-night basis, the source exhibits mild bluer-when-brighter nature. The interaction of shocks with local inhomogeneities in the jet appears to cause intra-night variations, while microvariations could be due to small-scale perturbations intrinsic to the jet.

Key words: BL Lacertae objects: individual (S5 0716+71) – galaxies: active – galaxies: photometry – methods: observational

Online-only material: machine-readable table

1. INTRODUCTION

Blazars are an extreme subclass of active galactic nuclei (AGNs), seen at a small angle ($\leqslant 10°$) to the relativistic jet emanating from very close to the black hole (Urry & Padovani 1995). They are characterized by strong variability in flux and polarization at almost all frequencies in the electromagnetic spectrum and their variability is often used to probe the central engine and nature of physical processes in AGNs. Blazars are known to show variations on different timescales ranging from years to months to days to hours and minutes. The variations that occur during the course of a night (few hours) are known as intra-night variations (INOVs), while microvariability is a change of a few tenths of magnitude in brightness during hours or less. Some authors use these terms interchangeably (Wagner & Witzel 1995; Miller et al. 1989). Fast variation, or microvariability, was first discovered in 1960s by Matthews & Sandage (1963), who found that the brightness of the BL Lac object 3C48 changes by 0.04 mag in the *V* band in 15 minutes, but their result was not taken seriously due to instrumental errors. However, now microvariability has been confirmed as an intrinsic feature of AGNs, especially blazars (Miller et al. 1989; Villata et al. 2008; Impiombato et al. 2011), and has become a subject of intensive study as its physical mechanisms are not understood well. Several models (e.g., Gopal-Krishna & Subramanian 1991; Mangalam & Wiita 1993; Marscher & Gear 1985; Qian et al. 1991; Marscher 1996; Gopal-Krishna & Wiita 1992) have been proposed in order to explain such fast variations. In order to constrain these models, long-term continuous observations with high temporal resolution (few minutes) are required.

The blazar S5 0716+71 (PKS 0716+714, redshift $z = 0.31$) is one of the brightest BL Lac objects that is highly variable from the radio to γ-rays with a very high duty cycle (Wagner & Witzel 1995). This source has been the target of a number of monitoring campaigns (e.g., Wagner et al. 1996; Qian et al. 2002; Raiteri et al. 2003; Villata et al. 2008). For the first time, INOV was detected in this source by Heidt & Wagner (1996). A decay in *J*-band brightness by 0.5 mag during 2003 December 10–12 was reported by Baliyan et al. (2005). Variations on various timescales have also been reported by many authors (e.g., Gupta et al. 2009; Montagni et al. 2006; Stalin et al. 2009, and references therein). Nesci et al. (2002) reported 0.02 mag hr^{-1} variations during their 52 night observation. Very recently, Carini et al. (2011) reported the *B*- and *I*-band microvariability study of S5 0716+71 based on their five-night observation during 2003 March 5–9. In their systematic statistical study, they detected variations at several timescales from days to few tens of minutes. Zhang et al. (2008) claim microvariability down to a 6 minute timescale but their sampling time is large (4–7 minutes). In the present paper, we report day-to-day and rapid variations in the optical brightness of the BL Lac object S5 0716+71 obtained in high temporal resolution observations during five nights in 2010 March.

The paper is organized as follows: Section 2 describes the observations and data analysis procedures, while Section 3 presents the results and their discussion. Conclusions from the study are presented in Section 4.

2. OBSERVATIONS AND DATA ANALYSIS

The photometric observations were carried out by using the liquid nitrogen cooled CCD Camera mounted at the $f/13$ Cassegrain focus of the 1.2 m Telescope at Mt. Abu Infrared Observatory, Gurushikhar, Rajasthan, operated by the Physical Research Laboratory, Ahmedabad, India. The PIXELLANT CCD Camera has 1296×1152 pixels^2 each of 22 μm size and a total read out time of about 13 s. With a scale of 0.29 arcsec pixel^{-1}, the total field of view is about 6.5×5.5 arcmin^2. The CCD read-out noise is four electrons and the dark current is negligible when cooled. The CCD-photometric system is equipped with a Johnson–Cousins *UBVRI* filter set.

The source was observed in two observing slots: during 2010 March 8–10 and 2010 March 19–20. All the observation nights were photometric with a seeing better than 1″.6. Several

Table 1
Observation Log for Monitoring in the *R* Band

Date	T_{start}(UT)	Duration (hr)	No. of Images
2010 Mar 8	14:53:51	3.2	248
2010 Mar 9	14:39:36	3.4	265
2010 Mar 10	14:44:44	4.0	294
2010 Mar 19	14:24:16	0.06	5
	17:24:27	0.30	24
2010 Mar 20	14:11:53	3.3	201

bias frames were taken every night at the beginning and the end of the observations. To construct master flats, we have taken a large number of evening twilight sky flats in all the bands each night. The observation strategy was to take four frames each in the *B*, *V*, *R*, and *I* bands and then to monitor the source in the *R* band for several hours. The field of view was large enough to accommodate several standard stars in the target frame to facilitate calibration. The exposure times were 30 s in the *I*, *R*, and *V* bands and 60 s in the *B* band.

Table 1 presents the details of the observations, giving the date, time (UT) of the starting observation, duration of monitoring (hours), and total number of observation points on the source. The data reduction is performed using standard routines in the IRAF[1] software. On the bias-subtracted, flat-fielded images, differential aperture photometry was performed using DAOPHOT package available in IRAF. The photometry is carried out using several aperture radii, ranging from 1 to 9 times the FWHM. The right size of the aperture is chosen, keeping in mind the optimum value of signal-to-noise ratio (S/N) and the prescription of Cellone et al. (2000) to avoid spurious variations. Based on these criteria, we use 4.5 arcsec as the aperture radius for the target and other stars used in the differential photometry. We have used standard stars 6 ($R = 13.26$ mag) and 5 ($R = 13.18$ mag) from Villata et al. (1998), having apparent magnitudes close to that of the source to check the variability of the blazar. Such a choice of comparison and control stars is necessary to avoid any disparity in the measured dispersions of the target-comparison and comparison-control light curves (Howell et al. 1988) due to photon statistics. One star is used to correct the source magnitude and the other as a control star to check the stability.

To check the significance of intra-night variability, we performed the *F*-test incorporated in the *R* statistical package. The *F*-statistic is the ratio of the sample variances, or $F = S_B^2/S_C^2$, where S_B^2 is the variance in the blazar magnitude and S_C^2 is that in the standard stars during the whole night of observations. For all the five nights, the *F*-values are greater than 9 with a significance level of 0.999995 or $\geqslant 5\sigma$. We have also calculated the intra-night variability amplitude, which is given by

$$\mathrm{Amp} = \sqrt{(A_{\max} - A_{\min})^2 - 2\sigma^2}, \tag{1}$$

where $A_{\max}$ and $A_{\min}$ are the maximum and minimum values in the light curves and σ is given as

$$\sigma = \sqrt{\frac{\Sigma(m_i - \bar{m})^2}{N - 1}}, \tag{2}$$

[1] IRAF is distributed by the National Optical Astronomy Observatory, which is operated by the Association of Universities for Research in Astronomy, Inc., under cooperative agreement with the National Science Foundation.

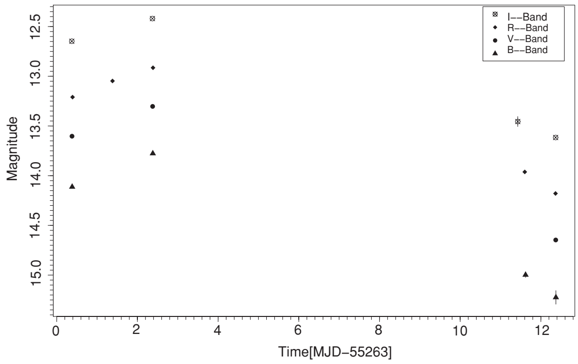

Figure 1. Nightly averaged *B*, *V*, *R*, and *I* magnitudes for S5 0716+71 as a function of time during 2010 March 8–10 and 19–20. Most of the error bars ($\pm\sigma$) lie within the symbol.

where $m_i = (m_{S6} - m_{S5})_i$ is the differential magnitude of stars 6 and 5 for the *i*th observation point, while $\bar{m} = (m_{S6} - m_{S5})$ is their differential magnitudes averaged over the entire data set, and *N* is the number of observation points obtained that night in a particular band. As the errors are subtracted from the total measured variability, Equation (1) gives a fairer estimate of the amplitude of variability in the source. The results from such analysis of our data for each night are discussed in the following section.

3. RESULTS AND DISCUSSION

The light curves for the source were obtained by adopting the abovementioned analysis procedure. The observed magnitudes of the source in the *B*, *V*, *R*, and *I* bands are calculated with respect to standard star 5 and nightly averaged values are plotted as a function of time in MJD in Figure 1 for 2010 March 8–10 and 19–20. In Figure 2, we plot *R*-band light curves showing intra-night variations during individual nights. The bottom curve in each panel shows the differential light curve of the stars. The observational uncertainties are the rms errors of the nightly differential magnitudes of calibration star 5 and check star 6 as given in Equation (2). The typical rms errors for the *R* band are less than 0.008 mag. These *R*-band magnitudes for S5 0716+71 for all the nights of observation are given in Table 2 in truncated form. The full data table is available electronically in a machine-readable form in the online version of the journal.

Table 3 lists the result of the *F*-test, giving the date of observation, *F*-value, standard deviation in the differential magnitudes of stars, and the amplitude of variation in the source each night. On March 19, we have five data points at the beginning and 24 data points at the end of the night, covering about 3.5 hr. The *F*-value for this night, therefore, is obtained from these limited measurements. The tabulated values for all the nights indicate that the source is significantly variable during the present observing run, showing 100% duty cycle for variation. A similar result has been reported by other workers (e.g., Wagner & Witzel 1995). The *F*-test results are in very good agreement with the values obtained from the variability test (Jang & Miller 1997). Here, the confidence level of variability is defined by the parameter $C = \sigma_T/\sigma$, where σ_T is the standard deviation in the differential light curve of the source and comparison star. The source is considered variable at the 99% confidence level if $C \geqslant 2.576$. Our values for the variability parameter for March 8, 9, 10, and 20 are, 7.66, 3.35,

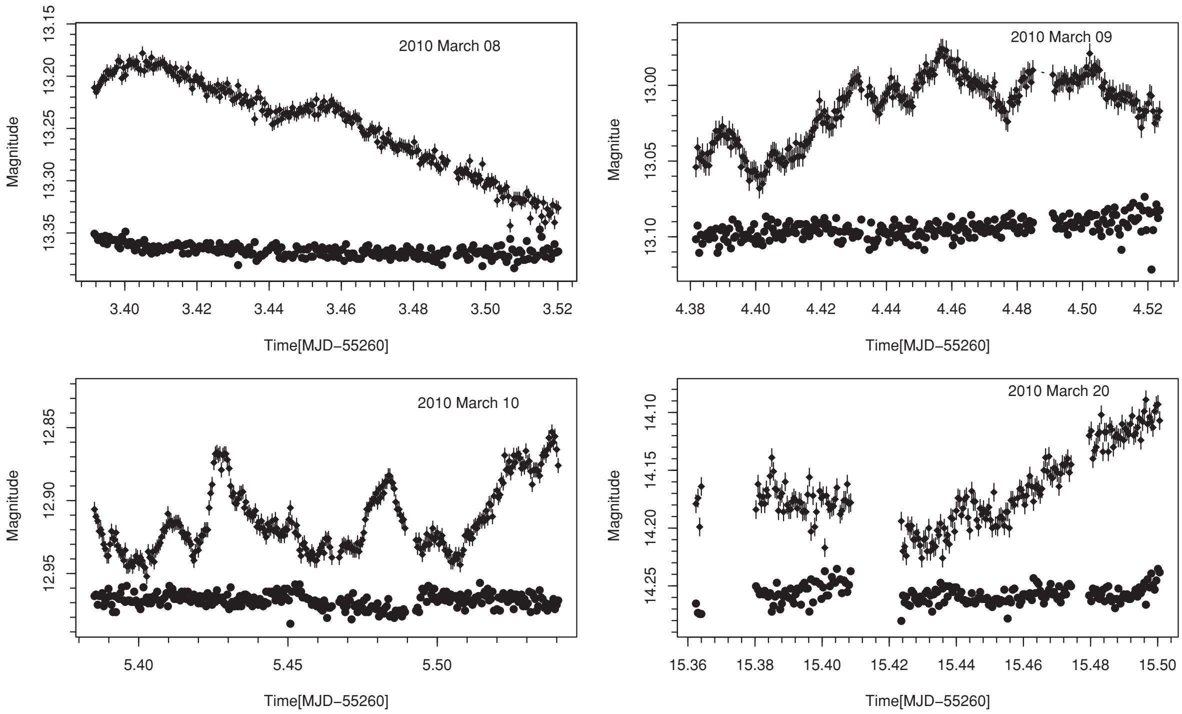

Figure 2. *R*-band light curves showing INOV for S5 0716+71 on 2010 March 8, 9, 10, and 20. The lower curve in each panel shows differential light curve for comparison and control stars plotted with appropriate offsets.

Table 2
R-band Photometric Data for S5 0716+71

Date	MJD (55200 +)	Mag	σ (mag)
2010 Mar 8	63.39160	13.211	0.007
	63.39210	13.215	0.007
	63.39260	13.211	0.007
	63.39310	13.208	0.007
	63.39360	13.204	0.007
2010 Mar 9	64.38170	13.054	0.006
	64.38220	13.041	0.006
	64.38270	13.048	0.006
	64.38320	13.049	0.006
	64.38370	13.045	0.006
2010 Mar 10	65.38520	12.906	0.005
	65.38570	12.911	0.005
	65.38630	12.914	0.005
	65.38680	12.921	0.005
	65.38730	12.920	0.005

(This table is available in its entirety in a machine-readable form in the online journal. A portion is shown here for guidance regarding its form and content.)

4.72, and 4.45, respectively, confirming significant variability in the source on all the nights. To further support the genuine nature of the microvariability reported here, we note that the host galaxy is more than 4 mag fainter as compared with the source (Nilsson et al. 2008), ruling out any significant effect on the source variability.

The variation rates (mag hr^{-1}) for various peaks appearing in the light curves of each night of observation are calculated by fitting a straight line in the rising and falling segments using a least-squares fitting algorithm. Nesci et al. (2002) studied the intra-night variability of S5 0716+71 for 52 nights and claimed a variation rate of 0.02 mag hr^{-1} along with a maximum rising rate of 0.16 mag hr^{-1}, while Montagni et al. (2006) reported equally fast variation rates of 0.1–0.16 mag hr^{-1}. In the following, we discuss results obtained in the present study.

Table 3
Intra-night Variability Results

Date	*F*-value	σ (mag)	Amp(%)
2010 Mar 8	38.82	0.006	16.8
2010 Mar 9	11.27	0.006	9.1
2010 Mar 10	20.51	0.005	9.9
2010 Mar 19	98.54	0.004	12.8
2010 Mar 20	19.73	0.008	14.4

3.1. Inter-night Variations

Figure 1 shows nightly averaged *B*, *V*, *R*, and *I* magnitudes as a function of time (MJD) for all five nights. It is evident that S5 0716+71 brightens by 0.34, 0.3, 0.3, and 0.24 mag in the *B*, *V*, *R*, and *I* bands, respectively, during 2010 March 8–10. During March 19–20, the source decreases in brightness by 0.23, 0.22, and 0.21 mag in the *B*, *R*, and *I* bands, respectively. Evidently, during our observations the blazar S5 0716+71 was brightest on March 10 ($R \approx 12.914 \pm 0.008$ mag) and faintest on March 20 ($R \approx 14.179 \pm 0.006$ mag). The figure also gives clear indication that the source is mildly bluer when brighter and redder when fainter. During the period of eight days (March 11–18), when we do not have observations, S5 0716+71 became fainter by about 1.10 (*R* band) and 1.49 (*B* band) mag, clearly showing an increase in the amplitude of variation with the frequency.

3.2. Intra-night Variations (INOVs)

From the light curves in Figure 2, it is evident that the blazar S5 0716+71 is showing significant INOVs on almost all of the nights it was monitored. Here we discuss the variability behavior night by night.

On 2010 March 8, the source brightens up to $R \sim 13.185$ mag at MJD = 55263.40. It then decays to $R \sim 13.335$ mag at MJD = 55263.52, a variation of 0.15 mag during 2.88 hr (decay rate $\approx$0.052 mag hr^{-1}). This smoothly falling curve is superposed by a flicker (between MJD55263.44 and MJD55263.465) that brightens the source by more than 2σ within a timescale of about 15 minutes.

The blazar S5 0716+71 appears to be very active during the night of 2010 March 9 (cf. Figure 2). The source is in the brightening phase with several rapid fluctuations modulating a smoothly varying intra-night light curve. During the first microvariability event of the night, the source fades by 0.032 mag ($>5\sigma$) with a timescale of $\approx$15 minutes. It then brightens to its highest value ($R = 12.976$ mag) at MJD = 55264.456 within a time span of about 1.24 hr (rise rate 0.063 mag hr^{-1}). The source then decays by 0.05 mag within 0.48 hr toward the end of the observations.

The statistical analysis of the light curves shows fast variation rates (up to $\sim$0.38 mag hr^{-1}) for several segments on March 10. During the entire night, the source remains in a bright state with rapid fluctuations in the intensity. We have recorded the most rapid fluctuation during this night. For the most significant peak, we have calculated the rise and fall rates to be $\sim$0.38 mag hr^{-1} and $\sim$0.08 mag hr^{-1}, respectively. Toward the end (from MJD 55265.502 to MJD 55265.539), S5 0716+71 brightens by 0.09 mag in the R band within about 53 minutes. The source also shows several microvariability events on a timescale of about 15 minutes. On March 19, we have few observation points in the beginning and end of the night. However, the trend shows significant variation, about 0.1 mag in 3.5 hr of duration. The light curve for this night is not shown here. On March 20, the source is initially stable but later (at MJD = 55275.43) starts brightening, changing by 0.12 mag in 1.68 hr (0.07 mag hr^{-1}). The source is generally faint during these two nights and microvariability, if any, is washed out in the relatively large scatter (0.008 mag).

Let us now discuss our results in detail. The present observations reveal significant variability at intra-night (1.24–2.88 hr) and inter-night (night-to-night to nine nights) timescales, as well as microvariability (15 minutes or more) or fast fluctuations. Similar behavior for S5 0716+71 is reported by Carini et al. (2011) in their 2003 March 5–9 observations made in the B and I bands. As mentioned above, to avoid the spurious variations caused by the variation in the seeing and/or contamination by the thermal emission from the unresolved host galaxy, we have carefully chosen aperture and comparison/control stars. In order to delineate small-scale fluctuations, we have used the best temporal resolution ($\approx$45 s) reported so far. Many authors have reported INOV and microvariability for this source at similar timescales (e.g., Quirrenbach et al. 1991; Villata et al. 2008; Carini et al. 2011) but with few minutes to tens of minutes temporal resolutions. Zhang et al. (2008) have reported fast variations at 6–33 minute timescales with an unusually large ($>$1 mag) amplitude of variations. They do not mention the aperture size adopted but have used exposures ranging from 4 to 7 minutes and have calibrated the source magnitude with the brightest star in the field. Some of these are prescriptions for spurious variations as investigated by Cellone et al. (2000).

The observed optical emission in blazars originates in a part of the accretion disk and the inner (pc-scale) regions of the jet. In light of this, one can discuss the possible reasons behind the variations over various timescales. We should also keep in mind that optical variability timescales shorter than a few hours would imply emitting regions to be smaller than the Schwarzschild radius for certain objects, depending upon their mass. There are a host of models to explain extrinsic and intrinsic variability in blazars: microlensing effect (Chang & Refsdal 1979), light house effect (Camenzind & Krockenberger 1992), accretion disk models (Chakrabarti & Wiita 1993; Mangalam & Wiita 1993), and shock-in-jet model (Marscher & Gear 1985). As far as our observations are concerned, we notice mild chromatic behavior (bluer when brighter) in the inter-night light curves. Our intra-night light curves do not show any symmetry or periodicity and the variability timescales are short, ranging from few tens of minutes to few hours. Such fast variations with amplitude of the variations reported here are difficult to explain using the accretion disk models. Since the blazar emission is dominated by the jet radiation, we concentrate on relativistic jet models.

A mild chromatic behavior in the long-term variation is explained by Villata et al. (2004) and Papadakis et al. (2007) for BL Lacertae, using the data obtained during several Whole Earth Blazar Telescope (WEBT[2]) campaigns covering the period from 1997 to 2002, by the variation in the Doppler factor due to the change in the viewing angle. They interpreted flux variability in terms of two components: a long-term (few days timescale) variation component as a mildly chromatic event and a fast (intra-day) varying component characterizing strong bluer-when-brighter chromatic behavior. If the intrinsic source spectrum is well described by a power law, a Doppler factor variation does not imply a color change. But mildly chromatic behavior could be due to Doppler factor variation on a spectrum slightly deviating from a power law. A change in the Doppler factor changes both the flux ($F_\nu \propto \delta^3$) and the frequency ($\nu \propto \delta$) of emission. The inter-night variations reported here for S5 0716+71, which show mild chromatic behavior, could be the result of the change in the Doppler factor.

Rapid variability can be produced when a relativistic shock wave or a blob propagates down the jet with turbulent plasma (Marscher et al. 1992; Qian et al. 1991). Synchrotron emission gets enhanced when the shock encounters particle or magnetic field overdensities. The amplitude and the timescale of the variation depend on the turbulence and shock thickness. Fast variations thus require shocks to be very thin and emission to originate from very close to the central engine. Based on our shortest intra-night variation timescale (t_v) of 1.24 hr, the upper limit on the size of the emission region, with Doppler boosting and cosmological corrections, is $R \leqslant t_v \delta c/(1+z) \approx 10^{15}$ cm, where c is the speed of light and δ is the Doppler factor (taken as 10 here). Considering this size as a bound on the Schwarzschild radius of the central engine, one can estimate its mass using $M \approx (c^2 R)/3G$, which comes out to be $\approx 1.1 \times 10^9\, M_\odot$. However, estimation of black hole mass using such fast optical variations must be taken with caution (Quirrenbach et al. 1991). The variations shorter than INOV (microvariations) amounting to few tens of minutes as reported here and by many other authors cannot possibly be explained by the shock-in-jet model. These are perhaps either due to small fluctuations intrinsic to the jet or imprinted by a small fraction of black hole horizon

2 http://www.to.astro.it/blazars/webt/

(Begelman et al. 2008). Such fast variations may not represent the linear dimension of an emission region.

4. CONCLUSIONS

Here we have reported intra-night variations and microvariability in the blazar S5 0716+71 as observed in the high temporal resolution observations carried out during 2010 March 8–10 and 19–20. We note that the source was variable with a 100% duty cycle at various timescales. Inter-night behavior of the source appears to be bluer when brighter from the limited observations. It is evident that S5 0716+71 was highly active during 2010 March 9, 10, and 20 with rapid flickers superposed on the slowly varying intra-night light curves. On March 19, it shows substantial decay but we do not have full coverage of the night to comment on the behavior of nightly variation.

The source shows various timescales for the variation, ranging from close to 2 hr to 15 minutes. The inter-night variations showing mild bluer-when-brighter nature could be due to variations in the Doppler factor. While intra-night variations with few-hour timescales are probably due to the interaction of fast-moving shocks in the jet with local small-scale inhomogeneities, it is very difficult to associate faster variations with the spatial extent of the emitting region. Perhaps these variations originate in a small region of the blob. Taking the shortest intra-night variability timescale of 1.24 hr, the linear size of the emitting region is estimated to be $\approx 10^{15}$ cm and with the corresponding Schwarzschild radius, $\approx 1.1 \times 10^9 M_\odot$ is the mass of the black hole.

This work is supported by the Department of Space, Government of India, India.

REFERENCES

Baliyan, K. S., Joshi, U. C., & Ganesh, S. 2005, Bull. Astron. Soc. India, 33, 181
Begelman, M. C., Fabian, A. C., & Rees, M. J. 2008, MNRAS, 384, L19
Camenzind, M., & Krockenberger, M. 1992, A&A, 255, 59
Carini, M. T., Walters, R., & Hopper, L. 2011, AJ, 141, 49
Cellone, S. A., Romero, G. E., & Combi, J. A. 2000, AJ, 119, 1534
Chakrabarti, S. K., & Wiita, P. J. 1993, ApJ, 411, 602
Chang, K., & Refsdal, S. 1979, Nature, 282, 561
Gopal-Krishna, & Subramanian, K. 1991, Nature, 349, 766
Gopal-Krishna, & Wiita, P. J. 1992, A&A, 259, 109
Gupta, A. C., Srivastava, A. K., & Wiita, P. J. 2009, ApJ, 690, 216
Heidt, J., & Wagner, S. J. 1996, A&A, 305, 42
Howell, S. B., Warnock, I. A., & Mitchell, K. J. 1988, AJ, 95, 247
Impiombato, D., et al. 2011, ApJS, 192, 12
Jang, M., & Miller, H. R. 1997, AJ, 114, 565
Mangalam, A. V., & Wiita, P. J. 1993, ApJ, 406, 420
Marscher, A. P. 1996, in ASP Conf. Ser. 110, Blazar Continuum Variability, ed. H. R. Miller, J. R. Webb, & J. C. Noble (San Francisco, CA: ASP), 248
Marscher, A. P., & Gear, W. K. 1985, ApJ, 298, 114
Marscher, A. P., Gear, W. K., & Travis, J. P. 1992, in Variability of Blazars, ed. E. Valtaoja & M. Valtonen (Cambridge: Cambridge Univ. Press), 85
Matthews, T. A., & Sandage, A. R. 1963, ApJ, 138, 30
Miller, H. R., Carini, M. T., & Goodrich, B. D. 1989, Nature, 337, 627
Montagni, F., Maselli, A., Massaro, E., Nesci, R., Sclavi, S., & Maesano, M. 2006, A&A, 451, 435
Nesci, R., Massaro, E., & Montagni, F. 2002, PASA, 19, 143
Nilsson, K., Pursimo, T., Sillanpää, A., Takalo, L. O., & Lindfors, E. 2008, A&A, 487, L29
Papadakis, I. E., Villata, M., & Raiteri, M. 2007, A&A, 470, 857
Qian, B., Tao, J., & Fan, J. 2002, AJ, 123, 678
Qian, S. J., Quirrenbach, A., Witzel, A., Krichbaum, T. P., Hummel, C. A., & Zensus, J. A. 1991, A&A, 241, 15
Quirrenbach, A., et al. 1991, ApJ, 372, L71
Raiteri, C. M., et al. 2003, A&A, 402, 151
Stalin, C. S., et al. 2009, MNRAS, 399, 1357
Urry, C. M., & Padovani, P. 1995, PASP, 107, 803
Villata, M., Raiteri, C. M., Lanteri, L., Sobrito, G., & Cavallone, M. 1998, A&AS, 130, 305
Villata, M., et al. 2004, A&A, 421, 103
Villata, M., et al. 2008, A&A, 481, L79
Wagner, S. J., & Witzel, A. 1995, ARA&A, 33, 163
Wagner, S. J., et al. 1996, AJ, 111, 2187
Zhang, X., Zheng, Y. G., Zhang, H. J., Liu, Y., Wen, Y. B., & Wang, W. 2008, AJ, 136, 1846